



HAL
open science

Innate immune response to tissue-specific infection : notochord infection in the zebrafish embryo

Quang Tien Phan

► **To cite this version:**

Quang Tien Phan. Innate immune response to tissue-specific infection : notochord infection in the zebrafish embryo. Human health and pathology. Université Montpellier, 2016. English. NNT : 2016MONTT082 . tel-01559163

HAL Id: tel-01559163

<https://theses.hal.science/tel-01559163>

Submitted on 10 Jul 2017

HAL is a multi-disciplinary open access archive for the deposit and dissemination of scientific research documents, whether they are published or not. The documents may come from teaching and research institutions in France or abroad, or from public or private research centers.

L'archive ouverte pluridisciplinaire **HAL**, est destinée au dépôt et à la diffusion de documents scientifiques de niveau recherche, publiés ou non, émanant des établissements d'enseignement et de recherche français ou étrangers, des laboratoires publics ou privés.

THÈSE

Pour obtenir le grade de
Docteur

Délivré par **UNIVERSITÉ MONTPELLIER**

Préparée au sein de l'école doctorale CBS2
Et de l'unité de recherche UMR 5235-DIMNP

Spécialité : **Microbiologie et Immunologie**

Présentée par **PHAN Quang Tién**

**Innate immune response to tissue-specific
infection: Notochord infection in the
zebrafish embryo**

Soutenue le 22 Mars 2016 devant le jury composé de

Mme Emma COLUCCI-GUYON, Dr, Institut Pasteur
M Serge MOSTOWY, Dr, Imperial College London
Mme Annemarie H. MEIJER, Prof, Universiteit Leiden
M Victoriano MULERO, Prof, Universidad de Murcia
Mme Mai NGUYEN-CHI, Dr, Université Montpellier
M Georges LUTFALLA, Dr, CNRS Montpellier

Rapporteur
Rapporteur
Examineur
Examineur
Examineur
Directeur de thèse



Résumé

Lors des infections bactériennes, selon les tissus infectés, et selon la nature des pathogènes, l'organisme répond en mobilisant différents acteurs. Nous avons décidé d'utiliser le modèle du zebrafish ou Danio rério pour étudier la réponse immunitaire innée dans les situations d'infection bactérienne où les phagocytes professionnels ne peuvent pas venir au contact direct des bactéries. Pour cela, j'ai développé un modèle d'infection de la notochorde de l'embryon de zebrafish. Lors de l'injection des bactéries dans ce compartiment, les bactéries se retrouvent protégées par une épaisse gaine de collagène. Les phagocytes ne peuvent pas pénétrer. Alors que les mycobactéries, protégées par la gaine de collagène ne sont pas détectées par les phagocytes, les bactéries E. coli sont immédiatement détectées ce qui déclenche une importante inflammation locale autour de la notochorde. Alors que les bactéries E. coli, bien qu'inaccessibles à la phagocytose sont éliminées dans les premières 24 heures qui suivent l'injection, l'inflammation dure plusieurs jours.

J'ai étudié les mécanismes qui conduisent à cette inflammation persistante et ses conséquences à long terme sur le développement du poisson. J'ai montré le rôle central de la cytokine IL1 β dans ce processus, et j'ai développé une lignée transgénique qui permet d'étudier l'induction de cette cytokine in vivo chez le poisson.

J'ai ensuite étudié le rôle des deux principales populations de phagocytes dans l'élimination des bactéries E coli. J'ai montré que les macrophages ne sont pas impliqués dans la disparition des bactéries alors que les neutrophiles, bien qu'incapable de pénétrer à l'intérieur de la gaine de collagène sont nécessaires à l'élimination des bactéries.

J'ai ensuite montré que la myéloperoxydase et le monoxyde d'azote ne sont pas impliqués dans l'élimination des bactéries alors que les espèces réactives de l'oxygène produites par les neutrophiles sont nécessaires pour éradiquer l'infection.

Summary

In bacterial infections, according to the infected tissue and the nature of pathogens, the body responds by mobilizing various actors. I decided to use zebrafish or *Danio rerio* model to study the innate immune response to bacterial infection in the situations that professional phagocytes cannot come in direct contact with the bacteria. For this, I developed a model of infection in the notochord of zebrafish embryo. Upon injection of bacteria in this compartment, the microbes find themselves protected by the thick collagen sheath where the phagocytes cannot penetrate. While mycobacteria are not detected by phagocytes; *E. coli* bacteria are sensed and a significant local inflammation around the notochord is mounted. The *E. coli*, although inaccessible to phagocytosis are eliminated within the first 24 hours after injection, the inflammation lasts several days.

I studied the mechanisms that lead to this persistent inflammation and its long term consequences on the development of the fish. I showed the central role of the cytokine IL1B in this process, and I developed a transgenic line that allows studying *in vivo* the induction of this cytokine in fish.

I then studied the roles of the two main populations of phagocytes in the elimination of *E. coli*. I revealed that macrophages are not involved in the removal of bacteria but neutrophils, although unable to penetrate inside the collagen casing, are necessary for the bacterial elimination.

I also confirmed that myeloperoxidase and nitrogen monoxide are not involved in the removal of bacteria, rather the reactive oxygen species produced by neutrophils are needed to eradicate the infection.

ACKNOWLEDGEMENTS

The weather looks good for today and I am very pleased to take this chance to express my gratefulness to all people who are always supportive to help create this thesis!

First and foremost I thankfully acknowledge my supervisor, Georges LUTFALLA and my mentor, Mai NGUYEN-CHI for offering me this fantastic opportunity to pursue my PhD thesis at University of Montpellier, and for all their advices during my lab time. It is my huge pleasure working with them!

I would also like to thank all people from the FishForPharma Network who are so friendly, funny and always available to share their facilities and opinions at any time. I have special thanks to Annemarie H. Meijer and other PIs for their giant efforts setting up this network for me and other students to learn about the zebrafish model in an international and cooperative environment!

This work could never be accomplished without advices, discussions and supports from people at DIMNP, especially Etienne LELIEVRE, Jana TRAVNICKOVA, Paul GUGLIELMI, Suma CHOORAPOIKAYIL, Karima KISSA. Also, I would like to give my gratitude to Annette VERGUNST and Jean-Pierre LEVRAUD for their fabulous advices and for being members of my Comité de thèse, thanks to all!

I am joyful to mention Catherine GONZALEZ, Richard CASTEL, Stéphane CASTEL who are not only extremely supportive to my lab work and the “*French*” administrative paper work. These amazing people always make my life in France just like home!

Being away is not easy. Fortunately thanks to all friends at the Association of Vietnamese Students in Montpellier, we have got lot of fun together!

Lastly, the deepest gratitude goes to my parents, my brothers and sisters and my wife, Thanh Trúć. Thanks all for treating me with love, always!



Contents

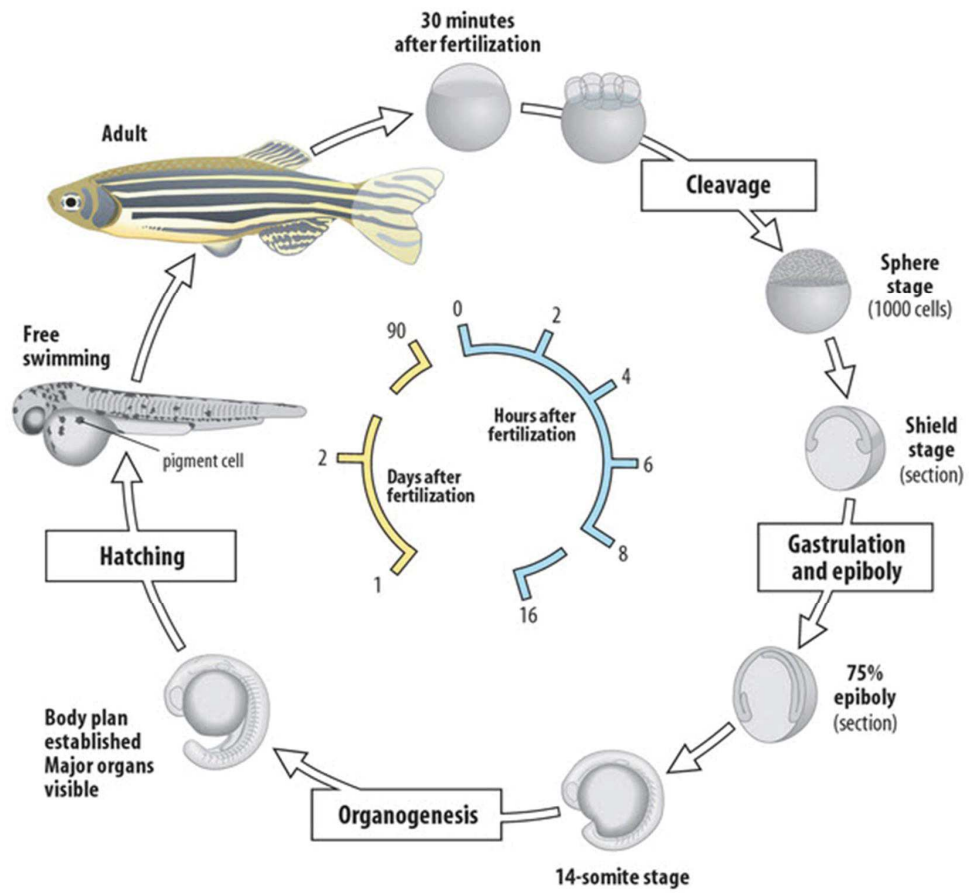
Résumé.....	1
Summary	2
ACKNOWLEDGEMENTS	3
CHAPTER I: INTRODUCTION	7
I. Innate immune system in human	7
I.1. General introduction	7
I.2. Innate immune response to bacterial infection.....	7
I.3. ROS productions and functions.....	22
I.4. Cytokines and immunoregulation	27
I.4.1. Resources and functions of cytokines	27
I.5. Characteristics and functions of inflammation	34
II. Zebrafish model for study of host-pathogen interaction.....	36
II.1. Zebrafish biology and experimental advantages	36
II.2. Zebrafish immune system.....	37
II.3. Innate immune response to bacterial infection.....	39
II.4. The zebrafish notochord.....	45
AIM OF THE THESIS.....	47
OUTLINE OF THE RESULTS.....	49
Part I: Transient infection of zebrafish notochord with E. coli induces chronic inflammation	49
Part II: Neutrophils control notochord infection at a distance with superoxide.....	49
Part III: Identification of polarized macrophage subsets in zebrafish.....	50
Part IV: Rearing zebrafish larvae with Tetrahymenas	50
PART I	51
PART II	52
Abstract	53
Introduction	54
Materials and Methods	56
Discussion	63
Acknowledgements	66
FIGURES AND LEGENDS.....	68
References.....	82
PART III	85



PART IV	86
Abstract	87
Introduction	88
Materials and Methods	89
Results	91
Discussion	95
Acknowledgements	97
References	97
CHAPTER III: DISCUSSION AND PERSPECTIVES	99
1. Innate immune response to tissue-specific infection	99
2. Roles of cytokines in chronic inflammation and bone diseases	100
2.1. Interleukin 1 β	100
2.2. TNF α	102
3. Combat of neutrophils and <i>E. coli</i> , victory for the crowd.....	103
General conclusion.....	106
ANNEXES	107
1. Only live bacteria could induce chronic inflammation.....	107
2. Chronic inflammation affects vertebral column ossification.....	109
LIST OF TABLES.....	110
ABBREVIATIONS	110
LISTS OF FIGURES	111
REFERENCES.....	112

CHAPTER I

INTRODUCTION



Zebrafish cycle

Memorial University

CHAPTER I: INTRODUCTION

I. Innate immune system in human

I.1. General introduction

The human innate immunity is made up with layer-to-layer of defensive structures ranging from physical and cellular to molecular entities which can be recognized as followed: 1) The first barrier is the epithelium which is highly structured with keratin. 2) The less structured mucosal membranes of the respiratory and gastrointestinal tracts yet are equipped with thick protective mucus. 3) The phagocyte population consists of neutrophils, macrophages, dendritic cells, mast cells, eosinophils, basophils and NK cells which are able to engulf microbes and destroy them with lysosomal and granular toxic components. 4) The intracellular or secretory proteins including: a) complements synthesized in the liver and in other local tissues, and b) antimicrobial compounds mostly produced by epithelia and by phagocytes are among the most important artillery of the innate immune system (Klebanoff et al., 2013; Li et al., 2007; Paiva and Bozza, 2014). The common function of all the aforementioned defensive layers is to deal with attacks or invasions of any harmful foreign agents such as microbes, toxins or dangerous molecules in the unspecific manners. The innate immunity also signals to activate the adaptive immune system, the other arm of the host immune system (Charles A Janeway et al., 2001).

I.2. Innate immune response to bacterial infection

The innate immunity plays crucial role in the control of wide range of microbial infections. Dysfunction of this arm of the host defense results in sepsis and other fatal symptoms (Albiger et al., 2007; Kobayashi and DeLeo). This thesis focuses more on the functions of two most important cellular actors of the innate immune system, neutrophils and macrophages.

I.2.1. Neutrophils

I.2.1.1. Biology and function of neutrophils

The polymorphonuclear neutrophil is a member of granulocyte family which includes also eosinophil and basophil. After being generated and matured in the bone marrow neutrophils possessing pro-inflammatory molecules such as cytokines, chemokines, antimicrobial and lytic compounds (depicted in figure 1) are released into the circulation where they join the innate immunity and perform protective function (Rosenbauer and Tenen, 2007). Neutrophils are the most abundant population of leukocytes in the blood (ATHENS et al., 1961; Dancey et al., 1976). The normal number of neutrophils in the body is actively regulated by hematopoietic organ and is known as steady-state density. Upon infection neutrophils are massively produced in response to the demand of fighting infection, this process is described as emergency granulopoiesis (Manz and Boettcher, 2014; Panopoulos and Watowich, 2008). In human, although having short-live characteristics, neutrophils are produced massively at daily basis of approximately 100 billion cells.

The correct population of neutrophils is critical for host protection from infections (Courtney et al., 2007; Donadieu et al., 2009). Patients with neutropenia or impaired neutrophil function suffer severe viral, bacterial and fungal infections which result in high rate of morbidity and mortality (Geiszt et al., 2001; Newburger, 2006).

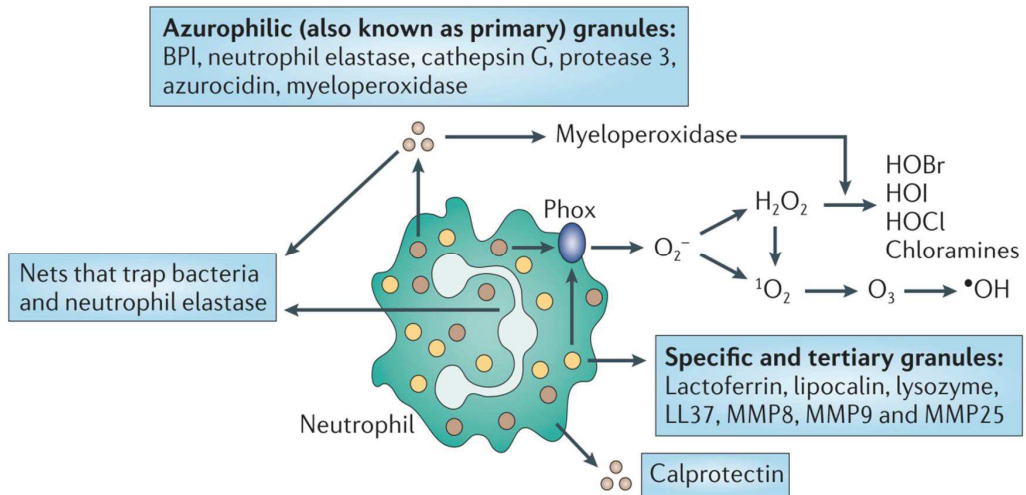


Figure 1: Neutrophils deliver multiple anti-microbial molecules

Microbicidal products arise from most compartments of the neutrophil: azurophilic granules (also known as primary granules), specific granules (also known as secondary granules) and tertiary granules, plasma and phagosomal membranes, the nucleus and the cytosol. BPI, bactericidal permeability increasing protein; H_2O_2 , hydrogen peroxide; HOBr, hypobromous acid; HOCl, hypochlorous acid; HOI, hypoiodous acid; MMP, matrix metalloproteinase; 1O_2 , singlet oxygen; O_2^- , superoxide; O_3 , ozone; $\bullet OH$, hydroxyl radical; phox, phagocyte oxidase. Adapted from (Nathan, 2006).

I.2.1.2. Mechanism of bacterial killing by neutrophils

Neutrophils have been shown to use different mechanisms to control infections (depicted in figure 3). The primary mean is professional phagocytosis in which neutrophils engulf microbes into their phagosomes. Following phagocytosis, infecting microorganisms are destroyed in the phagosomes by abundant and diverse sets of antimicrobial compounds including Reactive Oxygen Species (ROS), mainly produced by nadph oxidase complexes, and other toxic molecules such as myeloperoxidase, neutrophil elastase, defensins, azurocidin, protease 3, cathepsin G, lysozyme, lipocalin delivered from granules in the cytoplasm. These granular antimicrobial molecules, mostly from specific granules, could also be released to the extracellular environment to cope with invading agents as well as to facilitate the extracellular matrix degradations (Abdel-Latif et al., 2005; Fang, 2011; Kolaczowska and Kubes, 2013a). The massive production of ROS, especially the superoxide, in the phagosome is suggested to cause damage and make the ingested bacteria susceptible to other granular antimicrobial effectors (Slauch, 2011). In addition to the intracellular decomposition by phagocytosis, neutrophils were also described by Brinkmann in 2004 to perform the extracellular killing mechanism named Neutrophil Extracellular Traps (NETs).

In this process neutrophils usefully suicide themselves to trap the spreading of microbes by expelling their chromatin associated with range of antimicrobial molecules (Brinkmann et al., 2004; Halverson et al., 2015; Papayannopoulos and Zychlinsky, 2009). Recently the growing data have demonstrated that NETs are used in response to varieties of stimuli, such as: PMA, LPS, fungi, bacteria and protozoan (Fuchs et al., 2007; Guimarães-Costa et al., 2009; Remijsen et al., 2011c). Interestingly, neutrophils have been shown to release NETs in response to large pathogens which could not be engulfed by conventional phagocytosis such as *C. albicans* hyphae (Branzk et al., 2014).

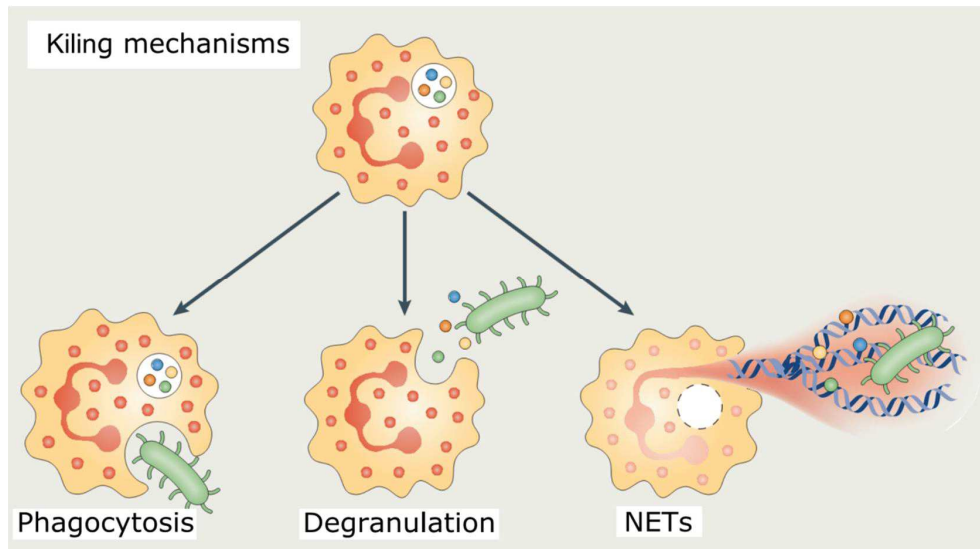


Figure 2: Killing mechanisms of neutrophil

Neutrophils can eliminate pathogens by multiple means, both intra- and extracellular. When neutrophils encounter microorganisms, they phagocytose them. After being encapsulated in phagosomes, the pathogens are killed by NADPH oxygenase-dependent pathway through reactive oxygen species or by antibacterial proteins such as cathepsins, defensins, lactoferrin and lysozyme. These molecules are released from the neutrophil granules either into phagosomes or into the extracellular milieu, thus acting on either intra- or extracellular pathogens, respectively. Highly activated neutrophils can stop the spreading and eliminate extracellular microorganisms by releasing neutrophil extracellular traps (NETs). NETs are composed of a core DNA element to which histones, antimicrobial proteins (for example, lactoferrin and cathepsins) and enzymes (for example, MPO and neutrophil elastase) that are released from neutrophil granules are attached. Adapted from (Kolaczowska and Kubes, 2013a).

The formation of NETs need stimulation and correct contribution of key cellular components. ROS is one of the important players and its role was shown in patients with Chronic Granulomatous Disease whose neutrophils failed to produce ROS due to mutation in the gene encoding nadph oxidase complex (Fuchs et al., 2007). The nadph oxidase-derived superoxide, a major member of ROS, was also shown to involve in the activation of neutrophil elastase (NE) another actor of NETs forming process (Reeves et al., 2002). Upon stimulation NE and Myeloperoxidase are translocated from cytosolic granules into the nucleus where NE promotes fragmentation of chromatin and NETs expulsion (Metzler et al., 2011; Papayannopoulos et al., 2010).

For all three neutrophil killing mechanisms, neutrophil granules with their components exhibit central regulatory function. Generally the neutrophil granules are classified into three groups: the primary or azurophilic granule contains BPI, neutrophil elastase, cathepsin G, protease 3, azurocidin, myeloperoxidase; the secondary or specific granule and the tertiary or gelatinase granule contain Lactoferrin, lipocalin, lysozyme, matrix metalloproteinase (MMP8-9). Since these granular microbicides are also devastating to host cells, it is crucial that their deliveries into phagosomes (depicted in figure 3) are correctly regulated to avoid host tissue damages (Nathan, 2006).

Although facing different neutrophil effectors, many microbes have evolved variety of mechanisms to survive neutrophil elimination; some of which include turning on stress response, avoiding contact with neutrophils, inhibiting phagocytosis, surviving intracellular, inducing cell death or destroying NETs (Corleis et al., 2012; de Haas et al., 2004; Fradin et al., 2005; Rubin-Bejerano et al., 2003; Urban et al., 2006).

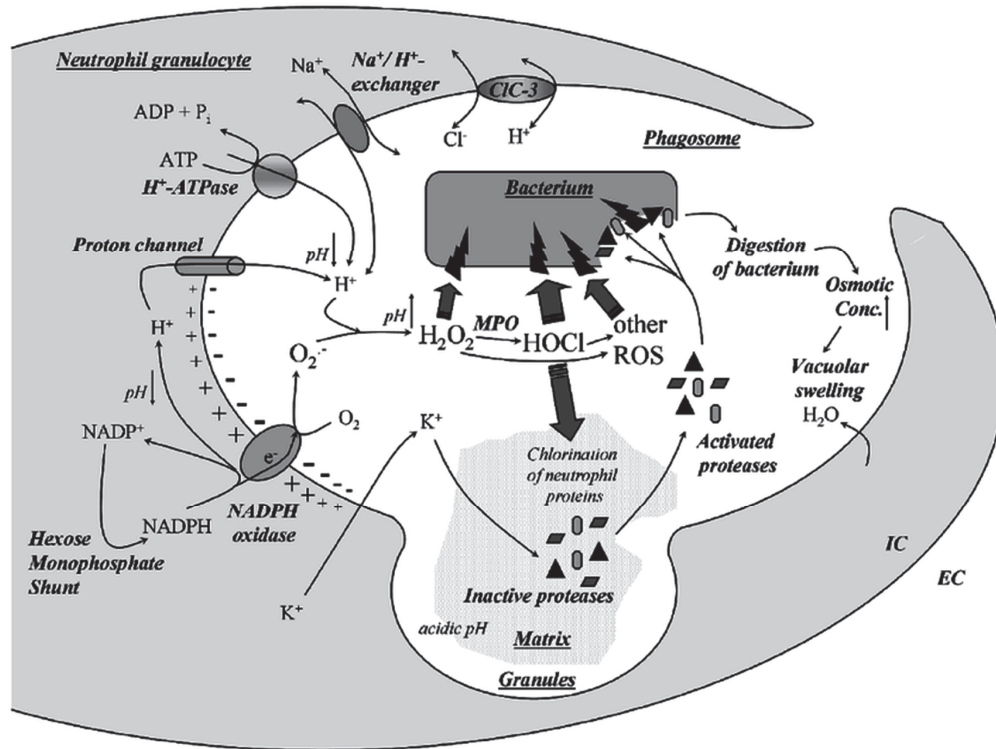


Figure 3: Killing of bacteria in neutrophil phagosome

Upon engulfment of bacteria into the neutrophil phagosome, granules fuse with the phagosome and the phagocytic NADPH oxidase is assembled and activated on the phagosomal membrane. By transporting electrons from cytosolic NADPH, the phagosomal membrane depolarizes as superoxide is produced in the phagosome lumen. Superoxide gives rise to the whole spectrum of reactive oxygen species that are highly reactive and attack bacteria. The Nox2-generated depolarization drives protons and potassium ions into the phagosome. The protons maintain a neutral pH in the phagosome required for optimal protease activity and sustained oxidase function. Potassium ions liberate and activate latent proteases from the granule matrix, allowing them to attack and destroy bacteria. Adapted from (Rada and Leto, 2008).

I.2.2. Macrophages

I.2.2.1. Biology and function of macrophages

The mononuclear phagocyte, macrophage, was originally discovered by Metchnikoff to have the ability to phagocytose. Macrophages are found in many different tissues throughout the body with diverse appearances and functions and known as resident macrophages (Wynn et al., 2013). They are produced in the yolk sac, the fetal liver and then by the bone marrow and distributed towards specific tissues during embryonic development and persisted in tissues until adulthood partly by self-renewal mechanism (depicted in figure 4-5) (Gautier et al., 2012; Ginhoux and Jung, 2014). From the functional aspect, macrophages are categorized in two main phenotypes M1 and M2 with different profiles of gene expressions, functions and general behaviors in response to infections or host homeostasis. Upon infections with gram-negative or gram-positive bacteria M1 macrophages express relatively similar transcriptional profiles of genes involved in pro-inflammation process, while M2 macrophages are reported to play important roles in the inflammation resolution, tissues repair and homeostasis by expressing anti-inflammatory genes (Benoit et al., 2008). Although having different mechanisms of activity, both functional M1 and M2 macrophages are crucial for the clearance of cellular debris and the control of inflammation and infections with bacteria or viruses. Macrophages perform their protective function through diverse modulations of sets of cytokines, chemokines and receptors. Mice deficient for TNF or IFN- γ , two of the important cytokines produced by M1 macrophages, or their respective receptors are susceptible to *Listeria monocytogenes* infection (Pfeffer et al., 1993). The intense inflammatory reaction promoted by uncontrolled expression of cytokines in macrophages is also fatal in certain conditions. In severe sepsis patients macrophages produce high level of type-1 cytokines which in turn induce death through heart arrest and block of perfusion (Bozza et al., 2007; Smith et al., 2007). As professional phagocytes, macrophages also act as antigen presenting cells (Hume, 2008; Koppensteiner et al., 2012).

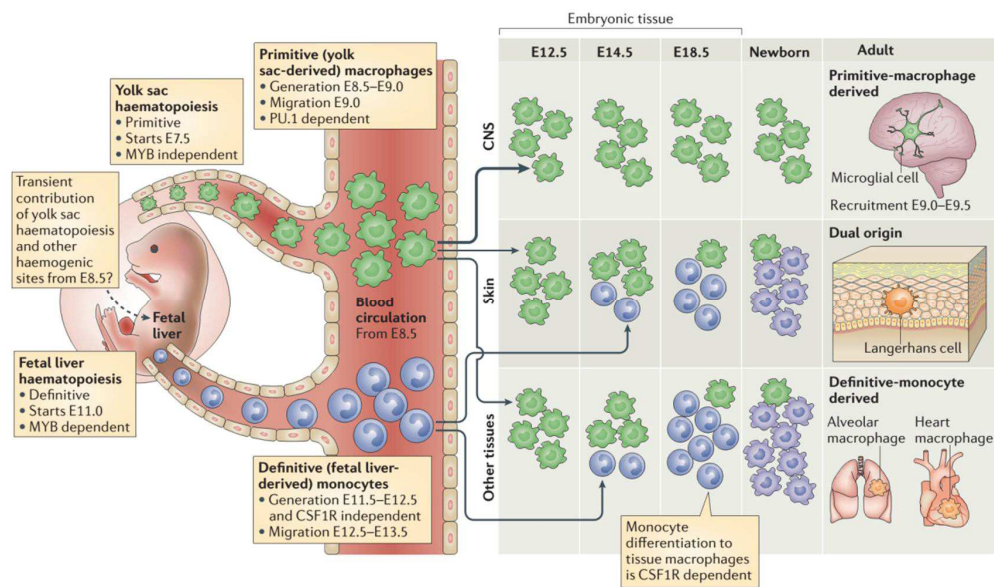


Figure 4: Embryonic macrophage development

Primitive haematopoietic progenitors generated in the yolk sac blood islands gives rise to primitive macrophages from embryonic day 8.5–9.0 (E8.5–E9.0). They populate embryos upon the formation of the blood circulatory system and colonize the whole embryo from E9.0–E10.0 to develop into fetal primitive macrophages. In parallel, definitive haematopoiesis occurs in the aorta–gonads–mesonephros (AGM) from E10.5 and is responsible for the generation of haematopoietic stem cells (HSCs) with multi-lineage haematopoietic potential, that give rise to progenitors that colonize the fetal liver. Haematopoiesis in the fetal liver generates monocytes around E11.5–E12.5 that migrate into the blood (E12.5–E13.5) and then invade embryonic tissues around E13.5–E14.5, a few days after yolk sac-derived macrophage colonization. Of note, yolk sac progenitors can also contribute to fetal liver haematopoiesis during the middle phase of embryonic development (from E8.5) and might contribute to the generation of fetal liver monocytes (dashed arrow). Once inside the tissues, fetal liver-derived monocytes proliferate and differentiate into macrophages and markedly dilute the population of yolk sac-derived macrophages as shown in the lungs and in the heart. Exceptions are the microglia, which arise predominantly from yolk sac-derived macrophages; and Langerhans cells, which mainly arise from fetal liver-derived monocytes but retain a detectable yolk sac-derived macrophage component. These recent findings reveal that the origin of adult macrophages in the steady state can vary considerably between tissues. Moreover, in the steady state, particular tissues — such as the skin and gut — contain adult monocyte-derived macrophages. CNS, central nervous system; CSF1R, colony-stimulating factor 1 receptor. Adapted from (Ginhoux and Jung, 2014).

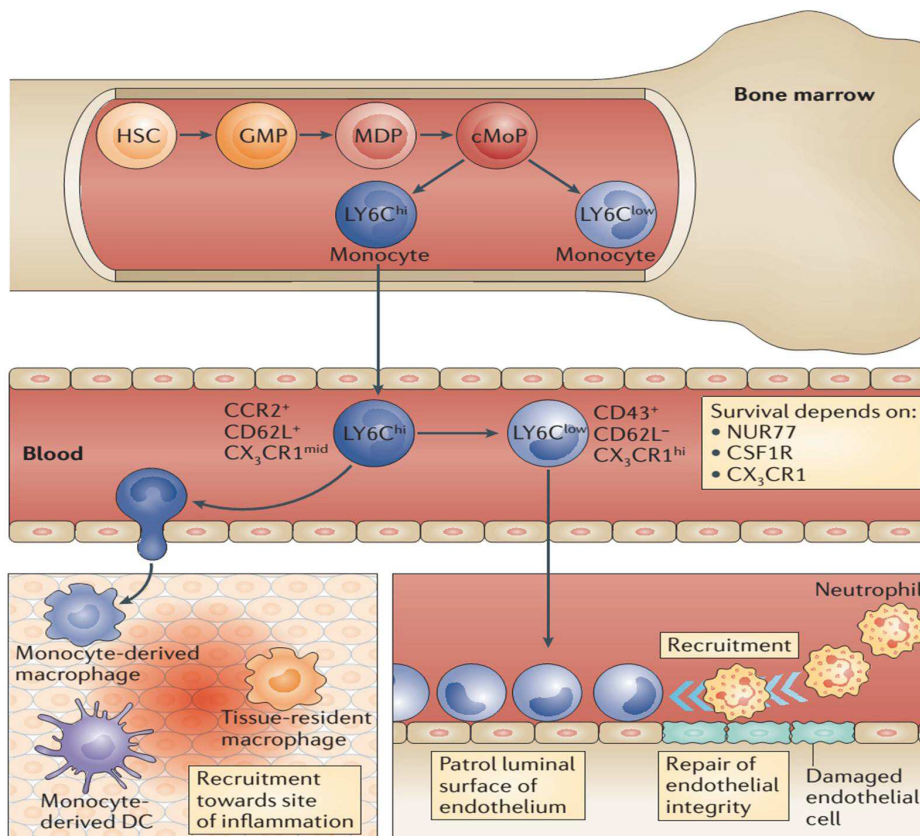


Figure 5: Monocyte-derived macrophage development

Monocytes are continuously generated in the bone marrow from haematopoietic stem cells (HSCs) via macrophage and dendritic cell (DC) precursor (MDP) and common monocyte progenitor (cMoP) intermediates. In the steady state, LY6C^{hi} and LY6C^{low} monocyte subsets in the circulation form a developmental continuum but are functionally distinct. Macrophage-like LY6C^{low} cells in the blood vessel lumen patrol the endothelial surface and coordinate its repair by recruiting neutrophils as required. LY6C^{hi} monocytes are rapidly recruited to sites of inflammation and sites of tissue remodeling, where they extravasate and can give rise to monocyte-derived DCs and monocyte-derived macrophages. Mouse LY6C^{hi} and LY6C^{low} cells are the equivalent of human CD14⁺ and CD14^{low}CD16⁺ monocyte subsets, respectively. CCR2, CC-chemokine receptor2; CSF1R, colony-stimulating factor 1 receptor; CX3CR1, CX3C-chemokine receptor1; GMP, granulocyte–macrophage progenitor. Adapted from (Ginhoux and Jung, 2014).

I.2.2.2. Mechanism of bacterial killing by macrophages

Besides the roles in tissue repair and cellular debris cleaning, tissue-resident macrophages guard the epithelial layer and actively join other professional phagocytes of the innate immune system to fight invading pathogens at the very early phase of attack (depicted in figure 6). To support phagocytosis, macrophages possess classes of pattern recognition receptors (PRRs) located on the extracellular- or intracellular- or vesical surface which help sense directly the pathogens through their pathogen-associated molecular patterns (PAMPS) on the bacterial surface such as peptidoglycans or lipoproteins and promote internalization of these bacteria into phagosomes. In some cases the foreign objects or the altered-self are opsonized by soluble PRRs and components of the complement system so that they would be recognized by other types of phagocytic receptors, for example Fc γ receptor (Fc γ R), complement C3 receptor (CR3), and internalized by the phagocytes (depicted in figure 7) (Litvack and Palaniyar, 2010; Weiss and Schaible, 2015). Upon contact with microbes, cascades of pro-inflammatory signals linked to PRRs are activated to promote production of other alarming molecules such as cytokines, chemokines and antimicrobial compounds. These signaling molecules such as interleukin-1b (IL1b), interleukin-6 (IL6), interleukin-8 (IL8), tumor necrosis factor alpha (TNFa) activate other phagocytes including neutrophils and promote recruitment of these leukocytes to join the fight at the site of infection (Arango Duque and Descoteaux, 2014; Kapetanovic et al., 2007). It is noted that the downstream signaling cascades of each PRR is activated differently for that particular PRR-mediated internalization. For Fc γ receptor for example, the pseudopod growing requires actin polymerization and is controlled by Rac1/2 plus the cell division control protein 42 (Cdc42) (Caron and Hall, 1998). In contrast, the CR3-mediated phagocytosis is regulated by interaction of diaphanous-related formin Dia1 and Ras GTPase-Activating-Like Protein IQGAP1 (Brandt et al., 2007).

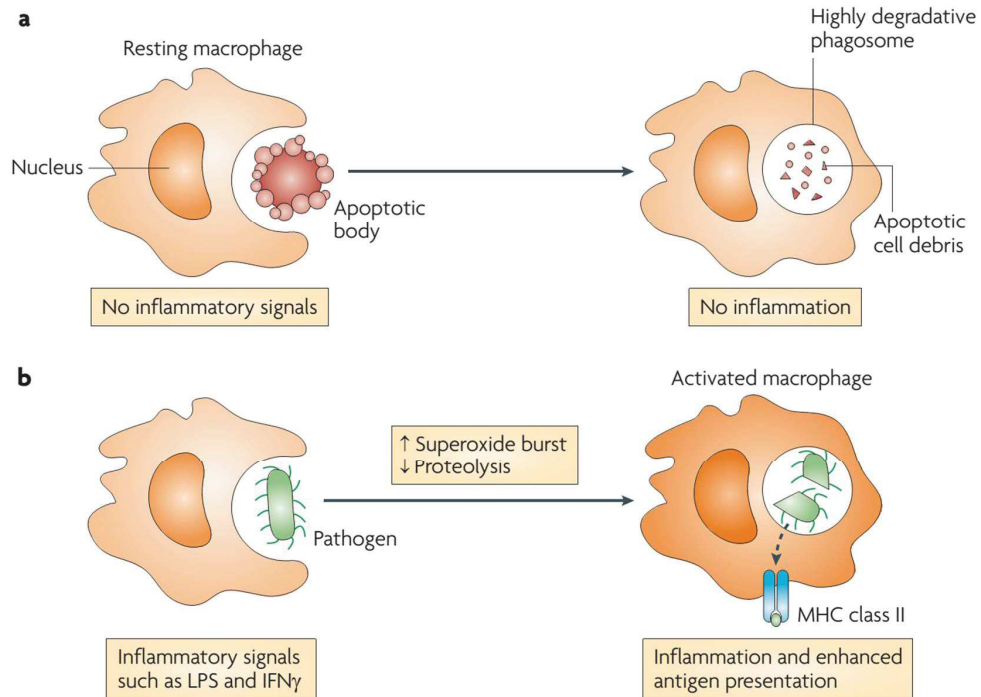


Figure 6: Phagocytic function of macrophages

The functions carried out by macrophages are modulated by their degree of stimulation by exogenous mediators, such as microorganism-derived Toll-like receptor (TLR) agonists, or endogenous activators, including cytokines and chemokines. **a** | resting macrophages function in the absence of any inflammatory stimuli and their primary role is to remove cellular debris such as apoptotic cells from the body. **b** | By contrast, macrophages activated by exposure to TLR agonists, such as lipopolysaccharide (LPS), or cytokines, such as interferon- γ (IFN γ), show alterations in several aspects of phagosome physiology. The superoxide burst is enhanced; microbial killing in activated macrophages relies on the production of reactive oxygen and nitrogen intermediates. Adapted from (Russell et al., 2009).



Following the phagocytosis, a phagosome carrying bacteria is translocated into the cytoplasm and matures through multiple interactions and fusions with endosomal and other vesical body, and eventually fuse with lysosomes for the degradation of the engulfed items (Zimmerli et al., 1996).

The interactions and fusions of the phagosome with cytoplasmic vesical compartments require involvements of different factors that first bring the fusing bodies close to each other and then bridge and join the compartments. This process is regulated by cytoplasmic effectors such as the family of Rab GTPases proteins and soluble N-ethylmaleimide-sensitive factor attachment protein receptor (SNARE) (Becken et al., 2010), During this process phagosomes become acidified to the low pH of 4-4.5, which is usually optimal for the activities of most lysosomal proteases.

Continuing accumulation and alteration the intracellular components result in maturation of phagosome which possessing a diverse sets of lytic oxidative compounds that are highly toxic and degradative to the trapped agents (Weiss and Schaible, 2015). However, some intracellular bacteria have developed strategies to survive in the phagosome of macrophages and eventually spread their infections systemically. Being engulfed in the macrophage *Salmonella Typhimurium* can modify its outer membrane to become more resistant to antimicrobial peptides and evade recognition by host (Ernst et al., 2001). The intracellular bacteria *Francisella tularensis* is able to survive macrophage killing by altering the maturation of its phagosome and accessing the host cell cytoplasm (Clemens et al., 2004).



Table 1: Receptors involved in the phagocytosis

Type of phagocytosis	Receptors	Ligands
Opsonic phagocytosis	Fc receptor family (FcγRI, FcγRIIA and FcγRIIA)	Antibody-opsonized targets
	Complement receptors (CR1, CR3 and CR4)	Complement-opsonized targets
	α5β1 integrin	Fibronectin
Non-opsonic phagocytosis	Dectin 1	β-glucan
	Macrophage receptor MARCO	Bacteria (undefined specific ligand)
	Scavenger receptor A	Bacteria (diverse charged molecules)
	αVβ5 integrin	Apoptotic cells
Triggered (nonspecific) phagocytosis	Toll-like receptors	Various, including lipopolysaccharides and lipopeptides

FcγR, Fc receptor for IgG (Underhill and Goodridge, 2012)

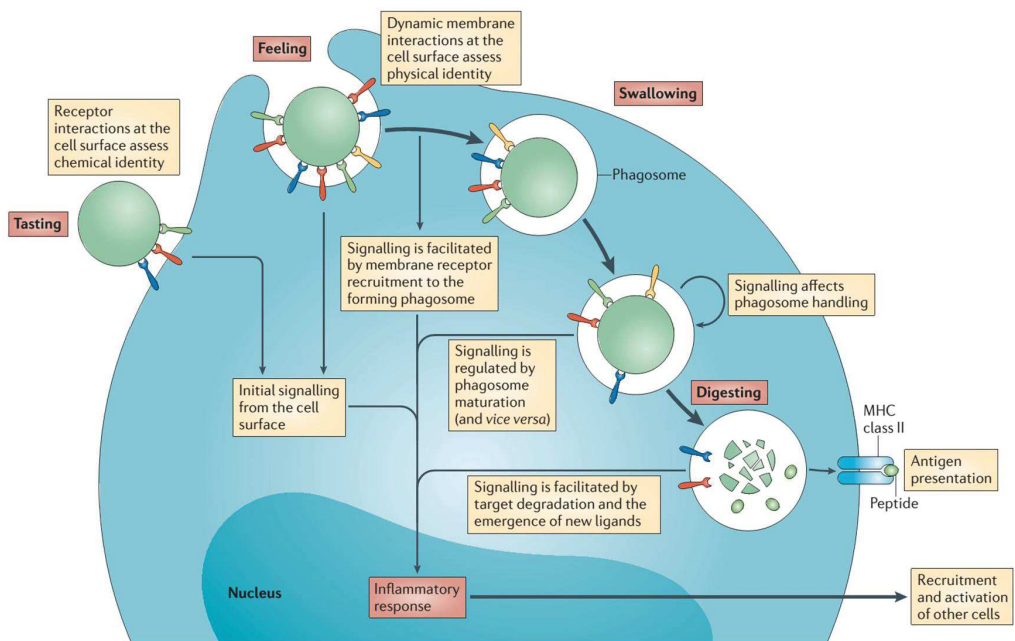


Figure 7: Process of the phagocytosis

As phagocytosis proceeds from the initial binding of a target to actin-dependent internalization and ultimately to degradation of the target in the phagolysosome, myeloid cells acquire information about the target through a variety of mechanisms. At the cell surface, receptors sample the chemical constituents of the particle and membrane dynamics facilitate an assessment of its physical properties. Additional information is gathered as the phagosome pinches off from the plasma membrane and as it matures through interactions with other intracellular compartments. Finally, the degradation of the target exposes ligands that were not previously accessible and releases ligands into the cytosol for detection by intracellular receptors. The information gathered by all of these processes is integrated to shape the ensuing immune response. MHC: major histocompatibility complex. Adapted from (Underhill and Goodridge, 2012).

I.3. ROS productions and functions

ROS are highly reactive oxygen-derived molecules produced by transmembrane multiprotein NADPH Oxidase complexes (NOXs) and DUOX enzymes that are present in many different cell types and tissues throughout the body. The NOX family comprises five isoforms named NOX1-NOX5 which work as electron transporters once assembled with other particular units such as p40, p47, p22^{phox} and Racs (depicted in figure 8). The DUOX enzymes encoded by *duox1* and *duox2* genes which found to be mostly expressed in thyroid (Bedard and Krause, 2007). While located on different chromosomes *Duox* genes share similar functional domain with *Noxs* in the conversion of oxygen into superoxide. While both *Duox1* and *Duox2* are highly expressed in thyroid, *Duox1* expression is also detected in respiratory epithelia and prostate, and *Duox2* found in gastrointestinal tract and rectal mucosa (De Deken et al., 2000; Dupuy et al., 1999; Forteza et al., 2005; Geiszt et al., 2003; Schwarzer et al., 2004). In recent years the most intensively studied species of ROS include superoxide anion, hydrogen peroxide, singlet oxygen and peroxynitrite, whose half-lives vary from milliseconds to seconds and hours in most biological processes with diverse and complicated functions (Bedard and Krause, 2007; Lushchak, 2014). Through NOX complexes, oxygen is converted into superoxide which subsequently reduced to hydrogen peroxide and other halide radicals by superoxide dismutase and peroxidase respectively (Fridovich, 1997). It is suggested that based on the concentrations in their microenvironments ROS have distinct biological functions in signaling, cell death, tissue homeostasis, inflammation and control of infections (Dupré-Crochet et al., 2013; Henrotin et al., 2003).

Hundreds of publications have revealed the wide spectrum of ROS productions and functions in many cell types and tissues. Their correct balances affect critically the regular function and physiology of the adipose tissue in response to insulin; the maturation of and function of spermatocytes; cardiovascular system, central nervous system, endocrine organs, gastrointestinal system, liver, kidney, urinary tract, lung and airways (Bedard and Krause, 2007; Mikkelsen and Wardman, 2003).

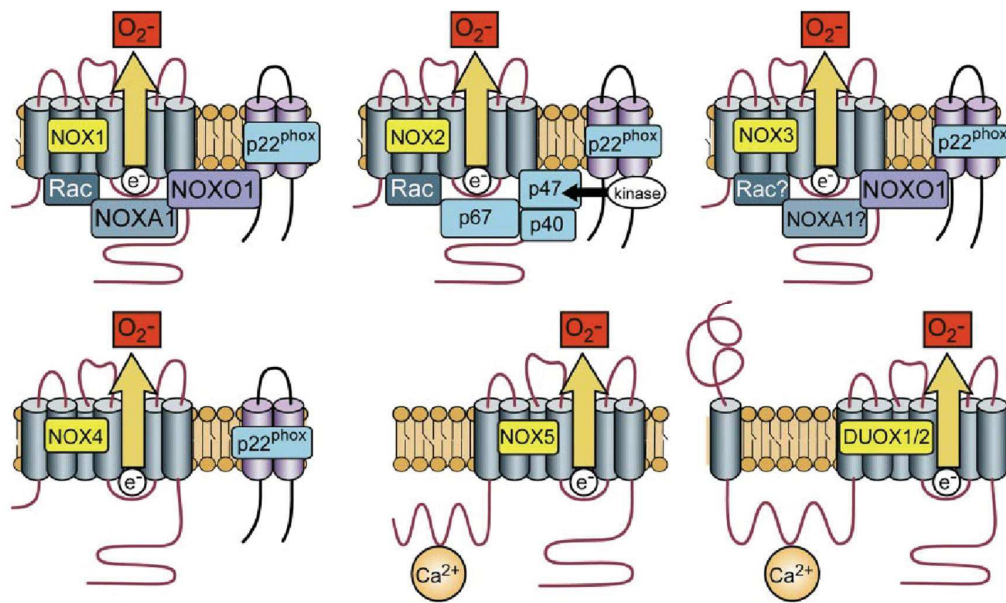


Figure 8: NADPH oxidase and DUOX isoforms

Despite their similar structure and enzymatic function, NOX family enzymes differ in their mechanism of activation. NOX1 activity requires p22^{phox}, NOXO1 (or possibly p47^{phox} in some cases) and NOXA1, and the small GTPase Rac. NOX2 requires p22^{phox}, p47^{phox}, p67^{phox}, and Rac; p47^{phox} phosphorylation is required for NOX2 activation. Although not absolutely required, p40^{phox} also associates with this complex and may contribute to activation. NOX3 requires p22^{phox} and NOXO1; the requirement for NOXA1 may be species dependent, and the requirement of Rac is still debated. NOX4 requires p22^{phox}, but in reconstitute systems it is constitutively active without the requirement for other subunits. However, in native NOX4-expressing cells, activation, possibly including Rac, has been described. NOX5, DUOX1, and DUOX2 are activated by Ca²⁺ and do not appear to require subunits. Adapted from (Bedard and Krause, 2007).



Table 2: NOX enzymes expression in different tissues

	High-Level Expression	Intermediate- to Low-Level Expression
NOX1	Colon	Smooth muscle, endothelium, uterus, placenta, prostate, osteoclasts, retinal pericytes
NOX2	Phagocytes	B lymphocytes, neurons, cardiomyocytes, skeletal muscle, hepatocytes, endothelium, hematopoietic stem cells, smooth muscle
NOX3	Inner ear	Fetal kidney, fetal spleen, skull bone, brain
NOX4	Kidney, blood vessels	Osteoclasts, endothelium, smooth muscle, hematopoietic stem cells, fibroblasts, keratinocytes, melanoma cells, neurons
NOX5	Lymphoid tissue, testis	Endothelium, smooth muscle, pancreas, placenta, ovary, uterus, stomach, various fetal tissues
DUOX1	Thyroid	Airway epithelia, tongue epithelium, cerebellum, testis
DUOX2	Thyroid	Salivary and rectal glands, gastrointestinal epithelia, airway epithelia, uterus, gall bladder, pancreatic islets

(adapted from (Bedard and Krause, 2007)

In the context of the bone, ROS are produced in osteoclasts, macrophage-like cells which function in bone resorption, and they play roles in osteoclast differentiation and activity (Lee et al., 2005; Yang et al., 2001). ROS production has also been found to cause matrix remodeling, cartilage degradation and inflammation of the articular joint tissues usually seen in osteoarthritis and rheumatoid arthritis (Henrotin et al., 2003).

In phagocytes ROS are generated, especially by NOX2, in response to infections. Patients with severe defect in the control of infection in chronic granuloma disease were found to lose oxidative burst activity due to mutations effecting the functional assemble of NOX complexes (Klebanoff, 2005; Stasia and Li, 2008). With the above observation, ROS were previously mentioned as effectors of bacterial killing. However, researchers also found that the neutrophils from CGD patients did not need NOX2 to clear many types of other bacteria (Winkelstein et al., 2000). While the presence of ROS is important for the control of many types of infection, their chemical interactions with diverse sets of granular compounds in phagocytes have been shown to contribute critically to the clearance of bacterial infections.



Upon bacterial infection, phagocytes engulf microbes into their phagosomes. During the phagosomal maturation, together with the delivery of other antimicrobial compounds, superoxide is massively produced by NADPH Oxidase complexes into the bacterial containing phagosomes. Superoxide together with H₂O₂, another ROS, are also the inputs of productions of other ROS such as singlet oxygen, ozone, hydroxyl radical which are essential for the bacterial killing and degradation in the direct manner (Rada and Leto, 2008; Robinson, 2008). Alternatively, Segal proposed that the high quantity of negatively charged superoxide released into the phagosome by NADPH Oxidase complexes must be compensated by ions; proton transferring into phagosome would in turn creates conductive electrophysiology which is deleterious to microbes (Segal, 2006). However, other hypotheses have suggested that the cooperation between superoxide and antimicrobial peptides seems instrumental for the bacterial killing (Slauch, 2011).

Recent studies have pointed out that, as the requirement of autophagy, ROS also have a function in the formation of NETs promote the translocations of Neutrophil Elastase (NE) and Myeloperoxidase (MPO) into the nucleus, these components subsequently induce de-condensation and fragmentation of the chromatin, a critical step in NETosis (Björnsdóttir et al., 2015; Papayannopoulos et al., 2010; Remijsen et al., 2011a; Remijsen et al., 2011b; Stoiber et al., 2015). Action mechanism of ROS are depicted in figure 9.

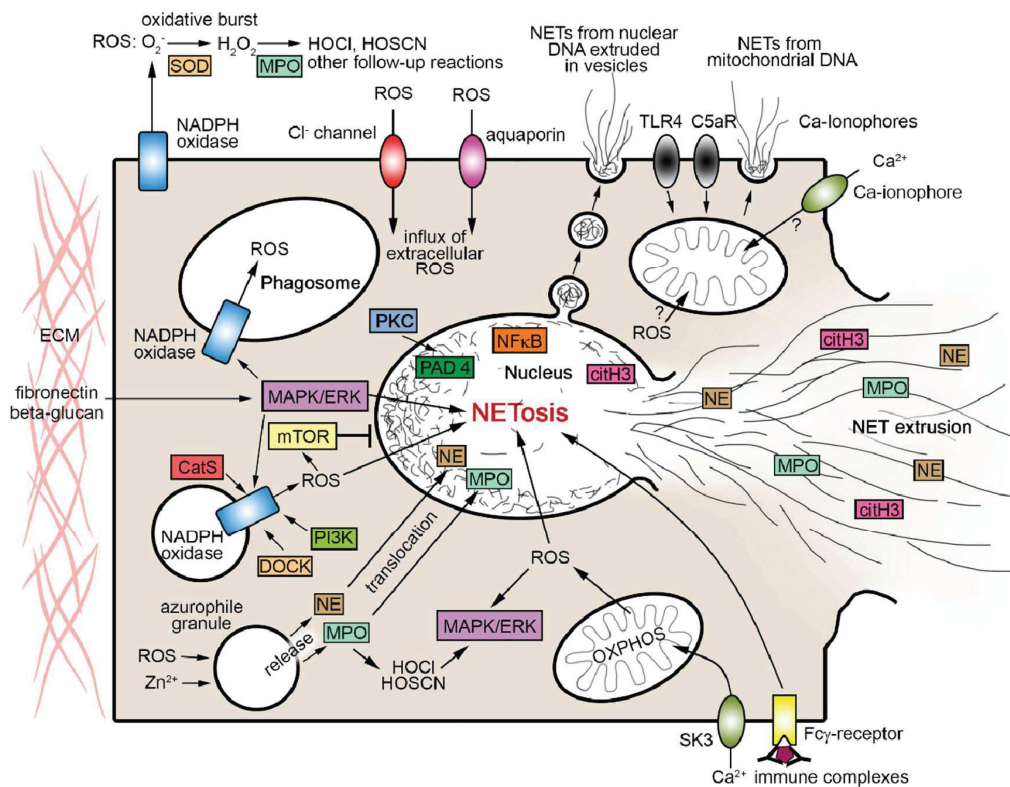


Figure 9: Distribution of ROS and their interactions with NETs formation

Arrows indicate directions of effects. Note that only some of the processes shown can co-occur. CatS cathepsin S; citH3 citrullinated histone H3; C5aR complement component 5a receptor; DOCK dedicator of cytokinesis proteins; HOCl hypochlorous acid; HOSCN hypothiocyanous acid; MAPK mitogen-activated protein kinases, ERK extracellular signal-regulated kinases, positive regulators of autophagy; PI3K phosphoinositide-3-kinase, mTOR mammalian target of rapamycin, negative regulators of autophagy and apoptosis; MPO myeloperoxidase; NE neutrophil elastase; NFκB nuclear factor kappa-light-chain-enhancer of activated B cells; OXPHOS oxidative phosphorylation; PAD4 peptidylarginine deiminase 4; PKC protein kinase C; SK3 small conductance calcium-activated potassium channel 3; SOD superoxide dismutase; TLR4 toll-like receptor 4. Adapted from (Stoiber et al., 2015).

I.4. Cytokines and immunoregulation

I.4.1. Resources and functions of cytokines

Cytokines are the extremely diverse group of small soluble proteins and glycoproteins whose functions are to transfer signaling messages from cells to cells throughout the body, which help regulate the host immune activity, tissue homeostasis and hematopoiesis in both physiological and pathological conditions (Foster, 2001).

The general acting mechanism of cytokines is their pleiotropic bindings to transmembrane receptors which in turn trigger cascades of intracellular reactions leading to downstream modifications in gene expression patterns. Cytokines can act autonomously (autocrine), on the neighboring cells (paracrine), or on the cells at a distance (endocrine). Functionally, depending on particular stimulating signals different cytokines might have stimulatory or inhibitory effects and synergistic or antagonistic effects (Matsumoto and Kanmatsuse, 2000).

Many types of cells may produce cytokines including immune cells, kidney cells, liver cells and fibroblasts. However, the main sources of cytokines are epithelial cells, leukocytes and lymphocytes. According to their functions and origins cytokines are known by other names such as lymphokine, which is produced by lymphocytes; monokine, produced by monocytes; interleukin, produced by leukocytes; chemokine, having chemotactic property. Their expressions are strictly and dynamically regulated when host encounters stimulating signals from for example infection, trauma, injury, cancer and physiological disorder (Hanada and Yoshimura; Orman et al., 2011). Accumulating evidence has disclosed the functions of cytokines in many different pathological conditions such as neurodegeneration, cancer, hepatocellular injury, cirrhosis, neoplasia, hematopoiesis disorders, infectious and inflammatory diseases (Elenkov et al., 2005; Lucey et al., 1996; Martins et al., 2010; O'Shea et al., 2002). Function, production, classification and receptors of some known cytokines are depicted in figure 11, table 3 and table 4.

Table 3: Cytokines production and function

Cytokines		Main sources	Target cell	Major function
Interleukins	IL-1	Macrophages, B cells, DCs	B cells, NK cells, T-cells	Pyrogenic, proinflammatory, proliferation, differentiation, BM cell proliferation
	IL-2	T cells	Activated B-and T-cells, NK cells	Proliferation and activation
	IL-3	T cells, NK cells	Stem cells	Hematopoietic precursor proliferation and differentiation
	IL-4	Th cells	B cells, T cells, macrophages	Proliferation of B and cytotoxic T cells, enhances MHC class II expression, stimulates IgG and IgE production
	IL-5	Th cells	Eosinophils, B-cells	Proliferation and maturation, stimulates IgA and IgM production
	IL-6	Th cells, macrophages, fibroblasts	Activated B-cells, plasma cells	Differentiation into plasma cells, IgG production
	IL-7	BM stromal cells, epithelial cells	Stem cells	B and T cell growth factor
	IL-8	Macrophages	Neutrophils	Chemotaxis, pro-inflammatory
	IL-9	T cell	T cell	Growth and proliferation
	IL-10	T cell	B cells, macrophages	Inhibits cytokine production and mononuclear cell function, anti-inflammatory
	IL-11	BM stromal cells	B cells	Differentiation, induces acute phase proteins
	IL-12	T cells	NK cells	Activates NK cells
TNFs	TNF- α	Macrophages	Macrophages	Phagocyte cell activation, endotoxic shock
	TNF- β	Monocytes, T-cells	Tumour cells, Phagocytes	Tumour cytotoxicity, cachexia, Chemotactic, phagocytosis, oncostatic, induces other cytokines
interferons	IFN- α	Leukocytes	Various	Anti-viral
	IFN- β	Fibroblasts	Various	Anti-viral, anti-proliferative
	IFN- γ	T-cells	Various	Anti-viral, macrophage activation, increases neutrophil and monocyte function, MHC-I and -II expression on cells
CSF	G-CSF	Fibroblasts, endothelium	Stem cells in BM	Granulocyte production
	GM-CSF	T cells, macrophages, fibroblasts	Stem cells	Granulocyte, monocyte, eosinophil production
	M-CSF	Fibroblast, endothelium	Stem cells	Monocyte production and activation
	Erythropoietin	Endothelium	Stem cells	Red blood cell production
Others	TGF- β	T cells and B cells	Activated T and B cells	Inhibit T and B cell proliferation, inhibit haematopoiesis, promote wound healing

BM, bone marrow; DCs, dendritic cells; G-CSF, granulocyte-colony stimulating factors; M-CSF, macrophage colony stimulating factor; Th, T helper cells; TNFs, Tumour Necrosis Factors. Adapted from (Turner et al., 2014).

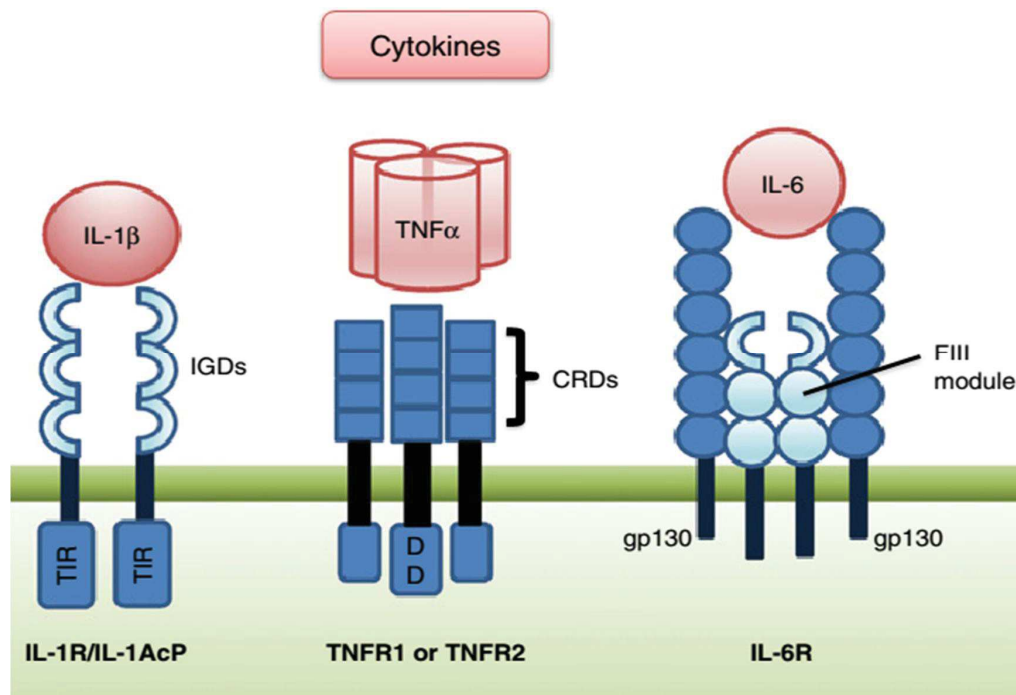


Figure 10: Some cytokines and their receptors

Cytokines signal via oligomers of single-pass, type I transmembrane receptors, with distinct extracellular domains for ligand binding and intracellular domains that allow signal transduction. The receptor for IL-1 is a complex of IL-1R1 and the IL-1 receptor accessory protein (IL-1RAcP) formed following ligand binding to the extracellular immunoglobulin domains (IGDs); intracellular signaling is mediated via the Toll/IL-1R (TIR) domain. Trimeric TNF α binds to the cysteine-rich domains (CRDs) of the pre-assembled trimers of the TNF receptor (TNFR) and signaling is mediated via the receptor's death domain (DD). Finally, the IL-6R is a multimeric structure with IL-6R chains complexed with gp130. The ligand-binding region is within the fibronectin III (FIII) modules of the IL-6R chains but signal transduction is via the associated gp130 molecules. Adapted from (Turner et al., 2014).

I.4.2. Roles of cytokines during infection and inflammation

Cytokines are dynamically expressed by variety of immune cells, and also epithelial cells in response to infectious agents or inflammatory stimuli. Very quickly following the onsets of infection or inflammation a primary set of cytokines is transcribed to mount the inflammation called pro-inflammatory cytokines. At the later phase another set of cytokines is produced to resolve the inflammation known as anti-inflammatory cytokines.

The best characterized pro-inflammatory cytokines, including interleukin-1 family (IL-1), interleukin-6 family (IL-6), interleukin-17 (IL-17), interleukin-18 (IL18), Tumor Necrosis Factor alpha (TNF α), interferon gamma (IFN γ) and set of chemokines such as G-CSF, GM-CSF, Eotaxin, MCP-1 (CCL2), MIP-1 (CCL3) etc., promote inflammation by sending out signals to stimulated and/or guide the recruitments of immune cells and other effectors to the site of infection to help control the infection. In the case of severe infections, the recruited cells then also actively produce large amount of pro-inflammatory cytokines to attract more innate immune components to the inflammatory foci.

After clearing the infecting agents or danger signals immune cells at the inflammatory foci change their programs to produce anti-inflammatory cytokines including interleukin-4 (IL-4), interleukin-10 (IL-10), interleukin-13 (IL-13) etc., to stop the recruitment of immune cells, promote inflammation resolution and tissue healing. The modulations of pro-inflammatory and anti-inflammatory cytokines are strictly controlled. However, very often they have time-overlapping of their expressions; also some cytokines have both pro- and anti-inflammatory effects such as interleukin-4, interleukin-6 (Scheller et al., 2011; Seruga et al., 2008; Van Kampen et al., 2005).

The correct productions of cytokines are critical in many infectious and inflammatory diseases. Patients with Inflammatory Bowel Disease (IBD) or Rheumatoid arthritis (RA) who have imbalance between pro-inflammatory and anti-inflammatory cytokines usually experience serious damages caused by chronic inflammations. In case of RA the uncontrolled prolonged expression of pro-inflammatory cytokines especially TNF α and interleukin-1 β leads to severe

destruction of cartilage and loss of the bone (Baum and Gravallesse, 2014; Neurath, 2014; Schett, 2011; Schuerwegh et al., 2003) .

Upon infections with pneumococcus or influenza virus cytokines appear to have important role for the outcome of infections. First they are produced with other chemokines as a network to regulate the inflammation by activating the recruited neutrophils. The activated neutrophils then produce microbicides such as reactive oxygen species, defensins, proteolytic enzymes, myeloperoxidase etc., to control the infections. It is observed in many cases that the above cytotoxic agents from neutrophils might be massively released into the extracellular microenvironment and cause devastating damages to host tissues by the overstimulation of pro-inflammatory cytokines (Barnes, 2008; Bordon et al., 2013; Goodman et al., 2003).

Table 4: Classification of cytokines by immune responses

Function	Family	Members
Adaptive Immunity	Common γ chain receptor ligands	IL-2, IL-4, IL-7, IL-9, IL-15, IL21
	Common β chain (CD131) receptor ligands	IL-3, IL-5, GM-CSF
	Shared IL-2 β chain (CD122)	IL-2, IL-15
	Shared receptors	IL-13, IL-13R-IL-4R complex
TSLP (TSLPR-IL-7R complex)		
Pro-inflammatory signaling	IL-1	IL-1 α , IL-1 β , IL-1RA, IL-18, IL-33, IL-36 α , IL-36 β , IL-36 γ , IL-36RA, IL-37, IL-1Hy2
	IL-6	IL-6, IL-11, IL-31, CNTF, CT-1, LIF, OPN, OSM
	TNF α	TNF α , TNF β , BAFF, APRIL
	IL-17	IL-17A-F, IL-25 (IL-17E)
	Type I IFN	IFN α , IFN β , IFN ω , IFN κ , Limitin
	Type II IFN	IFN γ
	Type III IFN	IFN λ 1 (IL-29), IFN λ 2 (IL-28A), IFN λ 3 (IL-28B)
Anti-inflammatory signaling	IL-12	IL-12, IL-23, IL-27, IL-35
	IL-10	IL-10, IL-19, IL-20, IL-22, IL-24, IL-26, IL-28, IL-29

TSLP: Thymic Stromal Lymphopietin; CNTF: ciliary neurotrophic factor; CT-1: cardiotrophin-1; GM-CSF: granulocyte macrophage-colony stimulating factor; IFN: interferon; LIF: leukaemia inhibitory factor; OPN: osteopontin; OSM: oncostatin M; TSLP, thymic stromal lymphopietin; BAFF: B cell activating factor; APRIL : a proliferation inducing ligand. Adapted from (Turner et al., 2014).

I.4.3. Targeting cytokines as therapeutics of inflammatory diseases

Thanks to the understandings of cytokine-receptor interaction mechanisms many cytokine-based therapeutics have been developed rapidly over the past decades. The treatment formulation is based on the seemingly simple strategies which are either to suppress or induce the ligand or/and receptor expressions, or to inhibit the interaction between them by antagonistic molecules or antibodies.

Since the onset of this application in 1960s recombinant cytokines have been successfully produced and used in clinics; exemplified as the utilizations of colony stimulating factors to induce granulopoiesis in patients suffering neutropenia during the course of chemotherapy, or of recombinant interferons as treatments for chronic hepatitis and osteosarcoma (Garcia-Carbonero et al., 2001; Gresser et al., 1969; Müller-Redetzky et al., 2015; Vilcek and Feldmann, 2004).

Treatment of Rheumatoid arthritis (RA) by blocking TNF activity with monoclonal antibodies and recombinant TNF receptor has been demonstrated to be effective. However, the recent data have marked the inefficacy and failure in response to certain TNF antagonists (Emery, 2012; Rubbert-Roth and Finckh, 2009; Solau-Gervais et al., 2006). Interleukin-1 and Interleukin-6 antagonists have also been developed for treatments of RA and other autoimmune and chronic inflammatory diseases (Hennigan and Kavanaugh, 2008; Jones and Moreland, 1999; Krishnan, 1999; Tanaka and Kishimoto, 2012). The combination therapy using antagonists of both cytokines TNF and IL-1 appeared to have higher curing efficacy by preventing bone erosion and cartilage damage (Zwerina et al., 2004).

I.5. Characteristics and functions of inflammation

In mammal the immunity plays indispensable function in orchestrating host adaptation to harmful stimuli such as infection and tissue injury, by employing a fundamental mechanism called inflammation. The inflammatory response is usually ignited when components of the immune system encounter immunogenic signals from exogenous origins such as microbes, microbial remnants, allergens, irritants, toxic compounds; or signals from endogenous physiopathological disorders like cancer metastasis, tissue injury, trauma, cell death. However, the current knowledge reveals some inflammations occur with unknown causes like the case of Rheumatoid arthritis (Barton, 2008; Dinh et al., 2014; Medzhitov, 2008; Rock and Kono, 2008; Rodrigues Viana et al., 2015). Few characteristics of inflammation are simplified below in figure 11.

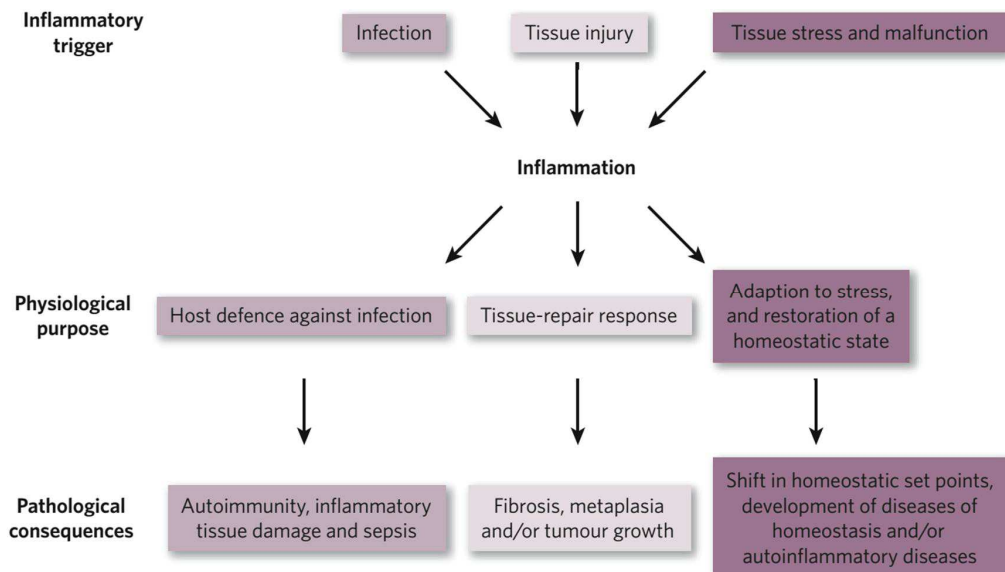


Figure 11: Causes, physiopathology and outcomes of inflammation

Depending on the triggers, the inflammatory response has a different physiological purpose and pathological consequences. Of the three possible initiating stimuli, only infection induced inflammation is coupled with the induction of an immune response. Adapted from (Medzhitov, 2008).

During the course of inflammation many different types of effectors of immunity, including neutrophils, macrophages, eosinophils, basophils, T cells, B cells platelets, and components of the complement system are recruited, activated, and produced to support the host protection and destruction of harmful interferences as well as the tissue healing (Hamann, 2000; Kolaczowska and Kubes, 2013a; Lalor et al., 2002; Shenoy et al., 2012).

Granulocytes such as neutrophils and eosinophils are reported to come first to the sites of inflammation for dealing with threatening agents. After cleaning the risks these leukocytes subsequently shutdown the alarm signals in a tightly controlled manner to stop recruitment of other effectors and undergo apoptosis and eventually promote resolution. Although being recruited later macrophages also crawl to the inflammation site and contribute important aspects of inflammatory resolution and tissue homeostasis normalization (Aggarwal et al., 2014; Maskrey et al., 2011; Serhan et al., 2007). This regulated program shortens the acute inflammation leading to less damage to the inflamed tissues. On the other hand, many serious diseases such as pulmonary fibrosis, Crohn's disease, and rheumatoid arthritis have been documented to be the results of uncontrolled prolonged inflammatory responses and denoted as chronic inflammation.

The causes of chronic inflammation in some cases are unknown. However, besides the massive recruitments of leukocytes, it includes the participation of other cell populations such as B cells and T cells. All these cells together are reservoir of uncontrolled productions of pro-inflammatory cytokines and chemokines which continuously promote inflammation and cause severe defects to host tissue at the site of inflammation (Chimen et al., 2015; Karmakar et al., 2010; Lalor et al., 2002; McInnes and Schett, 2007; Pène et al., 2008).

Upon both acute and chronic inflammations the host experiences some common symptoms such as fever, redness, swelling, pain, destruction and loss of functions of the inflamed tissues. Acute inflammations associated with infections have also been reported in number of patients with compromised immunities (Karin et al., 2006; Lawrence et al., 2002; Wright et al., 2001).

II. Zebrafish model for study of host-pathogen interaction

II.1. Zebrafish biology and experimental advantages

Danio rerio (zebrafish) is a small tropical freshwater fish native to Southeast Asia. Zebrafish was first used by Dr Georges Streisinger at University of Oregon in the late 1960s as he was trying to establish new vertebrate model for laboratory research. With many dominant advantages such as extremely rapid development, cost-effective husbandry, optical transparency of young embryo, easy genetic manipulation, zebrafish has been widely exploited by researchers worldwide as an excellent model to study vertebrate development. Its advantages have now been recognized in a wide variety of scientific fields, and it is used to establish research models of many human diseases (e.g. infections, immune responses, cancers, physiopathology, genetic disorders) and for high throughput drug screenings, (Dooley, 2000; Kar, 2013; Lieschke and Currie, 2007; Patton et al., 2014; Renshaw et al., 2006; Torraca et al., 2014; Ablain and Zon, 2013; Patton et al., 2014). However, some limitations are worth considering when using this model to

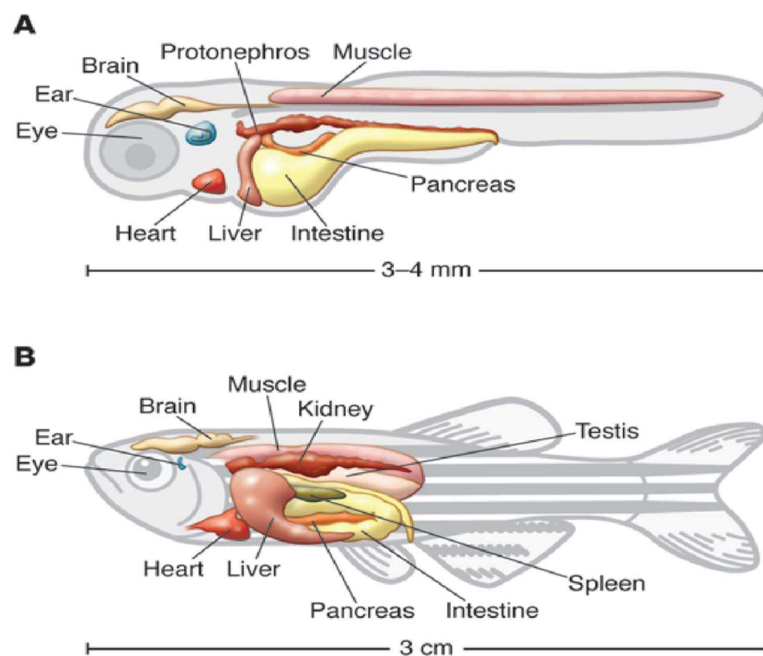


Figure 12: Zebrafish. Most organs are functionally formed at larval stage

A: Larva at 3-5 days post fertilization; B: Adult. Adapted from (Santoriello and Zon, 2012).

mimic human infectious diseases. One important example is the difference between fish housing temperature and the optimal temperature for human bacteria.

II.2. Zebrafish immune system

Protection from foreign invasion by the immune system is crucial for host survival and homeostasis. The immune system is remarkably well conserved in vertebrates from bony fish to human with the innate branch including the complement system and the adaptive branch (Amatruda and Zon, 1999; Hu et al., 2010; Trede et al., 2004).

At the early phase of embryonic development, like in mammal, zebrafish blood cells including erythrocytes and macrophages are produced by a primitive wave that is followed by a definitive wave of hematopoiesis (Davidson and Zon, 2004; Lieschke, 2001). The main difference between mammals and the zebrafish is the absence of lymphoid organs in the later. The primary lymphoid organ of mammals, the bone marrow is absent in fish. In fish, the primary lymphoid organ is the kidney (Ma et al., 2011; Murayama et al., 2006; Song et al., 2004).

Cells of the innate immune system such as macrophages and neutrophils are produced very early at the first day after fertilization by the primitive wave of hematopoiesis. Definitive hematopoiesis is initiated at about 30hpf by the emergence of hematopoietic stem cells from the ventral wall of the aorta. These stem cells migrate to the Caudal Hematopoietic Tissue (transient hematopoietic tissue) before to colonize the definitive hematopoietic tissue, the kidney. This definitive hematopoiesis will give raise to all blood cells including erythrocytes, lymphocytes and all myeloid cells (macrophages, neutrophils, dendritic cells, eosinophils, mast cells) (Balla et al., 2010; Herbomel et al., 1999; Lieschke, 2001; Lugo-Villarino et al., 2010). At 4 days post fertilization (dpf) components of the adaptive system could be detected: precursor T-cells expressing *recombinant activating gene 1 (rag1)* and *ikaros*. However, the full function of adaptive immunity has been reported at two to four weeks after the fertilization (Georgopoulos et al., 1997; Kissa et al., 2008; Langenau et al., 2004; Schorpp et al., 2006).

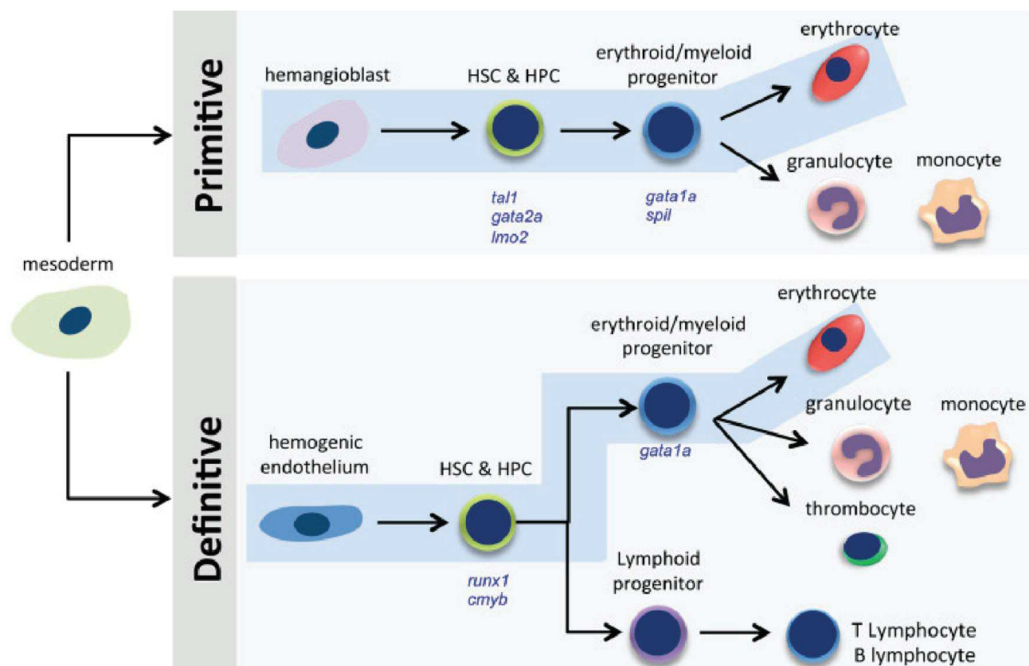


Figure 13: Scheme of primitive and definitive hematopoiesis during zebrafish embryogenesis

After gastrulation, hemangioblasts in the intermediate cell mass differentiate into either primitive hematopoietic stem cells (HSCs) and hematopoietic progenitor cells (HPCs) or vascular endothelial cells. Primitive HSCs and HPCs give rise to erythrocytes, granulocytes, and macrophages. For definitive hematopoiesis, HSCs and HPCs emerge from hemogenic endothelial cells lining the ventral wall of dorsal aorta in the aorta-gonad-mesonephros (AGM)-like region. These stem cells then enter the circulation and colonize to the caudal hematopoietic tissue, thymus, and pronephros (kidney), where they differentiate into erythroid/myeloid progenitors or lymphoid progenitor, and subsequently further differentiate into the indicated cell types. Transcription factors critical for HPCs and erythroid/myeloid progenitor cells are shown in blue in italics. *cmyb*, transcription factor cmyb; *csf1ra*, colony-stimulating factor 1 receptor a; *gata1a*, GATA-binding protein 1a; *gata2a*, GATA-binding protein 2a; *runx1*, runt-related transcription factor 1; *spi1*, spleen focus-forming virus proviral integration oncogene spi1; *tal1*, T-cell acute lymphocytic leukemia. Adapted from (Kulkeaw and Sugiyama, 2012).

II.3. Innate immune response to bacterial infection

II.3.1. Innate immune response

During the first week of embryonic development the adaptive arm of the immunity is not yet active, and the young larva relies solely on the innate immune system. Zebrafish larva possesses highly conserved innate immunity which comprises of different cell types as found in mammals such as neutrophils, eosinophils, macrophages, dendritic cells. These granulocytes and phagocytes express classes of membrane and soluble receptors which recognize microbial-associated molecular patterns (MAMPs) from microbes, and in turn trigger cascades of signaling and cytoskeleton modification to facilitate the engulfment of infectious agents (Levraud et al., 2007; Mostowy and Shenoy, 2015; van der Vaart et al., 2012; Varela et al., 2012).

The pattern recognition receptors (PRRs) of zebrafish phagocytes are diversely present on both cellular and phagosomal membranes including Toll-like receptor family (TLRs), Nod-like receptors (NLDs) respectively, and other soluble receptors like that of mammalian counterpart. In particular, some other non-mammalian TLRs have also been discovered in fish for example the soluble forms of TLR4 and TLR5 (sTLR4, sTLR5), TLR19, TLR20, TLR21, TLR22 and TLR23 (Jault et al., 2004; Palti, 2011; Quiniou et al., 2013). Although most TLRs are known for their ligands and functions, these novel receptors as well as the extra copies of the mammalian orthologs are somehow unclear for their interacting partners or signaling transduction mechanisms.

Upon infection leukocytes of the innate immunity also express extracellular messenger molecules especially the cytokines, chemokines and reactive oxygen species to mount the inflammation, a crucial process that facilitates the bacterial clearance and tissue homeostasis (Henrotin et al., 2003; Nguyen-Chi et al., 2014; Olavarría et al., 2010). At the site of inflammation neutrophils and macrophages are abundantly recruited and they phagocytose the bacteria. However, in some particular locations of infection these two phagocytes behave differently. Studies have shown that in the case of *E. coli* infection neutrophils are very efficient at clearing surface associated microbes in a

“vacuum-cleaner”-like behavior while macrophages are very efficient at engulfing microbes in the body fluids context using a “flypaper” strategy (Colucci-Guyon et al., 2011; Le Guyader et al., 2008; Nguyen-Chi et al., 2014).

While being instrumental in bacterial clearance and tissue physiological control, inflammatory responses in many cases are found destructive when recruited leukocytes, neutrophils in particular, become highly and uncontrolledly activated. Devastating symptoms are often seen in chronic inflammatory diseases of the lung or bone and joints of patients with pulmonary fibrosis or arthritis respectively (Karmakar et al., 2010; Wright et al., 2001). Furthermore, some pathogens use phagocytes as reservoirs and replicative niches for multiplication and dissemination (Mastroeni et al., 2009; Suzuki and Sasakawa, 2001; Vergunst et al., 2010).

II.3.2. Main effectors of zebrafish innate immunity

Zebrafish has a blood cell production mechanism similar to that of mammal which includes both primitive and definitive wave hematopoiesis (Paik and Zon, 2010; Warga et al., 2009). The professional phagocytes of the innate immune system, mainly neutrophils and macrophages, possess highly conserved functions and antimicrobial arsenals. These characteristics are important to the effectiveness of the innate immune responses (Elks et al., 2014; Nguyen-Chi et al., 2014; Palić et al., 2007).

II.3.2.1. Neutrophils

Zebrafish neutrophils have similar morphology and behavior to their human counterparts (Harvie and Huttenlocher, 2015; Lieschke et al., 2001). Early in the first day of fertilization neutrophils are produced from the primitive hematopoiesis in the yolk sac. They have the same origin as that of primitive macrophages (Le Guyader et al., 2008). During the later stage of development neutrophils are produced by definitive hematopoiesis that is initiated by the emergence of Hematopoietic Stem Cells in a region called the Aorta Gonad Mesonephros (AGM), their migration to the Caudal Hematopoietic Tissue (CHT) for maturation and then their colonization of Thymus and Kidney (Davidson and Zon, 2004; Murayama et al., 2006).

Like human granulocytes, zebrafish neutrophils are abundant and crucial for fighting infections by using wide range of conventional granular microbicides such as myeloperoxidase (Mpo), proteases, antimicrobial peptides (Henry et al., 2013; Leischke 2001). They also contain the NADPH Oxidase machinery that helps generate reactive oxygen species (Brothers et al., 2011). While being capable of sensing and engulfing pathogens, neutrophils isolated from kidney are also found to attack microbes extracellularly by releasing neutrophil extra cellular traps (NETs) (Palić et al., 2007). Transgenic reporter lines such as *tg(mpx:GFP)* and *tg(lyz:DsRed)* with fluorescently labelled neutrophils are helpful tools to study the *in vivo* behavior of these leukocytes in real time upon infection (Hall et al., 2007; Renshaw et al., 2006). In humans, neutrophils often become apoptotic after being activated at the inflammation site. Interestingly, most neutrophils of zebrafish were witnessed to skip apoptosis after the resolution of tail wound inflammation; instead, they reversely migrate away from the injured tail fin while maintaining their activated states and are able to phagocytose the *Staphylococcus aureus* infected at the other site of the larva (Ellett et al., 2015; Robertson et al., 2014). This highlights that zebrafish neutrophils do not behave exactly like human neutrophils; probably their life span is a major difference. Chronic inflammations with prolonged recruitment and activation of neutrophils, as seen in models of inflammatory bowel diseases and notochord infection, cause serious damages to the local tissues (Fleming et al., 2010; Nguyen-Chi et al., 2014).

II.3.2.2. Macrophages

In zebrafish macrophages are the first immune cells of the primitive hematopoiesis which arise in the yolk sac as early as 16 hours post fertilization. These cells then migrate to colonize specific tissues where part of them becomes highly differentiated into tissue resident macrophages with distinct functions as seen in mammal resident macrophages (Herbomel et al., 1999; Le Guyader et al., 2008). The other portion of macrophage remains less differentiated but functionally mature. These cells scatter to patrol throughout the body of embryo. The primarily produced macrophages at the early embryonic stage migrate and set their positions in brain and retina and further differentiate into resident macrophages called microglial cells. Zebrafish

microglial cells have highly ramified morphology as seen in the microglia of mammal (Morsch et al., 2015; Svahn et al., 2013). After populating brain and retina other macrophages set their fates to other tissues. Osteoclast-like cells which function as regulator of the bone development have also been described in zebrafish embryos (Chatani et al., 2011; Sharif et al., 2014).

The inflammatory macrophages with active transcription of macrophage expressed gene 1 (*mpeg1*) are most abundant among macrophage population in zebrafish embryo. These cells together with neutrophils are the main phagocytes to come to the infection and inflammation sites. The dynamic role and behavior of macrophages during infections have been widely investigated *in vivo* thanks to the release of *mpeg1*-driven fluorescent reporter transgenic lines (Ellett et al., 2011; Torraca et al., 2014). Upon notochord infection with *E. coli* macrophages are massively recruited to the site of infection. Interestingly, they remain persistently up to five or seven days post infection while the bacteria have been eliminated within the first day after the bacterial injection. In another study using double transgenic embryos *tg(mpeg1:mCherry/tnfa:GFP)* macrophages were shown to switch their stages in a timely manner from M1-like to M2-like macrophages when being recruited to the tail fin inflammation model (Nguyen-Chi et al., 2015). Revelation of zebrafish macrophages polarity vividly confirmed the previously described phenomenon found in mouse and human (Italiani and Boraschi, 2014; Mills and Ley, 2014; Stöger et al., 2012).

Phagocytosis of apoptotic cells and promotion of inflammation resolution are also featured in zebrafish macrophages. Likewise, macrophages have critical functions in tissue repair and regeneration. Depletion of macrophages was found to affect the resolution of inflammation and tail fin regeneration of zebrafish (Li et al., 2012; Petrie et al., 2014; van Ham et al., 2012).

Like other immune cells macrophages are susceptible to certain highly pathogenic bacteria. They are for example hijacked and killed by *Pseudomonas aeruginosa* and *Burkholderia cenocepacia*. These bacteria eventually disseminate to the whole body after escaping the infected macrophages (Belon et al., 2015; Vergunst et al., 2010).

II.3.3. Signalling modulations of innate immune response

Sensing and migrating to the sites of infection or injury of phagocytes need signaling messages. In most cases the information is transferred by diffusible cytokines, chemokines and reactive oxygen species.

II.3.3.1. Cytokines

Cytokines in fish are also small secreted proteins which act mainly as guiders for cell migrations in both normal physiological and pathological conditions. Accumulating data on cytokines and chemokines have been documented for the last two decades with differences when compare fish cytokines to those of human and even within fish species. Most cytokines have not been well characterized in zebrafish (Bird and Tafalla, 2015; DeVries et al., 2005). However, number of them present conserved functional properties as well as related signaling pathways (van der Vaart et al., 2012; Yeh et al., 2013).

While the main functions of most cytokines are to orchestrate the host immune responses to the variety of microbes, which are omnipresent in the aqua environment, some cytokines play important roles in the embryonic development (Candel et al., 2014; Harrison et al., 2015a; Ogryzko et al., 2014; Pozzoli et al., 2011). Chemokine receptor Cxcr4a together with myocardium-expressed ligand Cxcl12b are essential for coronary vessel formation and heart tissue regeneration, while Cxcl12a-Cxcr4b signaling functions as guider of lateral line primordium (Ghysen and Dambly-Chaudière, 2007; Harrison et al., 2015b). The known pro-inflammatory cytokine interleukin-1b (IL1b) of zebrafish is strongly expressed from 17-somite stage when the functional immunity is still not yet formed. This expression must facilitate the tissue homeostasis during embryonic development (Nguyen-Chi et al., 2014). In the inflammatory responses to gram-negative microbes or their bacterial components like LPS and DNA, a cascades of signaling transduction under toll like receptors (TLRs) recognition are activated and subsequently inducing transcriptions and activation of many cytokines, remarkably the interleukin-1 family, tumor necrosis factor alpha (tnf α) and other members of pro-inflammatory cytokines (H. Meijer and P. Spaik, 2011; Harvie et al., 2013; Pressley et al., 2005; Schett, 2011). Study of notochord infection has shown

that *il1b* and *tnfa* expressions are highly upregulated. During the notochord inflammation *il1b* is dynamically expressed first in the recruited macrophages and later in neutrophils. This cytokine prolongs the recruitment of neutrophils and contributes to the severe damage of the infected notochord (Nguyen-Chi et al., 2014). *Tnfa* has recently been recorded *in vivo* in M2-like macrophages at the tail wound of zebrafish (Laplace-Builhe et al., 2015).

II.3.3.2. Reactive oxygen species

Reactive oxygen species are produced by NADPH Oxidase (NOX) and Dual Oxidase (DUOX) complexes which locate on the cellular and cytosolic membranes of variety of cell types. Zebrafish possesses all NOX members except for NOX3 gene, and there is one copy of *Duox* found on its genome (Kawahara et al., 2007; Sumimoto, 2008). The correct regulation of ROS concentration is crucial in maintaining normal physiology during embryonic development (Covarrubias et al., 2008; Hagedorn et al., 2012).

Hydrogen peroxide (H₂O₂), one of the main functional components of ROS, appears to play important roles in signaling transduction in infection and tissue injury. In the tail fin amputation experiment a tissue-scale gradient of hydrogen peroxide is produced by cells proximal to the wound margin. This production of H₂O₂ acts as a signal to recruit phagocytes to the injured site. The recruited neutrophils then use their myeloperoxidase to downregulate the concentration of H₂O₂. Both signaling function of H₂O₂ and the recruitments of phagocytes help promote the epidermal proliferation which is essential for tissue regeneration (Gauron et al., 2013; Niethammer et al., 2009b; Pase et al., 2012). Other studies in cells transplantation also revealed the regulatory function of H₂O₂ while the DOUX-mediated H₂O₂ is produced by transformed cells and their neighboring cells (Feng et al., 2010). Superoxide and other halide radicals are also important members of ROS in the control of infection and inflammation. However, they remain to be better characterized in zebrafish.

II.4. The zebrafish notochord

The notochord is a transient compartment present at the early stage of development in chordates. In the developing chordate embryo, it is found ventral to the neural tube. The zebrafish notochord is made of a stack of vacuolated cells surrounded by an outer cell layer and packed within a thick collagen sheath. Vacuoles of the inner cells are fully filled with fluid to create an osmotic pressure against the collagen matrix which in turn forms a hydrostatic structure that serves as an axial skeleton for shaping the embryonic structure (Figure 14). The notochord lies between an upper structure, the floorplate and a lower structure, the hypochord that act as cables allowing only horizontal bending of the notochord during muscle contractions and therefore allowing the embryo and larvae to swim (Figure 15).

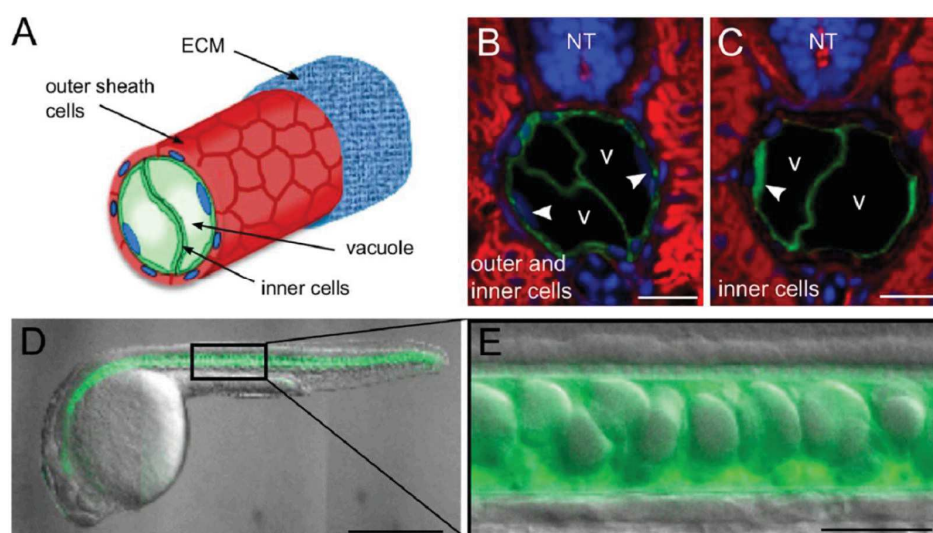


Figure 14: Zebrafish notochord

(A) Cartoon of a zebrafish notochord depicting outer and inner cell layers and the inner cell vacuoles. (B) Confocal image of a cross section of 3-dpf transgenic larva labeled with membrane GFP in the outer and inner cells of *tg(rcn3:GFP-CaaX)*. (C) Confocal image of a cross section of 3dpf transgenic larva expressing soluble GFP in the inner cells *tg(SAGFF214A:gal4/UAS:GFP)*. Cross sections were stained with phalloidin in red and DAPI in blue. V: vacuole; NT: neural tube; arrowheads show inner cell nuclei. (D, E) 24-hpf transgenic embryo *tg(rcn3:GFP-CaaX)* illustrating lateral view of the notochord. Adapted from (Ellis et al., 2013).

The notochord also gives developmental signals to pattern the neighboring tissue such as somites, neural tube and blood vessel. During larval development the notochordal cells undergo differentiation and segmentation and eventually transforms into nucleus pulposus of the intervertebral discs in adult fish (Ellis et al., 2013; Stemple, 2005; Glickman, 2003).

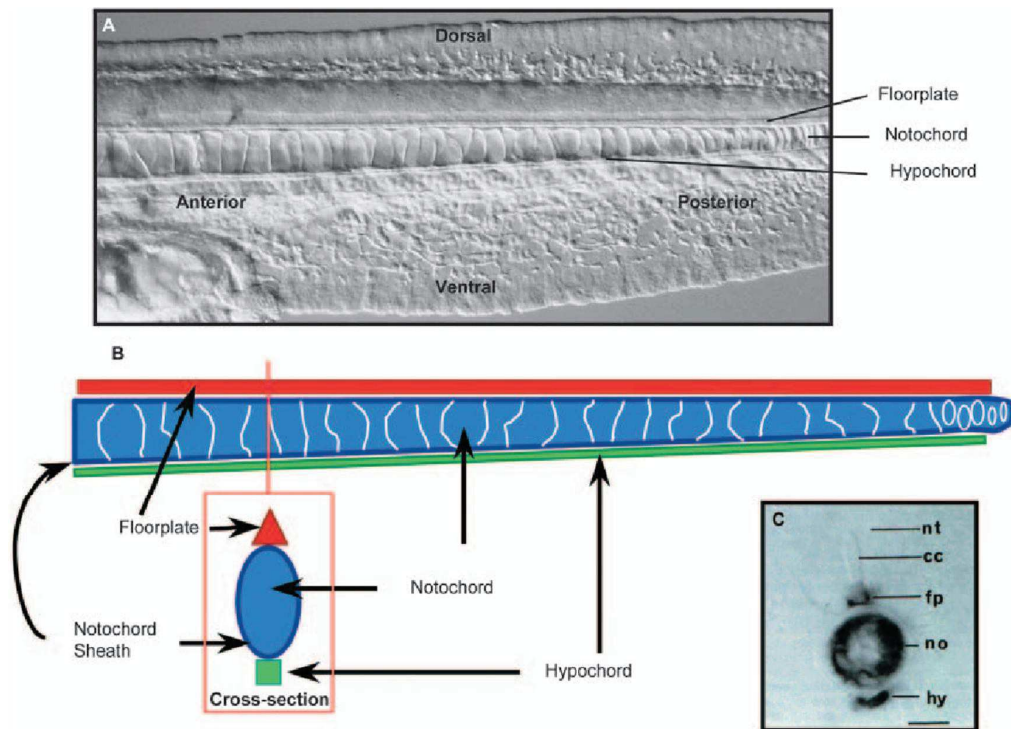


Figure 15: Structural aspects of the notochord

(A) A lateral view of a living zebrafish tail at 24 hpf, showing the main features of the notochord. Dorsal to the notochord is the floor plate, in the ventral-most part of the forming spinal cord. Ventral to the notochord is the hypochord.

(B) A schematic diagram of lateral and cross-sections of the notochord, showing the floor plate and hypochord acting as cables running along the top and bottom of the notochord. (C) As well as the notochord, the floor plate and hypochord express type II collagen (Yan et al., 1995). cc, central canal; fp, floor plate; hy, hypochord; no, notochord; nt, neural tube. Adapted from (Stemple, 2005).

AIM OF THE THESIS

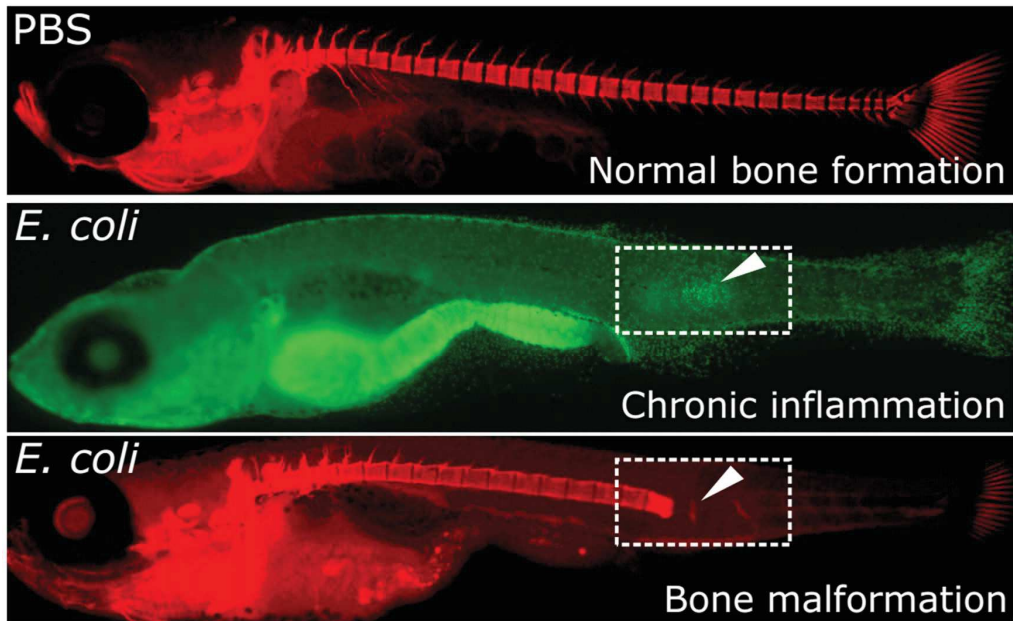
Outcome of a bacterial infection event is determined by nature of the microbe, multiplicity of bacterial cells, physiology of host and location of the infection.

The main aim of this thesis is to understand how the innate immune system responds to bacterial infection in an organ where the professional phagocytes cannot come in direct contact with the bacteria to perform their conventional phagocytic activity.

Since zebrafish is a powerful vertebrate model for study of infectious diseases, and its notochord, which comprises vacuolated cells encased in the thick collagen sheath, is inaccessible to phagocytes like neutrophils and macrophages; I developed an infection model in zebrafish embryo notochord and investigated the fate of the infected bacteria and the response of host innate immunity to this tissue-specific infection.

CHAPTER II

RESULTS



Transient notochord infection of *tg(mpx:GFP)* embryos at 2dpf, Alizarin staining at 20dpi

CHAPTER II: RESULTS

OUTLINE OF THE RESULTS

Part I: Transient infection of zebrafish notochord with *E. coli* induces chronic inflammation

Question: How the innate immune system responses to the bacterial infection in a specific tissue where the microbes could not be phagocytosed?

Strategy: Injection of non-pathogenic *E. coli* in the notochord of transgenic zebrafish embryo and investigate *in vivo* the behaviors of fluorescently labeled phagocytes and the modulation of cytokines using microscopy techniques.

Results:

- The injected *E.coli* is eliminated within 24 hours after the infection.
- Although neutrophils and macrophages could not access the notochord to phagocytose the injected bacteria, these leukocytes are massively recruited and persist for long period after the infection.
- Interleukin-1 β is dynamically expressed first by macrophage and later by neutrophils. This cytokine is crucial for neutrophils recruitment.
- Chronic inflammation causes severe defect on the notochord and subsequently malformation of the vertebral column.

Participation: I fully involved in the project.

Part II: Neutrophils control notochord infection at a distance with superoxide

Question: How is *E. coli* cleared in the notochord without phagocytosis event?

Strategy: Test the roles of neutrophils and macrophages in the bacterial killing by depletion each population at a time. Investigate the involvements of antimicrobial arsenals present in these leukocytes.

Results:

- Neutrophils but not macrophages are necessary for the *E. coli* killing.
- Neutrophils control *E. coli* at a distance through superoxide production.

- Neutrophils need proper cellular density to fight different levels of notochord infection with *E. coli*.

Participation: I fully involved in the project.

Part III: Identification of polarized macrophage subsets in zebrafish

Aim: Investigate the polarity of zebrafish macrophage during infection and inflammation.

Strategy: Induction of inflammation by tail fin amputation and by *E. coli* injection in double transgenic embryo *tg(mpeg1:mCherry-F/tnfa:GFP-F)*. Follow the behavior of fluorescently labelled macrophages and genetic markers for M1 and M2 subtypes macrophages using microscopy and FACS.

Results:

- Generation of transgenic line *tg(tnfa: GFP-F)*.
- Macrophages switch their phenotypes between M1 and M2 subtypes during the onset and the resolution of inflammation as seen in mammalian counterpart.

Participation: I partly involved in the generation of transgenic reporter line *tg(tnfa:GFP-F)*.

Part IV: Rearing zebrafish larvae with Tetrahymenas

Question: Could Tetrahymenas be an alternative food for young zebrafish embryo?

Strategy: 24-hour Tetrahymena culture in enriched medium is washes and the clean Tetrahymenas are used to feed zebrafish embryos starting from day 5 to day 10 after fertilization for one month. Survival and developmental characteristics of larvae are recorded.

Results

- Feeding the zebrafish larvae with Tetrahymenas at their early phase of embryonic development help increase fish survivals.
- Tetrahymenas help maintain good quality of larval medium.

Participation: Fully involved in the project



PART I

Transient infection of zebrafish notochord with *E. coli* induces chronic inflammation

Authors:

NGUYEN-CHI Mai*, **PHAN Quang Tien***, GONZALEZ Catherine,
DUBREMETZ Jean-François, LEVRAUD Jean-Pierre, and LUTFALLA
Georges

Disease models & Mechanisms

2014

RESEARCH ARTICLE

Transient infection of the zebrafish notochord with *E. coli* induces chronic inflammation

Mai Nguyen-Chi^{1,2,*‡}, Quang Tien Phan^{1,2,*}, Catherine Gonzalez^{1,2}, Jean-François Dubremetz^{1,2}, Jean-Pierre Levrard^{3,4} and Georges Lutfalla^{1,2,‡}

ABSTRACT

Zebrafish embryos and larvae are now well-established models in which to study infectious diseases. Infections with non-pathogenic Gram-negative *Escherichia coli* induce a strong and reproducible inflammatory response. Here, we study the cellular response of zebrafish larvae when *E. coli* bacteria are injected into the notochord and describe the effects. First, we provide direct evidence that the notochord is a unique organ that is inaccessible to leukocytes (macrophages and neutrophils) during the early stages of inflammation. Second, we show that notochord infection induces a host response that is characterised by rapid clearance of the bacteria, strong leukocyte recruitment around the notochord and prolonged inflammation that lasts several days after bacteria clearance. During this inflammatory response, *il1b* is first expressed in macrophages and subsequently at high levels in neutrophils. Moreover, knock down of *il1b* alters the recruitment of neutrophils to the notochord, demonstrating the important role of this cytokine in the maintenance of inflammation in the notochord. Eventually, infection of the notochord induces severe defects of the notochord that correlate with neutrophil degranulation occurring around this tissue. This is the first *in vivo* evidence that neutrophils can degranulate in the absence of a direct encounter with a pathogen. Persistent inflammation, neutrophil infiltration and restructuring of the extracellular matrix are defects that resemble those seen in bone infection and in some chondropathies. As the notochord is a transient embryonic structure that is closely related to cartilage and bone and that contributes to vertebral column formation, we propose infection of the notochord in zebrafish larvae as a new model to study the cellular and molecular mechanisms underlying cartilage and bone inflammation.

KEY WORDS: Zebrafish, Neutrophils, Inflammation, Interleukin-1 β

INTRODUCTION

Osteomyelitis, chondritis and septic arthritis are inflammatory diseases of bones, cartilage and joints, respectively, that are often caused by bacterial infections. These diseases are caused by local or systemic immune responses that lead to leukocyte infiltration,

damage to extracellular matrix, compression of vasculature and the progressive destruction of bone and joints (Wright and Nair, 2010). The bacteria that are involved are predominantly *Staphylococcus aureus*, *Streptococcus* spp. and members of Gram-negative Enterobacteriaceae, including *Escherichia coli* (Gutierrez, 2005; Lew and Waldvogel, 2004). Although the pathogen is often present within the infected site, it is occasionally undetectable, despite the persistence of immunological symptoms. Substantial evidence supports the importance of innate immunity in the physiopathology of these diseases; however, its exact role is still poorly understood (Lew and Waldvogel, 2004; Wright et al., 2010).

The innate immune response is the first defence of the host in the case of infection. Macrophages and neutrophils are two major effectors of innate immunity against microbes. Neutrophils are the first to be recruited to the infected tissue; they migrate rapidly by responding to gradients of chemoattractant molecules – such as the contents of damaged cells, bacterial products and host chemokines (Deng et al., 2013; Renshaw and Trede, 2012). Macrophages are recruited later in order to aid the removal of dead cells and microbes; they play a role in remodelling the injured tissue and activating adaptive immunity. Neutrophils and macrophages are both professional phagocytes, but the efficiency of phagocytosis depends on the site at which they encounter bacteria (Colucci-Guyon et al., 2011).

Although leukocytes can migrate rapidly and specifically to an infection site, most tissues have specific resident macrophages permanently patrolling the tissue, circulating through tissues to eliminate cellular debris and microorganisms. From this immunological perspective, bone and cartilage are very specific tissues in which, owing to their highly structured and resistant extracellular matrix, no specialised phagocytes patrol. The best-documented example is that of bones. Resident bone macrophages, OsteoMacs, are not present within the bone matrix but, with their stellate morphology, do extensively cover bone surfaces (Pettit et al., 2008). They probably act as guards to prevent microbes from entering or attacking the bone. By contrast, osteoblasts (that make bone) and osteoclasts (monocyte-macrophage lineage cells that resorb bone) are capable of phagocytosis, probably to compensate for the absence of professional phagocytes within the tissue. Some pathogens have even developed specific strategies to colonise these cells (Wright and Nair, 2010). Although documented to a lesser extent, the situation in cartilage is similar, with chondrocytes displaying phagocytic activity and a highly phagocytic cell population that specifically expresses the macrophage marker CD163, present below the superior zone at the periphery of cartilage (Castillo and Kouri, 2004; Jiao et al., 2013).

To address the complexity of the chronic inflammation of bones and joints, a number of mammalian infection models have been developed (Patel et al., 2009). Most of them rely on the injection of *Staphylococcus aureus*, or other bacteria, directly into the bone in

¹Dynamique des Interactions Membranaires Normales et Pathologiques, Université Montpellier 2, UMR 5235, case 107, Place Eugène Bataillon, 34095 Montpellier Cedex 05, France. ²CNRS; UMR 5235, Place Eugène Bataillon, 34095 Montpellier Cedex 05, France. ³Macrophages et Développement de l'Immunité, Institut Pasteur, Paris F-75015, France. ⁴CNRS URA2578, Paris F-75015, France. *These authors contributed equally to this work

[‡]Authors for correspondence (mai.nguyen-chi@univ-montp2.fr; lutfalla@univ-montp2.fr)

This is an Open Access article distributed under the terms of the Creative Commons Attribution License (<http://creativecommons.org/licenses/by/3.0>), which permits unrestricted use, distribution and reproduction in any medium provided that the original work is properly attributed.

TRANSLATIONAL IMPACT**Clinical issue**

Osteomyelitis, chondritis and septic arthritis are inflammatory diseases of bone, cartilage and joints that are often caused by bacterial infections. In these diseases, local or systemic immune responses lead to leukocyte infiltration and the progressive destruction of bone and joints. Special culture cell systems and several mammalian infection models have been developed to understand these diseases and to tune antibiotic therapies. However, the study of the complex dynamic interactions that occur during inflammation requires non-invasive models in which pathogens and immune cells can be imaged in the context of three-dimensional tissue architecture in the host. In the last decade, the zebrafish, owing to the transparency of its embryo and the ease with which it can be genetically manipulated, has emerged as an exquisite system for visualising the immune response to pathogen infections *in vivo* and in real time.

Results

Here, the authors develop a zebrafish model to investigate the inflammatory response that is induced by infection of the notochord, a cartilaginous-like embryonic tissue that participates in vertebral column formation and shares many similarities with chondrocytes. Using multi-dimensional confocal imaging, the authors show that, during the early stages of inflammation, infected zebrafish notochord is inaccessible to leukocytes, even though these professional phagocytes engulf microbes that had been injected into other tissues of the zebrafish embryo. Using *Escherichia coli*, a pathogen that cannot develop within the notochord, the authors show that a transient infection in this tissue triggers a severe and persistent inflammation that is characterised by a massive recruitment of leukocytes, extensive degranulation of neutrophils and leukocyte infiltration into the notochord. Notably, this non-resolved inflammation is accompanied by extracellular matrix remodelling and by the development of notochord lesions and dysmorphic vertebrae development. Finally, the authors report that an Il1b cytokine burst occurs during notochord inflammation that is specifically required for the establishment of the inflammatory episode and of notochord lesions.

Implications and future directions

These findings establish this *in vivo* approach as a relevant new vertebrate model of chronic inflammation in matrix-enriched tissues, such as bones and cartilage. Indeed, the symptoms exhibited by the notochord-infected larvae are reminiscent of those seen in bone and cartilage infection in mammals. Furthermore, these findings provide the first *in vivo* evidence that neutrophils can degranulate in the absence of a direct encounter with a pathogen. Thus, transient infection of the zebrafish notochord provides a unique model in which to visualise at high resolution the cellular events underlying pathological inflammation.

combination with an adjuvant or a trauma. Owing to these models, advances have been made in understanding the disease and in tuning antibiotic therapies; however, to understand the complexity of dynamic interactions during inflammation, non-invasive and tractable models in which pathogens and immune cells can be imaged in the context of three-dimensional tissue architecture in the host are required. Owing to its exceptional transparency, the zebrafish embryo is an exquisite vertebrate model for the study of tissue-specific infections and the inflammatory consequences within a homologous tissue.

At the embryonic and early-larval stages, zebrafish do not possess bone. However, the notochord, a transient embryonic structure that is present in all chordates, in addition to its essential roles in vertebrate patterning during development, serves as an axial skeleton of the embryo until other structures, such as the vertebrae, form (Stemple, 2005). The notochord comprises vacuolated cells that are encased in a sheath of collagen. Osmotic pressure within the vacuoles exerts such a pressure on the thick collagenous sheath that it forms a hydrostatic skeleton in the embryo and young larva.

Notochordal cells that express many cartilage-specific genes are most closely related to chondrocytes, but as development proceeds, they become ossified in regions of developing vertebrae and contribute to the formation of the centre of the intervertebral discs in a structure called the nucleus pulposus (Stemple, 2005). The notochord can be studied to dissect the molecular mechanisms that are involved in the immune response to infection in a chondrocyte-like tissue. Previous results from our laboratory have shown that the injection of an attenuated mutant of *Mycobacterium marinum*, TesA:Tn, into the notochord allows active replication of the bacteria, whereas the infection is easily controlled by professional phagocytes when injected at other locations (Alibaud et al., 2011). The drawback of this infection model is that the active replication of the mycobacteria within the notochord ultimately leads to the death of the host. As neither macrophage nor neutrophil infiltration is observed (by using electron microscopy), we hypothesised that the notochord is an organ that is inaccessible to leukocytes and that this organ could be a good model in which to study the outcome of an infection in a tissue where leukocytes cannot reach the pathogen.

Here, we show that the injection of non-pathogenic Gram-negative bacteria *Escherichia coli* K12 into the notochord of zebrafish embryos induces a strong immune response without compromising the survival of the host. Using a combination of imaging and genetic techniques, we investigate the fate of the bacteria in this organ, analyse the interaction between the bacteria and the leukocytes, describe the inflammation induced by the infection and analyse the consequences of this inflammation.

RESULTS**Zebrafish larvae rapidly clear *E. coli* infection in the notochord**

To characterise the immune response to notochord infection, we first injected 3×10^3 bacteria of an *Escherichia coli* K12 strain that expressed the fluorescent protein DsRed (*E. coli*-DsRed) into the notochord of zebrafish embryos at 45 hours post-fertilisation (hpf) (Fig. 1A). Injection through the collagen sheath, just posterior to the yolk extension, leads to the anterior sliding of the bacteria around the notochordal cells inside of the collagen sheath. Fifteen minutes after injection, the embryos were fixed, and the localisation of the bacteria was checked by using transmission electron microscopy (TEM). Bacteria were found inside the notochord, mainly at the periphery, pinned against the collagen sheath by the turgescence of notochordal cells (Fig. 1B,C). The fate of the bacteria in the notochord was monitored by live-imaging microscopy and compared to the fate of bacteria that were injected inside muscles. When injected into muscles, bacteria were restricted to the injected somite for the first hours, but after 24 hours, their fluorescent remnants were observed within motile cells that migrated away from the site of injection (Fig. 1D). By contrast, in most cases (73%, 57 out of 78), the day following injection into the notochord, fluorescent bacteria were not observed in the notochord, suggesting that bacteria had been removed (Fig. 1E). In the other 27% (21 out of 78) – presumably those embryos that received the higher bacterial load – bacteria proliferated within the notochord (Fig. 1F-I) and led to larval death within 3 days, as illustrated by the reduced survival of the embryos in which bacteria had been injected into the notochord (Fig. 1J). Further experiments were performed using lower bacterial loads (2×10^3); at this load, all embryos survived and bacterial division was not observed (by using TEM; data not shown). The clearance of bacteria from the notochord of most of the infected fishes was confirmed by counting colony-forming units

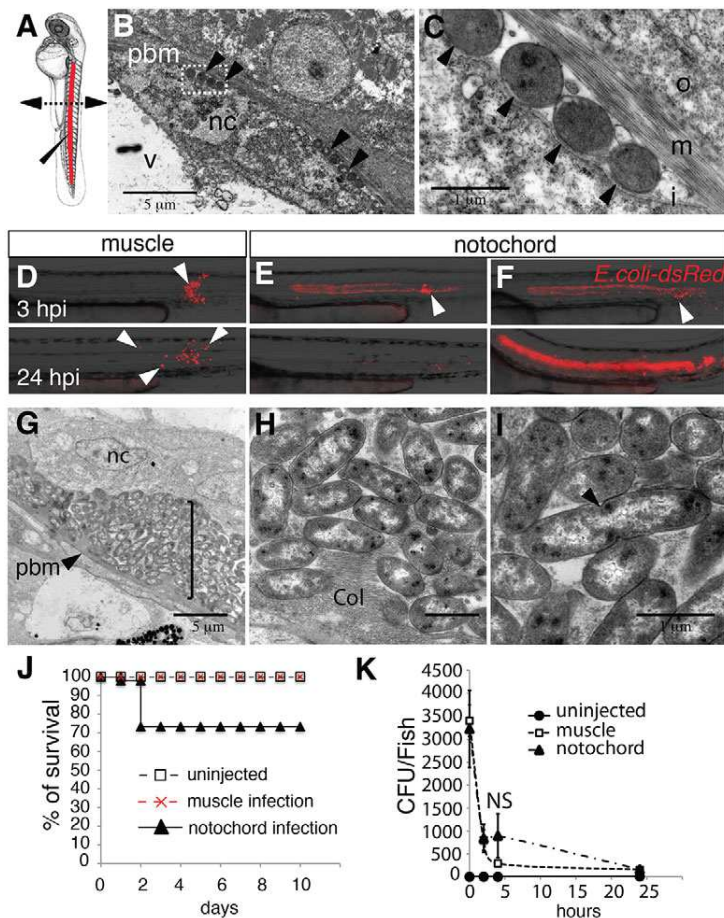


Fig. 1. Injection of *Escherichia coli* into the notochord of zebrafish larvae. (A) Embryos at 48 hpf. Bacteria were injected (elongated arrowhead) into the notochord (red) dorsal to the urogenital opening. The dashed line with arrowheads shows the region where cross-sections have been performed for electron microscopy. (B,C) Transmission electron microscopy analysis of a larva 15 minutes after injection of bacteria into the notochord; C is a higher magnification of the boxed region in B. Arrowheads indicate bacteria. Nc, notochordal cell; v, vacuole; pbm, peri-notochordal basement membrane that comprises three layers – o, outer; m, medium (collagen); l, inner. (D-F) The fate and distribution of DsRed-expressing *E. coli* (red) after infection of muscle with 3000 CFU (D) or notochord with 2000 CFU (E) and 3000 CFU (F). Each larva was followed and imaged at 3 (top row) and 24 (bottom row) hpi. Arrowheads indicate clusters of bacteria. (G-I) Transmission electron microscopy analysis of the notochord of larvae that had been infected in the notochord (11 hpi); H,I show magnifications of regions of G. (G) Numerous bacteria (bracket) are found between the peri-notochordal basement membrane (pbm, arrowheads) and notochord cells (nc). (H) Collagen (col) disorganisation is observed next to bacteria. (I) Extracellularly replicating bacterium (arrowhead). (J) Survival was scored of uninfected larvae and those that were infected in the muscle or notochord ($n > 24$ each). These results are representative of three independent experiments, $P < 0.0005$ for notochord injection versus uninjected. (K) Whole embryo bacterial counts of *E. coli* when injected into the muscle or notochord. Results are expressed as the mean number of CFU per larvae \pm s.e.m. ($n > 5$ larvae per timepoint). NS: not significant. Scale bars: 5 μ m (B,G); 1 μ m (C,H,I).

(CFUs) (Fig. 1K), indicating that bacteria, if not too numerous, are efficiently cleared from the notochord within the first 24 hours of infection.

Neutrophils and macrophages fail to reach, and engulf, bacteria in the notochord

During the first weeks of development, the zebrafish larva has no functional adaptive immune system, relying mostly on macrophages and neutrophils, to fight infections (Lieschke et al., 2001; Meijer and Spaik, 2011; Renshaw and Trede, 2012). Therefore, we determined whether these cells were able to reach the bacteria in the notochord in order to phagocytose and/or kill them. To study neutrophil-microbe interactions, we injected fluorescent *E. coli* into *Tg(mpx:GFP)* embryos, which expressed green fluorescent protein (GFP) under the control of the neutrophil-specific promoter of *myeloperoxidase* (*mpx*) (Renshaw et al., 2006), and we then imaged neutrophil behaviour by using confocal time-lapse microscopy from 2 hours post-infection (hpi). In contrast to PBS-injected controls (data not shown), neutrophils were primarily attracted to the injection site, then, arriving from the ventral side of the larvae (Fig. 2A,B; supplementary material Movies 1, 2), they crawled along the outside of the infected notochord, spreading towards the anterior region (Fig. 2B; supplementary material Movie 1). Although neutrophils appeared to be attempting to try to phagocytose bacteria (i.e. crawling forward and backward in the vicinity of bacteria, emitting cytoplasmic protrusions), they failed to engulf them (supplementary material Movie 3). Only a few neutrophils contained engulfed bacteria, but these leukocytes were

carefully, and retrospectively, traced from the injection site, suggesting that they phagocytosed a few *E. coli* that were deposited at the injury site of the notochord (Fig. 2B; supplementary material Movie 1). This behaviour is in stark contrast with that observed in muscles, where many neutrophils displayed phagosomes that were full of bacteria at 2 hpi and still efficiently engulfed bacteria (data not shown; Colucci-Guyon et al., 2011).

To analyse macrophage-bacteria interactions, we constructed the *Tg(mpeg1:mCherryF)* line that expressed red fluorescent macrophages. Transgenic larvae were infected either in the bloodstream or in the notochord, and macrophage behaviour was recorded at 1 hpi. Similar to neutrophils, although less mobile, macrophages were recruited to the infected notochord and extended pseudopodal protrusions in attempts to engulf bacteria (Fig. 2A,C; supplementary material Movies 4, 5). In contrast to the numerous macrophages that were laden with *E. coli* after bloodstream infection (supplementary material Movie 6), macrophages were inefficient at engulfing the bacteria present in the notochord. It is noteworthy that no significant difference in the time to the first recruitment was detected between neutrophils and macrophages (data not shown).

The fact that leukocytes easily engulfed bacteria at the injection site, where the notochordal collagen sheath had been damaged by the injection, but not in the undamaged upstream region suggests that bacteria might not be accessible to leukocytes because of the physical properties of the notochord (data not shown). We tested this hypothesis by performing three-dimensional reconstruction of confocal acquisitions. From 2 hpi onwards, bacteria were found in the phagosomes of neutrophils and macrophages after injection into

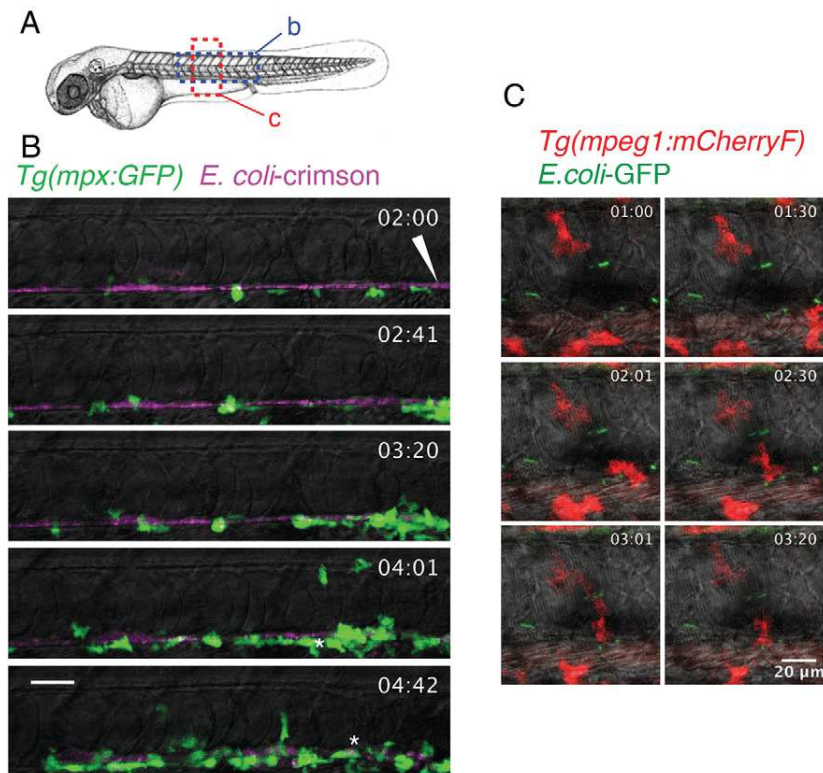


Fig. 2. Behaviour of neutrophils and macrophages following notochord infection. (A) Diagram showing the regions of the larvae imaged in B and C (dashed boxes). (B) *Tg(mpx:GFP)* larvae that had been infected with crimson-expressing *E. coli* (magenta) in the notochord at 48 hpf. The general behaviour of neutrophils (green) was imaged using four-dimensional confocal microscopy, starting at 2 hpi for a duration of 3 hours (the time post-infection is shown in the top right corner). *Neutrophils loaded with bacteria, the arrowhead indicates the injection site. (C) *Tg(mpeg1:mCherryF)* larvae that had been infected with GFP-expressing *E. coli* (green) at 48 hpf in the notochord were imaged in the region represented in A to visualise the behaviour of macrophages (red) using four-dimensional confocal microscopy at 1 hpi for a duration of 3 hours and 20 minutes. Scale bars: 20 μ m.

muscle (Fig. 3A) and the bloodstream, respectively (Fig. 3C); however, they remained next to, but outside of, immune cells after notochord infection (Fig. 3B,D). Indeed, many leukocytes accumulated around the notochord but could not infiltrate it, even at 24 hpi (Fig. 3E-G).

To confirm further that leukocytes could not reach the bacteria, and engulf them, in the notochord, we analysed the ultrastructure of the

notochord of infected larvae by using TEM at different timepoints following infection. At 15 minutes post-infection, bacteria were found in the periphery of the notochord, between notochordal cells and the collagen sheath as mentioned above (supplementary material Fig. S1A-C). At 2 hpi and 4 hpi, bacteria remained in the same location – in the extracellular space – although they were less numerous at 4 hpi (supplementary material Fig. S1D-F; data not shown for the 4 hpi

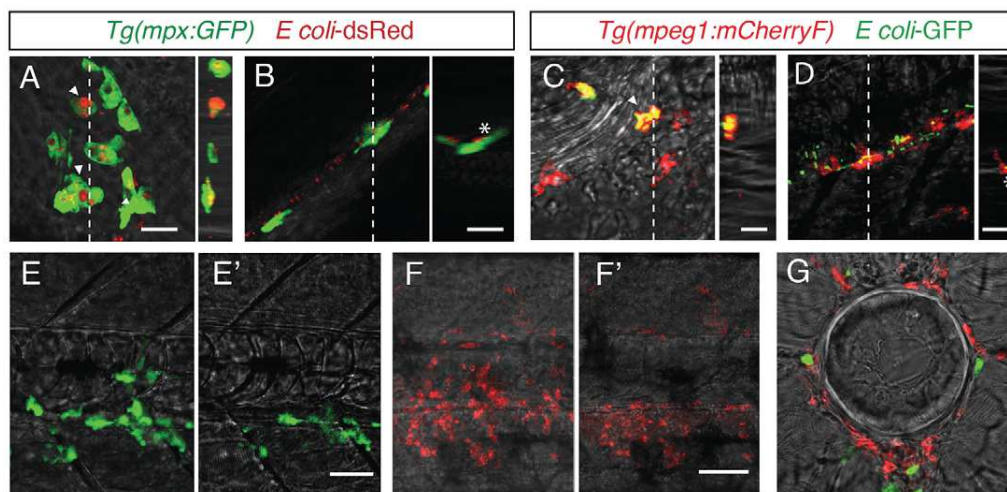


Fig. 3. Leukocytes do not enter the notochord during the early phase of infection. (A,B) Multiscan confocal analysis at 2 hpi of neutrophils (green) in *Tg(mpx:GFP)* larvae after muscle (A) or notochord infection (B) with DsRed-expressing *E. coli*. (C,D) Multiscan confocal analysis of macrophages (red) in *Tg(mpeg1:mCherryF)* larvae after intravenous (C) or notochord (D) infection with *E. coli-GFP* (green) at 2 hpi. In A-D, the left panels are xy maximum projections and the right panels are yz cross-section views at the position of the stippled line. Arrowheads show bacteria-containing leukocytes, *Leukocytes that were located next to bacteria but did not contain any. (E-G) Confocal analysis at 24 hpi of the notochord with fluorescent *E. coli*. Bacteria were no longer visible at 24 hpi. (E,E') *Tg(mpx:GFP)* larva showing neutrophils (green), (F,F') *Tg(mpeg1:mCherryF)* larva showing macrophages, (E,F) maximum projection, (E',F') single confocal scan. (G) Confocal analysis of a 60- μ m cross-section from a double-transgenic larva – neutrophils (green) and macrophages (red) accumulated around the notochord but did not enter this structure, as shown. Scale bars: 10 μ m (A-D); 20 μ m (E-G).

timepoint). Replicating bacteria were never observed under these conditions. This correlated with the observation that DsRed fluorescence in *E. coli* remained constant in the notochord for a few hours following injection before diminishing completely. Although a few leukocytes were detected outside of the notochord (data not shown), none were found inside, confirming that leukocytes cannot phagocytose bacteria in this structure (supplementary material Fig. S1). Strikingly, numerous *E. coli* displayed an altered morphology (supplementary material Fig. S1B,C,F), suggesting they are eliminated by a humoral lysis mechanism. No altered morphologies were observed when higher doses of bacteria were used, suggesting that the humoral lysis mechanism is overpowered when the notochord is injected with higher doses of *E. coli*.

Notochord infection induces a strong and persistent inflammatory reaction

We analysed the kinetics of immune cell recruitment using *Tg(mpx:GFP)* and *Tg(mpeg1:mCherryF)* lines by counting the leukocytes that accumulated around the infected notochord. As for muscle infections (Colucci-Guyon et al., 2011), notochord infections led to neutrophil recruitment within the very first hours following the injection. After injection of bacteria into the muscle, the number of neutrophils that had been recruited started decreasing at 24 hpi (Fig. 4A,C), whereas, in the notochord, neutrophil recruitment

continued to increase at 48 hpi and remained high up to 6 days post-infection (dpi), forming one to four clusters that were towards the anterior of the injection site (20 out of 26 fish; Fig. 4A,C). Macrophages migrated to both infected muscle and notochord in a similar manner (Fig. 4B) – in both cases, the recruitment of macrophages lasted for 6 days, but more macrophages were recruited to the infected notochord (23 out of 23 fish; Fig. 4B,D). The observed immune response was not a consequence of the injection per se in the notochord, because the injection of PBS or fluogreen Dextran caused neither neutrophil nor macrophage recruitment (Fig. 4C,D; supplementary material Fig. S2).

We conclude that infection of the notochord induces a massive recruitment of macrophages and neutrophils to its periphery; remarkably, this inflammatory response is not properly resolved, as leukocyte accumulation persists for days, despite the clearance of bacteria in a matter of hours.

Notochord inflammation induces notochord damage

Inflammation is fundamental in order to control bacterial infections. However, it is crucial that this inflammation resolves in a timely manner in order to prevent damage to the surrounding tissues. In order to analyse the consequences of notochord inflammation, we imaged larvae, in which bacteria had been injected into the notochord, for 10 days. At 5 dpi, most of the infected larvae

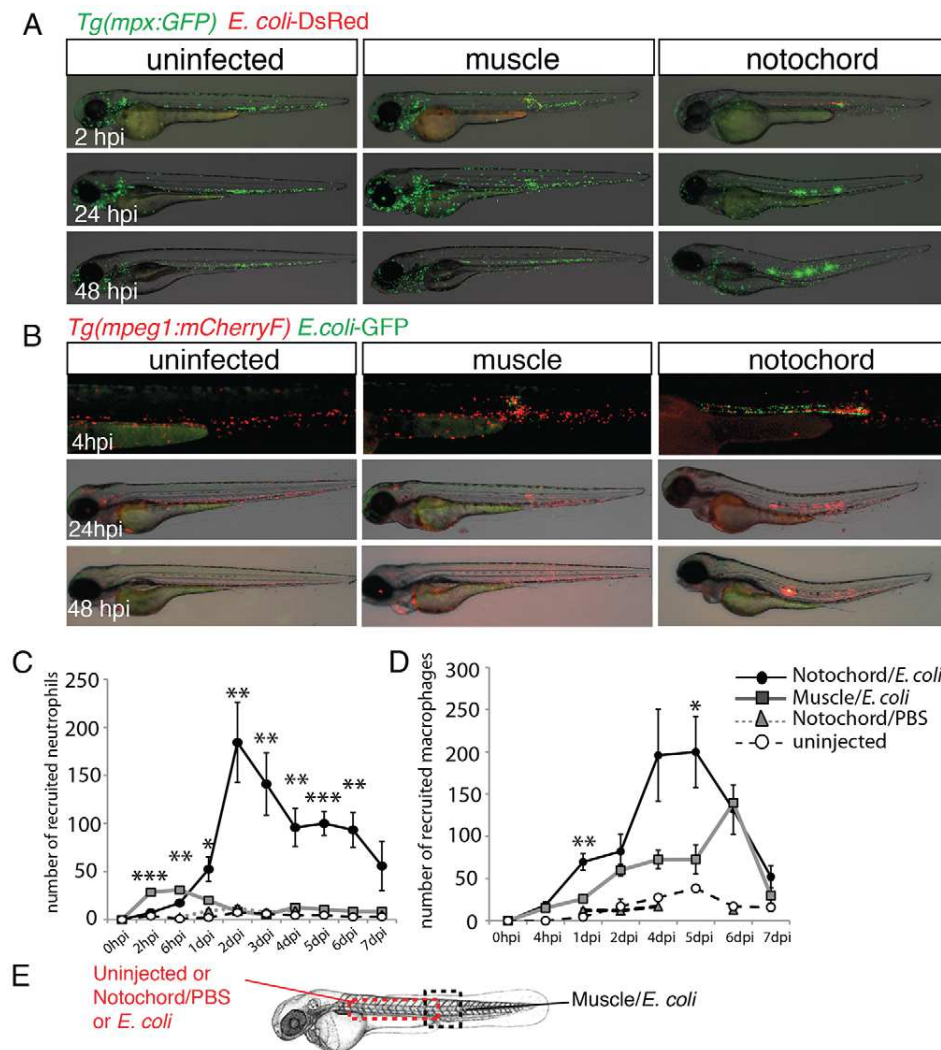


Fig. 4. Neutrophils and macrophages are recruited around the infected notochord. (A) *Tg(mpx:GFP)* larvae were either left uninfected or infected with DsRed-expressing *E. coli* (red) in the muscle or notochord at 48 hpf. Neutrophil recruitment (green) was imaged repeatedly in individual larvae at the indicated timepoints. (B) A similar experiment to that shown in A was performed in *Tg(mpeg1:mCherryF)* larvae that were either uninfected or infected with GFP-expressing *E. coli* (green) in muscle or the notochord at 48 hpf. (C,D) Corresponding counts of neutrophils (C) and macrophages (D) over the course of 1 week post-infection. Results are expressed as the mean number of cells ± s.e.m., five to nine fish were examined per timepoint, **P*<0.05, ***P*<0.005 and ****P*<0.001. (E) The dashed boxes in the diagram represent the zone where counting was performed.

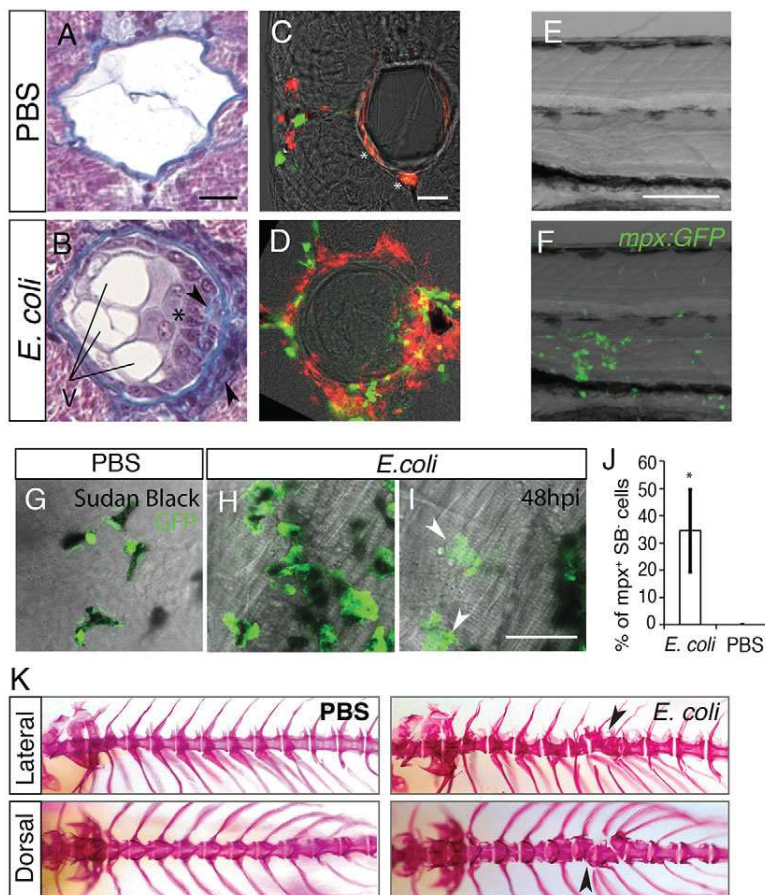


Fig. 5. Late consequences of notochord infection.

(A,B) Histological analysis at 5 dpi of larvae that had been injected in the notochord with PBS (A) or *E. coli* (B). Cross-sections (4 μ m) stained with Masson's Trichrome. In the infected larvae, collagen-enriched matrixes (blue) and supernumerary vacuoles (V) were seen. Cells inside the notochord (*) and ectopic matrix deposition (arrowhead) can be seen in the sections. (C,D) Neutrophil (green) and macrophage (red) infiltration in the notochord, multiscan confocal microscopy. Cross-sections (60 μ m) of *Tg(mpx:GFP; mpeg1:mCherryF)* larvae at 5 days following injection of the notochord with PBS (C) or with *E. coli* (D). *Nonspecific staining. (E,F) Notochord of *Tg(mpx:GFP)* larvae at 3 dpi. (E) Transmitted-light image, overlaid in F with a maximal projection of confocal fluorescence images that show neutrophils (green) clustered at the damaged zone. (G-I) Sudan-black (SB) staining (black) and GFP expression (green) in *Tg(mpx:GFP)* larvae at 48 hours post-injection of either PBS (G) or *E. coli* (H,I) into the notochord. Arrowheads indicate neutrophils that have degranulated. (J) Graphic representation of the percentage of GFP⁺SB⁻ cells under the indicated conditions, mean \pm s.e.m., five or six fish per condition were analysed. * $P < 0.05$ compared with the PBS control. (K) Infected larvae developed scoliosis and dysmorphic vertebrae. Larvae were injected with PBS or *E. coli* into the notochord at 48 hpf, grown to 60 dpf and fixed for analysis. Bones were stained with Alizarin red. Lateral and dorsal views of the anterior part of the vertebral column are shown. Arrowheads indicate mis-shaped and fused vertebral bodies. Scale bars: 20 μ m (A-D,G-I); 50 μ m (E,F).

presented curved malformation and lesions of the notochord, upstream of the injection site (43 out of 49 fish; supplementary material Fig. S3A,B). Although the defects were lessened, we still observed this malformation at 10 dpi (supplementary material Fig. S3C). Histological analysis of PBS-injected larvae at 5 dpi revealed normal architecture with highly vacuolated cells that were surrounded by a regular collagen sheath. By contrast, the infected larvae displayed swelling of the notochord at various locations along the antero-posterior axis (Fig. 5A,B; supplementary material Fig. S3D-K). At these spots, we observed an ectopic collagen-rich extracellular matrix, and an increased number of cells and vacuoles inside the notochord, suggesting the presence of supernumerary notochordal cells, rather than a phenomenon of fragmented vacuoles. Cells of a smaller size were also found clustered either outside or inside of the notochord; they were often trapped within the matrix, suggesting that they are infiltrating leukocytes (supplementary material Fig. S3J-K). Analysis by using confocal microscopy revealed that, although leukocytes were positioned at the margin of the myotome in PBS-injected larvae, they started infiltrating the notochord in *E. coli*-injected larvae from 2 dpi (Fig. 5C,D shows the 5 dpi timepoint; the data at 2 dpi is not shown), a timepoint that is long after bacterial clearance. Because notochord defects colocalised with neutrophil clusters (Fig. 5E,F), we asked whether neutrophil infiltration contributes to the destruction of host tissues. Indeed, this infiltration was concomitant with neutrophil degranulation – 35% of neutrophils in the inflammation region harboured no myeloperoxidase-containing granules, whereas all neutrophils in the control retained them (Fig. 5G-J). Taken together, these results show that infection of the notochord eventually leads to severe damage to

the notochord tissue, which correlates with late leukocytic infiltration and neutrophil degranulation.

Notochord inflammation triggers vertebral column defects

As the notochord participates to vertebral column formation we asked whether the inflammation of the notochord could trigger vertebral column defects. We thus examine the axial skeleton of juvenile fishes at 60 days post-fertilization (dpf) using Alizarin red staining. Zebrafish that had been previously injected with *E. coli* in the notochord developed scoliosis and dysmorphic vertebral column in their anterior region (upstream the injection site), characterised by fused and misshaped vertebral bodies and absence of intervertebral disc (11 out of 11 fish; Fig. 5K). No defects were observed in the PBS injected controls, excepting a single vertebral body that appeared more calcified at the injection site in few fishes (two out of 19 fish; Fig. 5K; data not shown).

Neutrophils but not macrophages expressed high levels of *il1b* in notochord infected embryos.

In order to decipher the molecular mechanisms that orchestrate the inflammatory response to notochord infection, we analyzed the expression of many cytokines and chemokines in larvae that had been infected in the notochord (supplementary material Table S1). The expression of most of the chemokines that we examined was unchanged, such as that of the chemokine Cxcl-c5c; however, transcripts of the proinflammatory cytokine *Il1b* were strongly upregulated from 1 dpi onwards (Fig. 6A,B).

To study the spatiotemporal behaviour of the cells that produce the *il1b* transcripts, we established a transgenic line that expressed

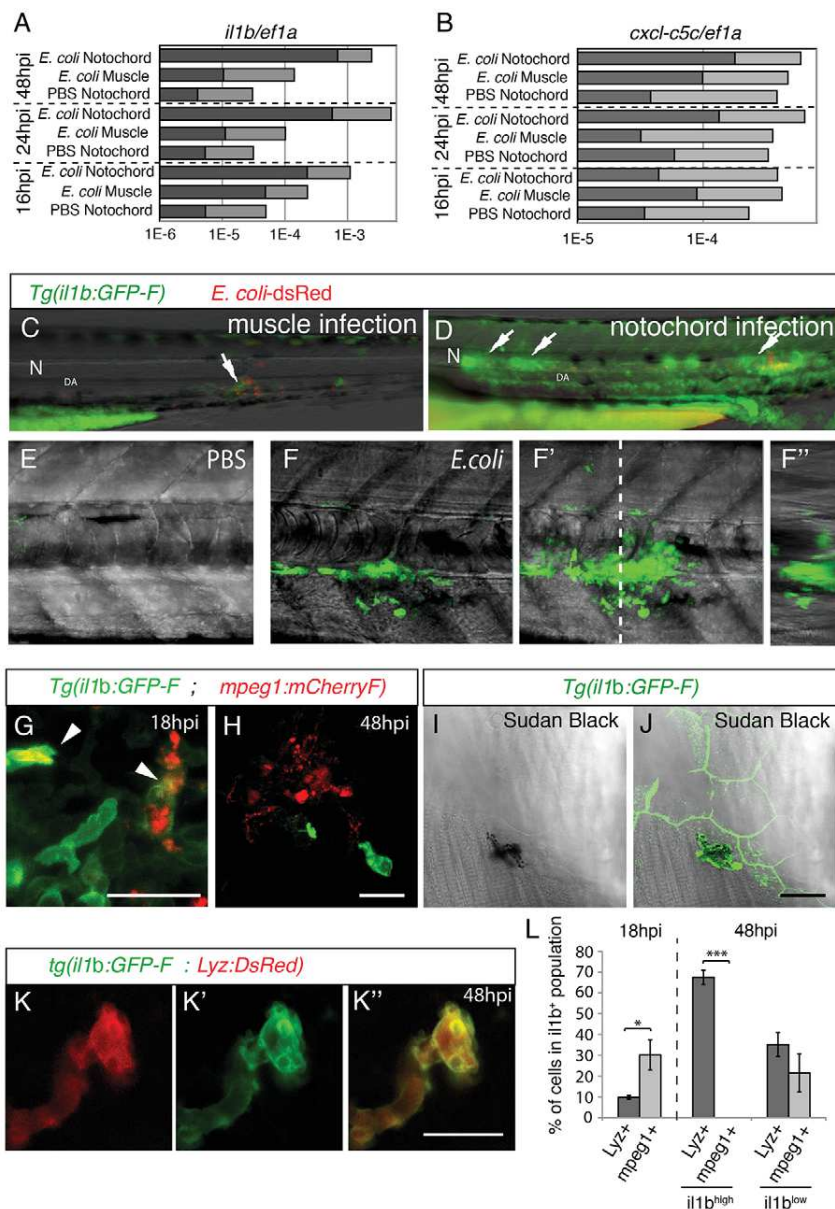


Fig. 6. GFP expression in *Tg(il1b:GFP-F)* infected larvae. (A,B) The relative expression of *il1b* (A) and of *cxcl-c5c* (B) at different timepoints post-infection, under three different conditions – PBS injected into the notochord, *E. coli* injected into muscle and *E. coli* injected into the notochord. Quantitative real-time RT-PCR on whole embryo RNA extracts using *ef1a* as a reference gene was performed; light grey bars represent the 95% confidence intervals (Student's *t*-test). Non-overlapping light grey bars indicate $P < 0.05$. These results are representative of three independent experiments. (C,D) GFP expression at 24 hpi in *Tg(il1b:GFP-F)* larvae that had been injected with *E. coli* (red) into muscle (C) or the notochord (D). Arrows indicate expression next to inflammation sites. N, notochord; DA, dorsal aorta. (E,F) Multiscale confocal analysis of GFP expression in *Tg(il1b:GFP-F)* larvae in the notochord region 48 hours following the injection of PBS or *E. coli*. (E-F) Maximum projections, (F) longitudinal- and (F'') cross-section views. The dashed line indicates the position of cross-section F'' relative to F. (G,H) The expression of mCherry (red) and GFP (green) in *Tg(mpeg1:mCherryF); il1b:GFP-F* double transgenic larvae at 18 (G) and 48 hpi (H) in the notochord region was analysed by using confocal microscopy. Arrowheads indicate macrophages expressing GFP. (I,J) Sudan-black staining and GFP expression in *Tg(il1b:GFP-F)* larvae was analysed by using confocal microscopy at 48 hpi. The images show a GFP⁺ neutrophil underneath GFP⁺ keratinocytes. (K-K'') The expression of DsRed (red) and GFP (green) in *Tg(Lyz:DsRed); il1b:GFP-F* double transgenic larvae at 48 hpi was analysed by using confocal microscopy. A merged image is shown on the right. (L) Quantification of *il1b*⁺; *mpegi*⁺ and *il1b*⁺; *Ly2z*⁺ cells in the inflammation region. Counts are expressed as the percentage of cells within the population expressing GFP (*il1b*⁺; *il1b*^{low} or *il1b*^{high}). * $P < 0.05$, ** $P < 0.005$ and *** $P < 0.001$. Scale bars: 20 μ m.

farnesylated GFP (membrane-targeted GFP; GFP-F) under the control of the *il1b* promoter *Tg(il1b:GFP-F)*. Uninfected *Tg(il1b:GFP-F)* developing embryos expressed GFP-F during the segmentation period in the elongating tail bud (supplementary material Fig. S4). At 24 hpf, GFP expression appeared in tail keratinocytes, the olfactory epithelium and individual cells on the yolk sac that behave as primitive leukocytes. At 35 hpf, when leukocytes appear in the caudal hematopoietic tissue (CHT), scattered GFP⁺ cells were also found in the CHT region. From 50 hpf, GFP was expressed in keratinocytes at the tip of the caudal fin, in fin buds, retina, neuromasts, gills and thymus (supplementary material Fig. S4; data not shown). Whole-mount *in situ* hybridisation analysis confirmed the expression of endogenous *il1b* mRNA in the different organs that are cited above, showing that *Tg(il1b:GFP-F)* recapitulates *il1b* transcriptional expression (supplementary material Fig. S5A,C). Furthermore, upon stimulation by 'danger signals', both the neutrophils and macrophages of *Tg(il1b:GFP-F)* larvae strongly expressed GFP,

correlating with the upregulation of the endogenous *il1b* mRNA that was observed in both leukocyte populations (supplementary material Fig. S6).

To study *il1b* transcription upon infection, we injected fluorescent bacteria (*E. coli*-DsRed) into the notochord of *Tg(il1b:GFP-F)* embryos. Specific expression of GFP was detected along the notochord as early as 18 hpi, which increased significantly by 48 hpi and was maintained up to 5 to 6 dpi before decreasing (24 out of 36 fish; Fig. 6D; supplementary material Fig. S5D). The induction of GFP upon infection correlated with the upregulation of *il1b* mRNA (supplementary material Fig. S5A-C). Conversely, control PBS and muscle injections, respectively, induced no and low expression of GFP around the injection site at 24 hpi and 48 hpi (Fig. 6C,E; supplementary material Fig. S5D). The analysis of larvae that had been injected in the notochord revealed that GFP was expressed by leukocytes that were clustered around the notochord but not by notochordal cells (Fig. 6F). Additional GFP expression was detected in leukocytes that were scattered throughout the body and in the

keratinocytes surrounding the inflammation site (supplementary material Fig. S5E,F; Fig. 6J).

By early timepoints (18 hpi) 30% of GFP-positive cells (*il1b*⁺) also expressed the macrophage marker *mpeg1* (*mpeg1*⁺), whereas only 10% expressed the neutrophil marker *lysosymeC* (*lyz*⁺) (Fig. 6G,L). During the late stages of inflammation (48 hpi), two distinct populations of GFP-expressing cells were observed around the inflamed notochord – cells that expressed a high level of GFP [*il1b*^{high}, 60±6.5% (mean±s.e.m.)] and those that expressed a low level of GFP (*il1b*^{low}, 40±6.5%). At 48 hpi, no macrophages were *il1b*^{high}, whereas neutrophils (*lyz*⁺) comprised 68% of these *il1b*^{high} cells. The other 32% of *il1b*^{high} cells were *mpeg1*⁻ and *lyz*⁻ and unidentifiable. The remaining *il1b*^{low} cell population comprised 35% neutrophils (*il1b*^{low} *lyz*⁺) and 27% macrophages (*il1b*^{low} *mpeg1*⁺) (Fig. 6H-L).

In conclusion, our data suggest that *Il1b* production dynamically shifts from early timepoints of the inflammatory response – at which both macrophages and neutrophils contribute to *Il1b* production – to late phases, when neutrophils are the main source of *Il1b*.

***Il1b* is required for the early and late recruitment of neutrophils but not macrophages**

Morpholino-mediated gene knockdown was used to investigate the role of zebrafish *Il1b* during severe notochord inflammation. Reverse transcription (RT)-PCR analysis, performed using primers on both sides of the splice site that is targeted by the morpholino, provided evidence of strong blocking of splicing, whereas overall morphology was not noticeably affected (Fig. 7A; the general

morphology of the morphants is not shown). The *il1b* morpholino was injected into *Tg(mpx:GFP ; mpeg1:mCherryF)* embryos, and the morphants were infected by the injection of *E. coli* into the notochord. In embryos that had not been injected with morpholino, or those that had been injected with control scrambled morpholino, both neutrophils and macrophages were recruited to the inflamed notochord in a normal manner. In *il1b* morphants, neutrophil recruitment was slightly reduced at 4 hpi and strongly reduced at 48 hpi compared with controls (Fig. 7C,E-G); only macrophages localised around the notochord of *il1b* morphants at 4 and 48 hpi (Fig. 7G; supplementary material Fig. S7). The decreased neutrophil recruitment was not caused by a general reduction of the neutrophil population under steady-state conditions because the total number of neutrophils in *il1b* morphants was similar to that in uninjected embryos or embryos that had been injected with the control scrambled morpholino at 4 hpi (Fig. 7D for *il1b* morpholino compared to scrambled morpholino; data not shown for *il1b* morphants compared to uninjected larvae). Additionally, a reduction of the overall inflammatory response was excluded because macrophage recruitment was unaffected (Fig. 7G). Long-term examination of the infected *il1b* morphants revealed that loss of *il1b* prevented formation of the lesions that were often detected in the rostral part of the notochord after infection (Fig. 7H-J, lesions were found in one out of 12 *il1b* morphant fish and seven out of 11 scrambled morpholino fish). Taken together, these results establish an important and specific role for *Il1b* in the recruitment of neutrophils during chronic inflammation of the notochord and subsequent sequelae.

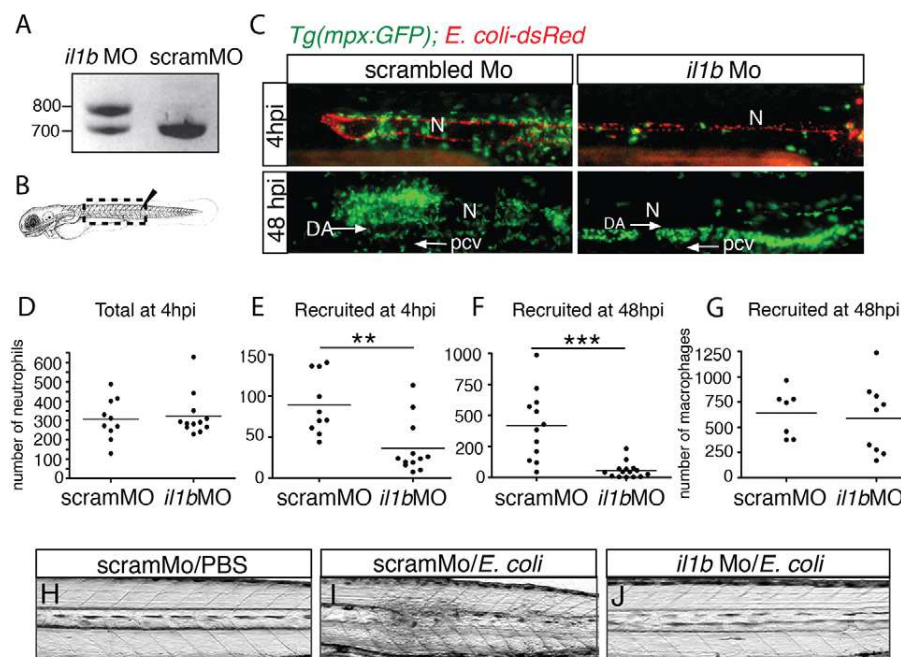


Fig. 7. *Il1b* is required for the early and late recruitment of neutrophils but not macrophages. PCR amplification of *il1b* cDNA from the 48 hpi intravenous-infected larvae, which had previously been injected with either scrambled morpholino (scramMO) or with a morpholino antisense oligonucleotide that blocked the splicing of intron 2 (*il1b*MO). (B) The diagram shows the region that is imaged in C (dashed box). (C) Recruitment of neutrophils (green) in *Tg(mpx:GFP)* larvae at 4 hours and 48 hours following the injection of DsRed-expressing *E. coli* (red) into the notochord. These larvae had been previously injected with scrambled morpholinos (scramMO) or *il1b* MO. N, notochord. At 48 hpi, many neutrophils were found in the AGM region, in between the dorsal aorta (DA) and the posterior caudal vein (pcv); arrows indicate the direction of blood flow. (D-G) Plots show the number of total neutrophils at 4 hpi (D) and the number of recruited neutrophils at 4 hpi (E) and 48 hpi (F). (G) The number of recruited macrophages at 48 hpi in similar experiments that were performed using *Tg(mpeg1:mCherryF)* larvae. Each point represents an individual larva, the bar represents the mean value. ***P*<0.005, ****P*<0.001. (H-J) Bright-field images of control (scramMO) and *il1b* morphants 3 days after injection of either PBS or *E. coli* into the notochord. Lateral views of the trunk region are shown in C,H,I,J.

DISCUSSION

This article describes a model of zebrafish notochord infection with *E. coli* that recapitulates several of the inflammatory aspects of bone and cartilage infection in human. We thus propose that the specific advantages of the larval zebrafish model system – transparency, genetic tractability – should facilitate the study of the early cellular and molecular inflammatory mechanisms that are related to matrix-tough tissue infections.

Notochord infection of the zebrafish larvae as a model to study inflammatory aspects of bone and cartilage infections

The similarity of the notochord with cartilage (in terms of transcriptional profile) and vertebral bone (in terms of structure and function) (Fleming et al., 2001; Stemple, 2005) prompted us to establish a model of the infection of this organ in order to mimic the inflammatory aspects of human osteomyelitis and osteoarthritis. As in some infections of human bones and joints, infection of the zebrafish notochord induces a severe inflammation that greatly outlasts the presence of live microbes and thus can be considered ‘chronic’ – taking into account due allowances. Indeed, injection of *E. coli* into the notochord leads to the rapid recruitment of both neutrophils and macrophages to the infected notochord within the first hour. The injection needle locally disrupts the collagen sheath, creating an opening for the leukocytes to phagocytose some bacteria in the notochord. However, probably because of the turgidity of the notochordal cells within the thick collagen sheath, neutrophils and macrophages fail to enter the notochord at sites distant from the injection site. This finding suggests that, in contrast to what is observed for transendothelial migration, leukocytes do not easily pass through all matrices. Even though the injected bacteria are cleared in less than one day, neutrophil and macrophage recruitment along the notochord persists for days, preventing the resolution of inflammation. Although they, initially, randomly spread around the notochord at 2 to 24 hpi, leukocytes accumulate in patches in the later stages of the response (from 48 hpi), suggesting that they are involved in the activation and recruitment of more leukocytes. Granules, the hallmarks of granulocytes, are stores of enzymes that participate in killing microbes and digesting tissues. We found that, from 2 dpi, despite the fact that injected microbes have been cleared by this point, neutrophils degranulate next to the notochord. Thus, the release and activation of proteolytic enzymes that are able to disassemble the collagen fibrils that impede neutrophil-bacteria contacts might explain the infiltration of neutrophils into the notochord, which is observed in the late phases of inflammation (Nathan, 2006). This neutrophil degranulation might be responsible for the tissue damage that is observed in notochord-infected larvae – including perturbation of extracellular matrix deposition, swelling and curvature of the notochord, and cellular clusters within the notochord that are reminiscent of the abscesses observed in human osteomyelitis (Lew and Waldvogel, 2004; Wright and Nair, 2010). The notochord lesion, which is induced by the severe inflammatory episode might contribute to the dismorphic vertebrae that were observed during adulthood. Although extracellular matrix deposition, neutrophil infiltration and tissue damage are the hallmarks of chronic infection, which occur in some osteomyelitis and septic arthritis individuals, curvature of the axial skeleton is reminiscent of that of observed in individuals that have bone tuberculosis. Indeed, also known as Pott disease, which accounts for 1–2% of overall tuberculosis cases, it is usually characterised by the spread of tuberculosis bacilli into the disc space from the vascular system, resulting in the destruction of the disc and progression to the bone of adjoining vertebral bodies. As the vertebrae degenerate and

collapse, a kyphotic deformity results (Moon, 1997). The chronic inflammation of the zebrafish notochord after bacterial clearance described here is also reminiscent of autoinflammatory disorders – such as chronic non-bacterial osteomyelitis, deficiency of IL-1 β receptor antagonist or neonatal-onset multisystem inflammatory disease. Although the etiology of chronic non-bacterial osteomyelitis is still unknown, deficiency of IL-1 β receptor antagonist and neonatal-onset multisystem inflammatory disease are caused by mutations in the *IL1RN* and *NLRP3* genes, respectively, and result in over-activation of the IL-1 β pathway (Morbach et al., 2013). Accordingly, neutrophil recruitment to the infected zebrafish notochord was found to be dependent on Il1b.

Elimination mechanism of *E. coli* in the notochord

Many bacteria avoid the immune response by hiding inside of cells of their host. By doing so, they are out of reach of the immune system and multiply within these cells before further invasion of the body. We have previously shown that, when injected into the notochord, non-pathogenic *Mycobacterium marinum* *Tes:A* mutant bacteria are internalised by notochordal cells as revealed, using TEM, by the presence of the bacteria in endosomes (Alibaud et al., 2011). Interestingly, similar bacterial internalisation has previously been reported for osteoblasts and chondrocytes (Diaz-Rodriguez et al., 2009; Wright and Nair, 2010; Jiao et al., 2013; Castillo and Kouri, 2004). All of these observations suggest that osteoblasts, chondrocytes and notochordal cells are non-professional phagocytes that engulf invader microbes. However, their phagocytic ability depends on the nature of these microbes. We observe here that notochordal cells do not phagocytose *E. coli*; bacteria remain extracellular for a few hours before being eliminated, as demonstrated by CFU assays, and fluorescence and electron microscopy. How are they killed? As leukocytes cannot phagocytose them, another mechanism must be used. The ‘unhealthy’ shape of some *E. coli* within the notochord, as observed by electron microscopy, suggests death by a humoral lysis mechanism that remains to be identified. The complement system is an obvious candidate, and we are currently studying the contribution of complement genes to the observed bacterial clearance.

Putative functions of Il1b in zebrafish

IL-1 β is a critical pro-inflammatory mediator of the host response to microbial infection. It acts on almost all cell types and has many functions – including growth and proliferation, the induction of adhesion molecules in epithelial cells, the activation of phagocytosis and release of proteases in macrophages and neutrophils, and the activation of B and T cells (Dinarello, 2009). Using transgenic zebrafish larvae that expressed farnesylated GFP under the control of the *il1b* promoter, we show here, for the first time, the dynamic transcriptional activity of *il1b* in a whole organism. Its expression during zebrafish development, especially in the keratinocytes of the caudal and pectoral fin bud, correlates with the regions of the body where active keratinocyte proliferation occurs. This is in agreement with findings in mammals where keratinocytes express IL-1 β (Kupper et al., 1986). However, resting keratinocytes express IL-1 β in its unprocessed biologically inactive form – pro-IL-1 β . Indeed, to be secreted as an active cytokine, pro-IL-1 β must be cleaved by caspases (caspase-1, caspase-11 and others), which are themselves activated through inflammasome assembly (Kayagaki et al., 2011). Although *il1b* transcription is low in most cell types and strongly inducible following the detection of microbial molecules – notably in myeloid cells – constitutive expression of pro-IL-1 β by some tissues should allow for a faster response to external injuries. This is logical for cells that are directly exposed to the environment –

such as keratinocytes, olfactory epithelial cells, enterocytes or neuromast cells – all cell types that were seen to spontaneously express endogenous *il1b* mRNA and GFP in the *Tg(il1b:GFP-F)* line. In zebrafish, *Il1b* has been shown to be structurally conserved compared with its human counterpart, and the *Il1b* pathway is also dependent on caspases (Ogryzko et al., 2014). Whether the active form of *Il1b* is produced in these zebrafish organs remains to be determined. Notably, spontaneous GFP expression in some cell types, such as those of neuromasts and the gut, mimics the spontaneous expression of GFP in the *Tg(NFκB:EGFP)* reporter transgenic zebrafish line (Kanther and Rawls, 2010), which is in agreement with the well-known contribution of NF-κB to *il1b* induction (Ogryzko et al., 2014).

In addition to its basal expression during development, GFP is also induced following *E. coli* infection in *Tg(il1b:GFP-F)* fish, which parallels endogenous *il1b* induction. This induction is strictly correlated in intensity and time with the recruitment of leukocytes. Indeed, infection in muscles induces a low level of expression that quickly resolves, whereas infection of the notochord induces strong and persistent expression. The GFP expression level decreases one day before the resolution of inflammation. In most mammalian systems, IL-1β has been reported to be mainly produced by circulating monocytes, tissue macrophages and dendritic cells (Dinarello, 2009). Here, we describe that, in our zebrafish notochord infection model, *il1b* is first expressed in macrophages during the early phase of inflammation and is mainly expressed by neutrophils during the late phases. This is reminiscent of the recent work of Karmakar and collaborators, which shows that neutrophils are the main source of *Il1b* in response to *Pseudomonas aeruginosa* in mouse, highlighting the importance of activated neutrophils in mediating inflammation (Karmakar et al., 2012).

One interesting question arising from the present work is which signal stimulates the recruitment of leukocytes to the infected notochord? Is it a primary signal that is actively emitted by the notochordal cells, does it come from the injected bacteria or does it correspond to bacterial leftovers after destruction within the notochord? We are currently investigating this latter hypothesis through the injection of different bacterial products into the notochord of larvae and evaluating their ability to recruit leukocytes.

Our data demonstrate that *il1b* is not expressed by notochordal cells after *E. coli* injection; however, it is partially required for the initial recruitment of neutrophils, even though a low number of neutrophils is still recruited to the infected notochord in the absence of *il1b*. *Il1b* is also required for the persistence of neutrophils at the inflammation site, but it has no effect on macrophage recruitment, suggesting that *Il1b* is a signal produced by recruited leukocytes themselves that amplifies the activation of neutrophils and prevents resolution of inflammation. If neutrophils do not encounter a bacterium, they are thought to degranulate to promote tissue digestion in order to gain access to bacteria (Nathan, 1987). Indeed, we show that the notochord is not directly accessible to neutrophils, thus degranulation might produce cellular and matrix debris that maintain inflammation around the notochord. Therefore, multiple different signals probably induce and maintain the inflammatory response.

IL-1β is a key player in the inflammatory process that occurs in bone diseases (Wright and Nair, 2010). The neutralisation of IL-1β signalling appears to be crucial for the potential therapy of osteomyelitis, but also for other inflammatory diseases, such as rheumatoid arthritis. Several specific drugs that inhibit this pathway are currently used to improve the symptoms of these diseases (Dinarello, 2004). Interestingly, in our model, knocking down *il1b*

suppressed the long lasting inflammation. We therefore consider the zebrafish model to be perfectly adapted to the challenge of dissecting the exact function of *il1b* during chronic inflammation of bone and joints.

MATERIALS AND METHODS

Ethics statement

All animal experiments that are described in the present study were conducted at the University Montpellier 2 according to European Union guidelines for the handling of laboratory animals (http://ec.europa.eu/environment/chemicals/lab_animals/home_en.htm) and were approved by the Direction Sanitaire et Vétérinaire de l'Hérault and Comité d'Éthique pour l'Expérimentation Animale under reference CEEA-LR-13007.

Zebrafish line and maintenance

Fish maintenance, staging and husbandry were as described previously (Alibaud et al., 2011) under standard conditions (Westerfield, 2007). Experiments were performed using the F1 golden zebrafish mutant (Lamason et al., 2005), originally purchased from Antinea, and using the transgenic line *Tg(mpx:GFP)* (kind gift from Steve Renshaw, MRC Centre for Developmental and Biomedical Genetics, Sheffield, UK) to visualise neutrophils. Embryos were obtained from pairs of adult fish by natural spawning and raised at 28.5°C in tank water. Embryos and larvae were staged as described previously (Kimmel et al., 1995).

Statistical analysis

Student's *t*-tests (two-tailed, unpaired) were performed in Fig. 1K; Fig. 4C,D; Fig. 5J; Fig. 6L and Fig. 7D-G.

For statistics on the survival of larvae that had been infected with *E. coli*, the survival rate of each of the populations of injected embryos was compared with that of the uninjected embryos using the log-rank (Mantel-Cox) test using GraphPad Prism 4 (Graphpad Software).

Transgenic line construction

Based upon the work of Ellett et al. (Ellett et al., 2011), we cloned a new version of the *mpeg1* promoter to drive the specific expression of a red fluorescent membrane-targeted protein. A 1.9-kb fragment of the *mpeg1* promoter was amplified from genomic DNA using primers zMpeg1P4 (5'-TTGGAGCACATCTGAC-3') and zMpeg1E2N2 (5'-TTATAGCGCCGCGAAATGCTCTTGACTTCATGA-3'), digested by NotI and then ligated to the reading frame of the farnesylated mCherry (mCherry-F) protein so that the *mpeg1* AUG was in-frame with the downstream mCherry-F open reading frame. The plasmid was injected in one-cell stage embryos together with the Tol2 transposase RNA. F0-microinjected embryos were screened using the expression of the transgene in macrophages, as described previously (Ellett et al., 2011), and stable lines were established. The same strategy was used to clone a 3.4-kb fragment of the *il1b* promoter using primers P2 (5'-ATGAGCTCCGAAATTCAGCTGG-3') and E2N (5'-TTATAGCGCCGCTTGCCCGCATGCCATCATTCTA-3').

Quantitative real-time RT-PCR analysis of cytokines

To determine the relative expression of *il1b* and *cxcl-c5c*, total RNA from infected larvae and controls (pools of ~10 larvae each) was prepared at different timepoints post-infection. RNA preparation, reverse transcription and quantitative real-time PCR, including statistical analysis, have been described elsewhere (Aggad et al., 2009). The primers used were as follows: zIL1b.fw, 5'-TGGACTTCGCAGCACAAAATG-3'; zIL1b.rv, 5'-GTTC-ACTTCACGCTCTTGATG-3'; zEF1a.fw, 5'-TTCTGTTACTCTGGC-AAAGGG-3'; zEF1a.rv, 5'-TTCAGTTTGTCCAACACCCA-3'; CXCL-C5C.fw, 5'-AACCAAGTCCATCCTGCTCA-3'; CXCL-C5C.rv, 5'-CGTTAGGATCCAAACACACCT-3'.

Embryo and larva manipulation

For *il1b* loss-of-function assays, we designed morpholino antisense oligonucleotides that specifically hybridised with the splicing site between intron 2 and exon 3 – morpholino sequence 5'-CCCACAACTGCAAAA-TATCAGCTT-3'. The oligonucleotides against *il1b* (3 nl at a final

concentration of 0.5 mM), or scrambled morpholinos (5'-AATCACAAG-CAGTGCAAGCATGATG-3', 3 nl at a final concentration of 0.5 mM) were injected into one-cell stage embryos. No side effect was observed. Efficiency was tested by using RT-PCR with primers for both sides of the morpholino target sequence: *zil1b.30*, 5'-TGCCGGTCTCCTTCCTGA-3' and *zil1b.50*, 5'-GCAGAGGAACCTAACAGCT-3' (Fig. 7A). Sequencing confirmed the retention of the second intron of *il1b*, leading to a frame shift and premature stop codon. Larvae were infected with *Escherichia coli* K12 bacteria that harboured DsRed (van der Sar et al., 2003), Crimson (Clontech), or a GFP expression plasmid and had been grown in Luria broth (LB) with appropriate antibiotics. Overnight stationary-phase cultures were centrifuged (1 minute, 10,000 g), and the bacteria were resuspended in sterile PBS (2×10^9 – 4×10^9 CFU/ml) and then injected into the muscle, caudal vein or notochord of 48- to 50-hpf larvae (Alibaud et al., 2011; Colucci-Guyon et al., 2011).

Imaging of live zebrafish larvae

Larvae were anaesthetised in 0.01% 3-amino benzoic acid ethylester (Tricaine), positioned on 35-mm glass-bottomed dishes (WillCo-dish®), immobilised in 0.8% low-melting-point agarose and covered with 2 ml of embryo water containing Tricaine. Epifluorescence microscopy was performed by using an MVX10 Olympus MacroView microscope that was equipped with MVPLAPO 1× objective and XC50 camera. Confocal microscopy was performed using a Leica SPE upright microscope with 40× HCX APO L 0.80 W and 20× CHX APO L 0.5 W objectives. Time-lapse acquisitions were performed at 23–26°C. The 4D files generated by the time-lapse acquisitions were processed using ImageJ. Three-dimensional reconstructions and optical sectioning were performed on the four-dimension files using Imaris (Bitplan AG, Zurich, Switzerland).

CFU count

Individual larvae were lysed in 1% Triton-X100 and homogenised with a 26G syringe five to six times. The resultant debris and notochords were washed twice in PBS and incubated for 30 minutes at 30°C with agitation in the presence of 10 mg/ml collagenase that had been dissolved in PBS supplemented with 1 mM CaCl₂. A fraction of the total lysate was plated on selective LB agar plates.

Histology and sectioning

Larvae were fixed at 4–5 days post-infection in Bouin's solution and washed in 70% ethanol. After successive dehydration, butanol and Paraplast baths, larvae were embedded in Paraplast X-TRA (Sigma), sectioned (using a Leitz Wetzlar Microtome), stained with Masson's trichrome and imaged (using a Nanozoomer Slide scanner with 40× objective). For bone staining, juvenile fish were fixed in 4% paraformaldehyde in PBS for 48 hours at 4°C, dehydrated with 100% ethanol over 4 days, stained with Alizarin red (Javidan and Schilling, 2004) and transferred to 100% glycerol over the course of 1 week before analysis and storage.

Isolation of mRNA from fluorescently labelled neutrophils and macrophages

Double transgenic larvae *Tg(mpx:eGFP/mpeg1:mCherry-F)* were injected with *E. coli* K12 or PBS into the notochord at 2 dpf. At 2 dpi, 40 anaesthetised larvae per sample were allocated to each well of a 6-well plate and dissociated in 2 ml of trypsin 0.25% with 0.5 mM EDTA for 1 hour at 33°C with pipetting every 10 minutes for correct dissociation. Reactions were stopped by the addition of CaCl₂ (final concentration 1 mM) and foetal calf serum (final concentration 10%). The lysates were passed through a 40-µm mesh filter, washed twice with 1% FCS in PBS and sorted by fluorescence-activated cell sorting (MoFlo Astrios EQ) for GFP-labelled neutrophils and mCherry-labelled macrophages for collection directly into lysate buffer solutions for mRNA extractions using the RNAqueous-micro kit (Ambion).

Larva dissociation and cell culture

Double transgenic larvae *Tg(il1b:eGFP/mpeg1:mCherry-F)* or *Tg(il1b:eGFP/LysC:mCherry)* at 4 dpf were anaesthetised and trypsinised individually in 6-well plates, as described above. After washing with 1% FCS in PBS, the cell

suspensions were cultured in Leibovitz L-15 medium (21083-027, Gibco) for 1 hour at 30°C. Non-attached cells were then removed, and the attached macrophages and neutrophils were supplied with fresh L-15 medium and incubated at 30°C for an additional 3 hours before confocal imaging.

This article is part of a Special Issue, Spotlight on Zebrafish: Translational Impact. See all the articles in the issue at <http://dmm.biologists.org/content/7/7.toc>.

Acknowledgements

We thank Karima Kissa, Paul Guglielmi and the members of DIMNP for helpful discussions; Evelyse Grousset for her help with histological sectioning; Pierre-Henri Commère for fluorescence-activated cell sorting, Steve Renshaw for providing the *Tg(mpx:GFP)* line and Vincent Domergue for helping to generate the *Tg(il1b:GFP-F)* line.

Competing interests

The authors declare no competing financial interests.

Author contributions

M.N.-C. and G.L. conceived and designed the experiments. M.N.-C., Q.T.P., C.G. and J.-F.D. performed the experiments. C.G. contributed reagents and materials. M.N.-C., Q.T.P., J.-F.D. and J.-P.L. analysed the data. M.N.-C. and G.L. wrote the paper.

Funding

This work was supported by the French Agence Nationale de la Recherche [ANR-10-MIDI-009, ZebraFlam]. The research leading to these results also received funding from the European Community's Seventh Framework Programme (FP7-PEOPLE-2011-ITN) under the Marie-Curie Initial Training Network FishForPharma [grant agreement no. PITN-GA-2011-289209]. Q.T.P. is a Marie-Curie fellow. We wish to thank the InfectioPôle Sud for funding part of the fish facility and the Montpellier RIO Imaging facility.

Supplementary material

Supplementary material available online at <http://dmm.biologists.org/lookup/suppl/doi:10.1242/dmm.014498/-/DC1>

References

- Aggad, D., Mazel, M., Boudinot, P., Mogensen, K. E., Hamming, O. J., Hartmann, R., Kotenko, S., Herbomel, P., Lutfalla, G. and Levraud, J. P. (2009). The two groups of zebrafish virus-induced interferons signal via distinct receptors with specific and shared chains. *J. Immunol.* **183**, 3924–3931.
- Alibaud, L., Rombouts, Y., Trivelli, X., Burguière, A., Cirillo, S. L., Cirillo, J. D., Dubremetz, J. F., Guérardel, Y., Lutfalla, G. and Kremer, L. (2011). A *Mycobacterium marinum* TesA mutant defective for major cell wall-associated lipids is highly attenuated in *Dictyostelium discoideum* and zebrafish embryos. *Mol. Microbiol.* **80**, 919–934.
- Castillo, E. C. and Kourí, J. B. (2004). A new role for chondrocytes as non-professional phagocytes. An in vitro study. *Microsc. Res. Tech.* **64**, 269–8.
- Colucci-Guyon, E., Tinevez, J. Y., Renshaw, S. A. and Herbomel, P. (2011). Strategies of professional phagocytes in vivo: unlike macrophages, neutrophils engulf only surface-associated microbes. *J. Cell Sci.* **124**, 3053–3059.
- Deng, Q., Sarris, M., Bennin, D. A., Green, J. M., Herbomel, P. and Huttenlocher, A. (2013). Localized bacterial infection induces systemic activation of neutrophils through Cxcr2 signaling in zebrafish. *J. Leukoc. Biol.* **93**, 761–769.
- Diaz-Rodriguez, L., Garcia-Martinez, O., Arroyo-Morales, M., Reyes-Botella, C. and Ruiz, C. (2009). Antigenic phenotype and phagocytic capacity of MG-63 osteosarcoma line. *Ann. N. Y. Acad. Sci.* **1173** Suppl 1, E46–54.
- Dinarelli, C. A. (2004). Therapeutic strategies to reduce IL-1 activity in treating local and systemic inflammation. *Curr. Opin. Pharmacol.* **4**, 378–385.
- Dinarelli, C. A. (2009). Immunological and inflammatory functions of the interleukin-1 family. *Annu. Rev. Immunol.* **27**, 519–550.
- Ellett, F., Pase, L., Hayman, J. W., Andrianopoulos, A. and Lieschke, G. J. (2011). *mpeg1* promoter transgenes direct macrophage-lineage expression in zebrafish. *Blood* **117**, e49–e56.
- Fleming, A., Keynes, R. J. and Tannahill, D. (2001). The role of the notochord in vertebral column formation. *J. Anat.* **199**, 177–180.
- Gutierrez, K. (2005). Bone and joint infections in children. *Pediatr. Clin. North Am.* **52**, 779–794, vi. (vi).
- Javidan, Y. and Schilling, T. F. (2004). Development of cartilage and bone. *Methods Cell Biol.* **76**, 415–436.
- Jiao, K., Zhang, J., Zhang, M., Wei, Y., Wu, Y., Qiu, Z. Y., He, J., Cao, Y., Hu, J., Zhu, H. et al. (2013). The identification of CD163 expressing phagocytic chondrocytes in joint cartilage and its novel scavenger role in cartilage degradation. *PLoS ONE* **8**, e53312.
- Kanther, M. and Rawls, J. F. (2010). Host-microbe interactions in the developing zebrafish. *Curr. Opin. Immunol.* **22**, 10–19.
- Karmakar, M., Sun, Y., Hise, A. G., Rietsch, A. and Pearlman, E. (2012). Cutting edge: IL-1β processing during *Pseudomonas aeruginosa* infection is mediated by

- neutrophil serine proteases and is independent of NLRC4 and caspase-1. *J. Immunol.* **189**, 4231-4235.
- Kayagaki, N., Warming, S., Lamkanfi, M., Vande Walle, L., Louie, S., Dong, J., Newton, K., Qu, Y., Liu, J., Heldens, S. et al. (2011). Non-canonical inflammasome activation targets caspase-11. *Nature* **479**, 117-121.
- Kimmel, C. B., Ballard, W. W., Kimmel, S. R., Ullmann, B. and Schilling, T. F. (1995). Stages of embryonic development of the zebrafish. *Dev. Dyn.* **203**, 253-310.
- Kupper, T. S., Ballard, D. W., Chua, A. O., McGuire, J. S., Flood, P. M., Horowitz, M. C., Langdon, R., Lightfoot, L. and Gubler, U. (1986). Human keratinocytes contain mRNA indistinguishable from monocyte interleukin 1 alpha and beta mRNA. Keratinocyte epidermal cell-derived thymocyte-activating factor is identical to interleukin 1. *J. Exp. Med.* **164**, 2095-2100.
- Lamason, R. L., Mohideen, M. A., Mest, J. R., Wong, A. C., Norton, H. L., Aros, M. C., Jurynech, M. J., Mao, X., Humphreville, V. R., Humbert, J. E. et al. (2005). SLC24A5, a putative cation exchanger, affects pigmentation in zebrafish and humans. *Science* **310**, 1782-1786.
- Lew, D. P. and Waldvogel, F. A. (2004). Osteomyelitis. *Lancet* **364**, 369-379.
- Lieschke, G. J., Oates, A. C., Crowhurst, M. O., Ward, A. C. and Layton, J. E. (2001). Morphologic and functional characterization of granulocytes and macrophages in embryonic and adult zebrafish. *Blood* **98**, 3087-3096.
- Meijer, A. H. and Spaik, H. P. (2011). Host-pathogen interactions made transparent with the zebrafish model. *Curr. Drug Targets* **12**, 1000-1017.
- Moon, M. S. (1997). Tuberculosis of the spine. Controversies and a new challenge. *Spine* **22**, 1791-1797.
- Morbach, H., Hedrich, C. M., Beer, M. and Girschick, H. J. (2013). Autoinflammatory bone disorders. *Clin. Immunol.* **147**, 185-196.
- Nathan, C. F. (1987). Neutrophil activation on biological surfaces. Massive secretion of hydrogen peroxide in response to products of macrophages and lymphocytes. *J. Clin. Invest.* **80**, 1550-1560.
- Nathan, C. (2006). Neutrophils and immunity: challenges and opportunities. *Nat. Rev. Immunol.* **6**, 173-182.
- Ogryzko, N. V., Hoggett, E. E., Solaymani-Kohal, S., Tazzyman, S., Chico, T. J., Renshaw, S. A. and Wilson, H. L. (2014). Zebrafish tissue injury causes up-regulation of interleukin-1 and caspase dependent amplification of the inflammatory response. *Dis. Model. Mech.* **7**, 259-264. PubMed
- Patel, M., Rojavin, Y., Jamali, A. A., Wasielewski, S. J. and Salgado, C. J. (2009). Animal models for the study of osteomyelitis. *Semin. Plast. Surg.* **23**, 148-154.
- Pettit, A. R., Chang, M. K., Hume, D. A. and Raggatt, L. J. (2008). Osteal macrophages: a new twist on coupling during bone dynamics. *Bone* **43**, 976-982.
- Renshaw, S. A. and Trede, N. S. (2012). A model 450 million years in the making: zebrafish and vertebrate immunity. *Dis. Model. Mech.* **5**, 38-47.
- Renshaw, S. A., Loynes, C. A., Trushell, D. M., Elworthy, S., Ingham, P. W. and Whyte, M. K. (2006). A transgenic zebrafish model of neutrophilic inflammation. *Blood* **108**, 3976-3978.
- Stemple, D. L. (2005). Structure and function of the notochord: an essential organ for chordate development. *Development* **132**, 2503-2512.
- van der Sar, A. M., Musters, R. J., van Eeden, F. J., Appelmeik, B. J., Vandenbroucke-Grauls, C. M. and Bitter, W. (2003). Zebrafish embryos as a model host for the real time analysis of Salmonella typhimurium infections. *Cell. Microbiol.* **5**, 601-611.
- Westerfield, M. (2007). *The Zebrafish Book: A Guide for the Laboratory Use of Zebrafish (Danio rerio)*, 5th edn. Eugene: University of Oregon Press.
- Wright, J. A. and Nair, S. P. (2010). Interaction of staphylococci with bone. *Int. J. Med. Microbiol.* **300**, 193-204.
- Wright, H. L., Moots, R. J., Bucknall, R. C. and Edwards, S. W. (2010). Neutrophil function in inflammation and inflammatory diseases. *Rheumatology (Oxford)* **49**, 1618-1631.

SUPPLEMENTARY FIGURES AND TABLES AND THEIR LEGENDS

Transient infection of the zebrafish notochord triggers chronic inflammation

Mai Nguyen-Chi ^{1,2,5}, Quang Tien Phan ^{1,2,5}, Catherine Gonzalez ^{1,2}, Jean-François Dubremetz ^{1,2}, Jean-Pierre Levraud ^{3,4} and Georges Lutfalla ^{1,2}.

¹Dynamique des Interactions Membranaires Normales et Pathologiques, Université Montpellier 2, UMR 5235, case 107, Place Eugène Bataillon, 34095 Montpellier Cedex 05, France.

²CNRS; UMR 5235, Place Eugène Bataillon, 34095 Montpellier Cedex 05, France.

³Macrophages et Développement de l'Immunité, Institut Pasteur, Paris F-75015, France.

⁴CNRS URA2578, Paris F-75015, France

⁵These authors contributed equally to this work

Correspondence to Mai Nguyen Chi and Georges Lutfalla, Dynamique des Interactions Membranaires Normales et Pathologiques, Université de Montpellier 2, UMR 5235, CNRS, case 107, Place Eugène Bataillon, 34095 Montpellier Cedex 05, France.

E-mail addresses: mai.nguyen-chi@univ-montp2.fr and lutfalla@univ-montp2.fr

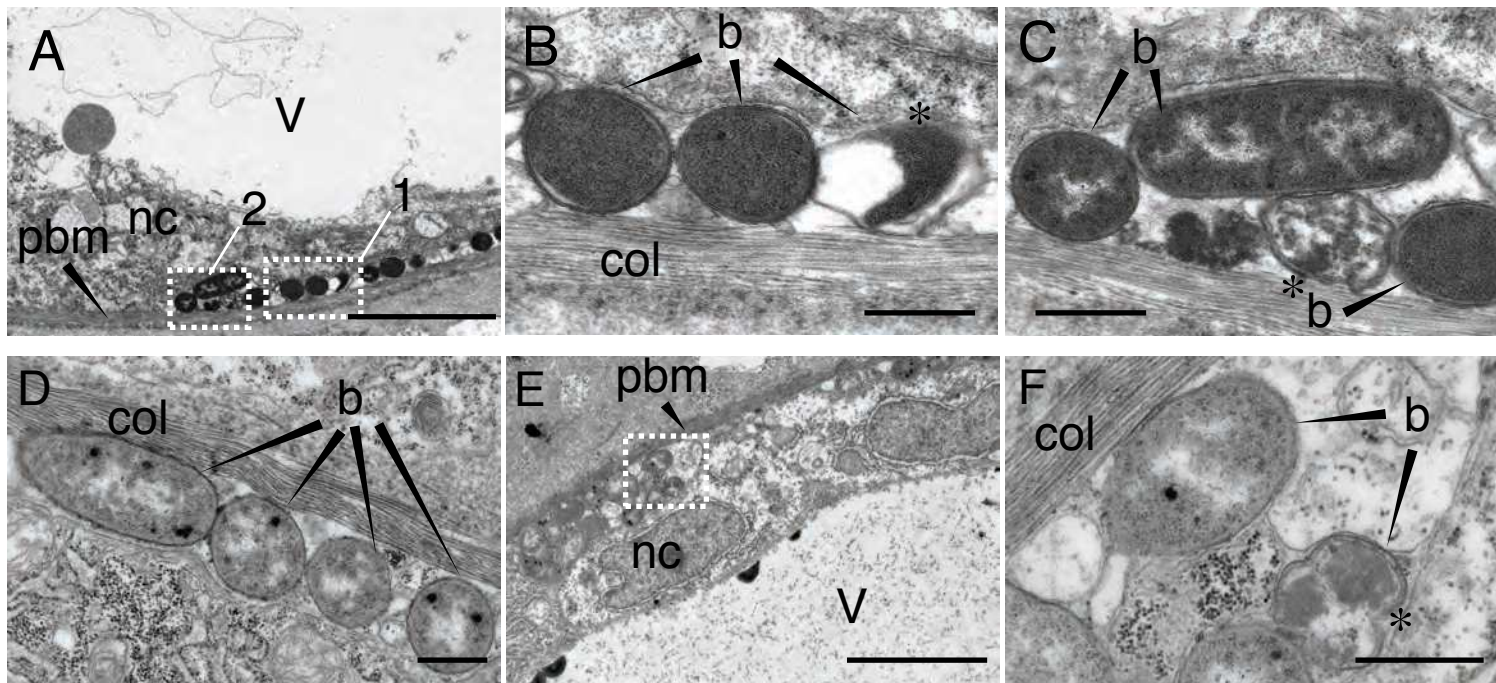


Figure S1: *E. coli* remains extracellular in the notochord of infected larvae.

Ultra-structural analysis using transmission electron microscopy of notochord infected larvae with *E. coli*, 15 min after infection (A-C) and 2 hpi (D-F). (B) and (C) are high magnification of regions boxed in (A), box 1 and 2, respectively. and (F) of region boxed in (E). Asterisks show bacteria whose morphology is altered. b: bacteria, pbm: peri-notochordal basement membrane, col: collagen sheath, nc: notochordal cell, v: vacuole. Scale bars : 5 μm in A and E, 0.5 μm in B, C, D and F.

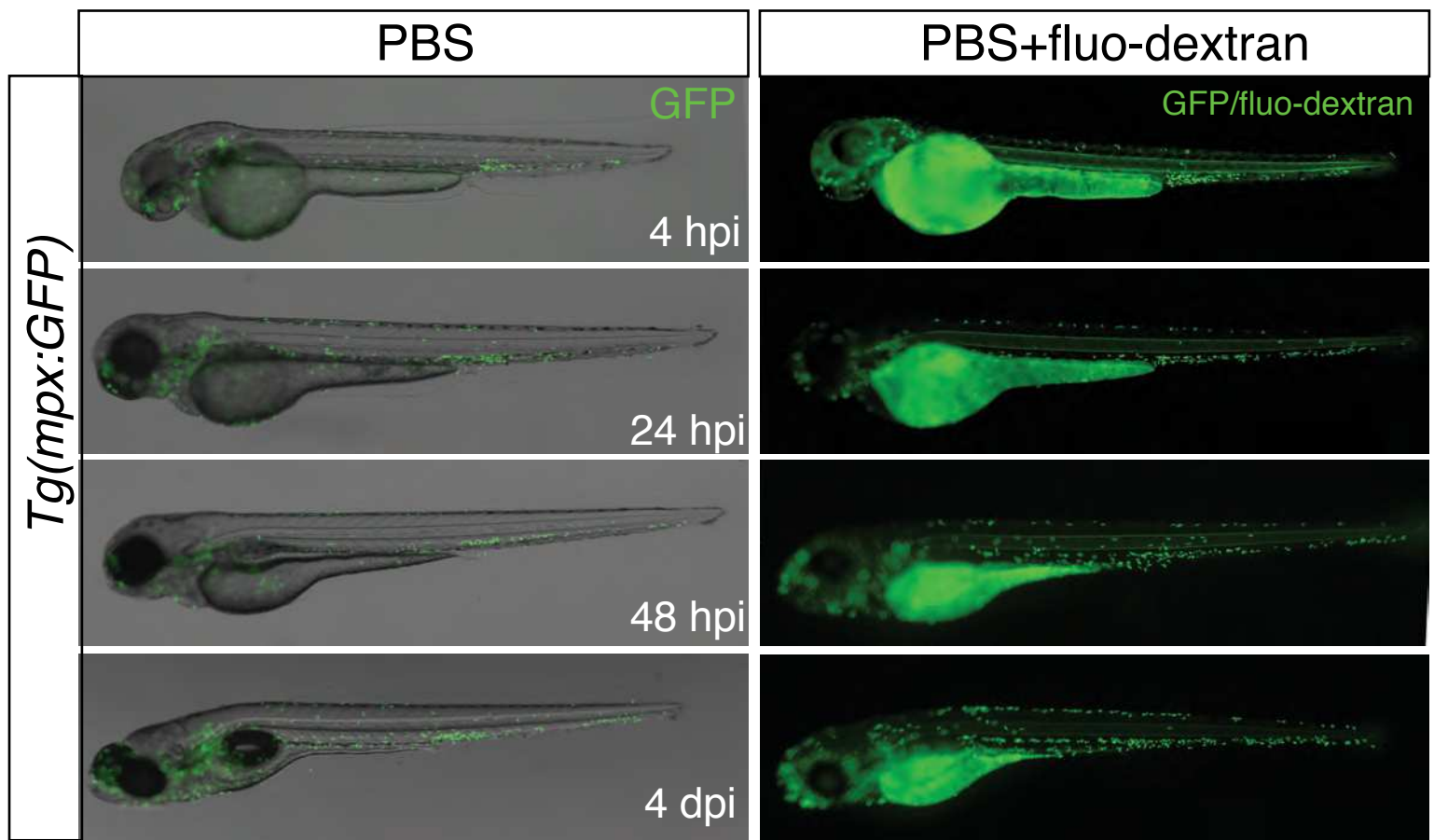
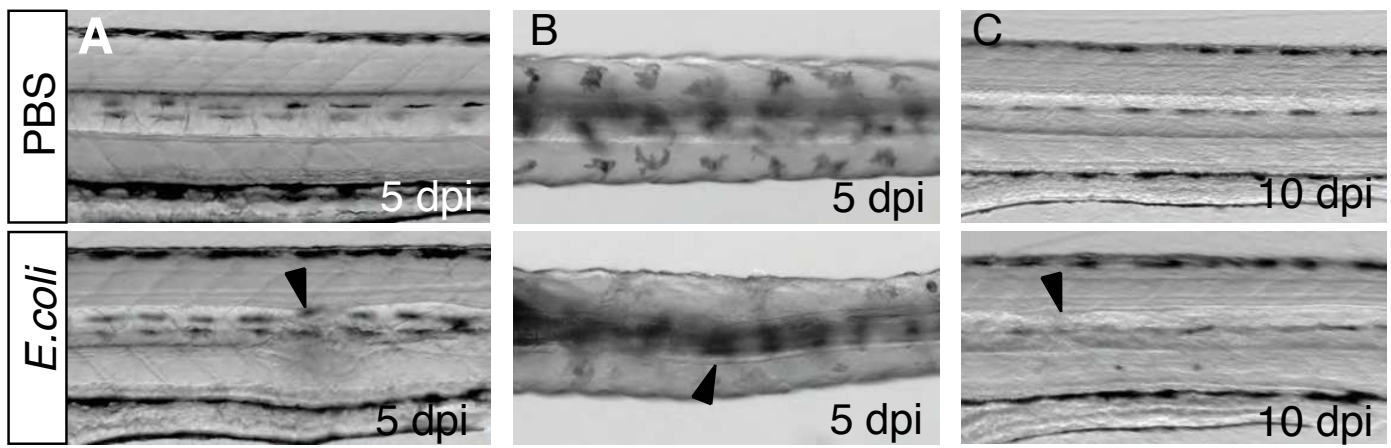
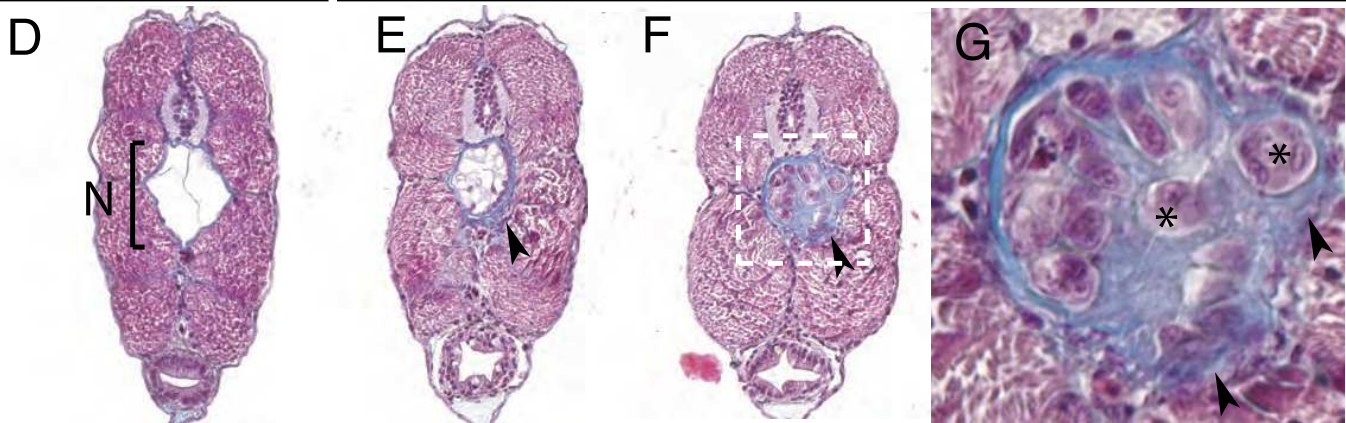


Figure S2: Effect of PBS injection in the notochord on neutrophil recruitment.

To check the effect of the injection in the notochord *per se* on neutrophil recruitment, PBS was injected in the notochord of *Tg(mpx:GFP)* larvae. No neutrophil was recruited to the notochord (visible with bright-field). To confirm and follow the injection in the notochord, PBS combined with Fluorecein-dextran (green) was injected in the notochord of *Tg(mpx:GFP)* larvae. Larvae were imaged at different time points following injection: 4, 24, 48 hpi and 4dpi and no recruited neutrophils (green) was detected.



PBS	<i>E. coli</i>
-----	----------------



PBS	<i>E. coli</i>
-----	----------------

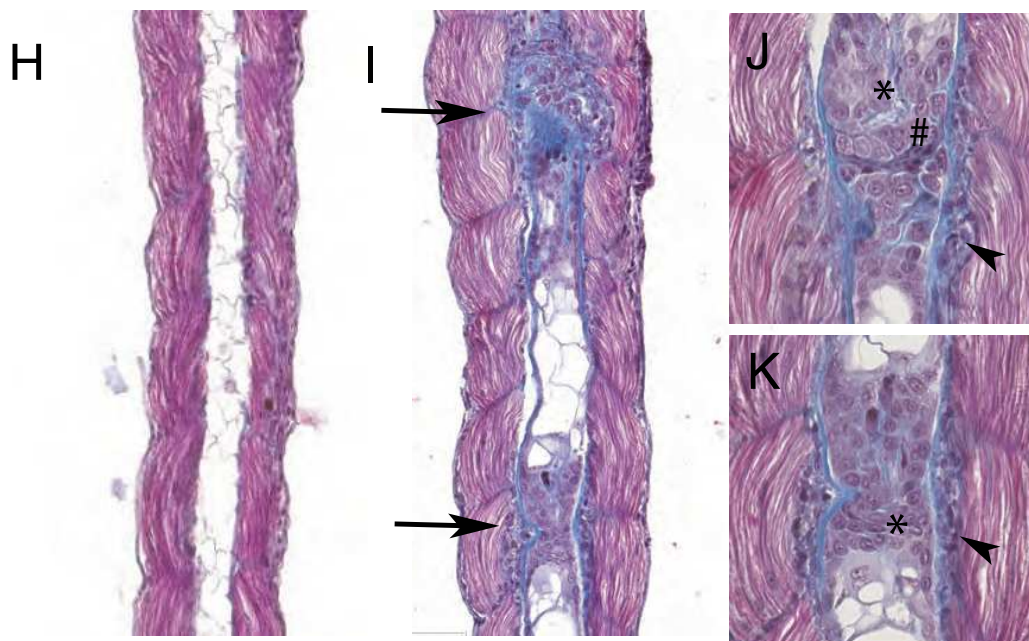


Figure S3: Notochord infection induces notochord defects

Bright-field images of PBS or *E. coli* injected larvae in the notochord at 5 dpi (A-B) and 10 dpi (C). A, C lateral views; B, dorsal view. Arrowheads show defects in the notochord anterior of the injection site (5 to 10 somites away). (D-G) 4 μ m cross sections of PBS (D) or *E. coli* (E-G) injected larvae stained with Masson's Trichrome. While PBS injected larvae present a notochord (N, bracket) filled mainly with 2 or 3 big vacuolated cells (white) and delimited with a regular, unaffected collagen membrane (blue), *E. coli* injected larvae present several abnormalities of the notochord. Numerous cells and vacuoles are found inside the notochord. Increase of collagen deposition appears inside and outside the notochord (arrowhead). Many cells are embedded inside the collagen sheath (asterisks). (G) is a high magnification image of the region boxed in (F). (H-K) 4 μ m longitudinal sections of PBS (H) or *E. coli* (I-K) infected larvae stained with Masson's Trichrome. As described above, PBS injected larvae present a notochord filled mainly with vacuolated cells (H), while *E. coli* infected larvae present several massive cell aggregates within the notochord (I). In these locations, the notochord is surrounded with cells embedded in the matrix (arrow heads) and cells with different

Tg(il1b:GFP-F)

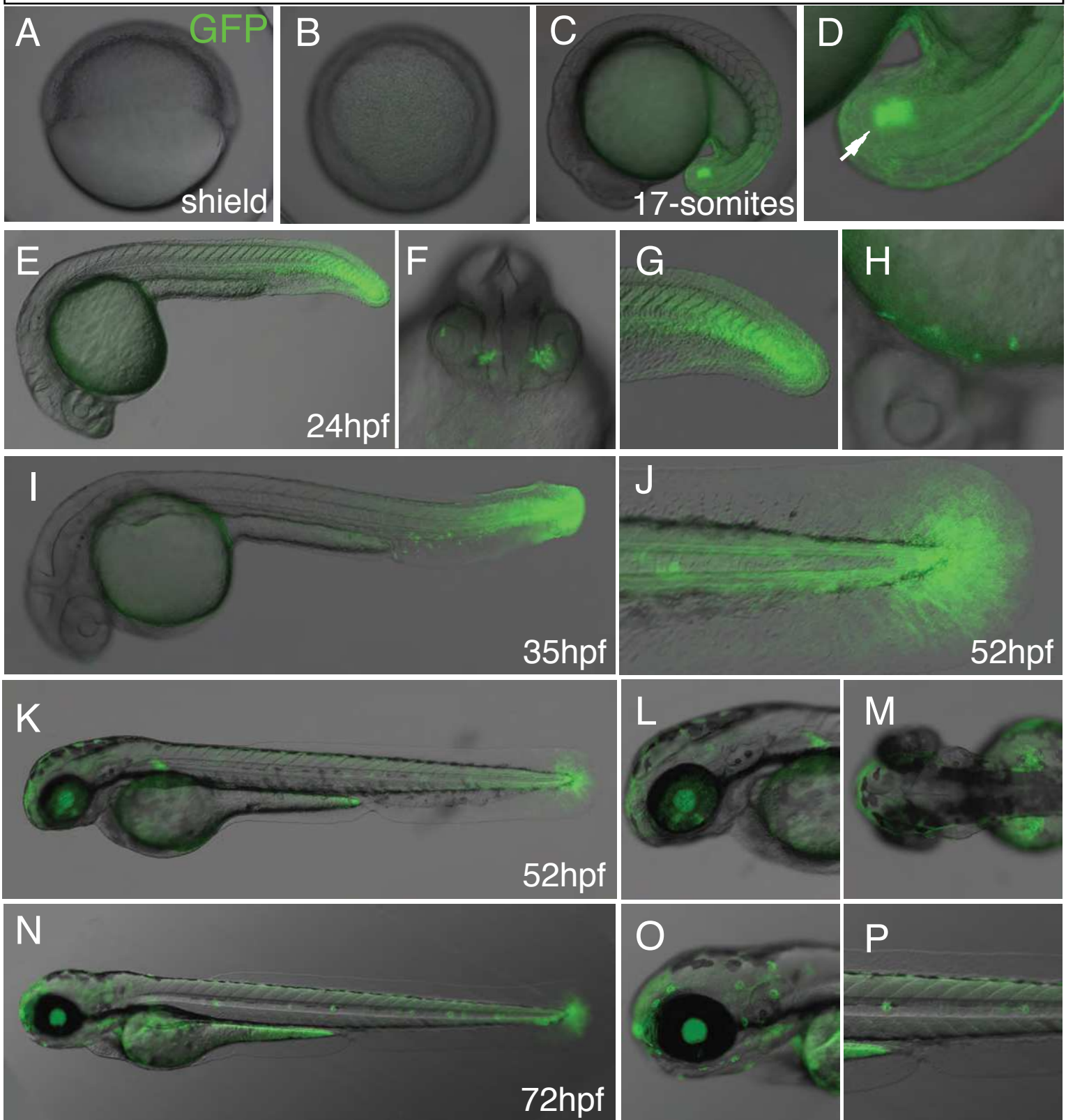
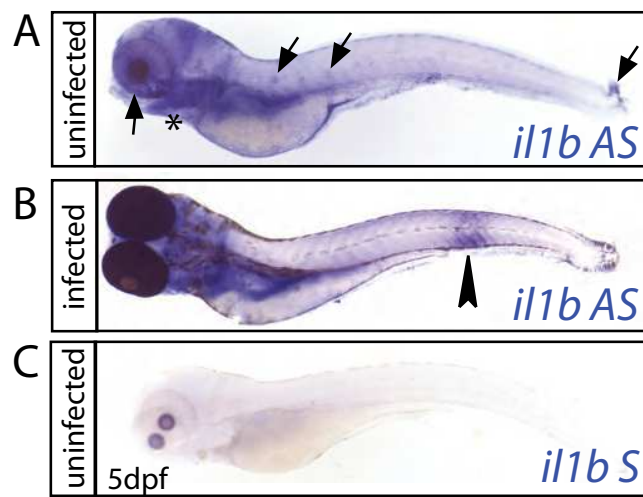


Figure S4: GFP expression in *Tg(il1b:GFP-F)* embryos and larvae during normal development.

(A-B) GFP is not detected during gastrulation: Shield stage, side view with animal pole on top (A) and animal pole view (B). (C-D) GFP is first detected during segmentation in the tail bud, especially in the tip (arrow). (E-I) This expression pattern is seen at 24 and 35hpf, with in addition expression in the olfactory epithelium (F) and in scattered cells on the yolk sac (H). (J-P) From 50 hpf GFP is detected in the tip of the tail and of the caudal fin, especially in the keratinocytes. In addition it is observed in the pectoral fin bud, the retina and the neuromasts. This expression was constant during one month. (C-P) lateral views except (F) (front) and (M) (dorsal).



D *Tg(il1b:F-GFP)* *E.coli-DsRed*

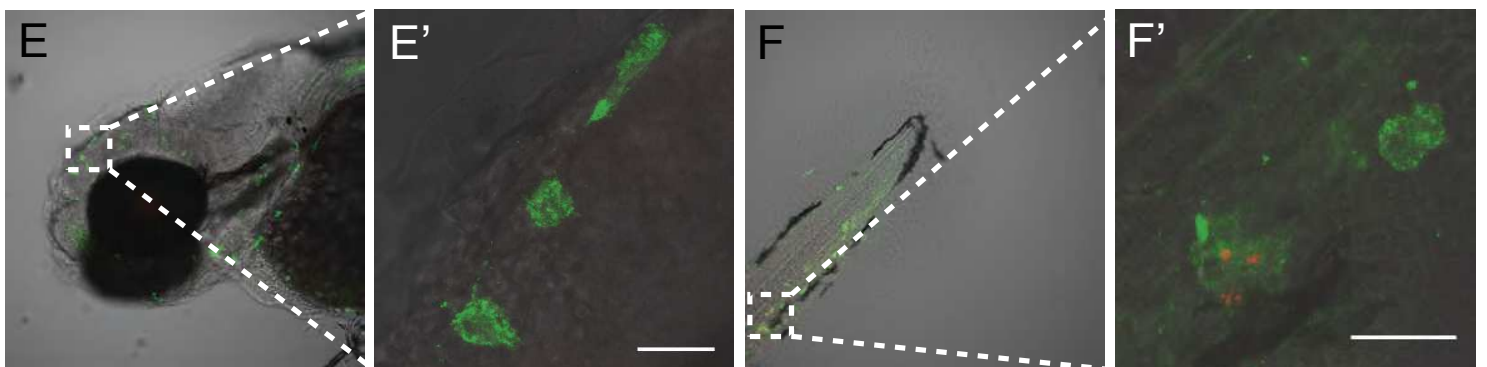
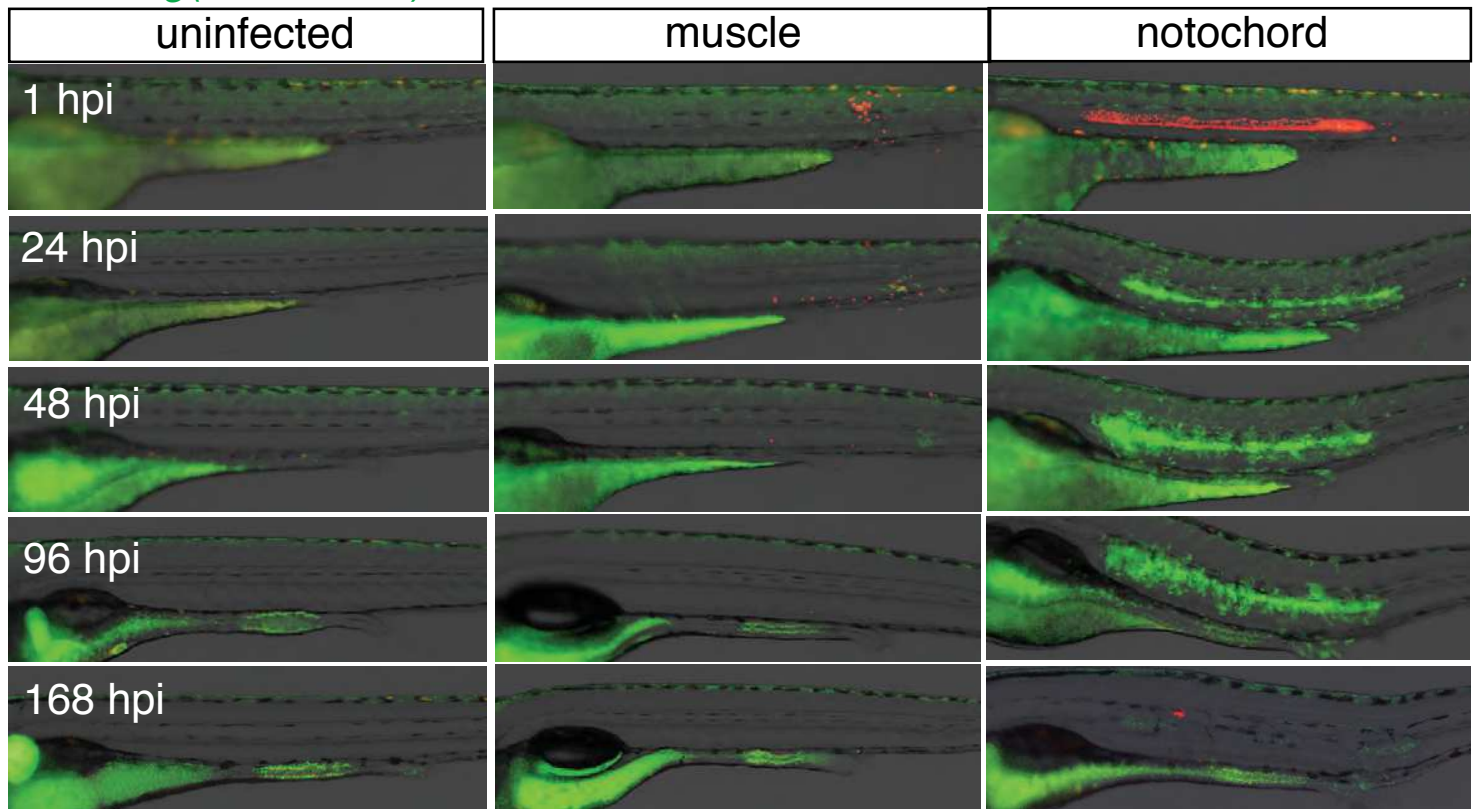


Figure S5: transcriptional activation of *il1b* upon infection with *E. coli*

(A-B) Whole mount in situ hybridization with *il1b* anti-sense (*il1b* AS) probe in 5dpf larvae uninfected (A) and infected with *E. coli* in the notochord (3dpi) (B). Probe signal is detected in the tip of the caudal fin, the skin, the neuromast, eyes (arrows) and gills (asterisks). After infection, larvae overexpress *il1b* mRNA in the inflamed region (arrowhead). (C) No signal is detected using *il1b* sense probe (*il1b* S) (C). (D) GFP (green) expression in *Tg(il1b:GFP-F)* larvae. Larvae were imaged without infection or at different time points following infection with a DsRed expressing *E. coli* (red) in the muscle or in notochord. Each column shows images from a single larva image repeatedly. (E-F) Confocal analysis of GFP expression in *Tg(il1b:-GFP-F)* in the head (G) and the tail (H) regions 24h following *E. coli* injection. Maximum projections, lateral views, scale bars=20μm. (E') and (F') are high magnification images of regions boxed in E and F.

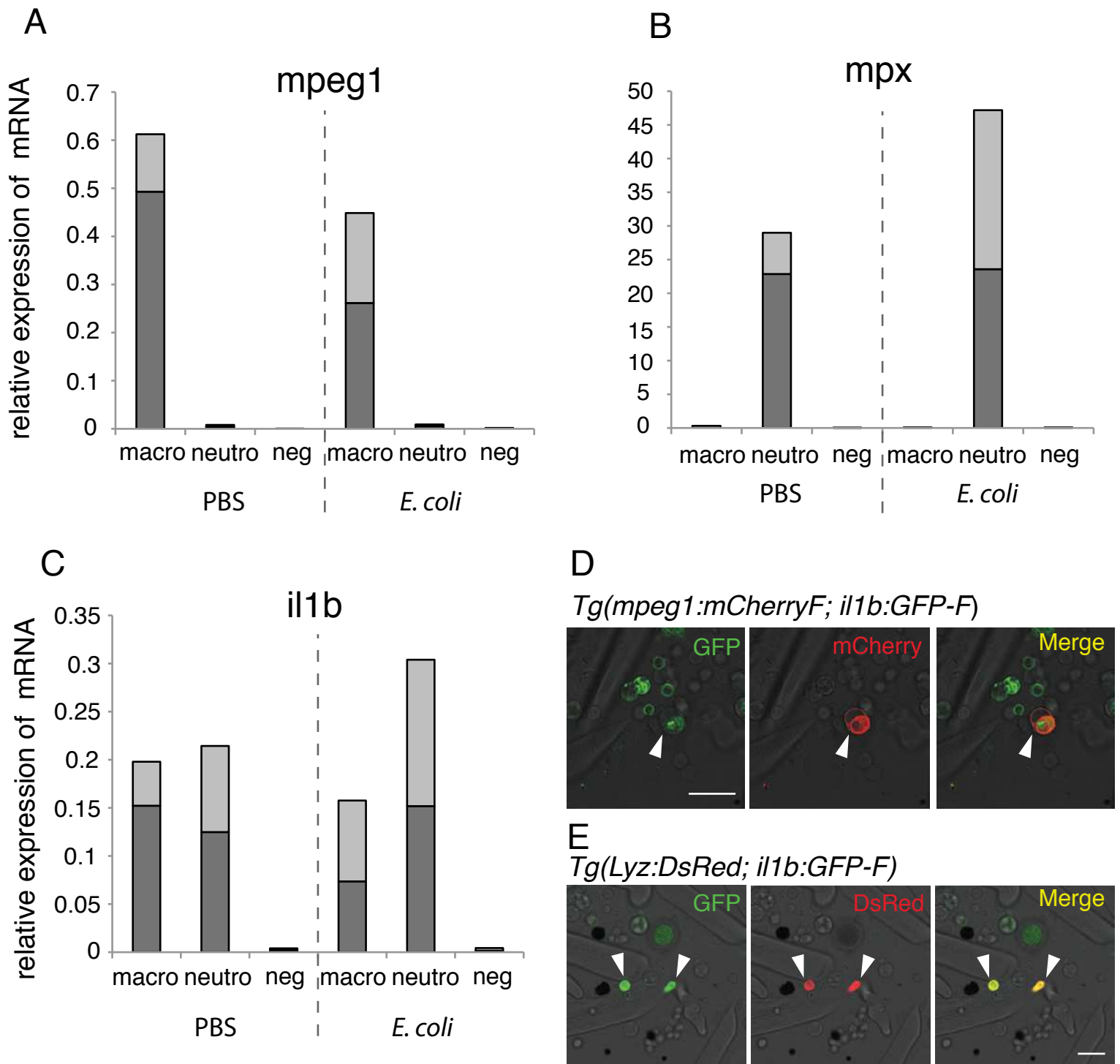


Figure S6 : GFP expression in *Tg(il1b:GFP-F)* line recapitulates endogenous *il1b* mRNA expression in activated leukocytes

Trypsinization of 4dpf larvae was used to generate single cell suspensions for FACS sorting, and was found to activate macrophages and neutrophils, allowing us to compare endogenous *il1b* transcription and GFP expression triggered by a stimulus irrespective of an infection,

(A-C) To test whether *Tg(il1b:GFP-F)* can be used to study the dynamic expression of *il1b* in activated leukocytes, macrophages (macro), neutrophils (neutro), and non leukocyte cells (neg) were FACS sorted from *Tg(mpx:GFP; mpeg1:mCherryF)* 4dpf-larvae first injected with either PBS or *E. coli*. Q-RT-PCR was used to measure the relative expression of *mpeg1* (A) and *mpx* (B) in the different populations, confirming purity of sorted populations. Measurement of *il1b* expression (C) shows that trypsinization and cell dissociation of larvae induced high level of *il1b* expression in macrophages and neutrophils as compared to non leukocyte cells in both PBS and *E. coli* injected embryos. Quantifications using *ef1a* as a reference gene; light grey bar represent 95% confidence interval (student T test). Non-overlapping light grey means $p < 0.05$.

(D-E) Using similar conditions to dissociate the embryos, leukocytes were cultured from *Tg(il1b:GFP-F; mpeg1:mCherryF)* (D) or *Tg(il1b:GFP-F; Lyz:DsRed)* (E). While no expression of GFP was observed in leukocytes before dissociation (in living larvae, not shown), 90% of the macrophages (red, D) and 100% of the neutrophils (red, E) expressed GFP (green) (arrowheads), showing that *Tg(il1b:GFP-F)* is a good reporter transgene in leukocytes. Confocal images, Scale bar= 20 μ m

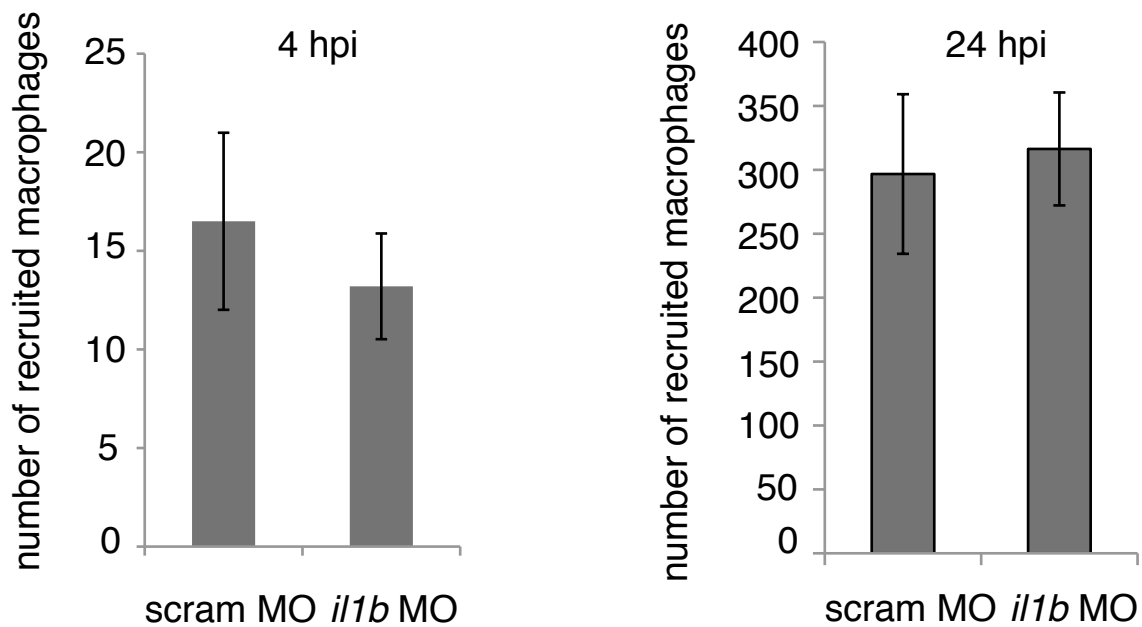


Figure S7: Macrophage recruitment is not affected by *il1b* loss-of-function upon notochord infection.

To evaluate the effect of *il1b* loss-of-function on macrophage recruitment, *Tg(mpeg1:mCherryF)* larvae were injected with either *il1b* (*il1b* MO) or scramble (scram MO) morpholinos. Then the larvae were infected with *E. coli*-GFP in the notochord and recruited macrophages counted. Plots represent the number of recruited macrophages to the notochord at 4 hpi (A) and at 24 hpi (B). The number of recruited macrophages in *il1b* morphans was similar to that of controls. Graphs are mean value \pm s.e.m. (A) $p=0.80$ and (B) $p=0.69$

	accession number	genes	Fold	s.e.m
increased	NM_212859.2	TNFa1	55.68	0.48
	NM_001024447.1	TNFa2	3.26	1.62
	NM_001020785	Il10	3.44	0.78
unchanged	NM_001082955.1	Il20	1.18	0.07
	NM_001020799	Il26	1.76	0.09
	NM_001111083.1	IFN ϕ 3	1.57	0.52
	NM_001020792	Il22	1.03	0.05
	XM_002662056.3	CXC11L	0.63	0.30
	NM_131834	CXCR4b	0.75	0.06
decreased	XM_005165411.1	CXC10L	0.40	0.19

Table S1: Induction of cytokines upon notochord infection with *E. coli*

The relative expression levels of cytokines and chemokines associated with *E. coli* infection in the notochord. Expressions were measured by real-time PCR (using *efl1a* as a reference gene) on cDNA made from RNA isolated from larvae injected with PBS or with *E. coli* in the notochord at 48 hpi. Results are represented as fold change in *E. coli* infection relative to PBS injection +/- standard error of the mean. $n=3$ independent samples of 10 pooled larvae. We detected no significant expression of interferon ϕ 1, ϕ 2, γ 1 and γ 2 in the different conditions.

MOVIE LEGENDS

Movie 1: General behaviour of neutrophils following notochord infection

Tg(mpx:GFP) larvae were infected with crimson expressing *E. coli* (magenta) in the notochord at 48hpf. General behaviour of neutrophil (green) was imaged using 4-dimensional confocal microscopy at 2 hpi during 3 hours. Scale bar: 20µm.

Movie 2: General behaviour of neutrophils following notochord infection

Tg(mpx:GFP) larvae were infected with DsRed expressing *E. coli* (red) in the notochord at 48hpf. Scale bar: 50µm. Neutrophil behaviour (green) was imaged at 1 hpi during 2 hours and 50 min.

Movie 3: Typical behaviour of one neutrophil following notochord infection

High magnification of a region of movie S2 shows the representative behaviour of one neutrophil that fail to engulf bacteria. Scale bar: 20µm.

Movie 4: General behaviour of macrophages following notochord infection

Tg(mpeg1:mCherryF) larvae were infected with GFP expressing *E. coli* (green) at 48hpf in the notochord. The behaviour of macrophages (red) was imaged using 4-dimensional confocal microscopy at 1 hpi during 3 hours. Scale bar: 50µm.

Movie 5: Typical behaviour of few macrophages following notochord infection

The representative behaviour of few macrophages was image in a similar experiment that describe in movie S5 from 1hpi during 3 hours 20 min. Scale bar: 20µm.

Movie 6: General behaviour of macrophages following systemic infection

Tg(mpeg1:mCherryF) larvae were infected with GFP expressing *E. coli* (green) at 48hpf in the posterior caudal vein. The behaviour of macrophages (red) was imaged using 4-dimensional confocal microscopy at 1 hpi during 1 hour. Scale bar: 50µm.



PART II

Neutrophils control *E. coli* infection at a distance with superoxide

Authors:

PHAN Quang Tien, GONZALEZ Catherine, LEVRAUD Jean-Pierre,
LUTFALLA Georges, and NGUYEN-CHI Mai

Submitted for publication

2016

Neutrophils control *E. coli* infection at a distance with superoxide

PHAN Quang Tien¹², GONZALEZ Catherine¹², LEVRAUD Jean-Pierre⁴,
LUTFALLA Georges¹² and NGUYEN-CHI Mai¹³

¹Dynamique des Interactions Membranaires Normales et Pathologiques,
Université Montpellier 2, UMR 5235, case 107, Place Eugène Bataillon, 34095
Montpellier Cedex 05, France.

²CNRS; UMR 5235, Place Eugène Bataillon, 34095 Montpellier Cedex 05,
France.

³INSERM; Institute for regenerative medicine and Biotherapies, CHRU
Montpellier, France.

⁴Macrophages et Développement de l'Immunité, Institut Pasteur, Paris F-
75015, France.

*Authors for correspondence (mai.nguyen-chi@univ-montp2.fr; lutfalla@univ-
montp2.fr)

Key points:

Neutrophils, but not macrophages, are instrumental in killing bacteria
when they cannot be reached for phagocytosis.

Superoxide produced by neutrophil oxidative burst is essential to clear
the infecting bacteria at a distance.

Abstract

Understanding the roles of neutrophils and macrophages in fighting bacterial
infections is a critical issue in human pathologies. Although phagocytic killing
has been extensively studied, little is known about how bacteria are eliminated
extracellularly in live vertebrates. We have recently developed an infection
model in the zebrafish embryo in which leucocytes cannot reach the injected
bacteria. We have described that when *E. coli* bacteria are injected within the

notochord, both neutrophils and macrophages are massively recruited during several days, but do not infiltrate the infected tissue presumably because of its tough collagen sheath. Interestingly, the bacteria are cleared during the first 24 hours, and we report here that macrophages are not involved in the control of the infection. On the contrary, using transgenic lines and chemical approaches, we show that the bactericidal action is achieved by production of superoxide by neutrophils and that the outcome of infection depends on the presence of a sufficient arsenal of neutrophils compared to bacterial load. We thus reveal a novel host effector mechanism mediated by neutrophils that eliminates bacteria that cannot be reached by phagocytes and that is independent of macrophages, NO synthase, Myeloperoxidase or NETs.

Introduction

The innate immune system, first line of defence of the host, includes large phagocytes (such as macrophages and granulocytes) equipped with a battery of weapons to destroy the invader within minutes or hours. Since the seminal work of Elie Metchnikoff¹, the defence mechanisms of leukocytes remain a challenging subject. When microbes penetrate the epithelial barrier, macrophages and neutrophils are rapidly recruited and upon contact, engulf the bacteria into a vacuole called a phagosome that fuses with intracellular granules or lysosomes to form the phagolysosome in which bacteria may be killed by a wide variety of mechanisms involving chemicals and enzymes^{2,3}. Non-oxidative effectors include antimicrobial proteins, while the oxygen-dependent mechanism, also known as the respiratory burst, involves the generation of reactive oxygen species (ROS)⁴⁻⁶. ROS production inside the phagocytic vacuole involves NADPH oxidase and the major ROS, superoxide (O_2^-) and hydrogen peroxide (H_2O_2), can directly or indirectly promote the death of the microbe, according to the nature of the pathogens⁷. Nitric oxide (NO), produced by NO synthase, can contribute to microbicidal activity and is essential for the defence against intracellular organisms such as *S. enterica* and mycobacteria^{8,9}.

Many microbes manage to survive within phagocytes after phagocytosis. While some cope with the phagolysosomal conditions (*Salmonella*

*typhimurium*¹⁰), others like *Listeria*, *Shigella* and some mycobacteria¹¹⁻¹³ are able to block the maturation of the phagosome or even to escape from these compartments. Host cells, however, have developed counter strategies to fight cytosolic bacteria including directing them to autophagosomes¹⁴.

While microbe killing inside the phagosome has been extensively studied, it is less well understood how phagocytes are capable of killing microbes extracellularly in whole organisms. Neutrophils can fight bacterial pathogens without phagocytosis either by release of toxic granule contents (degranulation)¹⁵ or by expelling neutrophil extracellular traps (NETs), which are networks of extracellular fibres built upon expulsion of chromatin¹⁶. However events such as these are very hard to disentangle from phagocytosis-mediated killing in the full context of tissue infection.

Thanks to its transparency and genetic amenability, the zebrafish embryo is a useful model for the study of host/pathogen interactions *in vivo*. The zebrafish model has been used to evaluate the respective roles of neutrophils and macrophages in eliminating invading bacteria^{9,17,18}; this relies not only on the nature of the invading microbe, but also on the anatomic site of infection and on the route of infection. One striking observation was that macrophages are very efficient at engulfing microbes from body fluids (“flypaper” strategy) while neutrophils may be very efficient at clearing surface associated microbes in a “vacuum-cleaner”-like behaviour¹⁹.

We have recently developed an infection model in the zebrafish embryo in which the bacteria are trapped in a tissue in which macrophages and neutrophils cannot enter. When non-pathogenic *Escherichia coli* (*E. coli*) bacteria are injected in the notochord, the swollen rod that provides axial stiffness to the developing embryo, they slip between notochord cells and the thick cylindrical collagen sheath that encases the cord. Although unable to thread their way through this envelope, neutrophils and macrophages are massively recruited all along the infected notochord where they stay in a highly activated state for days. Interestingly, these inaccessible bacteria are cleared within the first 24 hours²⁰. While zebrafish embryo notochord represents a physical barrier for leukocytes, there are differences in host responses to

notochord infection by different invaders as *E. coli* is immediately detected by leukocytes and induces heavy inflammation, whereas mycobacteria remain undetected and their proliferation results in notochord destruction²⁰⁻²².

Here we address the mechanisms of *E. coli* clearance in the notochord infection model where professional phagocytes cannot directly encounter the injected bacteria. We first investigate whether macrophages or neutrophils are involved in this clearance and then investigate the nature of the molecules instrumental for bacterial killing.

Materials and Methods

Ethics statement

Animal experimentation procedures were carried out according to the European Union guidelines for handling of laboratory animals (http://ec.europa.eu/environment/chemicals/lab_animals/home_en.htm) and were approved by the Direction Sanitaire et Vétérinaire de l'Hérault and Comité d'Ethique pour l'Expérimentation Animale under reference CEEA-LR-13007. Fish husbandry and experiments were performed at the University of Montpellier.

Fish husbandry

Fish maintenance, staging and husbandry were performed as described²⁰ with golden strain and transgenic lines. *Tg(mpeg1:mCherry-F)umpTg2*, referred as *tg(mpeg1:mCherry-F)*²³ was used to visualize macrophages. *Tg(mpx:GFP)i114* and *tg(lyz:DsRed)nz50* used to label neutrophils and the *mpx-/-NL144* 'spotless' mutant, are referred here as *tg(mpx:GFP)*²⁴, *tg(lyz:DsRed)*²⁵ and *mpx-/-*²⁷. *tg(mpx:Gal4/USA:nfsB-mCherry)* was used to ablate neutrophils²⁶. Embryos were obtained from pairs of adult fishes by natural spawning and raised at 28.5°C in tank water. Embryos and larvae were staged according to²⁸.

E. coli and *Salmonella* injections and CFU count

E. coli K12 or *Salmonella enterica* serovar Typhimurium (here called *Salmonella*) carrying plasmids encoding GFP or DsRed fluorescent proteins

were injected in the notochord of 2dpf embryos and counted as described²⁰. Four different doses of *E. coli* were used: very low (1000 CFU), low (<3000 CFU), high (3000<n<6000 CFU) and very high (>7000 CFU). 3000 CFU of *Salmonella* were injected in the hindbrain or in the notochord. Enteroinvasive *E. coli* AIEC bacteria strain LF82²⁹ and its mutants, LF82- Δ chiA³⁰ and LF82- Δ lpfA³¹ were injected at a low dose (CFU <3000) in the notochord.

Macrophage and neutrophil ablation and overproduction

To induce depletion of macrophages, 10nl of Lipo-Clodronate or Lipo-PBS (clodronateliposomes.com) was *i.v.* injected in *tg(mpeg1:mCherry-F)* transgenic larvae at 1dpf. Macrophage-depleted larvae were selected based on the reduction of red labelled macrophages 24h after the treatment²³. For depletion neutrophils, 3nl of antisense translational morpholino *csf3r* 0.7mM (5'GAAGCACAAGCGAGACGGATGCCAT3', Gene-Tools) was microinjected in the one-cell stage *tg(mpx:GFP)* embryos. Neutrophils were alternatively depleted using metronidazole treatment of *tg(mpx:gal4/UAS:nfsb-mCherry)* larvae (see below). Microinjection of *gcsf3a* or *gcsf3b* over-expressing plasmids³² at 1-cell stage was used to increase neutrophil supply in *tg(mpx:GFP)* embryos.

Drug treatments of zebrafish larvae

Tg(mpx:Gal4/USA:nfsB-mCherry) 2 dpf embryos expressing a Nitroreductase-mCherry fusion protein specifically in neutrophils, were placed in fish water containing 10mM Metronidazole and 0.1% DMSO (freshly prepared) for 24h. After 3 washes with fish water, neutrophil-depleted larvae were selected based on the number of red fluorescent cells. VAS2870 (Sigma-Aldrich SML0273) stock was prepared in DMSO at 15mM. Two dpf *tg(lyz:DsRed)* embryos were injected in the yolk with 5nl of 20 μ M VAS2870 diluted in milliQ water or with 5 nl of water-diluted DMSO. Apocynin (Santa Cruz, CAS498-02-2) was dissolved at 100mM in DMSO. *E. coli*-infected larvae were placed in fish water containing 250 μ M Apocynin for 1 day. Decrease of superoxide production was checked at 1dpi using DHE (Dihydroethidium, Santa Cruz CAS104821-25-2) staining (see below). Nitric Oxide inhibition was performed with the pan-NOS inhibitor NG-Nitro-L-Arginine Methyl Ester (L-NAME) (sigma, CAS 51298-62-

5). After Notochord injection, embryos were placed in 1mM L-NAME fish water for the whole time course of the experiments.

Staining and immuno-labelling in whole embryo

Mpx activity and neutrophils were detected in *tg(mpx:GFP)/mpx+/-* and *tg(mpx:GFP)/mpx-/-* larvae at 1dpi using Sudan black staining²⁰. DHE was added to the fish medium at 3 μ M at 1dpi for one hour and larvae washed 2 times before imaging³³. Nitric Oxide was stained with 4-Amino-5-methylamino-2',7'-difluorofluorescein diacetate, Diaminofluorescein-FM diacetate (DAF-FM-DA) (Sigma, CAS 254109-22-3)³⁴. Infected *tg(lyz:DsRed)* embryos were treated with DAF-FM-DA 5 μ M by adding it directly to the fish medium for 2 hours at 6, 10hpi and 1dpi (for *E. coli* infection) or 2hpi (for *Salmonella* infection). Larvae were then washed 3 times with fish water before imaging. H₂O₂ was stained with Pentafluorobenzen sulfonyl fluorescein (Santa Cruz, CAS 728912-45-6). Notochord infected *tg(lyz:DsRed)* embryos were soaked in 50 μ M of the fluorescent probe at 1dpi for 2 hours. The larvae were then washed in fish water 3 times before imaging. Apoptotic cells were detected using Acridine Orange staining; embryos were treated at 40hpi with 5 μ g/mL of Acridine Orange in fish water for 30 min, at 28.5 °C. Larvae were then rinsed three times in fish water before imaging. DHE: excitation/emission 518/605 nm, DAF-FM-DA: 495/515 nm, Acridine Orange 500/526 nm.

Statistics analysis

Prism 4.0 (GraphPad Software) was used to construct plots and analyze data in all figures except figures 4D and 6F, which were performed in Excel 2010 (Microsoft). A Mann-Whitney, two-tailed, unpaired t-test was used to calculate the statistical significance. Data are shown as means with SEM. The survival rate of treated embryos was compared with that of the DMSO/infected embryos using the log-rank (Mantel-Cox) test.

Imaging of live zebrafish larvae

Larvae were anesthetized and mounted as previously described²⁰. Epi-fluorescence microscopy was performed using a MVX10 Olympus microscope (MVPLAPO 1X objective; XC50 camera), and a confocal Leica SPE upright



microscope (40x HCX APO L 0.80 W and 20x CHX APO L 0.5 W objectives). Image stacks for time lapse movies were acquired at 23–26°C every 4 min, typically spanning 50 µm at 2 µm intervals, at 1024x512 or 512x512 pixel resolution. The 4D files generated from time-lapse acquisitions were processed using Image J, compressed into maximum intensity projections and cropped. Brightness, contrast, and colour levels were adjusted for maximal visibility.

Results

Macrophages are not required for the control of *E. coli* infection in the notochord

We first compared enteric adherent invasive *E. coli* strains³⁵ and laboratory K12 strains in our notochord infection model and observed that they behaved similarly (data not shown). We therefore performed our experiments with the laboratory K12 strain. To investigate the role of macrophages in the observed bacterial clearance, we injected liposome-encapsulated clodronate (Lipo-clodronate) that kills phagocytic macrophages^{36,37}. At one day post fertilization (1dpf), macrophage/neutrophil dual reporter embryos, *tg(mpeg1:mCherry-F)/tg(mpx:GFP)*, were injected with 10nl of Lipo-Clodronate in the posterior caudal vein (intravenous, i.v.). As previously described³⁶ 24h after Lipo-Clodronate injection, macrophages were efficiently eliminated without affecting the neutrophil population, nor inducing unspecific toxicity (Fig. 1A, B). Macrophage depleted larvae were selected and injected in the notochord with DsRed-expressing *E. coli*. Bacteria were cleared within the first 24 hours post infection (hpi) in both, macrophage-depleted larvae (Fig. 1C) and Lipo-PBS injected control larvae; the red signal observed along the notochord at 2dpi was due solely to macrophages. Importantly, upon notochord infection, neutrophils were normally recruited around the infected notochord regardless of the presence or absence of macrophages (Fig. 1C). Thus, macrophages are not required for bacterial clearance in this model.

Neutrophils are essential for the control of notochord infection by *E. coli*

To investigate the role of neutrophils in bacterial clearance, we ablated neutrophils by two independent approaches. First, we specifically inhibited neutrophil development by knocking down the G-CSF/GCSF3R pathway using a morpholino oligo (MO) specifically blocking *csf3r* translation (MO *csf3r*)³⁸. Injection of MO *csf3r* in the neutrophil reporter embryos, *tg(mpx:GFP)*, led to approximately 70% reduction in the total number of neutrophils as compared to larvae injected with a control morpholino (MO CTRL) at 3dpf (Fig. 2A-D). We infected these morphants with 2500 CFUs fluorescent *E. coli*. Bacteria were cleared in the control larvae (Fig. 2B, 2E) while they proliferated in neutrophil-depleted embryos (Fig. 2B, 2F). The bacterial proliferation correlates with a further dramatic reduction in neutrophil number at 1 and 2dpi suggesting neutrophil death (Fig. 2D). Subsequently, infected *csf3r* morphants died at 2-3dpi with overwhelming bacterial proliferation and neutropenia.

We also ablate neutrophils, using *tg(mpx:Gal4/UAS:nfsB-mCherry)* embryos in which the *myeloperoxidase* promoter (*mpx*) indirectly drives the expression of *E. coli* nitroreductase enzyme (*nfsB*) in neutrophils. Treatment of *tg(mpx:Gal4/UAS:nfsB-mCherry)* embryos with the pro-drug metronidazole (MTZ) at 2dpf specifically depleted neutrophils (Fig. S1A, B)³⁹. Similarly to *csf3r* morphants, bacteria were cleared in control larvae, while bacteria proliferated in embryos with low neutrophil density (Fig. S1A). These two experiments demonstrate that neutrophils are essential for the control of notochord infection by *E. coli*.

Neutrophil/bacterial balance dictates infection outcome

We investigated the relationship between neutrophil supply and bacterial clearance in the notochord. Embryo with a higher number of neutrophils (overexpression of *csf3a*) can cope with higher amounts of injected bacteria (Fig 3D). Similar results were observed by overexpressing *csf3b* (not shown).

Our data reveal that the balance of neutrophils versus bacteria is instrumental for the outcome of the infection. Normal neutrophil levels are necessary to eliminate small amounts of bacteria (Fig 3A), but embryos with depressed

neutrophil populations are killed even by low bacterial loads (Fig 3C) and embryo injected with higher amount of bacteria need a larger neutrophil population to eliminate the bacteria (Fig 3B & D). This shows that neutrophil populations are limiting in fighting the infection. Acridine Orange staining of embryos experiencing neutropenia suggests that when the neutrophil versus bacteria balance is not correct, neutrophils die by apoptosis (fig S2).

The neutrophil Myeloperoxidase is not required to control notochord infection

Our previous study revealed that approximate 35% of recruited neutrophils undergo degranulation of their primary granules around infected notochords²⁰. We therefore investigated the role of the neutrophil-specific myeloperoxidase (Mpx) that is present in the azurophilic granules, in bacterial clearance. We introduced the *mpx:GFP* transgene in the *mpx*-null mutant 'spotless'²⁷ to generate *tg(mpx:GFP)/mpx-/-* offspring in which neutrophils express the eGFP but lack Mpx activity²³. Sudan Black staining confirmed that neutrophils did not contain active Mpx in *tg(mpx:GFP)/mpx-/-* while in *tg(mpx:GFP)/mpx+/-* siblings, neutrophils contained active Mpx in their granules (Fig. 4A). A low dose of fluorescent *E. coli* was injected in the notochord of 2dpf *tg(mpx:GFP)/mpx-/-* embryos; neutrophils were normally recruited along the notochord, and the injected *E. coli* cleared at 1dpi as in the wild type (n>60 larvae, Fig. 4B). Mpx is therefore not required for the clearance of *E. coli* in the notochord.

Larvae without NADPH Oxidase activity are highly susceptible to notochord infection

Neutrophils use a wide variety of diffusible molecules to fight infections, including NO and ROS. We investigated NO production by neutrophils during the course of notochord infections using the NO reporter fluorescent probe DAF-FM-DA. We used *Salmonella* infected embryos as controls to detect NO production in neutrophils within the Aorta-Gonad-Mesonephros (AGM) (Fig. S3A)⁴⁰. As described³⁴, the notochord itself was labelled by DAF-FM-DA in uninfected embryos, but we could not observe any evidence of NO production by neutrophils in our notochord infection model (Fig. S3B). Next we specifically

inhibited NO synthases using L-NAME and injected *E. coli* into the thus treated embryos. We did not observe any difference in the outcome of the infection in L-NAME-treated larvae compared to controls (DMSO) (not shown).

To examine the role of ROS in the bacterial clearance, we used VAS2870 (VAS), a NADPH oxidase (NOX) inhibitor⁴¹. Injection of VAS in the yolk of 2dpf *tg(lyz:DsRed)* embryos did not induce any toxicity. One hour after VAS treatment, embryos were infected with low-dose GFP-expressing *E. coli* in the notochord (Fig. 5A). At 1dpi, VAS treatment had no effect on the total neutrophil population as seen in PBS control-injected embryos (Fig. 5B). While bacteria were cleared in DMSO-treated embryos, *E. coli* proliferated in the notochord of VAS treated larvae despite comparable neutrophil recruitment followed by neutropenia and death in 74% of infected larvae between 2 and 3dpi (Fig. 5B-D), showing the essential role of NOX in the control of bacterial infection. The effect was specific to the clearance of bacteria in this notochord infection model since VAS treatment did not interfere with the clearance of bacteria injected in muscle of the embryo where phagocytosis occurs (data not shown).

Superoxide is produced in neutrophils of bacterial infected embryos

To check H₂O₂ production by neutrophils, we stained infected *tg(lyz:DsRed)* embryos with the fluorescent probe Pentafluorobenzenesulfonyl fluorescein that specifically detects H₂O₂. We did not detect fluorescence in recruited neutrophils along the infected notochord during the first 24 h (data not shown). As a control, we checked that, as reported⁴¹, H₂O₂ was produced by cells at the amputated fin (data not shown). This suggests that H₂O₂ is not important for bacterial clearance.

Another major ROS produced by neutrophils, superoxide, is also involved in bacterial killing⁴². To detect superoxide production in *tg(mpx:GFP)* embryos infected with *E. coli*, we used Dihydroethidium (DHE), a fluorescent probe that turns red after reacting with superoxide³³. First, we imaged the injection site, where some bacteria initially leak from the pierced notochord and get engulfed by neutrophils and observed that these phagocytosing leukocytes, abundantly produced superoxide in intracellular compartments harboring bacteria, which



are most probably phagosomes (Fig. 6B). Green fluorescent *E. coli* were rapidly lysed within 20 minutes in the putative phagosome (Fig. 6B). We then image the upstream region, where bacteria are separated from the recruited neutrophils by the notochord collagen sheath. Interestingly, these recruited neutrophils also produced large amounts of superoxide, even though they had not phagocytosed bacteria (Fig. 6C).

Apocynin decreases superoxide production and prevents bacterial killing

We decided to investigate whether this superoxide production could be involved in the control of bacterial proliferation by neutrophils. Apocynin, like VAS, is a NOX inhibitor, but it targets phagocytes more specifically^{43,44}. Upon notochord infection, Apocynin-treated embryos had reduced number of superoxide producing cells, including recruited neutrophils at the site of inflammation, as compared to DMSO-treated larvae (Fig. 7A, B, C). We infected *tg(lyz:DsRed)* embryos with a very low dose of *E. coli* ($10^3 \pm 20$ CFUs) in the notochord. Even with the very low dose infection, 80% of Apocynin-treated embryos failed to clear bacteria, while all bacteria were efficiently killed in DMSO-control embryo. Apocynin treated embryo displayed unrestricted bacterial growth in the notochord at 1dpi, neutropenia and eventually death at 2-3dpi (Fig. 7 A, D, E, F). These data show that inhibition of superoxide production in neutrophils increases susceptibility to notochord infection.

Discussion

Many studies have used the zebrafish embryo model to address the respective roles of neutrophils and macrophages in eliminating invading bacteria, but in all instances, at least one of these two cellular populations had direct access to the bacteria. In our model neither neutrophils nor macrophages could reach the bacteria. We first observed an active recruitment of both macrophages and neutrophils around the infected notochord that is correlated with the clearing of the bacteria within the notochord in less than 24 hours. By specific depletion of individual myeloid populations, we have investigated their contribution in the clearance of *E. coli* at a distance and describe how neutrophil may eliminate inaccessible bacteria.



Using chemical ablation of macrophages, we revealed that despite being massively recruited to the notochord, macrophages are not required for the bacterial killing. Whichever the strategy to lower the amount of neutrophils within the developing zebrafish, the embryo becomes unable to cope with low-dose infection, leading to bacterial proliferation and death of the embryo. Importantly, we highlight the importance of the numerical balance between neutrophils and bacteria in the control of notochord infection suggesting that the molecules produced by the neutrophils to fight the bacteria are produced in limiting amount. During *Salmonella* infections, the correct population of neutrophils is maintained through a mechanism of demand-driven granulopoiesis in the main site of hematopoietic stem cells emergence, i.e., the AGM⁴⁰. Similarly, we show here, that when a low amount of bacteria is injected, the host may increase the neutrophil pool to control notochord infection. We also report that either increasing bacterial load or decreasing the number of neutrophils results in bacterial proliferation, onset of neutropenia, and death within 2 to 3 dpi. Conversely, we show that embryos with an increased number of neutrophils can cope with a very high dose of bacteria.

To capture and kill microbes they cannot phagocytize, neutrophils have been described to expel their chromatin to form Neutrophil Extracellular Traps (NETs), but this may lead to neutrophil death (Netosis)^{45,46}. NET formation relies on complex intracellular processes involving the activity, among others, of myeloperoxidase⁴⁷. Myeloperoxidase activity is not necessary to fight the infection in our experimental system and we found no indication of NET expulsion (data not shown). Since it is clear that the main cause of death of the neutrophils is not NETosis, it will be very interesting to investigate the signals triggering neutrophil death in our model.

Interestingly, neutrophils do not employ their traditional defence mechanisms, phagocytosis and NETosis, to cope with notochord infection by *E. coli*; we demonstrate that NOX activity and the production of superoxide by neutrophils are essential. Indeed, treatment of embryos with a specific inhibitor of NOX assembly, VAS2870, leads to bacterial proliferation. Using fluorescent probes, we showed that neutrophils do not produce significant amount of H₂O₂ but produce large amounts of superoxide. Apocynin blocks superoxide production

specifically in phagocytes expressing Mpx⁴⁴. Indeed, infected embryos treated with Apocynin have a significantly reduced superoxide production and increased susceptibility to notochord infection consistent with an essential role of superoxide in the clearance of *E. coli* without direct phagocytosis (Fig. 7F).

The present work raises different questions related to the death of the different actors, the bacteria, the neutrophils, and the embryo. Foremost is the question as to how bacteria are killed at a distance by neutrophils. Neutrophils massively degranulate around the infected notochord and we show here that an oxidative burst is necessary for bacterial elimination. As hypothesised by JM Slauch, we propose that bacterial death is the result of cooperation between superoxide and antimicrobial peptides⁴⁸. A massive release of toxic molecules is consistent with the tissue-induced damage and subsequent spine malformations that we previously observed as a consequence of this transient infection²⁰. Why do neutrophils die when the bacteria/neutrophil ratio is too much in favor of the invaders? If bacteria are not rapidly killed and start proliferating within the infected notochord, then neutrophils massively die and the embryo becomes neutropenic. This could be due to a factor released by the densely packed bacteria within the notochord, possibly induced through a quorum sensing mechanism. However, there is no reason why this virulence factor would specifically kill neutrophils while sparing the highly endocytic macrophages that are also massively recruited to the notochord but not affected by bacterial proliferation. For this reason, we propose that death of neutrophils could rather be a consequence of the excessive number of bacteria triggering hyper activation of the neutrophils and leading to their death⁴⁹. This death would not be purely due to an excessive release of ROS since it is not prevented by our NOX inhibitors; there is, however, a wide choice of toxic molecules released by activated neutrophils besides ROS. This hyper activation, akin to a cytokine burst is probably also responsible for the death of the embryo in cases where *E. coli* proliferates within the notochord. Importantly, we have no indication that the bacteria used in this study could kill the embryo by themselves; injection of up to $5 \cdot 10^4$ CFU of *E. coli* within the blood circulation does not lead to embryo death and phagocytes can easily eliminate these huge amounts of bacteria (JPL, unpublished observations).

We consider that in cases where the embryos die, it is the consequence of their heavy inflammatory status mimicking a cytokine storm. This hypothesis is consistent with our experiments with mycobacteria. We have demonstrated that mycobacteria can replicate within the notochord without triggering the heavy inflammation described here with *E. coli*. Mycobacteria remain almost undetected within the notochord and proliferate, ultimately leading to notochord break down. The subsequent fate of the embryo depends on the virulence of the mycobacteria. The non-virulent *Mycobacterium smegmatis* is eliminated by phagocytosis, leading to the host survival while *M. marinum* resists destruction by phagocytosis and keeps proliferating until the host dies (Alibaud et al 2011). Conversely, *E. coli* only effectively kills infected embryos when injected in excessive amounts in the notochord where this triggers a heavy inflammation that kills the neutrophils and ultimately the embryo.

To overcome killing by neutrophils, some pathogenic bacteria developed a strategy to prevent engulfment. Indeed *Yersinia pestis* (bubonic and pneumonic plague), *Yersinia pseudotuberculosis* (gastroenteritis) and *Yersinia enterocolitica* (gastroenteritis and mesenteric adenitis) are able to inhibit the actin cytoskeleton required for engulfment, by the secretion of effector proteins into the cytoplasm of the immune cell, which results in the decrease phagocytosis by neutrophils and increased virulence³. Oxidative burst at a distance is an alternative mechanism employed by neutrophils to control such infections. Further investigations should determine whether host targeted therapeutic strategies may be beneficial against medically relevant infections where bacteria cannot be engulfed by phagocytes.

Acknowledgements

We have special thanks to Annette Vergunst, Paul Guglielmi, Etienne Lelièvre and the members of DIMNP for helpful discussions. We thank David Stachura for the gift of the Csf3 over-expressing plasmids, Nicolas Darnish for LF82 *E. coli* strain and Steve Renshaw for transgenic lines. This work was supported by a grant from the European Community's Seventh Framework Program (FP7- PEOPLE-2011-ITN) under the Marie-Curie Initial Training Network FishForPharma [grant agreement no. PITN-GA-2011-289209]. QTP is



currently supported by Fondation de la Recherche Médicale (FDT20150532259). We thank Montpellier Rio Imaging for access to the microscopes.

Author Contributions

Q.T.P., J-P. L., G.L. and M.N.-C. designed the project and the experiments, Q.T.P., C.G. G.L. and M.N.-C. performed the experiments and analysed the results. Q.T.P., G.L. and M.N.-C. wrote the manuscript with the input of J-P.L.

Conflict of Interest Disclosures

The authors declare that there are no conflicts of interest.

FIGURES AND LEGENDS

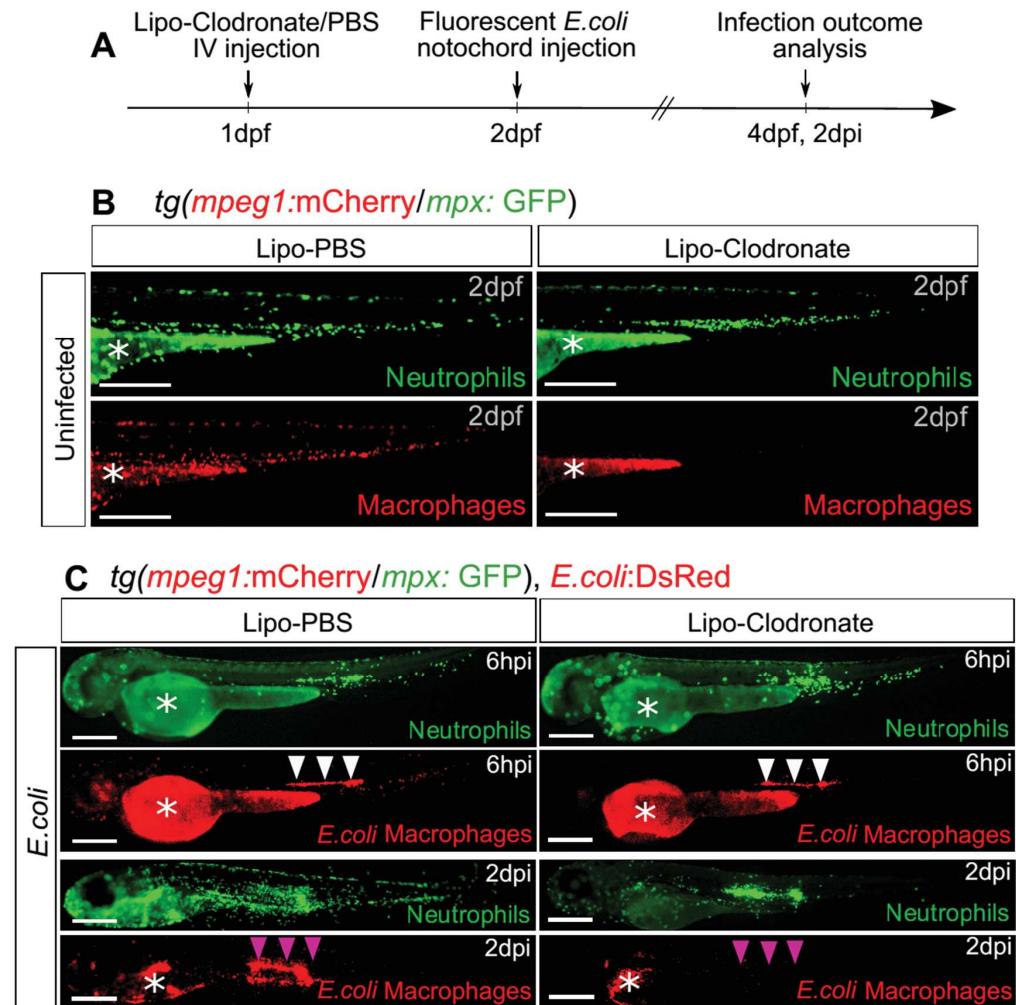


Figure 1: Macrophages are not involved in the clearance of bacteria injected within the notochord

(A) Experimental scheme. One dpf *tg(mpeg1:mCherry-F/mpx: GFP)* embryos were *i.v.* injected with Lipo-Clodronate or Lipo-PBS. Correctly depleted larvae were selected based on the loss of red fluorescence macrophages, and DsRed expressing *E. coli* were injected within their notochord at 2 dpf. The infection outcome was analyzed at 2 dpi using fluorescence microscopy. **(B)** Lipo-Clodronate efficiently depletes macrophages without affecting neutrophil population. Experiments were performed as described in (A). GFP (Neutrophils) and mCherry (macrophages) expression were analysed by fluorescence microscopy at 2 dpf. **(C)** *E. coli* infections in the notochord are cleared in the macrophage-depleted embryos. Experiments were

performed as described in (A). GFP (Neutrophils), mCherry (macrophages) and DsRed (*E. coli*) were imaged repeatedly in individual larvae using fluorescence microscopy at 6hpi and 2dpi. In both Lipo-PBS and lipo-clodronate conditions, DsRed-*E. coli* are present in the notochord at 6hpi (white arrowheads) but are cleared (pink arrowheads) at 2dpi. In (B) and (C) Asterisks indicate the auto-fluorescent of the yolk sac, Scale bar= 400 μ m.

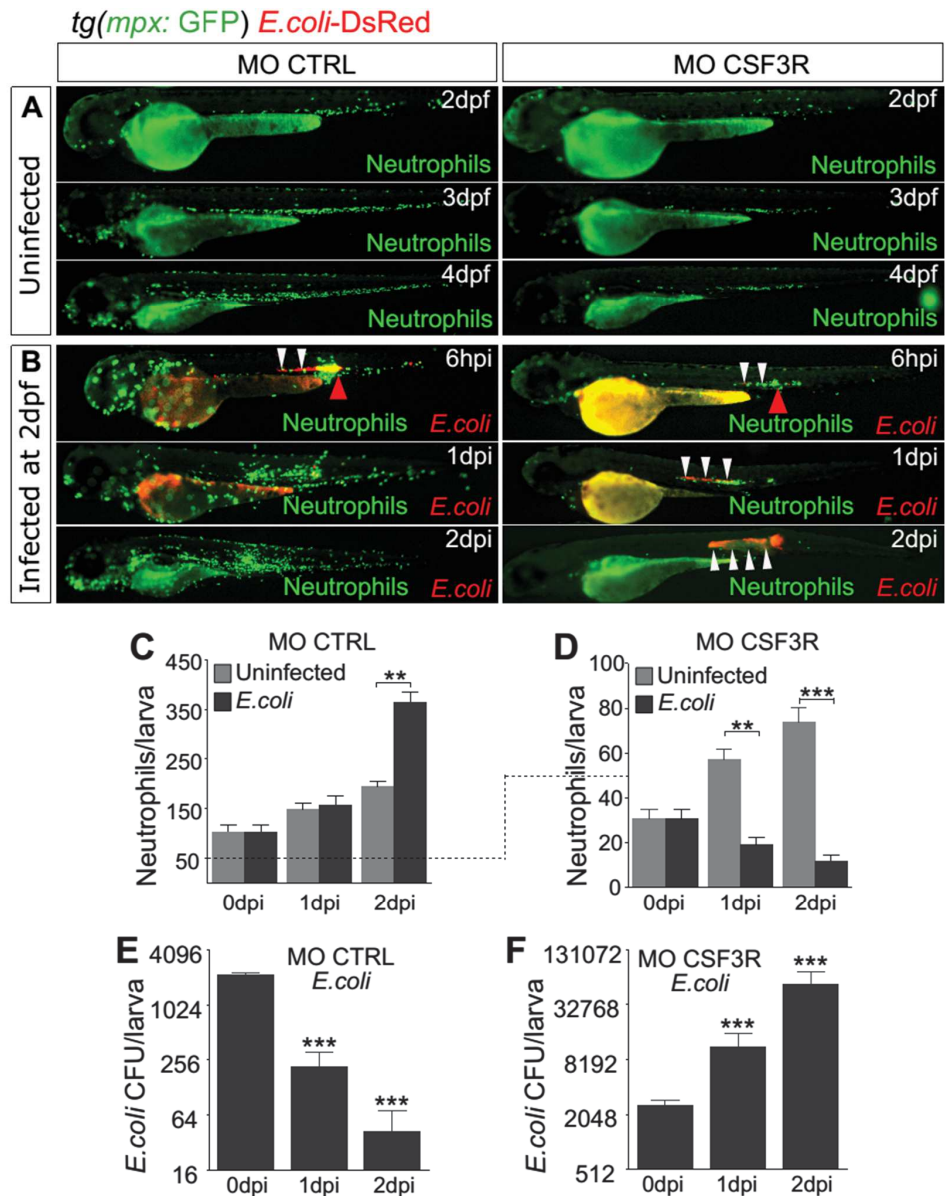


Figure 2: Neutrophils are essential for bacterial clearance

Tg(mpx:GFP) embryos were injected at the one cell stage with either *csf3r* morpholino (MO *csf3r*) to induce neutrophil depletion or a control morpholino (MO

CTRL). **(A)** The steady-state of the neutrophil population was imaged repeatedly in individual morphants using GFP fluorescence in both MO *csf3r* and control conditions between 2 and 4dpf. **(B)** Fluorescent *E. coli*-DsRed were injected in the notochord of *csf3r* and CTRL morphants (Red arrowheads: bacterial injection sites). GFP (Neutrophils) and DsRed (*E. coli*) fluorescence was imaged at indicated time points. *E. coli*-DsRed (red) disappeared from 1 dpi in the control embryos (left panel), while it increased in *csf3r* morphants at 1 and 2dpi (white arrowheads) with a concomitant decrease in neutrophil number (green, neutropenia). (**C,D**) Quantification of neutrophils in CTRL (**C**) and *csf3r* (**D**) morphants at the indicated time points following PBS (light grey columns) or *E. coli* (dark grey columns) injection. (**E, F**) *E. coli* log counts (CFU) in CTRL (**E**) and *csf3r* morphants (**F**). Neutrophils and CFU counts were taken in whole embryos and expressed as mean number of cells/CFU per larva \pm SEM, **p<0.005, ***p<0.001, 5<n<11.

E. coli-DsRed; tg(mpx :GFP)

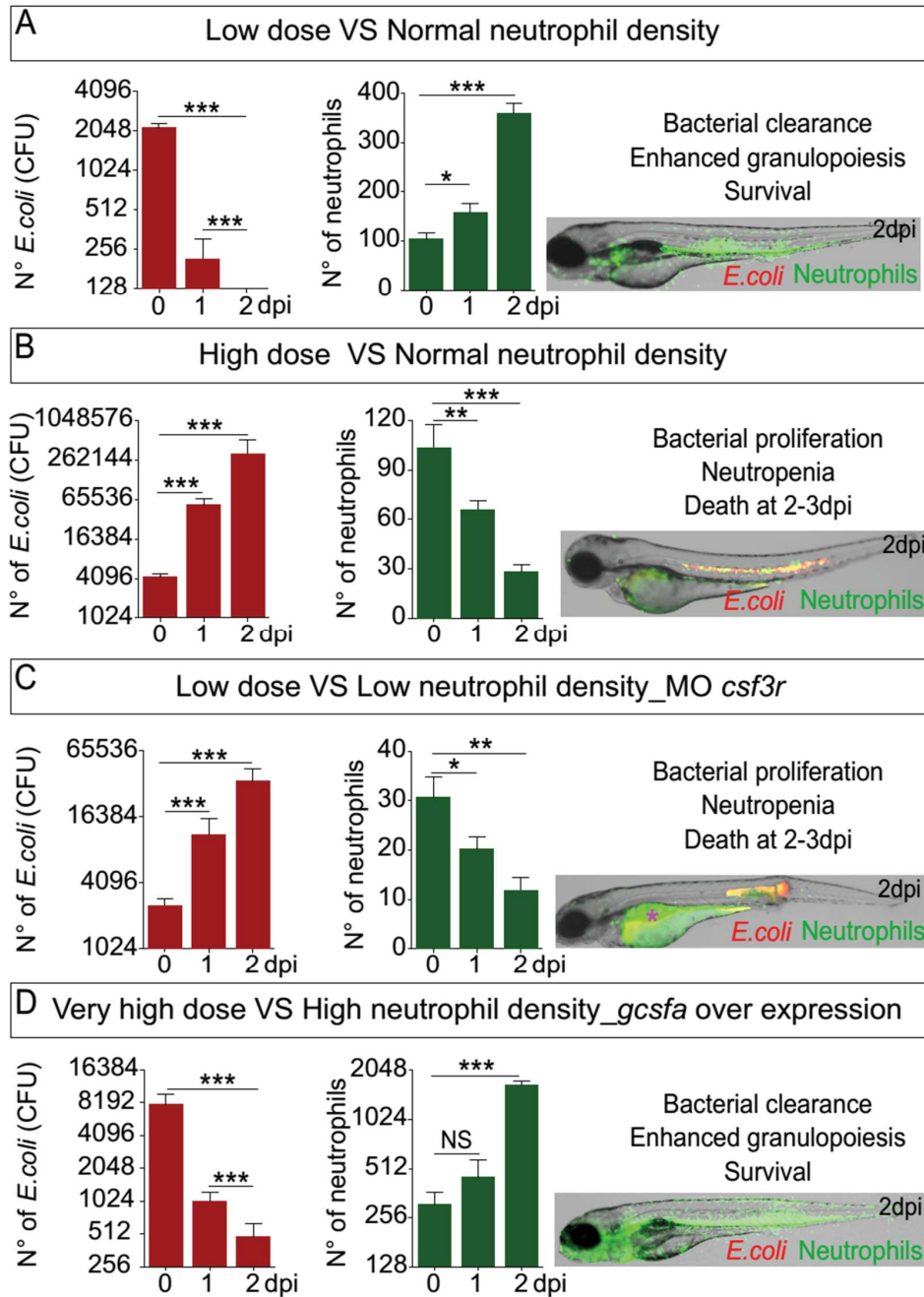


Figure 3: Embryo needs correct neutrophil densities to fight different levels of infection

(A, B) Two dpf *tg(mpx:GFP)* embryos were infected in the notochord with low dose (< 3000 CFUs, A) or high dose (> 4000 CFUs, B) DsRed fluorescent **E. coli**. Red-bar charts represent the CFU counts at 0, 1 and 2dpi. Green-bar charts show the quantification of total neutrophils at 0, 1 and 2dpi. Larvae images are representative

overlays of fluorescence (green neutrophils and red *E. coli*) and transmitted light images at 2dpi. **(C)**: To decrease neutrophil density, *tg(mpx:GFP)* embryos were injected at the one cell stage with the *csf3r* morpholino and then infected in the notochord at 2dpf with a low dose (<3000 CFUs) of red fluorescent *E. coli*-DsRed. **(D)** To increase neutrophil density, *tg(mpx:GFP)* embryos were injected at the one cell stage with the *gcsfa* over-expressing plasmid and then infected in the notochord at 2dpf with a very high dose (>7000 CFUs) of red fluorescent *E. coli*-DsRed. Charts correspond to CFU (red) and neutrophil (green) number counts at 0, 1 and 2dpi. *p<0.05, ** p<0.01 and ***p<0.001, with respect to 0hpi.

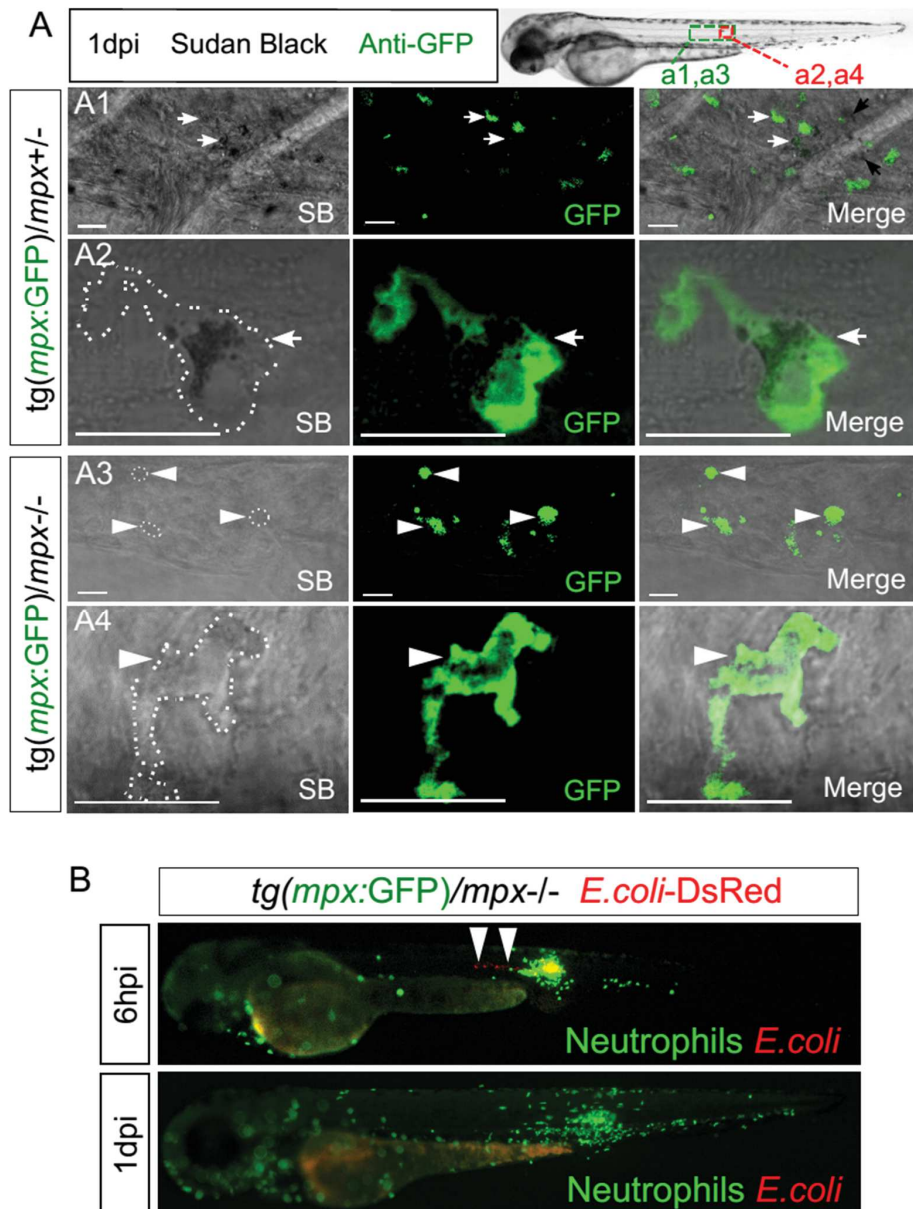


Figure 4: MPO is not required for bacterial clearance

Tg(mpx:GFP)/mpx+/- (A1, A2) and *tg(mpx:GFP)/mpx-/-* (A3, A4) embryos were infected with *E. coli* in the notochord. Sudan Black staining and immuno-detection of neutrophils (anti-GFP) were performed in whole embryos at 1dpi. The top right panel shows the regions imaged by confocal microscopy in the larvae in A1 and A3 (green box) and in A2 and A4 (red box). Representative transmitted light images, overlaid with a maximal projection of confocal fluorescence images show the presence of black granules in the neutrophils (white arrows) of *tg(mpx:GFP)/mpx+/-* embryos (A1

and A2), revealing MPX activity. MPX granules are absent in neutrophils (arrowheads) of *tg(mpx:GFP)/mpx-/-* embryos (A3 and A4). Scale bars: 10µm and white dotted lines outline neutrophils in (A2, A3 and A4). Leica SPE confocal microscope (488nm laser and bright field)

(B) *Tg(mpx:GFP)/mpx-/-* embryos were infected with *E. coli*-DsRed in the notochord. Neutrophils (GFP) and *E. coli* (DsRed) were imaged repeatedly in individual larvae using fluorescent microscopy at 6hpi and 1dpi. While *E. coli* locates in the notochord at 6hpi (arrowheads), it disappears at 1dpi. (N= 60 mpx mutant embryos displaying bacterial clearance similarly to the control embryos from three independent experiments).

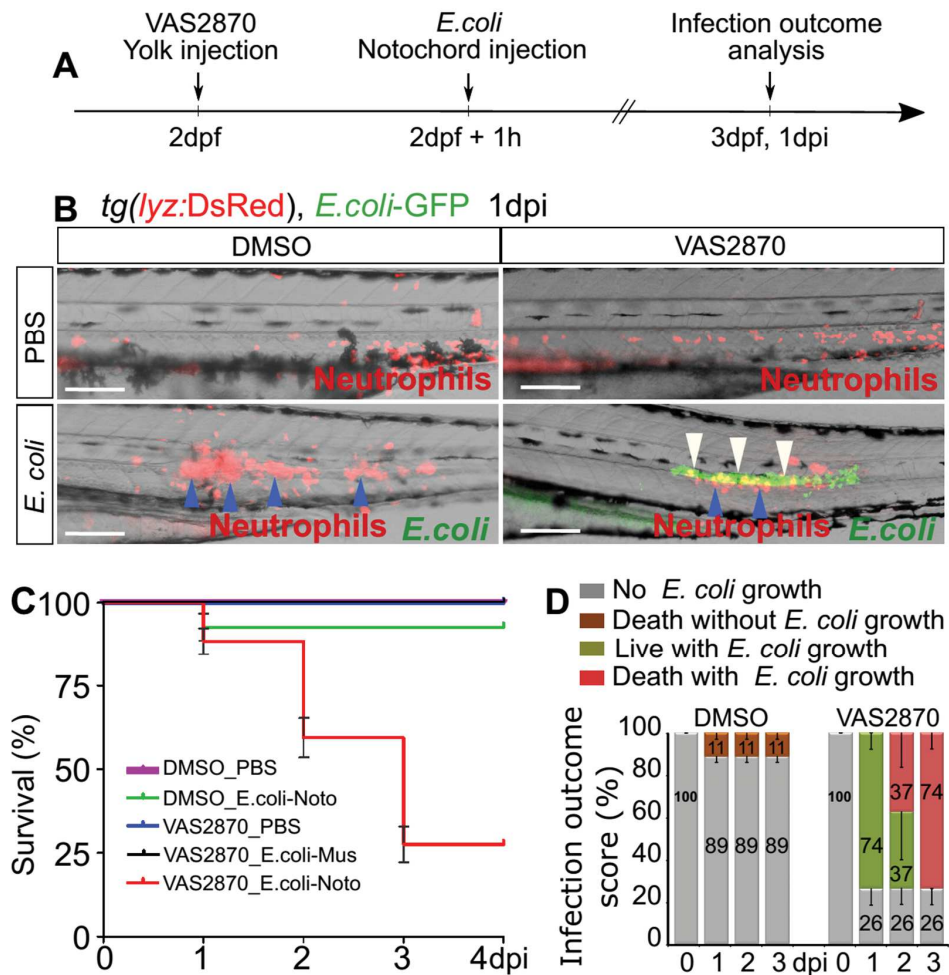


Figure 5: Larvae are more susceptible to notochord infection in the presence of NADPH oxidase inhibitors



Figure 5: Larvae are more susceptible to notochord infection in the presence of NADPH oxidase inhibitors

(A) Experimental scheme. VAS2870 was injected in the yolk of *tg(lyz:DsRed)* embryos at 2dpf. One hour later, *E. coli*-GFP bacteria were injected in the notochord. Injected embryos were scored from 1dpi. **(B, C, D)** The consequences of VAS2870 treatment on neutrophil recruitment and *E. coli* infection. Trunk images are representative overlays of DsRed, GFP and transmitted light images at 1dpi. Scale bars: 100 μ m. White arrowheads: *E. coli* in the notochord, blue arrowheads: neutrophils around the notochord. **(C)** Larva survival was scored for uninfected and *E. coli*-infected embryos, previously treated with either DMSO or VAS2870 ($n > 24$ each). These results are representative of three independent experiments; mean number of larvae \pm SEM, error bar $p < 0.0001$. **(D)** Zebrafish larvae were treated as described in (A). At 1 dpi larvae phenotype and bacterial outcome were scored. Larvae with no defects and complete bacterial clearance were scored as having no bacterial proliferation (grey). Results showed the mean percentage \pm SEM, numbers on bars are percentages, $42 < n < 69$.

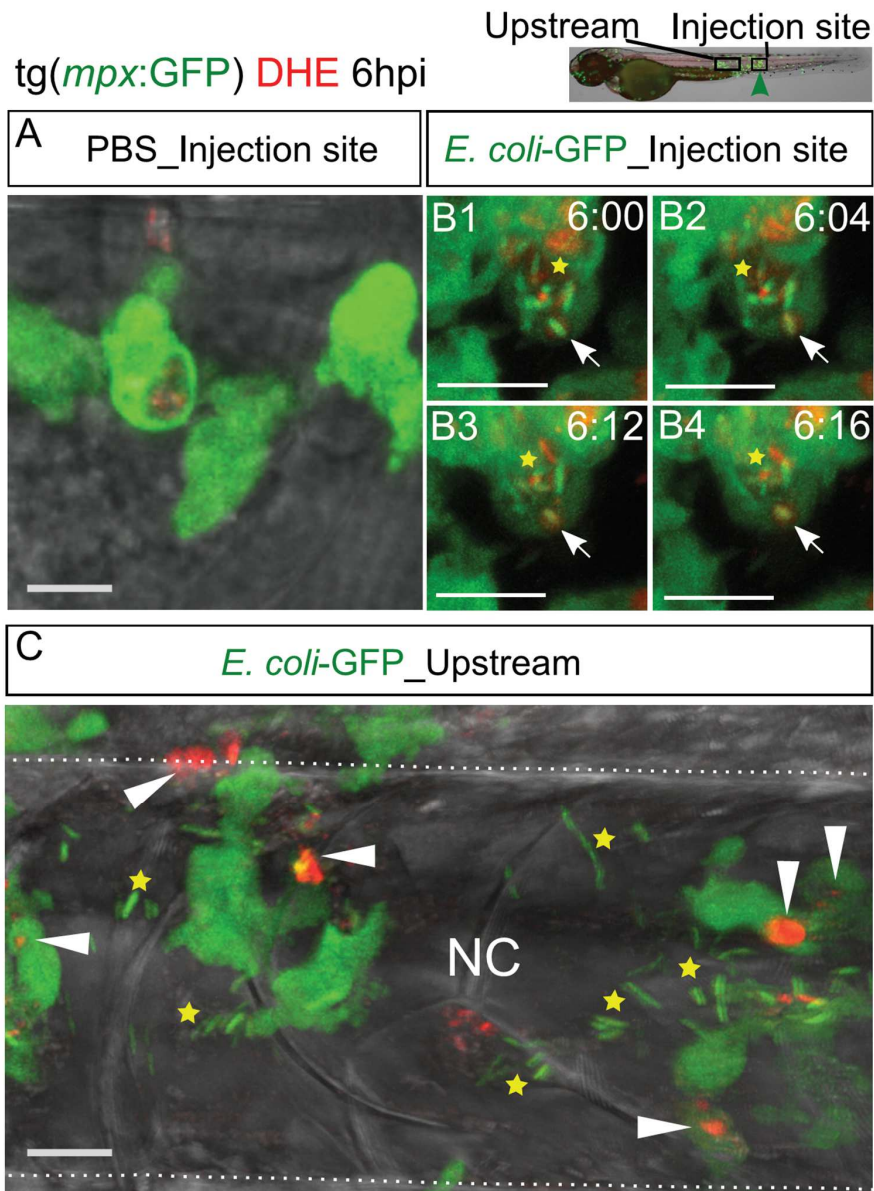


Figure 6: Superoxide is produced in neutrophils of infected embryos

Two dpf *tg(mpx:GFP)* embryos were either injected with PBS (A) or infected with *E. coli-GFP* in the notochord (B,C). At 6hpi, Superoxide was detected using Dihydroethidium (DHE, red) and neutrophils were visualized using GFP fluorescence (green). (Top panel) Black boxes in the larva image show the regions imaged by high resolution confocal microscopy. (A) Representative transmitted light images, overlaid with a maximal projection of confocal fluorescence images show that superoxide is lightly produced in the recruited neutrophil due to injury at the injection site. (B) Representative time-lapse maximum projections starting 6hpi during 16min, show

superoxide presence in phagosomes (white arrows) bearing bacteria (yellow stars: *E. coli*-GFP, Green) in recruited neutrophils at the injection site. Time is in minutes. (C): Representative transmitted light images, overlaid with a maximal projection of confocal fluorescence images show that, in the upstream region of the injection site, superoxide is detected intracellularly (white arrowheads) over the *E. coli* (yellow stars) infected notochord. Scale bars: 15µm, dotted line encases the notochord (NC).

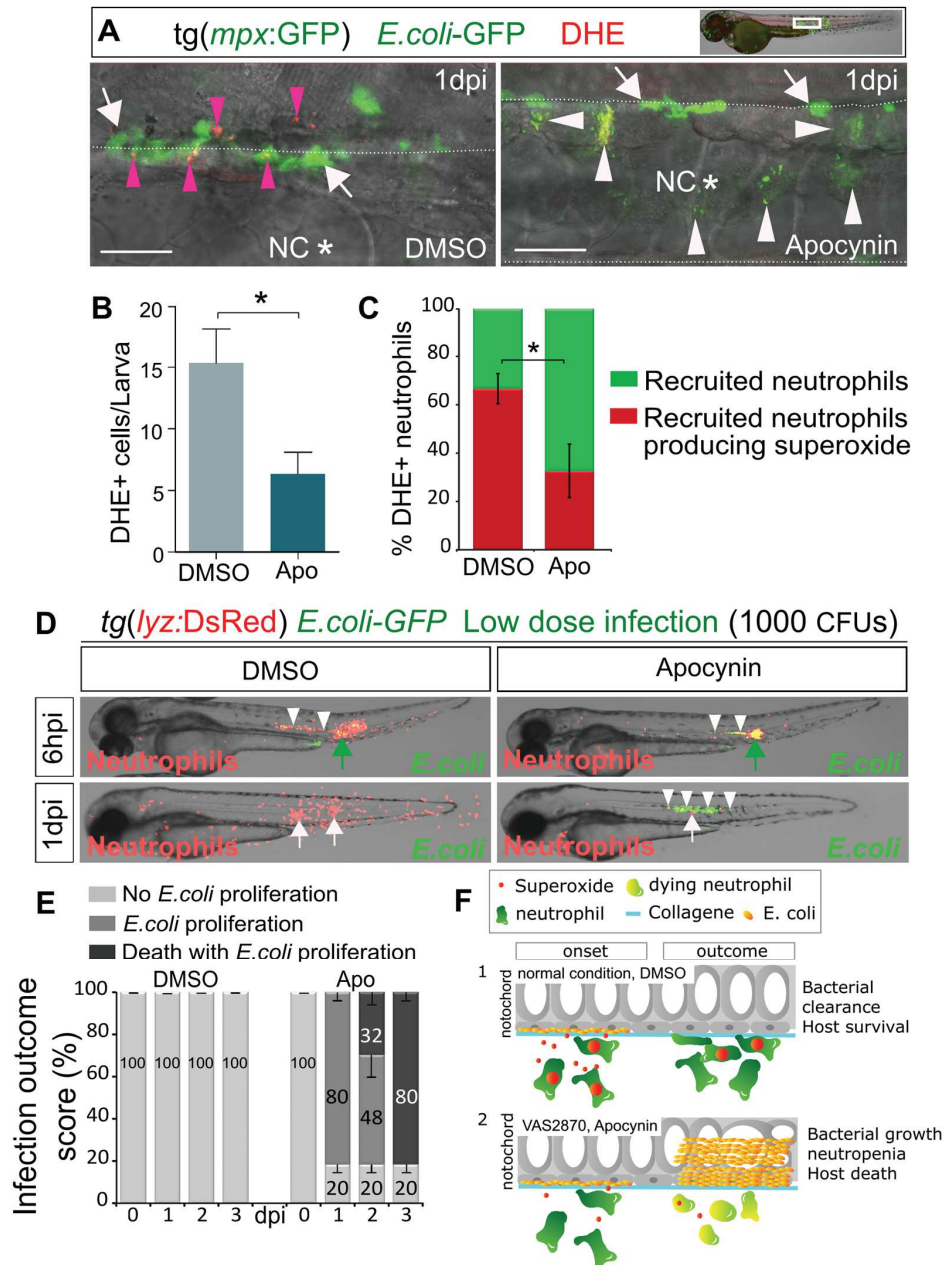


Figure 7: Larvae with Phagocyte-specific superoxide inhibition are more susceptible to notochord infection

Figure 7: Larvae with Phagocyte-specific superoxide inhibition are more susceptible to notochord infection

(A,B,C) GFP fluorescent *E. coli* were injected in 2dpf *tg(mpx:GFP)* embryos immediately followed by either DMSO or 250 μ M Apocynin treatment. **(A)** At 1dpi, superoxide production was visualised using dihydroethidium (DHE, red) and, neutrophils and *E. coli* were detected using GFP by confocal microscopy. Representative transmitted light images, overlaid with a maximal projection of confocal fluorescence images show that Apocynin-treated larvae have less DHE-positive neutrophils than DMSO-treated larvae (pink arrowheads). White arrows: neutrophils DHE-, white arrowheads: *E. coli*, NC*: mid of notochord, scale bars: 30 μ m. **(B)** Quantification of DHE-positive cells in DMSO- and Apocynin-treated larvae. Results were expressed as the mean of DHE-positive cells per larva \pm SEM, n>5 larvae. **(C)** Corresponding percentage of DHE-positive neutrophils that were recruited to the notochord; mean percentage \pm SEM, n>5 larvae.

(D, E, F) Two dpf *tg(lyz:DsRed)* embryos were infected in the notochord with *E.coli*-GFP (green arrows: injection sites) and immediately treated with 250 μ M Apocynin. **(D)** Neutrophils (DsRed) and *E. coli* (GFP) were imaged repeatedly in individual larvae using fluorescent microscopy at 6hpi and 1dpi. Bacteria (white arrowheads) were present at 6hpi in both DMSO- and Apocynin-treated embryos. At 1dpi, bacteria disappeared in DMSO-treated embryos (arrows) while their number increased in Apocynin-treated embryos (white arrowheads). Bacterial proliferation was accompanied by a decreased number of neutrophils (neutropenia). **(E)** Larvae survival was scored for uninfected and *E. coli* infected embryos, treated with either DMSO or Apocynine. Results represent the mean of three independent experiments, error bar: \pm -SEM, p<0.0001, 20<n<27. **(F)** Graphical abstract of host response during notochord infection. 1/ Low dose of *E. coli* infection in the notochord leads to the rapid recruitment of neutrophils to the notochord. During the first phase of infection, neutrophils cannot penetrate the collagen sheath and engulf bacteria. NOX activity in recruited neutrophils leads to the production of the ROS superoxide. Superoxide production participates in bacterial clearance without neutrophil-microbe physical contact, as early as 24hpi and results in host survival. 2/ Reducing the ROS superoxide using a drug that inhibits NADPH Oxidase assembly (VAS2870) or a drug that specifically blocks NADPH Oxidase in the leukocytes results in bacteria growth in the notochord and host neutropenia and death. Increasing the ratio (*E. coli* CFU)/(neutrophil number) either by genetic manipulation or higher dose of bacterial injections leads to a similar outcome.

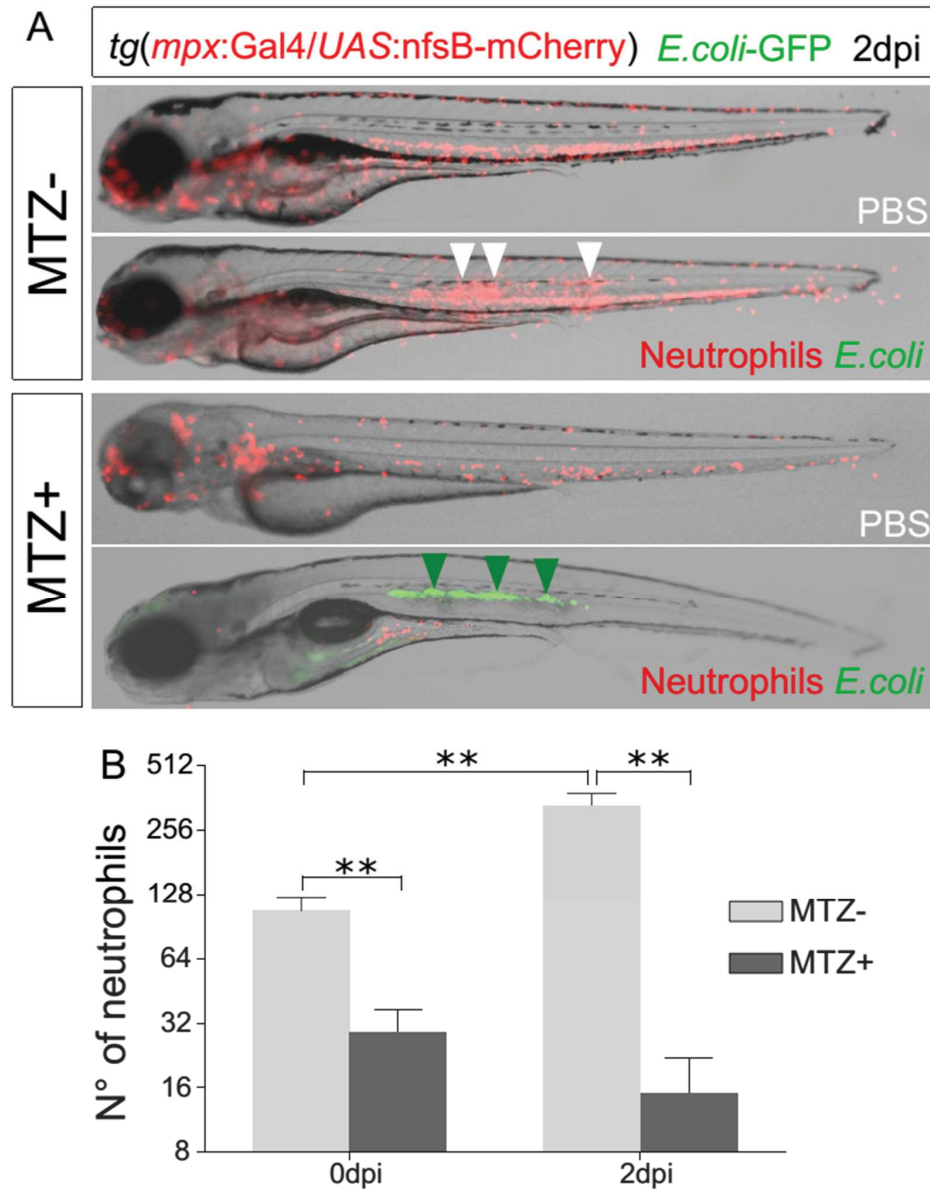


Figure S1: Neutrophils are essential for the control of notochord infection

(A) Two dpf $tg(mpx:Gal4/UAS:nfsB-mCherry)$ embryos were treated with 10mM Metronidazole (Mtz) in fish water for 24 hours. At 3dpf, larvae with neutrophil depletion were selected and injected either with PBS or *E. coli*-GFP in the notochord. The outcome of the infection was analysed by fluorescent microscopy. Larvae images are representative overlays of fluorescence (DsRed and GFP) and transmitted light images at 2dpi. In the absence of Mtz, neutrophils are massively recruited to the notochord and *E. coli* is cleared (white arrowheads). In Mtz-treated larvae, *E. coli* (green, white arrowheads) grew heavily. This correlated with a dramatic decrease in

the number of neutrophils (neutropenia). **(B)** Corresponding count of total neutrophils in neutrophil-ablated and control embryos at 0 and 2dpi. The graph corresponds to a representative experiment, values are expressed as the mean number of neutrophils per larva \pm SEM, ** $p < 0.005$, $n > 5$ larvae.

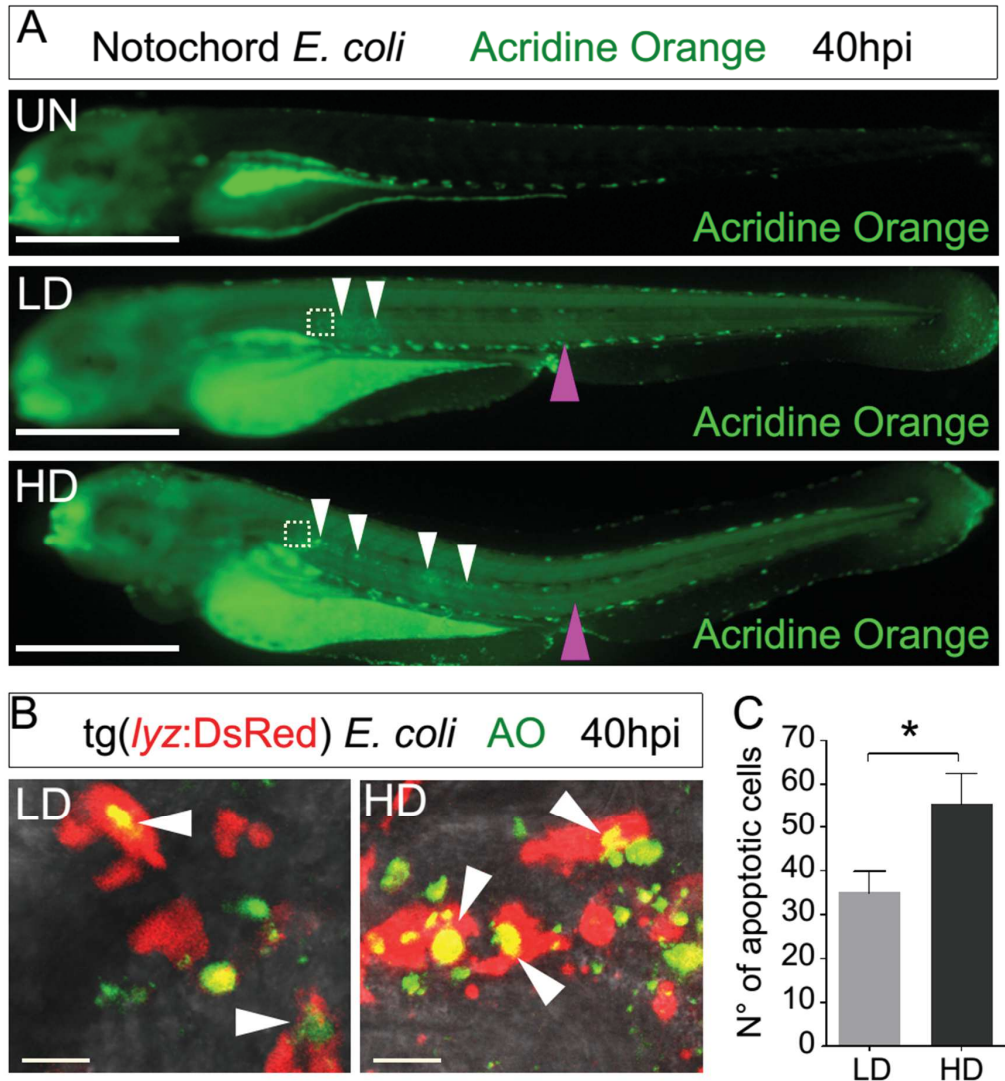


Figure S2: Cell death at the inflamed notochords of low dose and high dose infected larvae.

(A) Larvae were either uninfected (UN) or infected with low dose (LD) or high dose (HD) of *E. coli* in the notochord. They were then stained with 4 μ g/ml of Acridine Orange. Pink arrowheads indicate the injection site and white arrowheads show dead cells at the inflammation sites along the notochord. Boxes show the positions of images in B. Scale bar 600 μ m. **(B)** *Tg(lyz:DsRed)* embryos were infected with a low

dose (LD) or a high dose (HD) of *E. coli* in the notochord. Representative transmitted light images, overlaid with a maximal projection of confocal fluorescence images show neutrophils stained with Acridine Orange (AO) (Arrowheads) at the inflammation sites. **(C)** The number of Acridine Orange positive cells around the infected notochord in indicated conditions. Scale bar 10µm. Error bar: mean ± SEM, *P<0.05 (0.035), ***p<0.001.

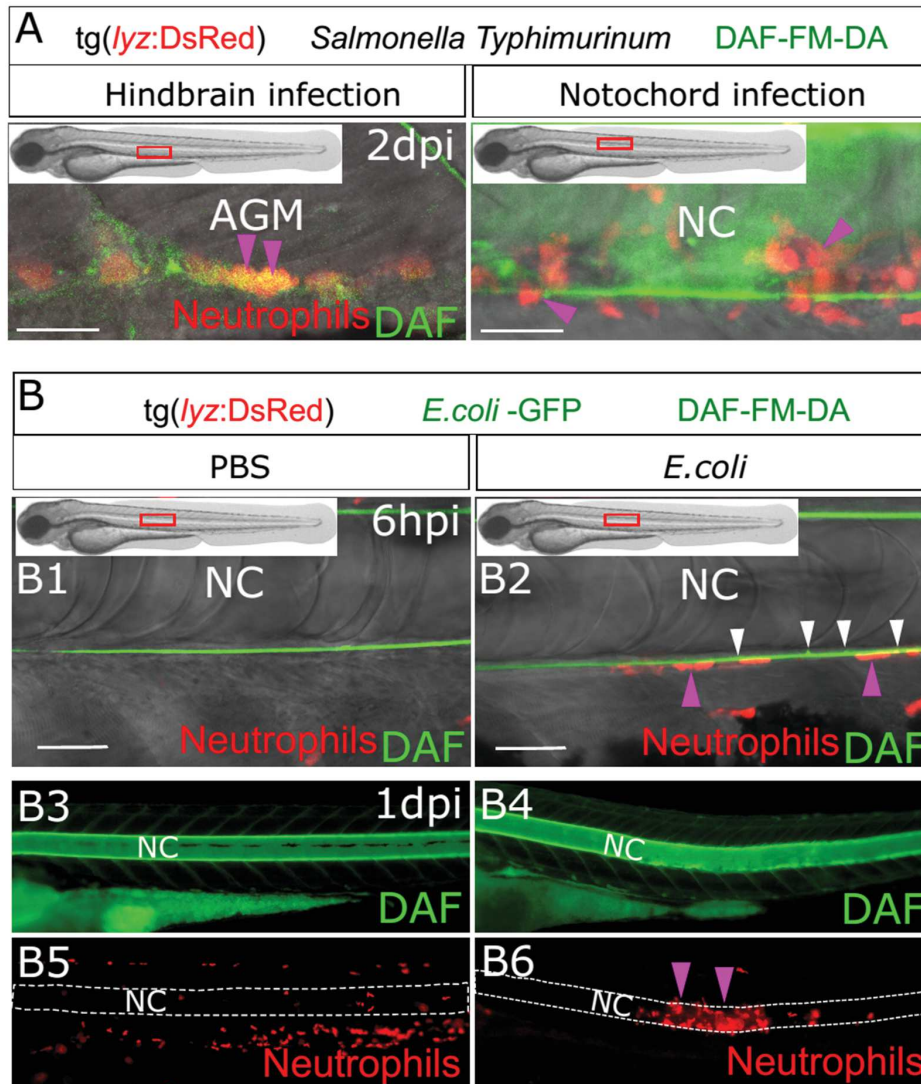


Figure S3: Recruited neutrophils do not produce detectable Nitric Oxide

(A) Nitric oxide is produced by neutrophils in the AGM following *Salmonella Typhimurium* infection. Two dpf *tg(lyz:DsRed)* embryos were infected in the hindbrain or in the notochord with *Salmonella Typhimurium*. At 2dpi Nitric oxide was detected with DAF-FM-DA (green) using confocal microscopy. Representative overlay of

maximum projections of multi scan acquisitions (DsRed and DAF-FM-DA) with transmitted light images shows that Nitric oxide is produced by neutrophils in the AGM (A left panel) and in the notochord (A right panel), but not in the recruited neutrophils (A right panel).

(B) Two dpf *tg(lyz:DsRed)* embryos were infected with *E. coli*-GFP in the notochord. **(B1, B2)** Representative overlay of maximum projections of multi-scan acquisitions (DsRed and DAF-FM-DA) with transmitted light images shows that Nitric oxide (green) is produced constitutively in the notochord (white arrowheads) but not in recruited neutrophils at 6hpi (pink arrowheads). **(B3-B6)** Trunk images are representative DAF-FM-DA fluorescence **(B3-B4)** and DsRed fluorescence images **(B5-B6)** from PBS- or *E. coli*-injected embryos at 1dpi. AGM: Aorta-gonad-mesonephros, NC: notochord, scale bars: 30µm

References

1. Metchnikoff É. Leçons Sur La Pathologie Comparée de L ' Inflammation : Faites à L ' Institut Pasteur En Avril et Mai 1891 / Par Élie Metchnikoff. Edited by G Masson. 1892;1 vol.(XI-. Paris: Librairie de l'académie de médecine, 120, Boulevard Saint-Germain, Paris.
2. Flannagan RS, Cosio G, Grinstein S. Antimicrobial mechanisms of phagocytes and bacterial evasion strategies. *Nat Rev Microbiol.* 2009;7:355-366.
3. Urban CF, Lourido S, Zychlinsky A. How do microbes evade neutrophil killing? *Cell Microbiol.* 2006;8:1687-1696.
4. Dupre-Crochet S, Erard M, Nubetae O. ROS production in phagocytes: why, when, and where? *J Leukoc Biol.* 2013;94:657-670.
5. Paiva CN, Bozza MT. Are reactive oxygen species always detrimental to pathogens? *Antioxid Redox Signal.* 2014;20:1000-1037.
6. Segal AW. How neutrophils kill microbes. *Annu Rev Immunol.* 2005;23:197-223.
7. Staudinger BJ, Oberdoerster MA, Lewis PJ, Rosen H. mRNA expression profiles for *Escherichia coli* ingested by normal and phagocyte oxidase-deficient human neutrophils. *J Clin Invest.* 2002;110:1151-1163.
8. Chakravorty D, Hensel M. Inducible nitric oxide synthase and control of intracellular bacterial pathogens. *Microbes Infect.* 2003;5:621-627.
9. Yang CT, Cambier CJ, Davis JM, Hall CJ, Crosier PS, Ramakrishnan L. Neutrophils exert protection in the early tuberculous granuloma by oxidative killing of mycobacteria phagocytosed from infected macrophages. *Cell Host Microbe.* 2012;12:301-312.
10. Eswarappa SM, Negi VD, Chakraborty S, Chandrasekhar Sagar BK, Chakravorty D. Division of the *Salmonella*-containing vacuole and depletion of acidic lysosomes in *Salmonella*-infected host cells are novel strategies of *Salmonella enterica* to avoid lysosomes. *Infect Immun.* 2010;78:68-79.
11. Pieters J. *Mycobacterium tuberculosis* and the macrophage: maintaining a balance. *Cell Host Microbe.* 2008;3:399-407.
12. Ray K, Marteyn B, Sansonetti PJ, Tang CM. Life on the inside: the intracellular lifestyle of cytosolic bacteria. *Nat Rev Microbiol.* 2009;7:333-340.

13. Tilney LG, Portnoy DA. Actin filaments and the growth, movement, and spread of the intracellular bacterial parasite, *Listeria monocytogenes*. *J Cell Biol.* 1989;109:1597-1608.
14. Mostowy S. Autophagy and bacterial clearance: a not so clear picture. *Cell Microbiol.* 2013;15:395-402.
15. Nathan C. Neutrophils and immunity: challenges and opportunities. *Nat Rev Immunol.* 2006;6:173-182.
16. Brinkmann V, Reichard U, Goosmann C, et al. Neutrophil extracellular traps kill bacteria. *Science.* 2004;303:1532-1535.
17. Pagan AJ, Yang CT, Cameron J, et al. Myeloid Growth Factors Promote Resistance to Mycobacterial Infection by Curtailing Granuloma Necrosis through Macrophage Replenishment. *Cell Host Microbe.* 2015;18:15-26.
18. Torraca V, Masud S, Spaik HP, Meijer AH. Macrophage-pathogen interactions in infectious diseases: new therapeutic insights from the zebrafish host model. *Dis Model Mech.* 2014;7:785-797.
19. Colucci-Guyon E, Tinevez JY, Renshaw SA, Herbomel P. Strategies of professional phagocytes in vivo: unlike macrophages, neutrophils engulf only surface-associated microbes. *J Cell Sci.* 2011;124:3053-3059.
20. Nguyen-Chi M, Phan QT, Gonzalez C, Dubremetz JF, Levraud JP, Lutfalla G. Transient infection of the zebrafish notochord with *E. coli* induces chronic inflammation. *Dis Model Mech.* 2014;7:871-882.
21. Alibaud L, Rombouts Y, Trivelli X, et al. A *Mycobacterium marinum* TesA mutant defective for major cell wall-associated lipids is highly attenuated in *Dictyostelium discoideum* and zebrafish embryos. *Mol Microbiol.* 2011;80:919-934.
22. Benard EL, van der Sar AM, Ellett F, Lieschke GJ, Spaik HP, Meijer AH. Infection of zebrafish embryos with intracellular bacterial pathogens. *J Vis Exp.* 2012.
23. Bernut A, Herrmann JL, Kissa K, et al. *Mycobacterium abscessus* cording prevents phagocytosis and promotes abscess formation. *Proc Natl Acad Sci U S A.* 2014;111:E943-952.
24. Renshaw SA, Loynes CA, Trushell DM, Elworthy S, Ingham PW, Whyte MK. A transgenic zebrafish model of neutrophilic inflammation. *Blood.* 2006;108:3976-3978.
25. Hall C, Flores MV, Storm T, Crosier K, Crosier P. The zebrafish lysozyme C promoter drives myeloid-specific expression in transgenic fish. *BMC Dev Biol.* 2007;7:42.
26. Robertson AL, Holmes GR, Bojarczuk AN, et al. A zebrafish compound screen reveals modulation of neutrophil reverse migration as an anti-inflammatory mechanism. *Sci Transl Med.* 2014;6:225ra229.
27. Elks PM, van der Vaart M, van Hensbergen V, et al. Mycobacteria counteract a TLR-mediated nitrosative defense mechanism in a zebrafish infection model. *PLoS One.* 2014;9:e100928.
28. Kimmel CB, Ballard WW, Kimmel SR, Ullmann B, Schilling TF. Stages of embryonic development of the zebrafish. *Dev Dyn.* 1995;203:253-310.
29. Boudeau J, Glasser AL, Masseret E, Joly B, Darfeuille-Michaud A. Invasive ability of an *Escherichia coli* strain isolated from the ileal mucosa of a patient with Crohn's disease. *Infect Immun.* 1999;67:4499-4509.
30. Low D, Tran HT, Lee IA, et al. Chitin-binding domains of *Escherichia coli* ChiA mediate interactions with intestinal epithelial cells in mice with colitis. *Gastroenterology.* 2013;145:602-612 e609.

31. Chassaing B, Rolhion N, de Vallee A, et al. Crohn disease--associated adherent-invasive E. coli bacteria target mouse and human Peyer's patches via long polar fimbriae. *J Clin Invest*. 2011;121:966-975.
32. Stachura DL, Svoboda O, Campbell CA, et al. The zebrafish granulocyte colony-stimulating factors (Gcsfs): 2 paralogous cytokines and their roles in hematopoietic development and maintenance. *Blood*. 2013;122:3918-3928.
33. Morash MG, Douglas SE, Robotham A, Ridley CM, Gallant JW, Soanes KH. The zebrafish embryo as a tool for screening and characterizing pleurocidin host-defense peptides as anti-cancer agents. *Dis Model Mech*. 2011;4:622-633.
34. Lepiller S, Laurens V, Bouchot A, Herbomel P, Solary E, Chluba J. Imaging of nitric oxide in a living vertebrate using a diamino-fluorescein probe. *Free Radic Biol Med*. 2007;43:619-627.
35. Dreux N, Denizot J, Martinez-Medina M, et al. Point mutations in FimH adhesin of Crohn's disease-associated adherent-invasive Escherichia coli enhance intestinal inflammatory response. *PLoS Pathog*. 2013;9:e1003141.
36. Travnickova J, Tran Chau V, Julien E, et al. Primitive macrophages control HSPC mobilization and definitive haematopoiesis. *Nat Commun*. 2015;6:6227.
37. van Rooijen N, Sanders A, van den Berg TK. Apoptosis of macrophages induced by liposome-mediated intracellular delivery of clodronate and propamidine. *J Immunol Methods*. 1996;193:93-99.
38. Ellett F, Pase L, Hayman JW, Andrianopoulos A, Lieschke GJ. mpeg1 promoter transgenes direct macrophage-lineage expression in zebrafish. *Blood*. 2011;117:e49-56.
39. Palha N, Guivel-Benhassine F, Briolat V, et al. Real-time whole-body visualization of Chikungunya Virus infection and host interferon response in zebrafish. *PLoS Pathog*. 2013;9:e1003619.
40. Hall CJ, Flores MV, Oehlers SH, et al. Infection-responsive expansion of the hematopoietic stem and progenitor cell compartment in zebrafish is dependent upon inducible nitric oxide. *Cell Stem Cell*. 2012;10:198-209.
41. Niethammer P, Grabher C, Look AT, Mitchison TJ. A tissue-scale gradient of hydrogen peroxide mediates rapid wound detection in zebrafish. *Nature*. 2009;459:996-999.
42. Babior BM, Curnutte JT, Kipnes BS. Pyridine nucleotide-dependent superoxide production by a cell-free system from human granulocytes. *J Clin Invest*. 1975;56:1035-1042.
43. Altenhofer S, Radermacher KA, Kleikers PW, Wingler K, Schmidt HH. Evolution of NADPH Oxidase Inhibitors: Selectivity and Mechanisms for Target Engagement. *Antioxid Redox Signal*. 2015;23:406-427.
44. Vejrazka M, Micek R, Stipek S. Apocynin inhibits NADPH oxidase in phagocytes but stimulates ROS production in non-phagocytic cells. *Biochim Biophys Acta*. 2005;1722:143-147.
45. Urban CF, Reichard U, Brinkmann V, Zychlinsky A. Neutrophil extracellular traps capture and kill *Candida albicans* yeast and hyphal forms. *Cell Microbiol*. 2006;8:668-676.
46. Yousefi S, Mihalache C, Kozlowski E, Schmid I, Simon HU. Viable neutrophils release mitochondrial DNA to form neutrophil extracellular traps. *Cell Death Differ*. 2009;16:1438-1444.
47. Metzler KD, Fuchs TA, Nauseef WM, et al. Myeloperoxidase is required for neutrophil extracellular trap formation: implications for innate immunity. *Blood*. 2011;117:953-959.
48. Slauch JM. How does the oxidative burst of macrophages kill bacteria? Still an open question. *Mol Microbiol*. 2011;80:580-583.
49. Geering B, Simon HU. Peculiarities of cell death mechanisms in neutrophils. *Cell Death Differ*. 2011;18:1457-1469.



PART III

Identification of polarized macrophage subsets in zebrafish

Authors:

NGUYEN-CHI Mai, LAPLACE-BUILHE Béryl, TRAVNICKOVA Jana, LUZ-CRAWFORD Patricia, TEJEDOR Gautier, **PHAN Quang Tien**, DUROUX-RICHARD Isabelle, LEVRAUD Jean-Pierre, KISSA Karima, LUTFALLA Georges, JORGENSEN Christian, and DJOUAD Farida

eLIFE

2015



Identification of polarized macrophage subsets in zebrafish

Mai Nguyen-Chi^{1,2†}, Béryll Laplace-Builhe^{1,2†}, Jana Travnickova^{2,3},
Patricia Luz-Crawford^{1,2}, Gautier Tejedor^{1,2}, Quang Tien Phan³,
Isabelle Duroux-Richard^{1,2}, Jean-Pierre Levrud^{4,5}, Karima Kissa^{2,3},
Georges Lutfalla^{2,3}, Christian Jorgensen^{1,2,6‡}, Farida Djouad^{1,2*†}

¹Institut de Médecine Régénérative et Biothérapies, Institut national de la santé et de la recherche médicale, Montpellier, France; ²Université de Montpellier, Montpellier, France; ³Dynamique des Interactions Membranaires Normales et Pathologiques, Centre national de la recherche scientifique, Montpellier, France; ⁴Macrophages et Développement de l'Immunité, Institut Pasteur, Paris, France; ⁵Département de Biologie du Développement et Cellules Souches, Institut Pasteur, Paris, France; ⁶Clinical unit for osteoarticular diseases and Department for Biotherapy, Centre Hospitalier Universitaire, Montpellier, France

Abstract While the mammalian macrophage phenotypes have been intensively studied in vitro, the dynamic of their phenotypic polarization has never been investigated in live vertebrates. We used the zebrafish as a live model to identify and trail macrophage subtypes. We generated a transgenic line whose macrophages expressing *tumour necrosis factor alpha* (*tnfa*), a key feature of classically activated (M1) macrophages, express fluorescent proteins *Tg(mpeg1:mCherryF/tnfa:eGFP-F)*. Using 4D-confocal microscopy, we showed that both aseptic wounding and *Escherichia coli* inoculation triggered macrophage recruitment, some of which started to express *tnfa*. RT-qPCR on Fluorescence Activated Cell Sorting (FACS)-sorted *tnfa*⁺ and *tnfa*⁻ macrophages showed that they, respectively, expressed M1 and alternatively activated (M2) mammalian markers. Fate tracing of *tnfa*⁺ macrophages during the time-course of inflammation demonstrated that pro-inflammatory macrophages converted into M2-like phenotype during the resolution step. Our results reveal the diversity and plasticity of zebrafish macrophage subsets and underline the similarities with mammalian macrophages proposing a new system to study macrophage functional dynamic.

DOI: [10.7554/eLife.07288.001](https://doi.org/10.7554/eLife.07288.001)

*For correspondence: farida.djouad@inserm.fr

†These authors contributed equally to this work

‡These authors also contributed equally to this work

Competing interests: The authors declare that no competing interests exist.

Funding: See page 13

Received: 03 March 2015

Accepted: 07 July 2015

Published: 08 July 2015

Reviewing editor: Utpal Banerjee, University of California, Los Angeles, United States

© Copyright Nguyen Chi et al. This article is distributed under the terms of the [Creative Commons Attribution License](https://creativecommons.org/licenses/by/4.0/), which permits unrestricted use and redistribution provided that the original author and source are credited.

Introduction

Behind the generic name 'macrophage' hides various cell types with distinct phenotypes and functions. Currently, it is well established that macrophages are not just important immune effector cells but also cells with critical homeostatic roles, exerting a *myriad* of functions in development, homeostasis, and tissue repair and playing a pivotal role in disease progression (Wynn et al., 2013). Therefore, there is a high interest in a better characterization of these cells to establish an early and accurate diagnosis. The wide variety of macrophage functions might be explained by the outstanding plasticity and versatility of macrophages that efficiently respond to environmental challenges and changes in tissue physiology by modifying their phenotype (Mosser and Edwards, 2008). Although there is a consensus that macrophages are a diversified set of cells, macrophage subtypes are still poorly characterized. Indeed, although these cell populations have been extensively investigated in mouse and human, these studies were mostly performed in vitro using monocyte-derived macrophages induced under specific stimuli. A comprehensive characterization of macrophage

eLife digest Inflammation plays an important role in helping the body to heal wounds and fight off certain diseases. Immune cells called macrophages—which are perhaps best known for their ability to engulf and digest microbes and cell debris—help to control inflammation. In mammals, different types of macrophage exist; the most functionally extreme of which are the M1 macrophages that stimulate inflammation and M2 macrophages that reduce the inflammatory response.

Macrophages acquire different abilities through a process called polarization, which is controlled by signals produced by a macrophage's environment. Polarization has been well investigated in human and mouse cells grown in the laboratory, but less is understood about how this process occurs in live animals.

Nguyen Chi, Laplace-Builhe et al. investigated whether zebrafish larvae (which are naturally transparent) could form an experimental model in which to investigate macrophage polarization in living animals. Zebrafish were first genetically engineered to produce two fluorescent proteins: one that marks macrophages and one that marks M1 macrophages. These fluorescent proteins allow the movement and polarization of macrophages to be tracked in real time in living larvae using a technique called confocal microscopy. Nguyen Chi, Laplace-Builhe et al. also isolated macrophage cells from these zebrafish at different times during the inflammatory process to identify which macrophage subtypes form and when.

The results show that unpolarized macrophages move to the sites of inflammation (caused by wounds or bacterial infection), where they become polarized into M1 cells. Over time, these M1 macrophages progressively convert into an M2-like macrophage subtype, presumably to help clear up the inflammation.

Furthermore, Nguyen Chi, Laplace-Builhe et al. show that the M1 and M2 macrophage subtypes in zebrafish are similar to those found in mammals. Therefore, genetically engineered zebrafish larvae are likely to prove useful for studying macrophage activity and polarization in living animals.

DOI: [10.7554/eLife.07288.002](https://doi.org/10.7554/eLife.07288.002)

subsets that takes into account their specific behaviour, phenotypic diversity, functions, and modulation shall rely on a real-time tracking in the whole organism in response to environmental challenges.

Mouse and human macrophages have been classified according to their polarization state. In this classification, M1 macrophages, also referred as classically activated macrophages, are pro-inflammatory cells associated with the first phases of inflammation, while M2 macrophages, also known as alternatively activated macrophages, are involved in the resolution of inflammation and tissue remodelling (**Gordon, 2003; Biswas and Mantovani, 2010; Sica and Mantovani, 2012**). Differential cytokine and chemokine production and receptor expression define the polarization state of macrophages. However, it is worthwhile to note that such binary naming does not fully reflect the diversity of macrophage phenotypes in complex *in vivo* environments in which several cytokines and growth factors are released and adjust the final differentiated state (**Chazaud, 2013; Thomas and Mattila, 2014**). Macrophages might adopt *intermediate activation phenotypes* classified by the relative levels of macrophage subset-specific markers. Therefore, macrophage plasticity results in a full spectrum of macrophage subsets with a myriad of functions (**Mosser and Edwards, 2008; Xue et al., 2014**). Although the possible phenotype conversion of macrophages from M1 to M2 has been suggested in *in vitro* studies, a recent study argues for the sequential homing of M1 and M2 macrophages to the site of injury (**Stout et al., 2005; Sica and Mantovani, 2012; Shechter et al., 2013**). Such controversies highlight the lack of accurate real-time tracing of macrophage subtypes *in vivo* in the entire animal.

Inflammation is a model of choice to study the wide range of macrophage subsets involved from its initiation to its resolution. Therefore, in the present study, we propose to decipher *in vivo* in real time the kinetic of macrophage subset recruitment, their behaviour and their phenotypic plasticity at the molecular level during a multiple-step inflammatory process. We used the zebrafish larvae model for its easy genetic manipulation, transparency, and availability of fluorescent reporter lines to track macrophages (**Ellett et al., 2011**). While the existence of macrophage subtypes in zebrafish embryos

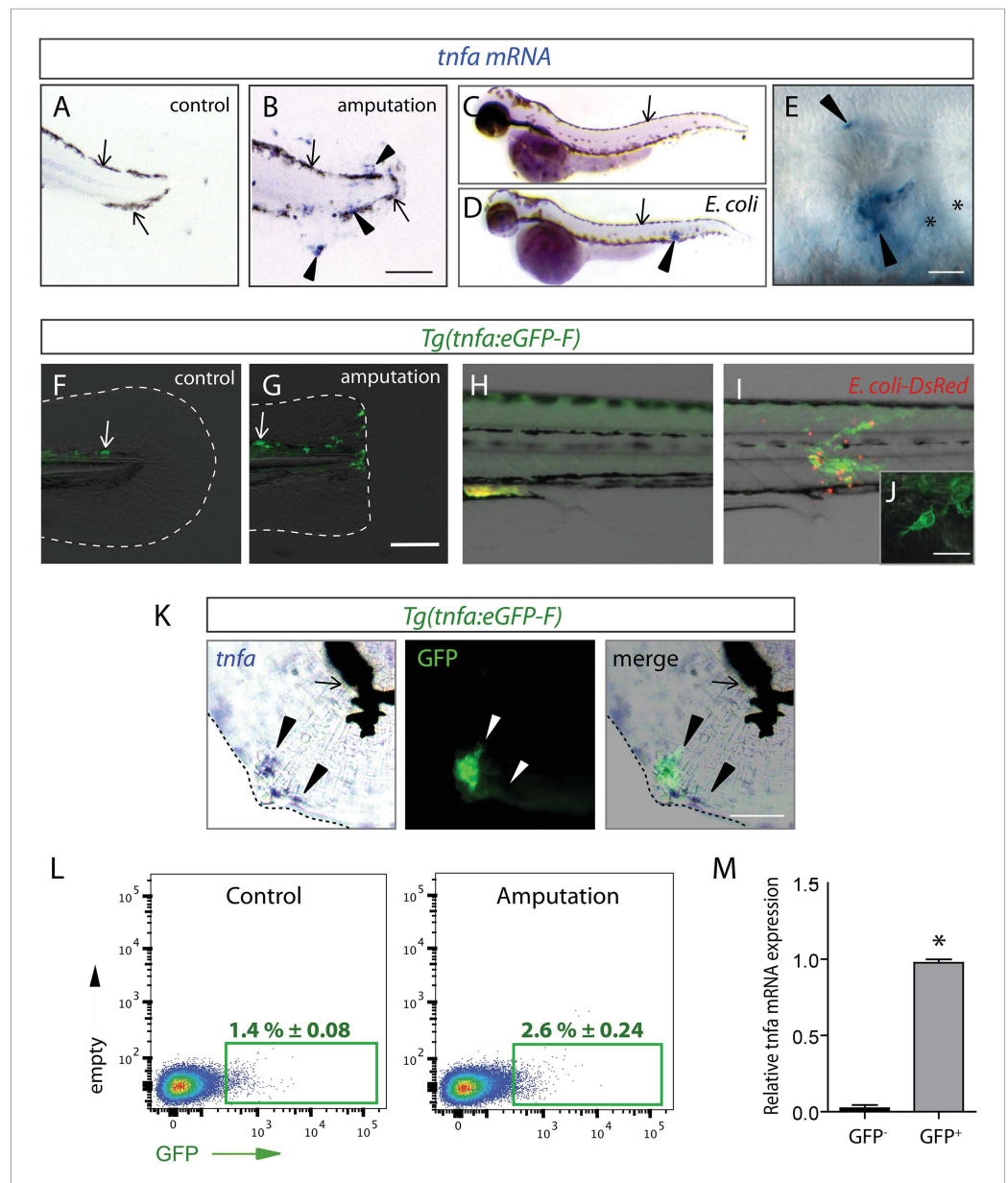


Figure 1. The (*tnfa:eGFP-F*) reporter line recapitulates transcriptional activation of *tnfa* upon wound-induced inflammation and *Escherichia coli* infection. (A–E) *Tumour necrosis factor alpha* (*tnfa*) mRNA expression (blue, arrowhead) was detected by in situ hybridization using *tnfa* anti-sense probe: at 6 hpa in (A) intact (control) and (B) amputated fins from 3 dpf WT larvae, (C) in uninfected larvae (54 hpf, hours post-fertilization) and (D, E) *E. coli* infected larvae (24 hpi, 54 hpf). Arrows show melanocytes (black). (E) Imaging of *tnfa* mRNA expression in the muscle at higher magnification, asterisks show muscle fibres, scale bar in (B) = 100 μ m and in (E) = 50 μ m. (F, G) eGFP fluorescence (green) was analyzed by fluorescent microscopy in (F) intact (control) and (G) amputated *Tg(tnfa:eGFP-F)* fins at 6 hpa, dotted lines outline the caudal fin, scale bar = 100 μ m and at 16 hpi in *Tg(tnfa:eGFP-F)* larvae injected with (H) PBS or (I, J) *E. coli* (red) in the muscle. Arrows show auto-fluorescent xanthophores. (J) Multi-scan confocal analysis of GFP expression in *E. coli*-infected *Tg(tnfa:eGFP-F)* larvae, scale bar = 20 μ m. (K) *tnfa* mRNA and eGFP-F expressions were analyzed using microscopy at 6 hpa in amputated fins from 3 dpf *Tg(tnfa:eGFP-F)* larvae. Dotted lines delimit the caudal fin, arrowheads show overlapping signals, and arrows show the pigments. Scale bar = 100 μ m. (L) Graphed data of representative fluorescence-activated flow cytometry analysis of eGFP⁺ cells in upon amputation. *Tg(tnfa:eGFP-F)* larvae were either kept intact (control) or amputated at 3 dpf, and cells were collected at 6 hr post-treatment. Green gates represent eGFP⁺ population and mean percentage of eGFP⁺ cells. (M) Bar graph showing relative *tnfa* mRNA expression in GFP⁻ and GFP⁺ cells. * indicates statistical significance. Figure 1. continued on next page

Figure 1. Continued

population \pm s.e.m is indicated. (M) Relative expression of *tnfa* in eGFP⁻ and GFP⁺ cells in amputated larvae. Real-time RT-PCR on separated cells using EF1a as a reference gene. Graph represents the mean value of three independent experiments \pm s.e.m. **p* < 0.05.

DOI: [10.7554/eLife.07288.003](https://doi.org/10.7554/eLife.07288.003)

has been suggested, they have not been fully characterized (Herbomel et al., 1999; Ellett et al., 2011; Cambier et al., 2013; Petrie et al., 2014). Here, we report a new reporter transgene for TNF α , a central inflammatory cytokine and well-established marker of M1 macrophages, instrumental to discriminate macrophage subsets during intravital imaging.

Results and discussion

In vivo visualization of macrophage activation and polarization

Fin wounding-induced inflammation and *Escherichia coli* inoculation in zebrafish larvae of 3 dpf are two well-established models triggering macrophage recruitment. Using in situ hybridization, we observed that the expression of the tumour necrosis factor alpha (*tnfa*), a consensus marker of M1 macrophages, was induced in cells accumulated in the caudal fin and the muscle following amputation ($n_{\text{larvae}} = 29/33$) and *E. coli* inoculation ($n_{\text{larvae}} = 12/12$), respectively (Figure 1A–E). To study the cells that express the *tnfa* transcripts, we established the *Tg(tnfa:eGFP-F)* transgenic zebrafish line expressing a farnesylated (membrane-bound) eGFP (eGFP-F) under the control of the *tnfa* promoter. While eGFP-F was undetectable in intact fins of *Tg(tnfa:eGFP-F)* larvae ($n_{\text{larvae}} = 10/10$), it was expressed in cells recruited to the wound at 6 hr post-amputation (hpA) ($n_{\text{larvae}} = 16/16$, Figure 1F,G). Similarly, eGFP-F expression was upregulated in cells accumulated in the muscle of *Tg(tnfa:eGFP-F)* larvae at 16 hr post-inoculation (hpi) of DsRed-expressing *E. coli* ($n_{\text{larvae}} = 8/8$), compared to Phosphate-buffered saline (PBS) injection ($n_{\text{larvae}} = 3/3$, Figure 1H,I). Confocal analysis confirmed the presence of a membrane-bound eGFP in cells displaying a typical myeloid morphology (Figure 1J). To demonstrate that the *Tg(tnfa:eGFP-F)* line recapitulates transcriptional activation of *tnfa*, we performed a simultaneous detection of *tnfa* mRNA by in situ hybridization and GFP-F protein by immunofluorescence in amputated larvae 6 hpA. We observed a consistent overlap between *tnfa* and GFP-F signal in the fin ($n_{\text{larvae}} = 11/11$), showing the direct correlation of eGFP-F and *tnfa* transcriptional activation in the fin of the reporter line (Figure 1K). In addition, we FACS-sorted GFP⁺ cells from wounded *Tg(TNF α :eGFP-F)* larvae 6 hpA and performed RT-qPCR to analyze *tnfa* expression. We observed a significant increase of *tnfa* mRNA level in eGFP⁺ cells as compared to eGFP⁻ cells (Figure 1L,M). All together these results indicate that the *Tg(TNF α :eGFP-F)* reporter line recapitulates transcriptional activation of *tnfa*. Then, with the ability to specifically track *tnfa*-expressing cells, we used *Tg(tnfa:eGFP-F)* fish to study macrophage activation by mating them with *Tg(mpeg1:mCherryF)* fish in which macrophages express farnesylated mCherry (mCherryF) under the control of the macrophage-specific *mpeg1* promoter (Ellett et al., 2011; Nguyen-Chi et al., 2014). In intact *Tg(tnfa:eGFP-F)/mpeg1:mCherryF* larvae, no eGFP-F was observed in macrophages (Figure 2A). We imaged double transgenic larvae *Tg(tnfa:eGFP-F)/mpeg1:mCherryF* using 4D confocal microscopy from 45 min post-amputation and found that macrophages were recruited to the wound from 1 hpA, some starting to express eGFP from 3 hpA (Figure 2B,C and Video 1). From 5 hpA already activated macrophages, that is, expressing *tnfa* arrived at the wound (Video 1 and Figure 2C). Similarly, infection with a crimson-expressing *E. coli* in the muscle induced the expression of *tnfa* in phagocytes few hours following the infection (Figure 2—figure supplement 1, Video 2). Imaging of the double transgenic larvae *Tg(tnfa:eGFP-F)/mpeg1:mCherryF* showed that *tnfa*-expressing phagocytes were mainly macrophages (Figure 2—figure supplement 1, Video 2). These results show the dynamic macrophage activation in real-time in vivo including recruitment and rapid phenotypic change. During the revision of this paper, a similar result has been published (Sanderson et al., 2015).

Morphology and behaviour of macrophage phenotypes

To test whether *tnfa*⁺ and *tnfa*⁻ macrophages harboured different cellular characteristics, we first analyzed their morphology in fin-wounded *Tg(tnfa:eGFP-F)/mpeg1:mCherryF* larvae. *tnfa*⁺*mpeg1*⁺ cells displayed flattened and lobulated morphology (Figure 2D), while *tnfa*⁻*mpeg1*⁺ were elongated

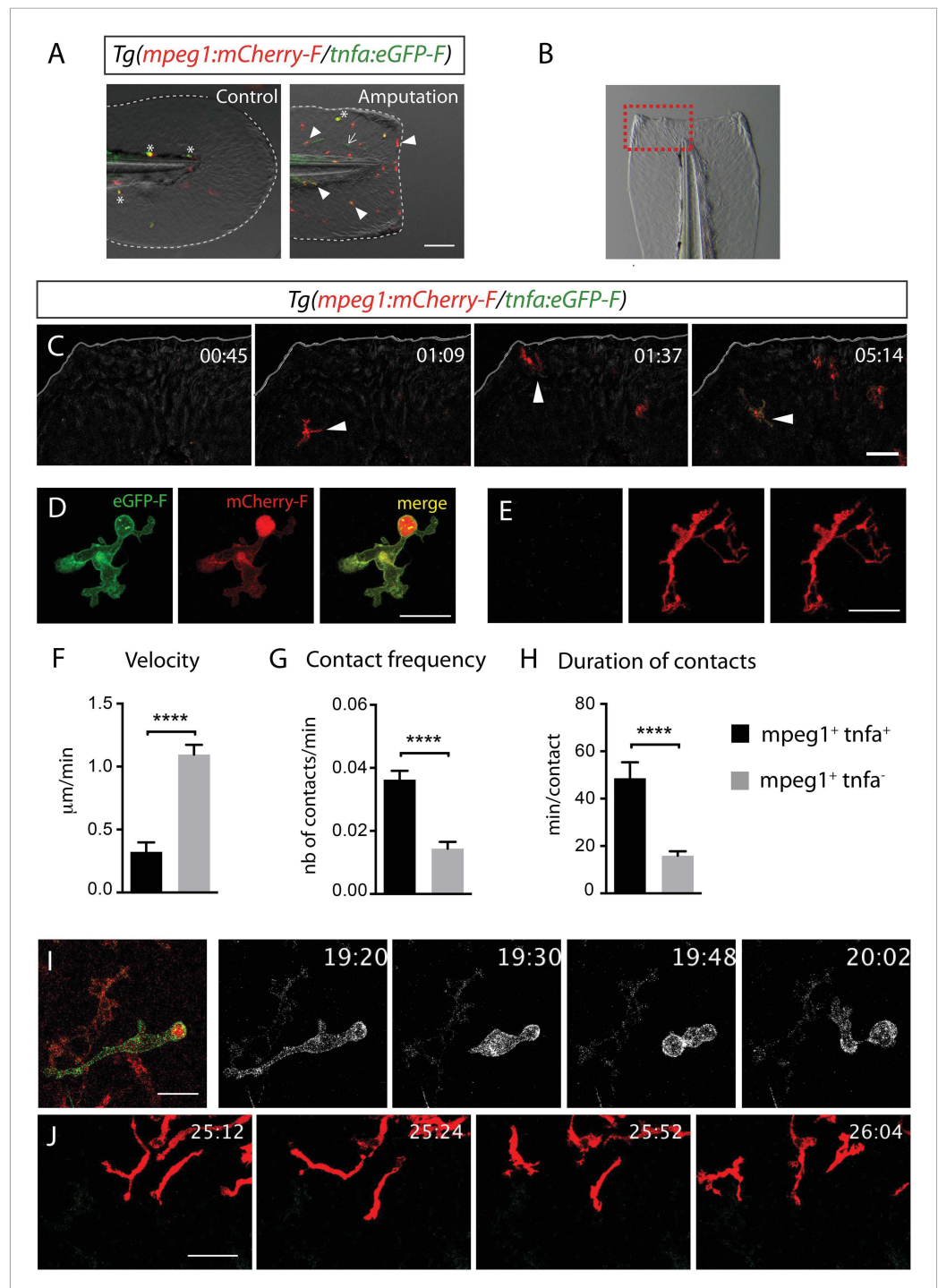


Figure 2. Activation, morphology, and behaviour of $\text{TNF-}\alpha^+$ macrophages in (*tnfa:eGFP-F/mpeg1:mCherry-F*) transgenic larvae upon wound-induced inflammation. **(A)** eGFP-F (green) and mCherryF (red) fluorescence was analyzed by fluorescent microscopy in intact (control) and amputated *Tg(mpeg1:mCherryF/tnfa:eGFP-F)* fins at 6 hpA of 3 dpf larvae. Arrowheads show recruited macrophages that express *tnfa*, arrows show *tnfa*⁺ cells that are not macrophages, and asterisks show auto-fluorescent pigments. Dotted lines outline the caudal fin, scale bar = 100 μm . **(B)** Bright-field image of the wounded fin of a 3 dpf *Tg(mpeg1:mCherryF/tnfa:eGFP-F)* larva. Dotted red box shows the region imaged in **C**. **(C)** Representative time-lapse maximum projections show the activation of macrophages arriving at the wound in 3 dpf amputated *Tg(mpeg1:mCherryF/tnfa:eGFP-F)*. The time pA is shown on top right *Figure 2. continued on next page*

Figure 2. Continued

corner and indicated in hours and minutes, white lines outline the caudal fin. The transcriptional activation of *tnfa* (green) in recruited macrophage (red, arrowhead) was first observed from 3 hpA. Scale bar = 30 μ m. White lines outline the caudal fin. (D, E) Maximum projections of confocal analysis of eGFP-F (green) and mCherryF (red) expressions in recruited macrophages at (D) 18 hpA and (E) 24 hpA in *Tg(mpeg1:mCherryF/tnfa:eGFP-F)*. *tnfa*⁺*mpeg1*⁺ macrophages exhibit a round and protrusive morphology, while *tnfa*⁻*mpeg1*⁺ macrophages exhibit a dendritic morphology. (F) Velocity of *tnfa*⁺*mpeg1*⁺ and *tnfa*⁻*mpeg1*⁺ macrophages (N = 18). (G) Frequency of macrophage–macrophage contacts and (H) time length of the contacts of *tnfa*⁻*mpeg1*⁺ and *tnfa*⁺*mpeg1*⁺ cells. Measurements were extracted from three independent videos of amputated *Tg(mpeg1:mCherryF/tnfa:eGFP-F)*, for contact frequency, N = 15 and for duration of the interaction, N = 11 macrophages. ****p < 0.0001. (I) Representative time-lapse maximum projections show the behaviour of *tnfa*⁺*mpeg1*⁺ macrophages, starting 19h20 pA during 42 min. Two macrophages (green + red) interact by cell–cell contact. These macrophages (eGFP in grey) remain attached up to 40 min. Scale bar 20 = μ m. (J) Representative time-lapse maximum projections show the behaviour of *tnfa*⁻*mpeg1*⁺ macrophages, starting 25h12 pA during 52 min. Macrophages (red) barely establish cell–cell contact. Scale bar = 30 μ m.

DOI: [10.7554/eLife.07288.004](https://doi.org/10.7554/eLife.07288.004)

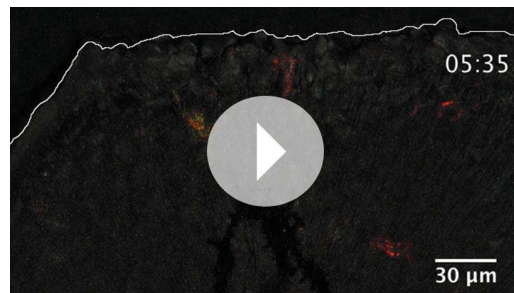
The following figure supplement is available for figure 2:

Figure supplement 1. Activation of *tnfa*⁺ macrophages in (*tnfa:eGFP-F/mpeg1:mCherry-F*) transgenic larvae upon *E. coli* infection.

DOI: [10.7554/eLife.07288.005](https://doi.org/10.7554/eLife.07288.005)

and dendritic (Figure 2E). As we observed that *tnfa*⁺*mpeg1*⁺ cells were predominant at the wound at 18 hpA and *tnfa*⁻*mpeg1*⁺ cells at 24 hpA (data not shown), we imaged the behaviour of these macrophage populations in wounded fins from *Tg(tnfa:eGFP-F/mpeg1:mCherryF)* larvae at these time points. *tnfa*⁺*mpeg1*⁺ cells presented a lower velocity (0.32 μ m/min) than *tnfa*⁻*mpeg1*⁺ macrophages (1.09 μ m/min, Figure 2F) but a higher cell–cell contact frequency (0.036 VS 0.016 contacts/min) with other macrophages (Figure 2G,I,J and Videos 3, 4). Measurements of the duration of macrophage–macrophages contacts showed that these contacts lasted longer (48.6 min/contact) than that of *tnfa*⁻*mpeg1*⁺ macrophages (15.9 min/contact, Figure 2H–J and Videos 3, 4). All together these data highlight different morphology and behaviour of macrophage phenotypes in live zebrafish

suggesting the existence of macrophage subsets exhibiting different functions.

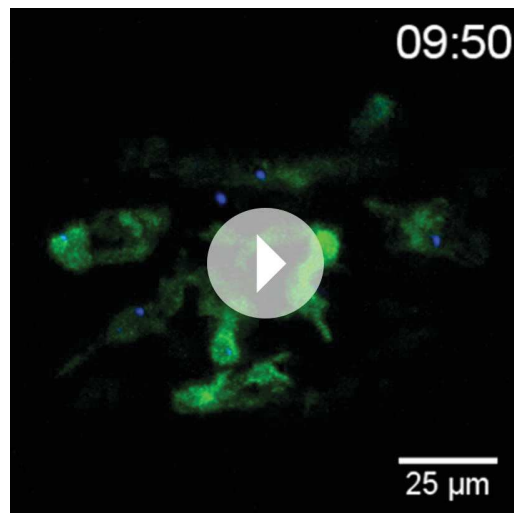


Video 1. Transcriptional activation of *tnfa* in macrophages of (*tnfa:eGFP-F/mpeg1:mCherry-F*) transgenic larvae upon amputation. Representative time-lapse maximum projections show the transcriptional activation of tumour necrosis factor alpha (*tnfa*) in macrophages arriving at the wound in 3 dpf amputated *Tg(mpeg1:mCherryF/tnfa:eGFP-F)*. The time pA is shown on top right corner, white line outline the caudal fin. Scale bar = 30 μ m. Image stacks were acquired every 3 min 30 s from 45 min pA to 7 hr 48 min pA at 2- μ m intervals, 1024 \times 512 pixel resolution using a confocal microscope TCSSP5 SP5 inverted equipped with a HCXPL APO 40x/1.25–0.75 oil objective (Leica). Excitation wavelengths used were 488 nm for EGFP-F and 570 nm for mCherryF.

DOI: [10.7554/eLife.07288.006](https://doi.org/10.7554/eLife.07288.006)

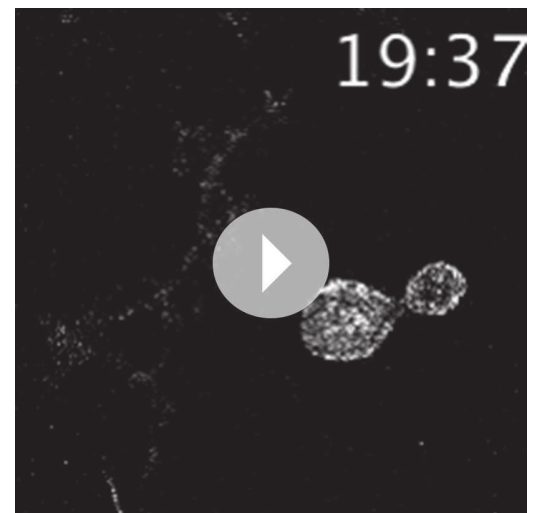
Macrophages phenotypes are activated in a time-dependant manner

To quantify the respective frequency of *tnfa*⁺ macrophages (mCherry⁺eGFP⁺ referred as *dbl*⁺) and *tnfa*⁻ macrophages (mCherry⁺eGFP⁻ referred as *mCh*⁺), we performed flow cytometry analysis on cells isolated from *Tg(tnfa:eGFP-F/mpeg1:mCherryF)* larvae at different time points following caudal fin amputation or *E. coli* inoculation (Figure 3A,B). While only 5.6% \pm 0.9 (s.e.m.) *dbl*⁺ cells were detected in the *mpeg1*⁺ population of the intact larvae, a steady increase of the *dbl*⁺ population from 6 to 20 hpA (up to 27.33 \pm 0.2%) was observed. This percentage decreased dramatically at 26 hpA to 8.75 \pm 1%. In *E. coli* inoculation experiments, the frequency of *dbl*⁺ cells increased as soon as 3 hpi (55.60 \pm 0.6%) and remained stable until 26 hpi. These results demonstrate that wound-induced macrophage activation is transient compared to infection-induced macrophage activation.



Video 2. Transcriptional activation of *tnfa* of (*tnfa*:eGFP-F/*mpeg1*:mCherry-F) transgenic larvae upon *E. coli* infection. *Tg(mpeg1*:mCherryF/*tnfa*:eGFP-F) larvae were infected with crimson-expressing *E. coli* (blue) at 3 dpf in the muscle and imaged from 30 min pi to 10 hr 30 min pi. Representative time-lapse maximum projections show the expression of *tnfa* (green) induced in myeloid-like cells at the infection site from 3 hpA. The time pA is shown on top right corner, scale bar = 25 µm. Image stacks were acquired every 3 min 30 s at 2-µm intervals, 512 × 512 pixel resolution with a X2 zoom using a confocal microscope TCSSP5 SP5 inverted equipped with a APO 20x objective (Leica). Excitation wavelengths used were 488 nm for EGFP-F and 580 nm for Crimson. To distinguish Crimson from mCherry, emission filter was adjusted from 630 to 750 nm.

DOI: [10.7554/eLife.07288.007](https://doi.org/10.7554/eLife.07288.007)

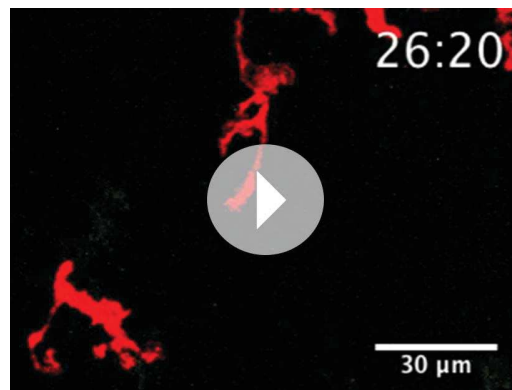


Video 3. *tnfa*⁺ macrophage behaviour following amputation. Representative time-lapse maximum projections show the behaviour of *tnfa*⁺*mpeg1*⁺ macrophages in *Tg(mpeg1*:mCherryF/*tnfa*:eGFP-F) larvae following amputation, starting 19h20 pA during 42 min. Two macrophages *tnfa*⁺*mpeg1*⁺ interact by cell-cell contact. These macrophages (GFP in grey) remain attached up to 40 min. Scale bar = 20 µm. Image stacks were acquired every 3 min 30 s at 2 µm-intervals, 1024 × 512 pixel resolution using a confocal microscope TCSSP5 SP5 inverted equipped with a HCXPL APO 40x/1.25–0.75 oil objective (Leica). Excitation wavelengths used were 488 nm for EGFP-F and 570 nm for mCherryF.

DOI: [10.7554/eLife.07288.008](https://doi.org/10.7554/eLife.07288.008)

Molecular signature of *tnfa*⁺ and *tnfa*⁻ macrophage populations

To characterize at the molecular level *tnfa*⁻ and *tnfa*⁺ macrophage populations during early and late phases of inflammation, we FACS-sorted *dbl*⁺ and *mCh*⁺ cells from *Tg(tnfa*:eGFP-F/*mpeg1*:mCherryF) tail-amputated larvae (**Figure 3C**) and analyzed them by qRT-PCR. In mammals, M1 and M2 macrophages are reported to be involved, respectively, in the initial phase of inflammation and in the resolution phase. Cell sorting was thus performed at 6 hpA and 26 hpA following caudal fin amputation since the kinetic analysis of macrophage subset activation (**Figure 3B**) suggested that these two time points correspond to initiation and resolution of inflammation, respectively. As expected, high levels of *mpeg1* expression was observed in the *mCh*⁺ and *dbl*⁺ sorted cells at 6 and 26 hpA (**Figure 3D**), and high levels of *tnfa* expression was detected in double-positive populations at 6 hpA (**Figure 3E**). These observations demonstrated that fluorescence of these transgenes can be efficiently used to track and separate macrophage sub-populations. At 6 hpA, *dbl*⁺ macrophages expressed high levels of *tnfb*, *il1b*, and *il6* compared to *mCh*⁺ macrophages (**Figure 3F,G**) that are well-known markers of M1 macrophages in mammals (**Mantovani et al., 2002; Martinez et al., 2006**). By contrast, *mCh*⁺ macrophages expressed low levels of these pro-inflammatory cytokines at both 6 and 26 hpA (**Figure 3F,G**), but expressed high levels of *tgfb1*, *ccr2*, and *cxcr4b* (**Figure 3H**), that are specifically expressed in mammalian M2 macrophages (**Mantovani et al., 2002; Martinez et al., 2006; Hao et al., 2012; Beider et al., 2014; Machado et al., 2014**). Of note, neither Arginase 1 (*Arg1*), which is largely used as a M2 marker in mouse but not in human (**Chinetti-Gbaguidi and Staels, 2011; Pourcet and Pineda-Torra, 2013**), nor *il10* (data not shown), a known M2 marker in mammals (**Mantovani et al., 2002**), was detected in zebrafish macrophages. Importantly, based on



Video 4. *tnfa*⁻ macrophage behaviour following amputation. *Tg(mpeg1:mCherryF/tnfa:eGFP-F)* caudal fins were amputated at 3 dpf. Representative time-lapse maximum projections show the behaviour of *tnfa*⁻ *mpeg1*⁺ macrophages, starting 25h12 pA during 42 min. Macrophages (red) scarcely establish cell–cell contact. Scale bar = 30 μm. Image stacks were acquired every 4 min at 2 μm-intervals at 1024 × 512 pixel resolution using a confocal microscope TCSSP5 SP5 inverted equipped with a HCXPL APO 40x/1.25–0.75 oil objective (Leica). Excitation wavelengths used were 488 nm for EGFP-F and 570 nm for mCherryF. DOI: 10.7554/eLife.07288.009

macrophages remain at the injury site and still express the GFP (**Figure 4A–C** and **Video 5**). The analysis of macrophage behaviour over time shows that among eGFP⁺ macrophages displaying an amyloid phenotype at the wound edge 6 hpA, 50% change toward a fibroblastic phenotype from 11 hpA when they moved distally (**Video 5**). All together these data show that pro-inflammatory macrophages underwent a phenotypic conversion toward an intermediate phenotype in which both M1 and M2 markers are expressed. In addition, this molecular characterization of macrophages in zebrafish reveals the conservation of macrophage subtypes between zebrafish and human.

In conclusion, we identified macrophage subsets in zebrafish and described their behaviour and fate during a process of inflammation (**Figure 4D**). Live imaging of transparent transgenic zebrafish larvae allowed the first real-time visualization of macrophage activation and polarization. In parallel, a molecular analysis of macrophage sub-populations highlights the evolutionary conservation of macrophages from fish to mammals. We propose that in response to wounding zebrafish, unpolarized macrophages are recruited to the inflammation site and adopt a M1-like phenotype. Subsequently, they progressively convert their functional phenotype from M1-like to M2-like in response to progressive inflammatory microenvironment changes within the tissue (**Figure 4D**). Live imaging of the new transgenic line we generated opens new avenues to study in real time in live vertebrates the full spectrum of macrophage activation, polarization, and functions.

Materials and methods

Ethics statement

All animal experiments described in the present study were conducted at the University of Montpellier according to European Union guidelines for handling of laboratory animals (http://ec.europa.eu/environment/chemicals/lab_animals/home_en.htm) and were approved by the Direction Sanitaire et Vétérinaire de l'Hérault and Comité d'Éthique pour l'Expérimentation Animale under reference CEEA-LR-13007.

the stability of the eGFP in *Tg(tnfa:eGFP-F/mpeg1:mCherryF)* larvae allowing us to specifically track the behaviour and fate of pro-inflammatory macrophages, we found that the *dbl*⁺ pro-inflammatory macrophages changed their phenotype at 26 hpA. Indeed, *dbl*⁺ macrophages negative for M2 markers at 6 hpA, displayed at 26 hpA, in parallel to a significant decrease of *tnfa*, *il1b*, and *il6* expression level, a significant increased expression level of *ccr2* and *cxcr4b* (**Figure 3E,H**). Of note, a tendency toward differential expression level was observed for *tnfb* and *tgfb1* between 6 and 26 hpA. To go further and demonstrate that the same macrophages are present at the wound site during inflammation and its resolution, we generated the *Tg(mpeg1:GAL4/UAS:Kaede)* larvae to track macrophages exploiting the conversion of the native green fluorescence of Kaede into red fluorescence under UV light. Recruited macrophages were photoconverted 6 hpA and imaged at 26 hpA revealing that early recruited macrophages were still present at the wound area 20 hr later (**Figure 4—figure supplement 1**). Then, GFP⁺ macrophages were specifically tracked using time-lapse imaging of wounded *Tg(mpeg1:mCherryF/TNFa:GFP-F)* fins from 6 to 26 hpA. We show that initially recruited eGFP⁺

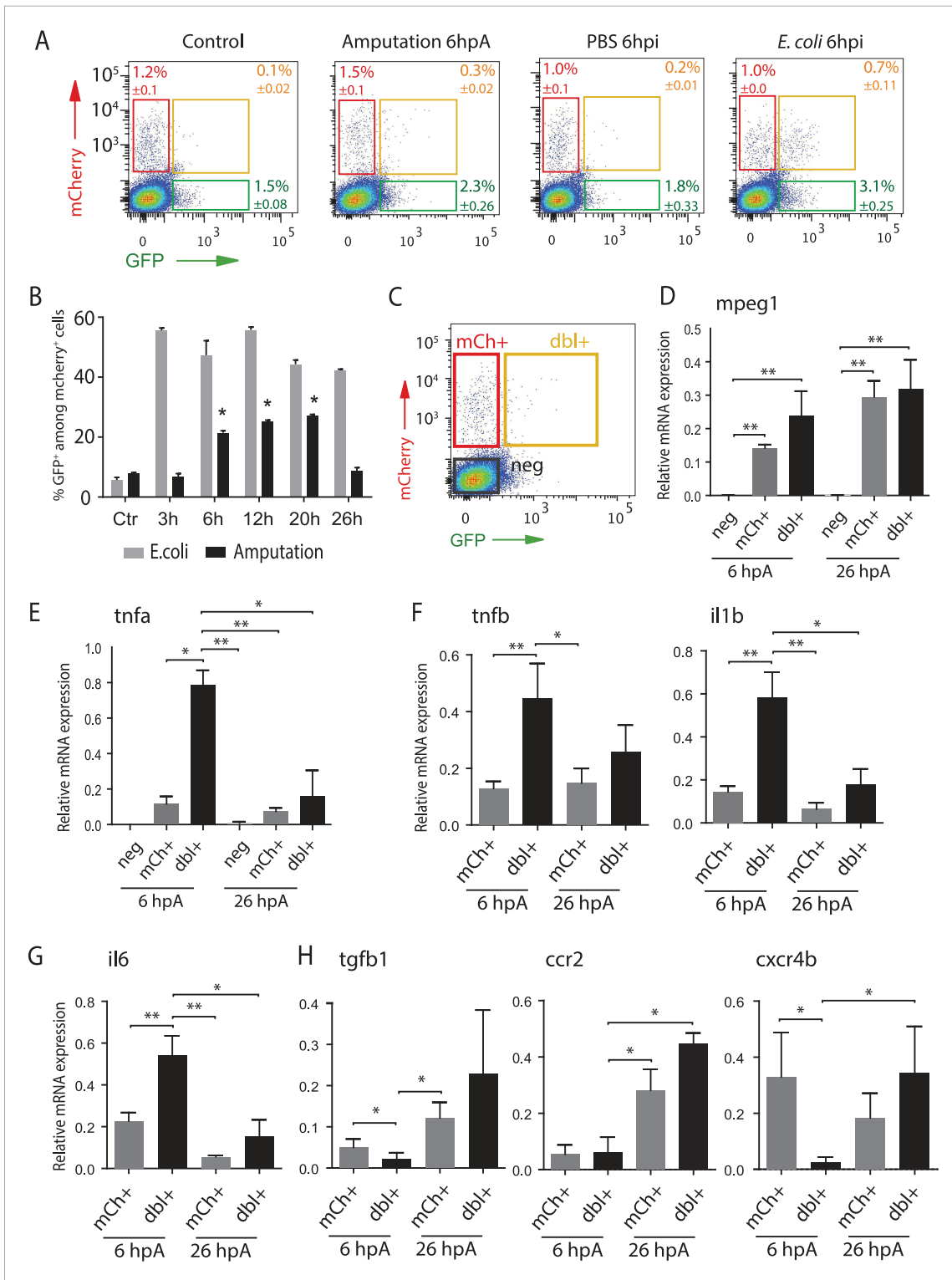


Figure 3. Isolation and molecular characterization of macrophage phenotypes. **(A)** Graphed data of representative fluorescence-activated flow cytometry analysis of *tnfa*⁺ and *tnfa*⁻ macrophages upon inflammatory stimulations. *Tg(mpeg1:mCherryF/tnfa:eGFP-F)* larvae were either kept intact (control), or amputated, or injected with PBS or with *E. coli* at 3 dpf, and cells were collected at 6 hr post-treatment. Red, green, and yellow gates represent mCherry⁺, eGFP⁺, and mCherry⁺eGFP⁺ populations, respectively. **(B)** Graph represents the kinetic of *mpeg1*⁺*tnfa*⁺ macrophages in macrophage population (*mpeg1*⁺) in three independent experiments following stimulation: amputation and *E. coli* infection (*E. coli*) at indicated time points. **p* < 0.05
Figure 3. continued on next page

Figure 3. Continued

vs 3 hpA, mean value of three experiments \pm s.e.m. (C) Gating strategy to isolate control cells (mCherry⁻ eGFP⁻, neg), *tnfa*⁻ macrophages (mCherry⁻ eGFP⁻, mCh⁺), *tnfa*⁺ macrophages (mCherry⁺eGFP⁺, dbl⁺). (D–H) Relative expression of (D) *mpeg1*, (E) *tnfa*, (F) *tnfb*, *il1b*, (G) *il6*, (H) *tgfb1*, *ccr2*, and *cxcr4b* in cells neg, mCh⁺, and dbl⁺. *Tg(mpeg1:mCherryF/tnfa:eGFP-F)* were amputated at 3 dpf and cells were collected and separated at 6 hpA and 26 hpA. Real-time RT-PCR on separated cells using *EF1a* as a reference gene. Graph represents the mean value of five independent experiments \pm s.e.m. Statistical significance between bars are indicated **p* < 0.05, ***p* < 0.01.

DOI: 10.7554/eLife.07288.010

Zebrafish line and maintenance

Fish and embryo maintenance, staging, and husbandry were as previously described (Nguyen-Chi et al., 2014). Experiments were performed using the AB zebrafish strain (ZIRC) and the transgenic line *Tg(mpeg1:mCherryF)* to visualize macrophages. For the photoconversion experiments, a cross of *Tg(mpeg1:Gal4)^{9/25}* and *Tg(UAS:kaede)^{rk8}* lines was used, using breeders selected for progeny with negligible silencing of the UAS transgene.

Transgenic line construction

The TNF α promoter (Gene ID: 405785) was amplified from zebrafish genomic DNA using primers zTNF α P4 (CCCGCATGCTCCACGTCTCC) and zTNF α E11N (TTATAGCGGCCCGCCGACTCTCAAGCTTCA). The resulting fragment was phosphorylated using T4PNK, digested by NotI and cloned in a farnesylated eGFP (eGFP-F) derivative of pBSK12 (Thermes et al., 2002). The resulting plasmid (pI2promTNF α :eGFP-F) harbours a 3.8-kb fragment of the zebrafish *tnfa* promoter, including part of the first coding exon. It uses the endogenous ATG codon of *tnfa* to drive the translation of eGFP-F. The expressed eGFP-F harbours the first 7 amino acids of zebrafish TNF α at its N-terminus (MKLESRA). The expression cassette is flanked by two I-SceI sites. pI2promTNF α :eGFP-F was co-injected in fertilized eggs with the enzyme I-SceI (New England Biolabs, France). Developing embryos were injected with non-pathogenic *E. coli* at 3 dpf (days post-fertilization), and those that developed a specific green fluorescence were raised as putative founders. The offspring of putative founders was tested the same way in order to establish the stable transgenic line. Low expression of eGFP in the pharynx at 3 dpf was used to check larvae for the presence of the transgene.

Larva manipulation for inflammation assays and imaging

Caudal fin amputation was performed on 3 dpf larvae as described in Pase et al. (2012). The caudal fin was transected with a sterile scalpel, posterior to muscle and notochord under anaesthesia with 0.016% Tricaine (ethyl 3-aminobenzoate, Sigma Aldrich, France) in zebrafish water. Larvae were inoculated at 3 dpf by 2.10^3 CFU *E. coli* K12 bacteria harbouring either DsRed (van der Sar et al., 2003) or Crimson (Clontech, France) expression plasmid or no plasmid. Imaging was performed as previously described (Nguyen-Chi et al., 2014) using a confocal TCS SP5 inverted microscope with a HCXPL APO 40 \times /1.25–0.75 oil objective (Leica, France). Image stacks for time-lapse videos were acquired every 3–5 min, typically spanning 30–60 μ m at 2- μ m intervals, 1024 \times 512 or 512 \times 512 pixel resolution. The 4D files generated from time-lapse acquisitions were processed using Image J. They were compressed into maximum intensity projections and cropped. Brightness, contrast, and colour levels were adjusted for maximal visibility. Velocity of macrophages was measured using Manual Tracking Image J plugin. Frequency of macrophage–macrophage interaction and duration of interactions were measured manually on stack images. For tracking of macrophages, eGFP-F⁺ mCherryF⁺ cells from *Tg(mpeg1:mCherryF/tnfa:eGFP-F)* wounded fins were tracked using time-lapse image series from 6 hpA (hours post-amputation) to 26 hpA.

FACS analysis, isolation of mRNA from macrophages and RT-qPCR

300 *Tg(tnfa:eGFP-F/mpeg1:mCherryF)* larvae were either amputated or infected as described above, then crushed on a 70- μ m cell strainer (Falcon, France). Isolated cells were washed in PBS/2 mM ethylenediaminetetraacetic acid (EDTA)/2% Foetal Calf Serum (FCS), filtered through a 40- μ m cell strainer, and counted. Counting of mCherry⁺eGFP⁻ and mCherry⁺eGFP⁺ cells was performed on LSRFortessa (BD Bioscience, France), and data analyzed using the Flowjo software (Tree start, Ashland, Or, USA). Sorting was done using FACS ARIA (BD Bioscience, France) and collected in 50% FCS/50% Leibovitz L-15 medium (21083-027, Gibco, France) on ice. To isolate total RNA, cells were

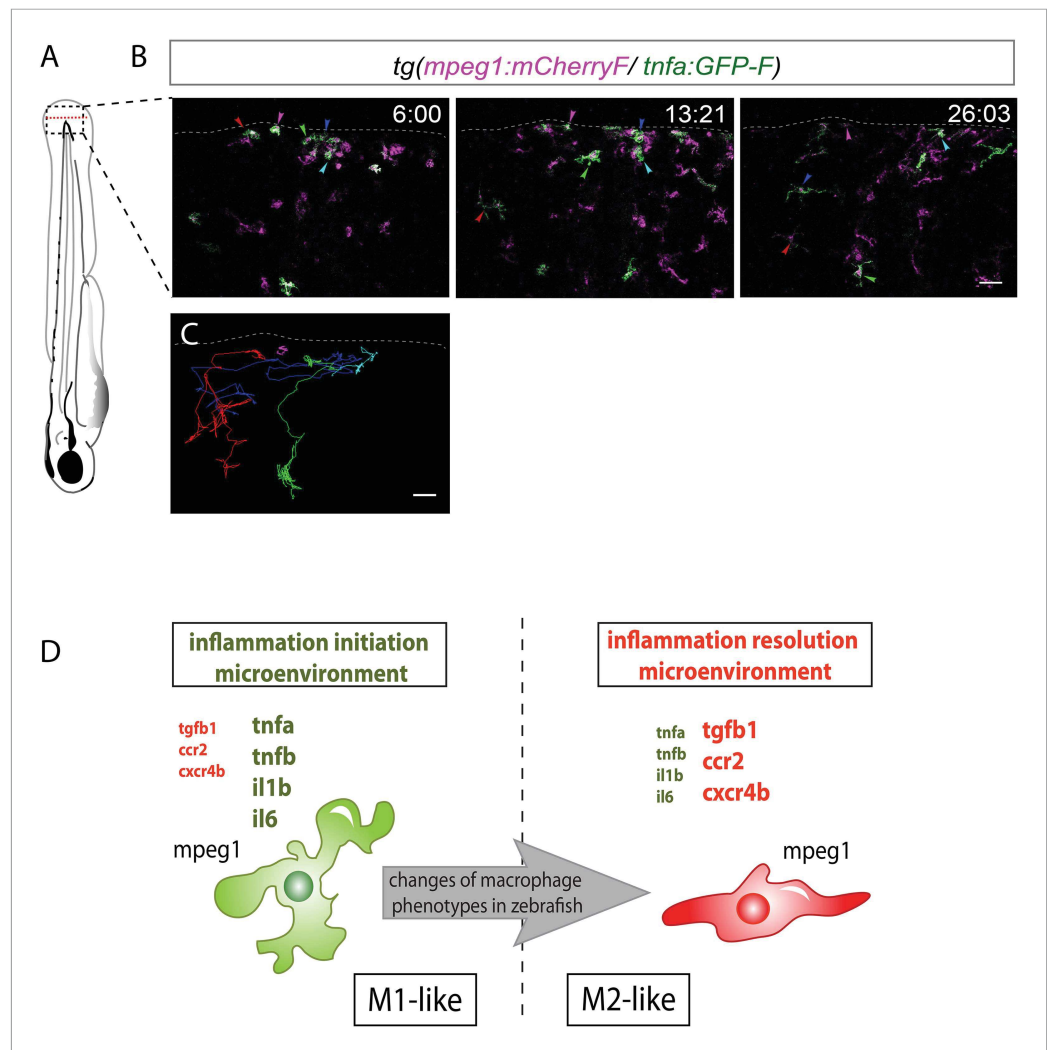


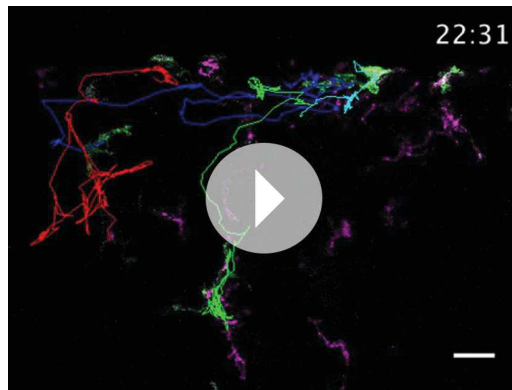
Figure 4. M1-like macrophages convert their phenotype toward M2-like phenotype in the wounded fin. **(A)** Diagram showing the site where caudal fin was transected (dotted red line) in 3 dpf *Tg(mpeg1:mCherryF/tnfa:eGFP-F)* larvae. The black dotted box represents the region imaged by confocal microscopy. **(B)** Representative time-lapse maximum projections of 3 dpf *Tg(mpeg1:mCherryF/tnfa:eGFP-F)* amputated fins showing the fate of *tnfa*⁺ macrophages (magenta + green) at the indicated times pA (hours:minutes) from 6 hpA to 26 hpA. White lines delimit the caudal fin. Scale bar = 30 μ m. **(C)** Tracking of *tnfa*⁺ macrophages from 6 to 26 hpA. The distinct colours of the lines correspond to the distinct macrophages that were indicated with an arrowhead in **B**. **(D)** Diagram representing macrophage activation and polarization in zebrafish. Unpolarized macrophages (*mpeg1*⁺) are mobilized and recruited to the wound following fin amputation. They are activated and polarized toward a M1-like phenotype (pro-inflammatory) few hours following fin amputation. After 24 hpA, in response to changes in environmental cues, the same macrophages progressively change their phenotype toward intermediate phenotypes and maybe fully polarized M2-like phenotype (non-inflammatory). Main markers of macrophage subtypes are indicated and resemble those found in human (*tnfa/b* indicates tumour necrosis factor alpha; *il1b*, interleukin 1-beta; *il6*, interleukin 6; *tgfb1*, tumour growth factor beta 1; *ccr2*, c-c chemokine receptor type 2; *cxcr4b*, chemokine (C-X-C motif) receptor 4b).

DOI: [10.7554/eLife.07288.011](https://doi.org/10.7554/eLife.07288.011)

The following figure supplement is available for figure 4:

Figure supplement 1. Recruited macrophages remain in the region of tissue injury at 26 hpA.

DOI: [10.7554/eLife.07288.012](https://doi.org/10.7554/eLife.07288.012)



Video 5. Recruited GFP⁺ macrophages persist in the region of tissue injury at 26 hpA. *Tg(mpeg1:mCherryF/tnfa:eGFP-F)* caudal fins were amputated at 3 dpf. Representative time-lapse maximum projections show the movements of *tnfa⁺mpeg1⁺* macrophages (green + magenta), starting 6 hpA to 26 hpA. Coloured lines correspond to eGFP⁺ macrophage tracking that stay in the wounded fin and still express eGFP at 26 hpA. Scale bar = 30 μ m. Image stacks were acquired every 4 min 40 s at 3.5- μ m intervals at 512 \times 512 pixel resolution using a confocal microscope TCSSP5 SP5 inverted equipped with a HCXPL APO 40x/1.25–0.75 oil objective (Leica). Excitation wavelengths used were 488 nm for EGFP-F and 570 nm for mCherryF.

DOI: [10.7554/eLife.07288.013](https://doi.org/10.7554/eLife.07288.013)

in vitro transcribed (Biolabs, France). In situ hybridizations on whole-mount embryos were as previously described (Nguyen-Chi et al., 2012). For simultaneous detection of eGFP-F proteins and *tnfa* mRNA by immuno-detection and in situ hybridization, fixed and rehydrated *Tg(tnfa:eGFP-F)* larvae were permeabilised in ice in 100% ethanol for 5 min, then in a mixture of 50% Xylene-50% ethanol for 1 hr and in 80% acetone for 10 min at -20°C as described in Nagaso et al. (2001). After washes in PBS-0.1% Tween, larvae were post-fixed in 4% paraformaldehyde (PFA) for 20 min. Subsequent steps of hybridization, washes, and staining with NBT-BCIP (Roche, France) were as previously described in Nguyen-Chi et al. (2012). Next, unspecific-binding sites were saturated in PBS-1% bovin serum albumin (BSA)-1% lamb serum-10% Goat serum and larvae incubated 3 days with an anti-GFP antibody (MBL, 1/500). After extensive washes, larvae were incubated with a goat anti-rabbit antibody. Stained embryos were imaged using a MVX10 Olympus microscope with MVPLAPO 1 \times objective and XC50 camera and using a Zeiss Axioimager with a Zeiss 40 \times Plan-Apo 1.3 oil objective.

Photoconversion of macrophage-specific Kaede protein

Tg(mpeg1:GAL4/UAS:Kaede) embryos were raised to 3 dpf in the dark, and caudal fin was transected as described above. At 6 hpA, larvae were mounted in 1% low-melting point agarose. A 405-nm Laser Cube 405-50C on a confocal TCS SP5 inverted microscope with a HCXPL APO 40x/1.25–0.75 oil objective (Leica) was used to photoconvert the Kaede-labelled cells using 6% laser power scanning for 60 s (optimized before the experiments; data not shown). Fins were imaged before and after the photoconversion (at 6 and 26 hpA) in the green and red channels.

Acknowledgements

This work was supported by Inserm and grants from the Medical Research Foundation (projet FRM 2011 'Comité Languedoc-Roussillon-Rouergue (LRR)'), from 'La region Languedoc-Roussillon projet Chercheurs d'avenir 2011' (chercheur avenir 2012-Q-173), from the French National Research Agency for 'Zebrafam' program n^o ANR-10-MIDI-009. We thank Myriam Boyer-Clavel from the Montpellier

lysed in QIAzol Lysis Reagent (Qiagen, France) and RNA extracted using miRNeasy mini kit (Qiagen-21704, France). 20 ng of total RNA was reverse transcribed using High Capacity RNA Reverse Transcription kit (Applied Biosystems, France). QPCR were performed on a LightCycler 480 system (Roche, France), following manufacturer's instructions (SYBR Green format, Roche Applied Science, Meylan, France) and using primers in **Supplementary file 1**: denaturation 15 s at 95°C , annealing 10 s at 64°C , and elongation 20 s at 72°C . Expression levels were determined with the LightCycler analysis software (version-3.5) from 5 independent experiments. The relative amount of a given mRNA was calculated by using the formulae $2^{-\Delta\text{Ct}}$ with *ef1a* as reference.

Statistical analysis

Significance testing for **Figures 1M, 3D–H** was done using Mann–Whitney unpaired t-test, one-tail and **Figure 2F–H** using Mann–Whitney unpaired t-test, two-tails using GraphPad Prism 6 Software. * $p < 0.05$, ** $p < 0.01$, **** $p < 0.0001$.

In situ hybridization

A *tnfa* probe was amplified from total cDNA by PCR using *tnfa.55* and *tnfa.58* primers (**Supplementary file 1**) and cloned in plasmid pCRII-TOPO. Digoxigenin (DIG)-labelled (Roche, France) sense and anti-sense RNA probes were in

RIO Imaging platform (MRI) for their help with cytometry and Pr Christine Dambly-Chaudière, U5235/CNRS, France for their help with in situ hybridization.

Additional information

Funding

Funder	Grant reference	Author
Conseil Régional Languedoc-Roussillon	chercheur avenir 2012-Q-173	Farida Djouad
Agence Nationale de la Recherche	ANR-10-MIDI-009	Jean-Pierre Levraud, Georges Lutfalla

Conseil Régional Languedoc-Roussillon: supported Farida Djouad's work by covering the expenses for reagent, imaging and animal facilities as well as the salary for an engineer. Agence Nationale de la Recherche: supported Jean-Pierre Levraud's work by covering animal facility expenses and expenses for reagent and Georges Lutfalla's work by covering animal facility expenses and some expenses for reagents. The funders had no role in study design, data collection and interpretation, or the decision to submit the work for publication.

Author contributions

MN-C, BL-B, FD, Conception and design, Acquisition of data, Analysis and interpretation of data, Drafting or revising the article; JT, PL-C, GT, QTP, ID-R, J-PL, GL, Acquisition of data, Analysis and interpretation of data; KK, CJ, Conception and design, Drafting or revising the article

Ethics

Animal experimentation: All animal experiments described in the present study were conducted at the University Montpellier 2 according to European Union guidelines for handling of laboratory animals (http://ec.europa.eu/environment/chemicals/lab_animals/home_en.htm) and were approved by the Direction Sanitaire et Vétérinaire de l'Hérault and Comité d'Éthique pour l'Expérimentation Animale under reference CEEA-LR-13007.

Additional files

Supplementary file

- Supplementary file 1. Genes, accession numbers, and sequences of the primers.

DOI: [10.7554/eLife.07288.014](https://doi.org/10.7554/eLife.07288.014)

References

- Beider K, Bitner H, Leiba M, Gutwein O, Koren-Michowitz M, Ostrovsky O, Abraham M, Wald H, Galun E, Peled A, Nagler A. 2014. Multiple myeloma cells recruit tumor-supportive macrophages through the CXCR4/CXCL12 axis and promote their polarization toward the M2 phenotype. *Oncotarget* **5**:11283–11296.
- Biswas SK, Mantovani A. 2010. Macrophage plasticity and interaction with lymphocyte subsets: cancer as a paradigm. *Nature Immunology* **11**:889–896. doi: [10.1038/ni.1937](https://doi.org/10.1038/ni.1937).
- Cambier CJ, Takaki KK, Larson RP, Hernandez RE, Tobin DM, Urdahl KB, Cosma CL, Ramakrishnan L. 2013. Mycobacteria manipulate macrophage recruitment through coordinated use of membrane lipids. *Nature* **505**:218–222. doi: [10.1038/nature12799](https://doi.org/10.1038/nature12799).
- Chazaud B. 2013. Macrophages: supportive cells for tissue repair and regeneration. *Immunobiology* **219**:172–178. doi: [10.1016/j.imbio.2013.09.001](https://doi.org/10.1016/j.imbio.2013.09.001).
- Chinetti-Gbaguidi G, Staels B. 2011. Macrophage polarization in metabolic disorders: functions and regulation. *Current Opinion in Lipidology* **22**:365–372. doi: [10.1097/MOL.0b013e32834a77b4](https://doi.org/10.1097/MOL.0b013e32834a77b4).
- Ellett F, Pase L, Hayman JW, Andrianopoulos A, Lieschke GJ. 2011. mpeg1 promoter transgenes direct macrophage-lineage expression in zebrafish. *Blood* **117**:e49–e56. doi: [10.1182/blood-2010-10-314120](https://doi.org/10.1182/blood-2010-10-314120).
- Gordon S. 2003. Alternative activation of macrophages. *Nature Reviews. Immunology* **3**:23–35. doi: [10.1038/nri978](https://doi.org/10.1038/nri978).
- Hao NB, Lu MH, Fan YH, Cao YL, Zhang ZR, Yang SM. 2012. Macrophages in tumor microenvironments and the progression of tumors. *Clinical & Developmental Immunology* **2012**:948098. doi: [10.1155/2012/948098](https://doi.org/10.1155/2012/948098).
- Herbomel P, Thisse B, Thisse C. 1999. Ontogeny and behaviour of early macrophages in the zebrafish embryo. *Development* **126**:3735–3745.

- Machado CM**, Andrade LN, Teixeira VR, Costa FF, Melo CM, dos Santos SN, Nonogaki S, Liu FT, Bernardes ES, Camargo AA, Chammas R. 2014. Galectin-3 disruption impaired tumoral angiogenesis by reducing VEGF secretion from TGFbeta1-induced macrophages. *Cancer Medicine* **3**:201–214. doi: [10.1002/cam4.173](https://doi.org/10.1002/cam4.173).
- Mantovani A**, Sozzani S, Locati M, Allavena P, Sica A. 2002. Macrophage polarization: tumor-associated macrophages as a paradigm for polarized M2 mononuclear phagocytes. *Trends in Immunology* **23**:549–555. doi: [10.1016/S1471-4906\(02\)02302-5](https://doi.org/10.1016/S1471-4906(02)02302-5).
- Martinez FO**, Gordon S, Locati M, Mantovani A. 2006. Transcriptional profiling of the human monocyte-to-macrophage differentiation and polarization: new molecules and patterns of gene expression. *The Journal of Immunology* **177**:7303–7311. doi: [10.4049/jimmunol.177.10.7303](https://doi.org/10.4049/jimmunol.177.10.7303).
- Mosser DM**, Edwards JP. 2008. Exploring the full spectrum of macrophage activation. *Nature Reviews Immunology* **8**:958–969. doi: [10.1038/nri2448](https://doi.org/10.1038/nri2448).
- Nagaso H**, Murata T, Day N, Yokoyama KK. 2001. Simultaneous detection of RNA and protein by in situ hybridization and immunological staining. *The Journal of Histochemistry and Cytochemistry* **49**:1177–1182. doi: [10.1177/002215540104900911](https://doi.org/10.1177/002215540104900911).
- Nguyen-Chi ME**, Bryson-Richardson R, Sonntag C, Hall TE, Gibson A, Sztal T, Chua W, Schilling TF, Currie PD. 2012. Morphogenesis and cell fate determination within the adaxial cell equivalence group of the zebrafish myotome. *PLOS Genetics* **8**:e1003014. doi: [10.1371/journal.pgen.1003014](https://doi.org/10.1371/journal.pgen.1003014).
- Nguyen-Chi M**, Phan QT, Gonzalez C, Dubremetz JF, Levraud JP, Lutfalla G. 2014. Transient infection of the zebrafish notochord with *E. coli* induces chronic inflammation. *Disease Models & Mechanisms* **7**:871–882. doi: [10.1242/dmm.014498](https://doi.org/10.1242/dmm.014498).
- Pase L**, Nowell CJ, Lieschke GJ. 2012. In vivo real-time visualization of leukocytes and intracellular hydrogen peroxide levels during a zebrafish acute inflammation assay. *Methods Enzymol* **506**:135–156. doi: [10.1016/B978-0-12-391856-7.00032-9](https://doi.org/10.1016/B978-0-12-391856-7.00032-9).
- Petrie TA**, Strand NS, Tsung-Yang C, Rabinowitz JS, Moon RT. 2014. Macrophages modulate adult zebrafish tail fin regeneration. *Development* **141**:2581–2591. doi: [10.1242/dev.098459](https://doi.org/10.1242/dev.098459).
- Pourcet B**, Pineda-Torra I. 2013. Transcriptional regulation of macrophage arginase 1 expression and its role in atherosclerosis. *Trends in Cardiovascular Medicine* **23**:143–152. doi: [10.1016/j.tcm.2012.10.003](https://doi.org/10.1016/j.tcm.2012.10.003).
- Sanderson LE**, Chien AT, Astin JW, Crosier KE, Crosier PS, Hall CJ. 2015. An inducible transgene reports activation of macrophages in live zebrafish larvae. *Developmental and Comparative Immunology* **53**:63–69. doi: [10.1016/j.dci.2015.06.013](https://doi.org/10.1016/j.dci.2015.06.013).
- Shechter R**, Miller O, Yovel G, Rosenzweig N, London A, Ruckh J, Kim KW, Klein E, Kalchenko V, Bendel P, Lira SA, Jung S, Schwartz M. 2013. Recruitment of beneficial M2 macrophages to injured spinal cord is orchestrated by remote brain choroid plexus. *Immunity* **38**:555–569. doi: [10.1016/j.immuni.2013.02.012](https://doi.org/10.1016/j.immuni.2013.02.012).
- Sica A**, Mantovani A. 2012. Macrophage plasticity and polarization: in vivo veritas. *The Journal of Clinical Investigation* **122**:787–795. doi: [10.1172/JCI59643](https://doi.org/10.1172/JCI59643).
- Stout RD**, Jiang C, Matta B, Tietzel I, Watkins SK, Suttles J. 2005. Macrophages sequentially change their functional phenotype in response to changes in microenvironmental influences. *The Journal of Immunology* **175**:342–349. doi: [10.4049/jimmunol.175.1.342](https://doi.org/10.4049/jimmunol.175.1.342).
- Thermes V**, Grabher C, Ristoratore F, Bourrat F, Choulika A, Wittbrodt J, Joly JS. 2002. I-SceI meganuclease mediates highly efficient transgenesis in fish. *Mechanisms of Development* **118**:91–98. doi: [10.1016/S0925-4773\(02\)00218-6](https://doi.org/10.1016/S0925-4773(02)00218-6).
- Thomas AC**, Mattila JT. 2014. ‘Of mice and men’: arginine metabolism in macrophages. *Front Immunol* **5**:479. doi: [10.3389/fimmu.2014.00479](https://doi.org/10.3389/fimmu.2014.00479).
- van der Sar AM**, Musters RJ, van Eeden FJ, Appelmelk BJ, Vandenbroucke-Grauls CM, Bitter W. 2003. Zebrafish embryos as a model host for the real time analysis of *Salmonella typhimurium* infections. *Cellular Microbiology* **5**:601–611. doi: [10.1046/j.1462-5822.2003.00303.x](https://doi.org/10.1046/j.1462-5822.2003.00303.x).
- Wynn TA**, Chawla A, Pollard JW. 2013. Macrophage biology in development, homeostasis and disease. *Nature* **496**:445–455. doi: [10.1038/nature12034](https://doi.org/10.1038/nature12034).
- Xue J**, Schmidt SV, Sander J, Draffehn A, Krebs W, Quester I, De Nardo D, Gohel TD, Emde M, Schmidleithner L, Ganesan H, Nino-Castro A, Mallmann MR, Labzin L, Theis H, Kraut M, Beyer M, Latz E, Freeman TC, Ulas T, Schultze JL. 2014. Transcriptome-based network analysis reveals a spectrum model of human macrophage activation. *Immunity* **40**:274–288. doi: [10.1016/j.immuni.2014.01.006](https://doi.org/10.1016/j.immuni.2014.01.006).



PART IV

Rearing zebrafish larvae with Tetrahymenas

Authors:

PHAN Quang Tien, NGUYEN-CHI Mai, GONZALEZ Catherine, LEVRAUD Jean-Pierre, and LUTFALLA Georges

Manuscript in preparation

2016

Rearing zebrafish larvae with Tetrahymenas

PHAN Quang Tien¹², NGUYEN-CHI Mai¹³, GONZALEZ Catherine¹²,
LEVRAUD Jean-Pierre⁴, and LUTFALLA Georges¹²

¹Dynamique des Interactions Membranaires Normales et Pathologiques, Université Montpellier 2, UMR 5235, case 107, Place Eugène Bataillon, 34095 Montpellier Cedex 05, France.

²CNRS; UMR 5235, Place Eugène Bataillon, 34095 Montpellier Cedex 05, France.

³INSERM; Institute for regenerative medicine and Biotherapies, CHRU Montpellier, France.

⁴Macrophages et Développement de l'Immunité, Institut Pasteur, Paris F-75015, France.

Abstract

Diet for the first feeding stages of zebrafish larvae is the critical issue for efficient rearing. We describe here a new rearing technique for zebrafish larvae using polycultures in static water with Tetrahymenas for the first month of development. We observe that the presence of Tetrahymenas helps maintaining high quality water during the first feeding stages. Using this technique, we addressed the question of the necessity to start feeding as soon as the mouth opens. We could see no differences between larvae for which feedings started from the fifth to the ninth day post fertilization. Starting the feeding the tenth day post fertilization, leads to a significant decrease in survival for the first month or rearing. However, the animals which reached that stage are then undistinguishable from those fed early. Setting up Tetrahymena cultures is so easy that it can be rapidly implemented in any laboratory with existing material in a couple of days.

Keywords: Zebrafish, nourishment, Tetrahymena

Introduction

The zebrafish is now a well-established animal model in many different fields of life sciences: development, host pathogen interactions, nutrition, behavior... While many very sophisticated techniques have been specifically developed to use embryo, larva and adult zebrafish for experimental purposes, fish husbandry remains a critical issue. Methods and tools for fish husbandry are still very different from one laboratory to another and still need to be improved. While researchers often consider getting reproducible batches of eggs as the critical point, larviculture is clearly the limiting point in most zebrafish facilities. Many authors have made significant contributions to increase the percentage of embryos that can be raised to adulthood. Two parameters are most often used to measure the efficiency of larviculture, the survival and the time needed to reach sexual maturity. The accepted thought is that larvae shall be fed as soon as the swimming bladder is inflated and the mouth open, that is around the fifth day of development. It is also generally accepted that living diet is the best for the raising zebrafish. The considered exquisite live diet for zebrafish is *Artemia nauplii*, but due to their relatively large size (over 400µm) as compared to the mouth opening of 5 to 9 dpf larvae, these nauplii are usually not used to feed the first feeding stages. Historically, *Paramecium* has been used as live diet for the first feeding stages of zebrafish larviculture. *Paramecium* has to be fed with bacteria and *Paramecium* cultures are not that easy to maintain but are still used in most laboratories for larvicultures. However, some authors consider that *Paramecium* does not possess adequate levels of key nutrients and therefore strongly recommend feeding zebrafish larvae with Rotifers. These rotifers are fed with microalgae-based feeds, harvested and added to the larvae tanks (Lawrence et al., 2012). In order for the rotifers to bring the maximum feed to the larvae, they are heavily fed prior to harvest; this is called "gut loading". Furthermore, as the larvae cannot immediately eat all the added rotifers, microalgae are added to the larvae tanks so that un-eaten rotifers could go on feeding and still be the optimal feed for the larvae. Reported survival indexes for larvae fed with rotifers are around 90%. Due to the relatively low density of rotifer cultures (in the order of million per liter) setting up rotifer cultures is not an easy task.

One of the important issues when rearing larvae is to find the correct equilibrium between the maintenance of suitable water quality and provision of ample food supply for the developing larvae. This is critical when rearing individual larvae for a follow up experiment involving many individuals. Based upon the numerous reported experiments of zebrafish larvae feeding, we decided to investigate the possibility of feeding zebrafish larvae with *Tetrahymena thermophila*. These rapidly growing protists have the size of 50 µm long similar to that of *Paramecium*. *Tetrahymena* can be grown simply in axenic conditions and handling them is much easier than handling *Paramecium*. *Tetrahymena* has two separate nutrient uptake systems; the first is phagocytosis that involves intake of particulate matter via its oral apparatus and nutrient digestion in food vacuoles, and the second is the surface uptake system which imports solute nutrients into the cell. This dual system is very convenient both to cultivate the *Tetrahymena* and to use them to clean the water of the larviculture tanks.

Larval feeding is a major constraint in experimental settings where animals have to be maintained individually. *Tetrahymena* are much less polluted than standard food sources and have actually been successfully used to extend the lifespan of germ-free larvae maintained individually, routinely up to 16 days at 28°C, without having to clean the wells (Rendueles et al., 2012).

Using *Tetrahymena* as an early feed for zebrafish larvae, we have decided to investigate the survival and time to reach sexual maturity of larvae first fed at different time points after fertilization. We also tested feeding conditions to rear individual larvae on a large scale in multi-well plates with *Tetrahymena* feeding and no well cleaning.

Materials and Methods

Fishes and embryos

Experiments were done using golden zebrafish mutants (Lamason et al., 2005) purchased from Singapore through a local company (Antinea) and housed in a Techniplast Zebtec aquaculture system at 28°C, 400 µSiemens (Instant Ocean salt), pH 7.5 (Bicarbonate). Photoperiod is set to 13 hours of

light, 11 hours of darkness. Embryos were obtained from pairs of adult fish by natural spawning rinsed in tap water and bleached by incubating in 0,005% bleach for 5 minutes at room temperature and thorough rinse with tap water. They are then transferred in 9 cm diameter plastic bacterial grade Petri dishes with 30 mL of embryo water. Embryo water is obtained by adding 60mg of Instant Ocean Salt and 40 μ L of 10 N NaOH to 1 L of 15 M Ω /cm Reverse Osmosis water. Next, embryos are kept at 28.5°C in these Petri dishes from day 0 to the first day of feeding and ages are expressed as hours post fertilization (hpf) or days post fertilization (dpf). We never house more than 100 embryos in these Petri dishes. The dishes are inspected daily to remove unfertilized eggs, empty chorions or abnormal embryos until first feeding.

Rearing larvae

Before first feeding, the larvae from each plastic Petri dish are transferred to a 20 cm diameter, 4 cm deep glass Petri dish with 200 mL of embryo water. As long as the larvae are kept in these glass dishes, each day, 3 million *Tetrahymenas* are added to the water. Starting from the fifth day, three times a day, 0.4 mg of NovoTom (JBL GmbH) powder diet is added to the surface of the water both to feed the *Tetrahymenas* and as surface feed for the larvae. From the sixth day of feeding, NovoTom is changed to ZM100 (ZM fish Food), and *Artemia* nauplii are added one to three times per day depending on the supply. One snail (*Planorbella* sp.) is added to each glass Petri dish. Dishes are cleaned one to three times a day by aspirating wastes, feces and possible dead embryo at the bottom allowing 20% renewal of water each day. The fiftieth day of feeding, ZM100, is changed to ZM200. One month after fertilization, juveniles are transferred to 20 L autonomous tanks and fed three times a day with *Artemia* nauplii and either ZM200, ZM300 or ZM400 or flakes according to their size. When they reach three months, the adults are transferred to a Techniplast Zebtec aquaculture system and fed two times per day either with flakes or *Artemias* or bloodworms.

Tetrahymena thermophila

Stock cultures of 15 ml are maintained at room temperature in 25 cm² Tissue Culture Flasks in PPYE medium: 0,25% Proteose-peptone (BD ref 211693)

and 0,25% Yeast extract. They are diluted 1/1000 once a week. Cultures are checked using an inverted microscope with 10x objective. In case of a bacterial contamination, an antibiotic brand is added to the PPYE cultures (PSN GIBCO 15640). Before being fed to larvae, *Tetrahymenas* are “gut loaded” at 33°C in the enriched MYE medium: 1% powder skim milk, 1% Yeast extract. 75 or 150 cm² Tissue Cultures Flasks are used for MYE cultures with 1/4 dilution each day. These media are autoclaved and dilutions are performed in a laminar flow cabinet (tissue culture hood). Cultures at 10⁶cells/mL are washed by centrifugation three times in conical centrifuge tubes (1500rpm, 5 mins, room temperature) and re-suspended in the same volume of embryo water. *Tetrahymenas* are counted using Roche CASY counter system (Roche CASY counter and analyzer).

Results

Cultivating *Tetrahymenas* to feed zebrafish larvae

Small volumes (15 ml) of *Tetrahymenas* stock cultures are maintained in minimal medium with weekly dilutions. These cultures can be kept few weeks at room temperature and are ready for inoculating the larger volume (50 or 100 ml Tissue Culture Flasks) cultures in rich medium MYE. The flask is held horizontally to offer a large surface/volume ratio which provides optimal oxygenation for the medium. The skim milk in MYE medium appears as aggregated particles that can be seen when the cultures are observed under the microscope with 10x objective. These MYE cultures are ready for larvae feeding when all the particles have been phagocytosed. At that time point, *Tetrahymenas* are full of the phagocytosed food and have perfect size for the opening mouth of young zebrafish larvae. These *Tetrahymena* cultures are rinsed in embryo water before being fed to larvae by adding directly into the glass disk with 100µL per larva per day.

Due to their high mobility, counting the *Tetrahymenas* is not an easy task. The only way to immobilize them is to fix them in PFA 2%, but we found that the easiest way to count them is to use the Roche CASY Counter.

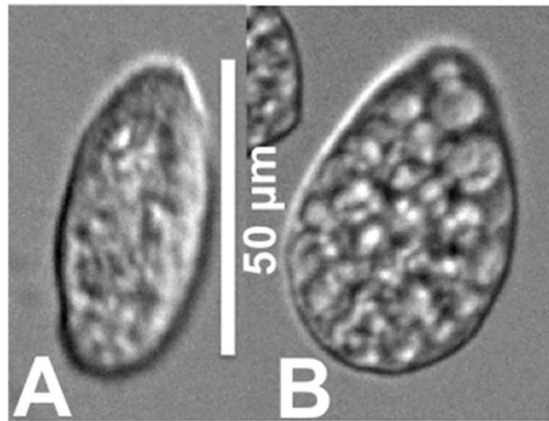


Figure 1: *Tetrahymena thermophila* cultivated either in minimal PPYE medium (A) or in rich medium MYE (B).

Larvicultures

Our preliminary result has showed that zebrafish larvae can feed on *Tetrahymenas*, we decided to test the influence of the day of first feeding on the survival as measured three months after fertilization. A single batch of eggs from one pair of golden fishes was collected, bleached and the unfertilized eggs were removed at 6 hpf. Empty chorions were removed from the Petri dishes as embryos hatch. From the fifth day post fertilization to the tenth day, each day, thirty embryos were transferred to 20 cm glass Petri dishes and fed with *Tetrahymenas*. As has been stressed by many authors, it is important that early feeding of larvae be as continuous as possible. For this reason, *Tetrahymenas* are added to the dishes together with powder diet that is both used by larvae as surface feed and by the *Tetrahymenas* for their continuous growths. We have observed that the presence of high concentrations of *Tetrahymenas* helps maintain good quality of water in the dishes. They both phagocytose many particles including the excess powder feed and bacteria that often proliferate in early larvicultures.

The larvae are maintained in glass Petri dishes for the first month with daily supply of *Tetrahymenas* and three times a day addition of either *Artemia* nauplii or dry food and thereon as described in Material and Methods. Larvae are counted one month after fertilization as they are transferred in 20L tanks and two months later as they are transferred in the ZebTEC system. As shown

in Table 1, first feeding of the larvae with *Tetrahymenas* is very efficient for rearing zebrafish larvae and it appears that it is absolutely not necessary to first feed the larvae before the ninth day of development.

Day of first feeding	6 th	7 th	8 th	9 th	10 th
One month	30/30/28	30/30/29	30/29/28	30/30/28	27/22/20
Three month	30/29/28	30/30/29	29/29/28	30/30/28	26/22/20

Table 1: Efficiency of rearing zebrafish larvae as a function of the first day of feeding. The experiment was performed three successive weeks. Embryos from one spawn were divided in five different batches of 30 embryos at 5dpf. Feeding started at the indicated day. Larvae were fed as mentioned in the result section and counted at 30 dpf as they were transferred to 20 L tanks and adults counted at 90 dpf as they reached adulthood and were transferred to the ZebTEC system. Counted numbers of living animals is reported in the table.

Rearing individual larvae in multiwell plates

Based on our previous experience (Rendueles, 2012), we tested more thoroughly this approach in conventional (i.e. not germ-free) settings, trying to improve survival and growth. Our goal was to keep the technique simple and practical, so we stuck to three feedings per week, on Monday, Wednesday and Friday morning, and no cleaning. We found that the addition of $\sim 10^4$ freshly washed, plump *Tetrahymena* per milliliter of water to individual larvae in 24 well plates, 3 times a week, was sufficient to extend their lifespan to an average of 25,5 days at 28°C.

We also tested variety of parameters in this setting. Increasing the volume of water from 1 to 2 ml in 24-well plates did not improve survival of larvae; provided evaporation was controlled (i.e. plates were maintained within transparent plastic boxes, and thus not directly exposed to the airflow of the

incubator; not shown). Keeping the larvae in small groups (6 larvae in 6 ml of water in the 6-well plates) did not change their survival either. Because some experiments require larvae to be maintained in the dark (as when larvae are injected with or harbor a transgene encoding for a photoconvertible dye), we also tested our feeding regimen to see whether it affects the survivals of larvae when boxes were covered in tin foil immediately after each feeding. Compared with the control larvae that were lit 14 hours a day, these larvae survived just as well (Figure 2), either kept individually or in small groups. This suggests that the density of *Tetrahymena* was sufficient for the larvae to eat enough without having to visually chase their prey.

To ensure that our protocol provided suitable nutrition to the larvae, we also evaluated their growth. In this case, larvae were maintained in groups of 6 larvae in 6-well plates, as size measurements require anesthetizing and pipetting the larvae multiple times, and it is easier to avoid damaging them when they are taken from a larger well. Measurements of standard length, as defined by (Parichy et al., 2009), revealed that larvae did grow under a strict diet of *Tetrahymena* (Figure 2). Although larvae were not followed individually, it was obvious that they grew at fairly different rates. This is a routine observation in zebrafish larviculture, often attributed to food competition; however, this could not be the main cause here, since *Tetrahymenas* were always abundant in the wells. Growth slowed down after two weeks of feeding, suggesting that some factor became limiting at this stage, consistent with the death of the juveniles about one week later. This limiting factor could be nutrition provided by *Tetrahymena* or quality of water, since no water changing has been performed during three weeks. In addition to length increase, typical features of larvae growing into juveniles were observed, such as upwards bending of the caudal spine, apparition of caudal fin rays, thickening of anal and dorsal fin primordia, and even in some cases formation of the secondary lobe of the swim bladder (Parichy et al., 2009).

growth of larvae fed with Tt - exps pooled

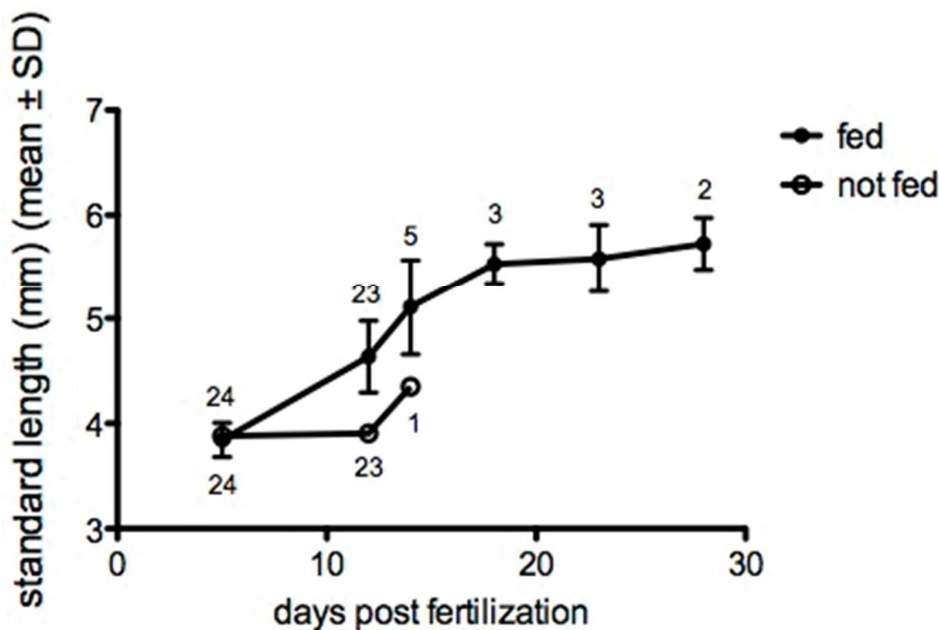


Figure 2: Survival and growth of zebrafish larvae fed with *Tetrahymena* as an only diet

A) Survival of larvae reared with *Tetrahymena* only diet in 24 wells plates B) Six larvae in six mL of embryo water per wells in six-well plates. Three times a week addition of $6 \cdot 10^4$ *Tetrahymenas*.

These features appeared in the same order and at the same sizes described for larvae fed with standard diet (not shown; (Parichy et al., 2009)). Thus, at least for the two first weeks following the inflation of the swim bladder in free-swimming larvae, a sufficiently abundant *Tetrahymena*-only diet is able to provide appropriate nutrition to larvae.

Discussion

When rearing zebrafish larvae, the important issue is to find the correct equilibrium between abundant and high quality food as well as correct water quality. Powder and processed diets often lead to poor quality water due to uneaten food that leads to bacterial or fungi proliferation. On the other end, Paramecium and Rotifers, the classical live diets for zebrafish feeding do not grow to high densities and they themselves need live diet supply. We therefore

decided to use to another protist as live diet. *Tetrahymenas* can be grown easily on defined axenic media and can be simply fattened up with skim milk. These plump *Tetrahymenas* are like bags of good food supply that can be used to feed the first feeding stages of the zebrafish larvae. They can be added directly to the larvae water at high densities, offering an abundant feed to the growing larvae and concomitantly constantly purifying the water. In order to get efficient long term rearing, daily partial renewal of the water is necessary for lessening nitrogen wastes that compromise larval survival. Addition of a snail in each vessel is an excellent cleaning solution specifically because *Tetrahymenas* cannot cope with fungi proliferation. In our experience *Tetrahymenas* are critical as a larval feed for the first week of feeding before larvae can eat Artemia nauplii. As soon as all the larvae in a given batch do take up nauplii, *Tetrahymenas* are mainly useful to help maintain a good quality of water as long as the fishes are not transferred in tanks with water recirculation and purification systems. However, despite the obvious benefit of the Artemia nauplii, a powder diet supplemented with *Tetrahymenas* is sufficient to raise batches zebrafish larvae for the first month without severely compromising their growth up to adulthood.

We have tested the possibility of feeding larvae in multi-well plates with individual larvae in the wells. In this case, without any water change, addition of *Tetrahymenas* thrice a week allows correct larval growth up to one month. However, with such regimen, larvae could not be raised longer, probably due to the quality of water and food supply. We therefore are currently testing the addition of 10^5 *Tetrahymenas* per well as a sole diet but with water change in order to raise the larvae up to one month without compromising their further growth to adulthood.

We have completely shifted our zebrafish nursery to the use of *Tetrahymena* polycultures for more than two years with a systematic high rate of growth and survival with many different lines including the AB reference line and casper mutants.

Acknowledgements

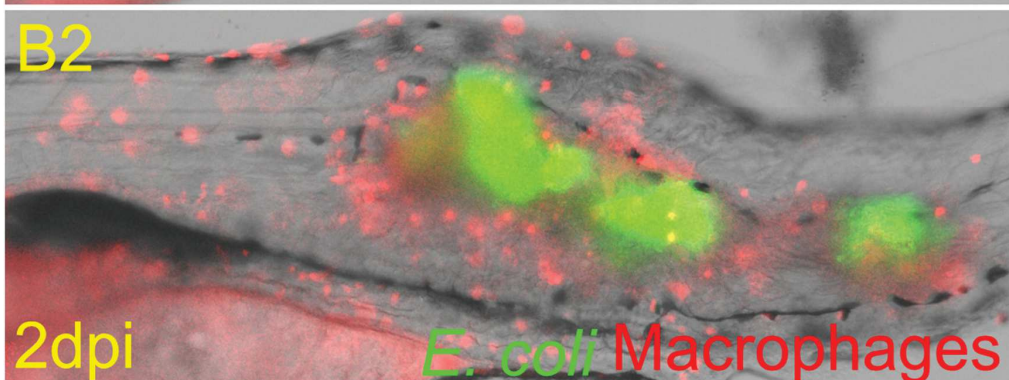
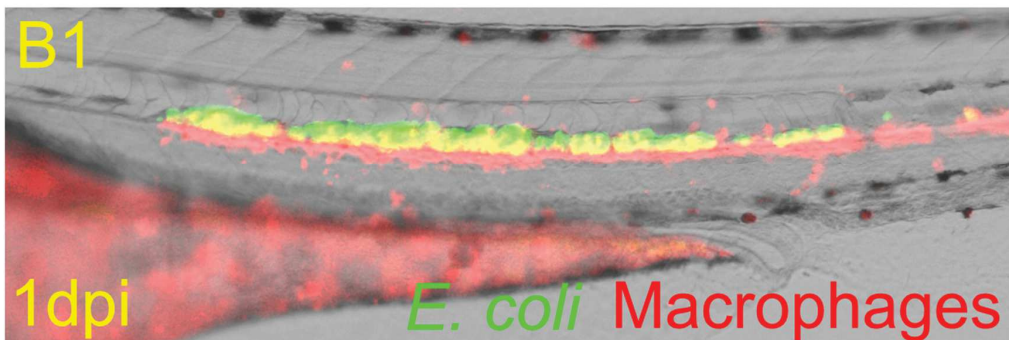
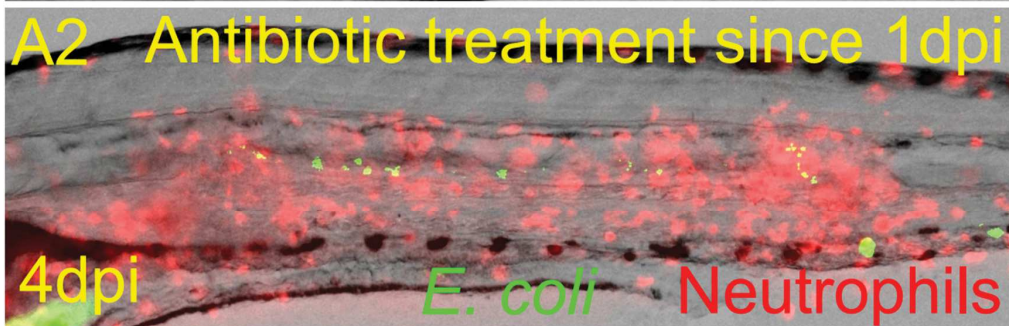
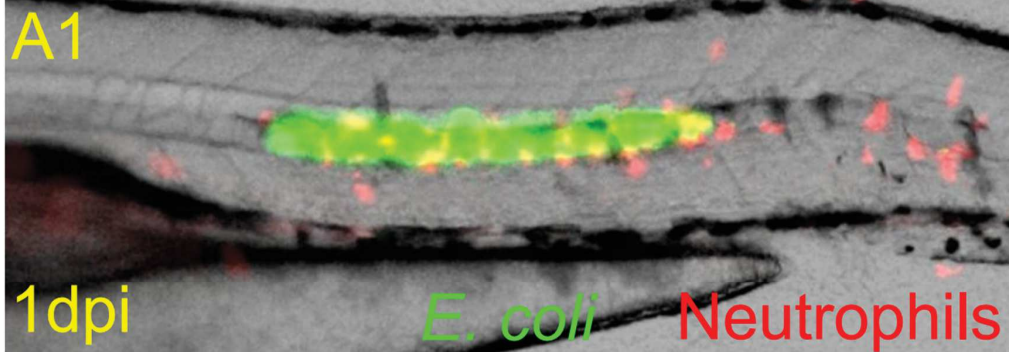
We would like to thank Karima Kissa, the members of DIMNP and Kris Rogowski for helpful discussions, Etienne Scwob and Simonetta Piaty for access to the Roche Casy counter and Nicolas Cubedo for help with fish husbandry. This study was funded by the french National Research Agency (ANR-10-MIDI-009; ZebraFlam) to MNC, JPL and GL. The research leading to these results has received funding from the European Community's Seventh Framework Programme [FP7-PEOPLE-2011-ITN] under grant agreement no. PITN-GA-2011-289209 for the Marie-Curie Initial Training Network FishForPharma. QTP is a Marie-Curie fellow. We wish to thank the InfectioPôle Sud for funding part of the fish facility and Vicky Diakou and the whole Montpellier RIO Imaging facility.

References

- Lamason, R. L., Mohideen, M.-A. P. K., Mest, J. R., Wong, A. C., Norton, H. L., Aros, M. C., Juryneec, M. J., Mao, X., Humphreville, V. R., Humbert, J. E., et al. (2005). SLC24A5, a putative cation exchanger, affects pigmentation in zebrafish and humans. *Science* 310, 1782–6.
- Lawrence, C., Sanders, E. and Henry, E. (2012). Methods for culturing saltwater rotifers (*Brachionus plicatilis*) for rearing larval zebrafish. *Zebrafish* 9, 140–6.
- Parichy, D. M., Elizondo, M. R., Mills, M. G., Gordon, T. N. and Engeszer, R. E. (2009). Normal table of postembryonic zebrafish development: staging by externally visible anatomy of the living fish. *Dev. Dyn.* 238, 2975–3015.
- Rendueles, O., Ferrières, L., Frétaud, M., Bégaud, E., Herbomel, P., Levraud, J.-P. and Ghigo, J.-M. (2012). A new zebrafish model of oro-intestinal pathogen colonization reveals a key role for adhesion in protection by probiotic bacteria. *PLoS Pathog.* 8, e1002815.

CHAPTER III

DISCUSSION AND PERSPECTIVES



High dose *E. coli* notochord infection in transgenic embryos *tg(lyz:DsRed)* (A1,A2) and *tg(mpeg1:mCherry-F)* (B1,B2) at 2dpf. A1: Neutropenia caused by severe infection; A2: Suppression of bacterial growth rescues granulopoiesis. B1,B2: Macrophage population remains abundant in neutropenic larvae.

CHAPTER III: DISCUSSION AND PERSPECTIVES

1. Innate immune response to tissue-specific infection

During evolution bacteria have accumulated diverse mechanisms to invade hosts and transmit their infections. In most cases either they produce cytotoxic molecules to suppress the immune response or they avoid the host killing by hiding themselves in specific cellular or structural compartments.

Neutrophils and macrophages are dynamic players of the innate immune system known as controller of different types of infections. However, their activities are limited by the nature of the infecting agents or by the specificity of tissues where infections take place. By studying the *E. coli* infection in zebrafish embryo Colucci has reported that although neutrophils are recruited early to the infection site, they are more efficiently in engulfing bacteria on the surface-based structure than the one located in fluid-filled cavity. It is contrary for macrophages which are very effective phagocytes in both environments (Colucci-Guyon et al., 2011). Through notochord infection model new observation regarding contributions of neutrophils and macrophages upon bacterial infections has also been described. First observation was made on the infection of *Tes:A* mutant of *Mycobacteria marinum* in which both neutrophils and macrophages were not actively sensing the bacteria encased within the thick collagen layer of the notochord. Only few leukocytes piling up the notochord were not able to control the injected mycobacteria. These bacteria then silently proliferated and eventually burst the notochord and caused death to the embryos (Alibaud et al., 2011; data not shown). The situation turned another direction by infection with low dose of non-pathogenic *E. coli*. Injection of *E. coli* in the notochord noisily triggered neutrophil and macrophage recruitments. However, both leukocytes could not come in contact to phagocytose the bacteria. By depletion of single myeloid population at a time the result clearly indicated that although present massively around the notochord macrophages did not participate to the bacterial killing. They rather functioned as cleaner of death cells and might play role in tissue homeostasis. Interestingly, while being inaccessible to the *E. coli* hidden behind the thick collagen sheath, neutrophils were responsible for the bacterial clearance at a distance. Further investigation revealed that this bacterial

elimination did not involve conventional effectors such as phagocytosis, NETs, or Myeloperoxidase degranulation. Neutrophils rather employed superoxide production through the activity of NADPH Oxidase complexes. Inhibition of the activity of these complexes decreased superoxide concentration which in turn made neutrophils unable to put out the notochord infection, even with very low dose of *E. coli*. Observations were also made on the *E. coli* infections in muscle and blood circulation. Very quickly after injections the bacteria were efficiently killed by both neutrophils and macrophages by phagocytosis, even with very high dose injection of up to 8000 CFUs of *E. coli*, while this high dose would not be controlled when injected in the notochord.

All these observations showed the very dynamic behaviors of phagocytes, especially neutrophils in response to wide variety of bacterial infections.

2. Roles of cytokines in chronic inflammation and bone diseases

The pro-inflammatory cytokines IL-1 β and TNF α are critical mediators of the host response to microbial infections.

2.1. Interleukin 1 β

The IL-1 β acts on different cell types and has many functions – including growth and proliferation, the induction of adhesion molecules in epithelial cells, the activation of phagocytosis and release of proteases in macrophages and neutrophils, and the activation of B and T cells (Dinarello, 2009). Using transgenic zebrafish larvae that expressed farnesylated GFP under the control of the *il1b* promoter, it is shown here, for the first time, the *in toto* dynamic transcriptional activity of *il1b*. Its expression during zebrafish development, especially in the keratinocytes of the caudal and pectoral fin bud, correlates with the regions of the body where active keratinocyte proliferation occurs. This is in agreement with findings in mammals where keratinocytes express IL-1 β (Kupper et al., 1986). However, resting keratinocytes express IL-1 β in its unprocessed biologically inactive form – pro-IL-1 β . Indeed, to be secreted as an active cytokine, pro-IL-1 β must be cleaved by caspases (caspase-1, caspase-11 and others), which are themselves activated through inflammasome assembly (Kayagaki et al., 2011). Although *il1b* transcription is low in most cell types and strongly inducible following the detection of

microbial molecules – notably in myeloid cells – constitutive expression of pro-IL-1 β by some tissues should allow for a faster response to external injuries. This is logical for cells that are directly exposed to the environment such as keratinocytes, olfactory epithelial cells, enterocytes or neuromast cells – all cell types that were seen to spontaneously express endogenous *il1b* mRNA and GFP in our transgenic line *tg(il1b:GFP-F)*.

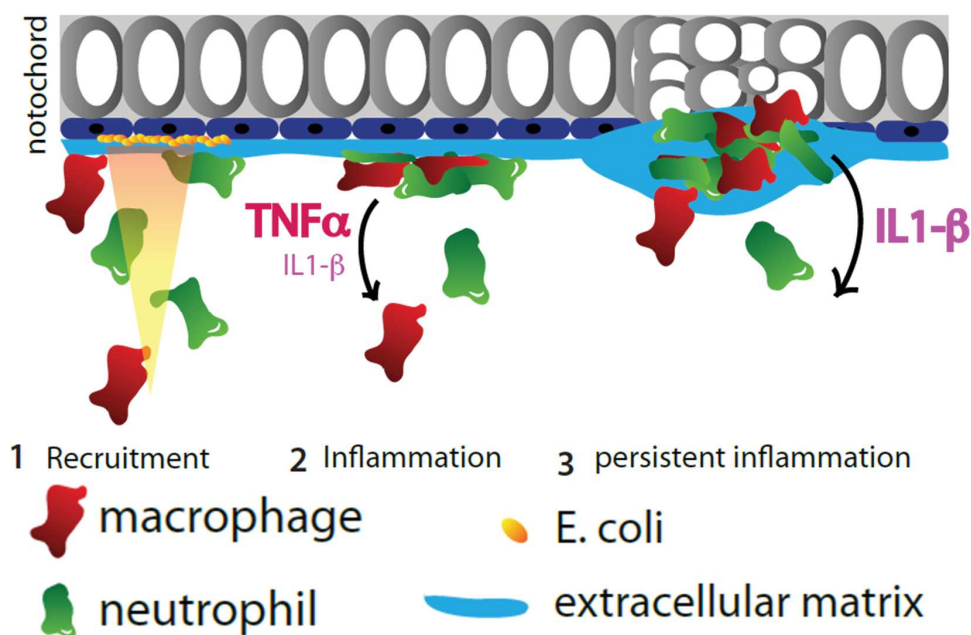


Figure 16: Modulations of *il1b* and *tnfa* during chronic inflammation

(1) Notochord infection triggers recruitment of neutrophils and macrophages along the notochord; (2) the recruited macrophages express strongly *tnfa* and low level of *il1b*; (3) *il1b* is highly transcribed in neutrophils and is crucial for the persistence of the inflammation; the chronic inflammation induces abnormal appearance of notochordal cells and reconstruction of the extra cellular matrix.

In addition to its basal expression during development, GFP is also induced following *E. coli* infection. This induction is strictly correlated in intensity and time with the recruitment of leukocytes. Indeed, infection in muscles induces a low level of expression that quickly lasts, whereas infection of the notochord promotes strong and persistent expression. The GFP expression level decreases one day before the resolution of inflammation. In most mammalian systems, IL-1 β has been reported to be mainly produced by circulating monocytes, tissue macrophages and dendritic cells (Dinarello, 2009). Here, we

describe that, in our zebrafish notochord infection model, *il1b* is first expressed in macrophages during the early phase of inflammation and is mainly expressed by neutrophils during the late phases (depicted in figure 16). This coincides with the recent work on mouse model (Karmakar et al., 2012), which showed that neutrophils were the main source of IL-1 β in response to *Pseudomonas aeruginosa*.

One interesting question arising in this work is which signal stimulates the recruitment and maintenance of leukocytes to the infected notochord? Is it a primary signal that is actively emitted by the notochordal cells, does it come from the injected bacteria or does it correspond to bacterial leftovers after destruction within the notochord? Our data demonstrate that IL-1 β is partially required for the initial recruitment of neutrophils and is also required for the persistence of neutrophils at the inflammation site. By injecting different components of bacteria such as LPS, DNA, heat-killed *E. coli*, PFA-fixed *E. coli* and the live bacteria we confirmed that only the live *E. coli* injection induced strong and prolonged inflammation (Annex1).

2.2. TNF α

TNF α and IL-1 β are key processors in bone inflammatory diseases (Wright and Nair, 2010). TNF α suppression has long been efficient treatment to relieve inflammation in rheumatoid arthritis. IL-1 β antagonists have also been intensively tested for these classes of diseases (Dinarello et al., 2012; Geiler et al., 2011). During the chronic inflammation of the notochord, while IL-1 β is dynamically expressed by macrophages and neutrophils, TNF α is strongly expressed by activated pro-inflammatory macrophages as seen in our transgenic line *tg(tnfa:GFP-F)*. Function of *tnfa* has not been deeply studied in the notochord infection and inflammation model; however, it is found to be dynamically expressed by recruited macrophages during the acute inflammation of tail fin amputation. This cytokine also contributes to the regeneration of the injured tail fin. Interestingly, in our notochord model, knocking down *il1b* suppressed the long lasting inflammation. This observation confirmed the significance of applying *il1b* targeting strategy as treatment of chronic inflammatory symptoms.

Interestingly, chronic inflammation in the absence of infection and bone loss during the inflammatory episode seen in this model (Figure 19) are mimicking the symptoms found in human bone and joints diseases. Altogether, we strongly consider the notochord infection to be a perfect model for study of infectious and inflammatory diseases of bone and cartilage.

3. Combat of neutrophils and *E. coli*, victory for the crowd

The outcome of an infection is determined by the nature of microbe, the state of host immunity and the site where infection takes place. The highly pathogenic genomes are able to induce severity to hosts with very low number of bacterial cells (Bernut et al., 2014; Vergunst et al., 2010). On the other hand, non-pathogenic bacteria, in normal conditions, present no threat even at high density as exemplified the microbial flora of the gastrointestinal tracts. Still, these bacteria reserve the infectivity when host immunity become compromised (Davis, 1996).

In this study, based on the context of notochord infection, we highlight the importance of the numerical balance between neutrophils and bacteria at the onset of notochord infection, simplified in figure 18. The normal neutrophil population is necessary for embryo to eliminate low amount of bacteria. However, to cope with high dose of infection it needs larger neutrophil population. This suggests that neutrophils are limited in producing antimicrobial molecules that act extracellularly. However, it is important to note that the infections of very high dose of *E. coli* in the muscle or blood could be controlled by normal density of neutrophils within the embryo. This could be explained by the fact that phagocytosis is the most efficient mechanism of clearance in the case of avirulent bacterial strains. Also, both macrophages and neutrophils participate in the control of infections in these tissues, while only neutrophils fight infection in the notochord.

In low dose notochord infection, after clearing the bacteria, embryo programs itself to produce more neutrophils known as demand-driven granulopoiesis at 2dpi. In the high dose infection, the normal population of neutrophils is gradually eliminated by apoptosis, but lack of granulopoiesis, making the embryo neutropenic and leading to larval death with overwhelming of bacterial

proliferation. This observation leads to two questions of 1) why do neutrophils die so rapidly upon recruitment, 2) why granulopoiesis is not correctly operational, and 3) why does the embryo die? One of the answers could be that the high density of bacteria in the notochord could get themselves armed via quorum sensing effect, which in turn releases cytotoxic compounds to induce deaths of recruited neutrophils, which in turn inhibiting the GCSF/GCSFR pathway where neutrophils are the source of GCSFR. While being injected in muscle or blood the bacteria would be separated by phagocytes so that they could not carry out the quorum sensing activity. During the inflammation triggered by high dose infection we recorded in our transgenic embryos a strong systemic induction of interleukin-1b. It, perhaps together with other pro-inflammatory cytokines might become out of control and subsequently cause devastating effect to neutrophils and dysfunctions of other organs as described in septic cytokines storm reports.

Figure 17: Embryo needs proper neutrophil density to fight different levels of infection

Notochord infection with different doses of *E. coli* and the outcomes of infections. The normal, but not the disrupted neutrophil population of zebrafish embryo is able to cope with low dose infection (<3000cfus). While this normal neutrophil population could not control high dose infection (>3000cfus), the larvae with ectopic neutrophilia can efficiently clear very high dose of infection (>7000cfus). Upon sensing the bacterial signals neutrophils come and kill bacteria in the notochord through superoxide production. However, when the bacterial density overwhelms the neutrophil population capacity, they proliferate and the recruited neutrophils die without adequate replenishment.

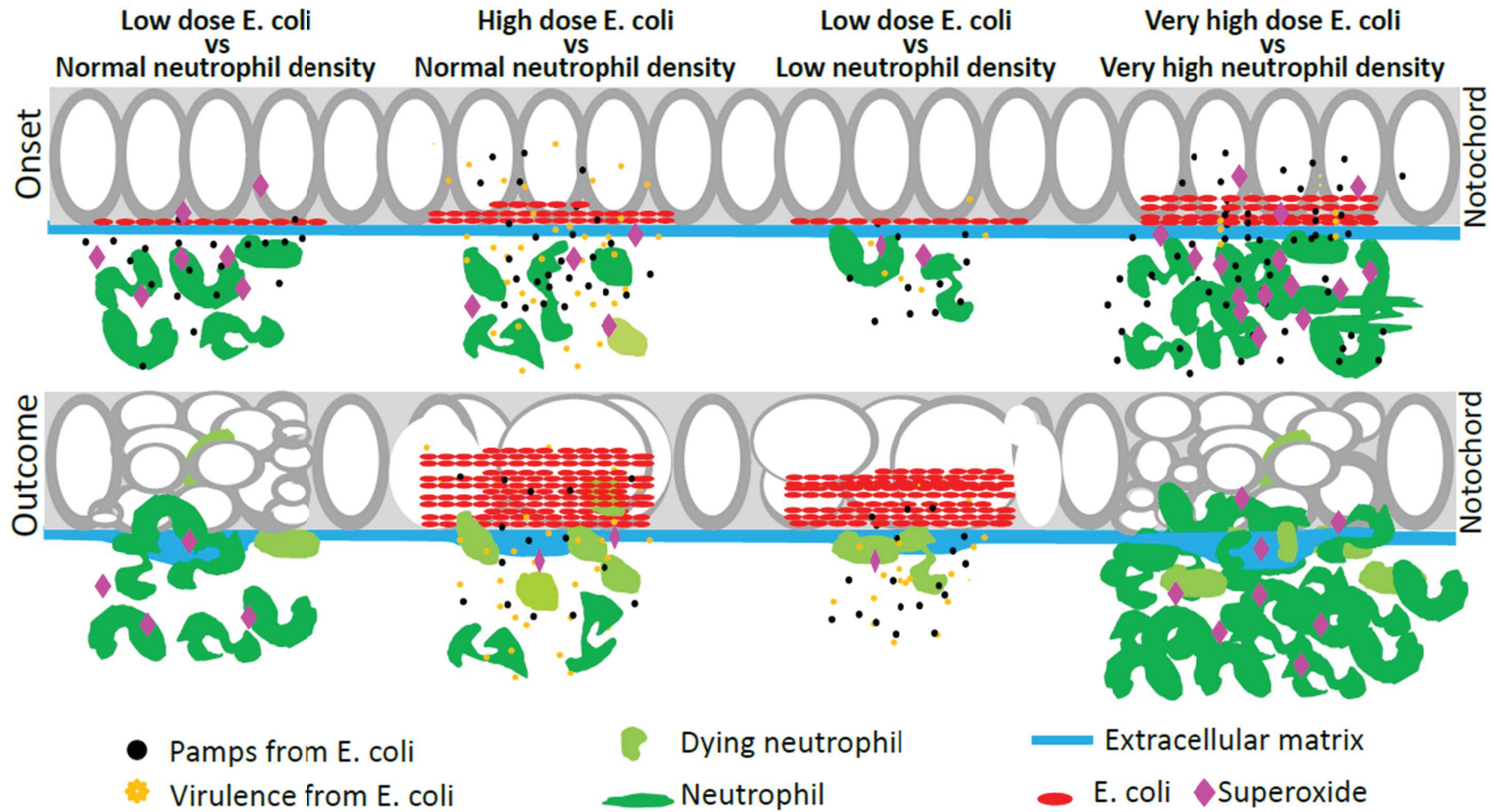


Figure 17: Embryo needs proper neutrophil density to fight different levels of infection

General conclusion

E. coli infection in the notochord of zebrafish embryo results in chronic inflammation, leukocyte infiltration, extracellular matrix reconstruction and vertebral column malformation. These characteristics resemble those seen in bone infection and in some chondropathies in human. With the availability of transgenic reporter lines of leukocytes and cytokines, which are the crucial players of the chronic inflammation, we strongly propose the notochord as a new model to study *in vivo* and *in toto* the cellular and molecular mechanisms in cartilage and bone infections.

Due to its very good efficiency, GCSF administration has long been used in neutropenic patients to help resist infections. This fact is interestingly conserved in zebrafish where GCSFa and/or GCSFb overexpression stimulates massive production of neutrophils, making the larvae highly immune to the severe infection. According to our preliminary data the GCSF injection might be, in this case, more efficient than antibiotic treatment, since addition of antibiotics to the severe *E. coli* infected larvae, even with very high dose, could not efficiently killed the bacteria once they have set their proliferating stages.

In this work we disclose the ability of neutrophils to control infection at a distance through superoxide production. However, the exact acting mechanism of this ROS remains to be further investigated.

ANNEXES

1. Only live bacteria could induce chronic inflammation

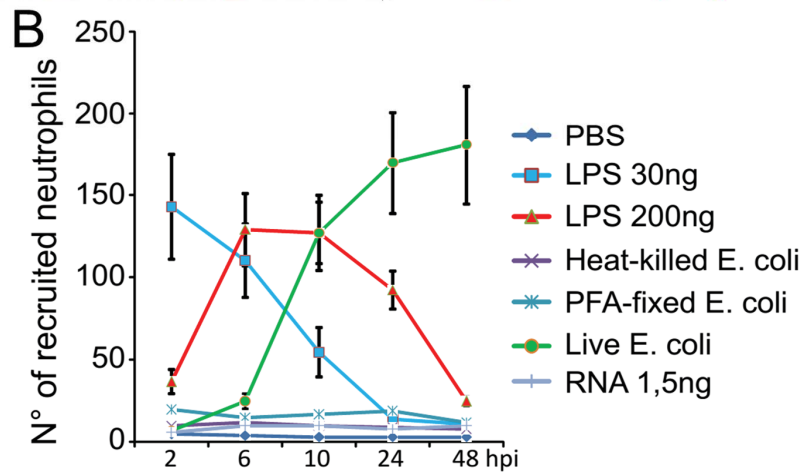
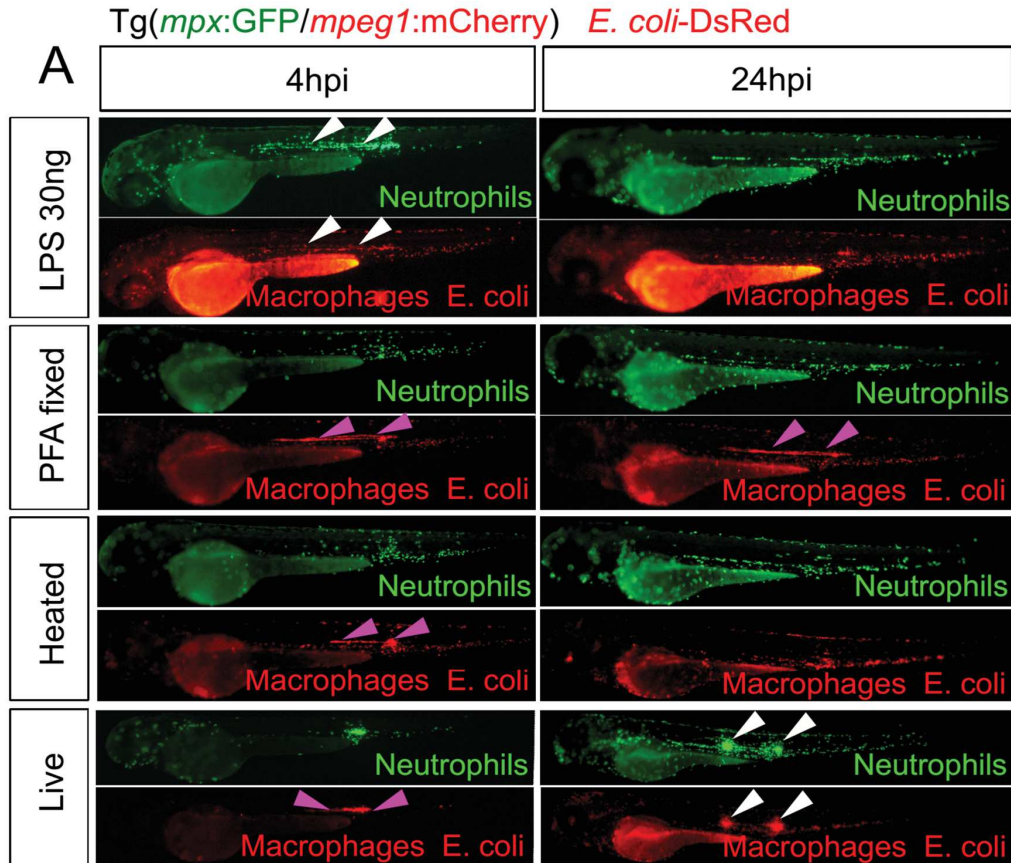


Figure 18: Only live *E. coli* bacteria induce chronic inflammation

Figure 18: Only live *E. coli* bacteria induce chronic inflammation

(A) Double transgenic embryos *tg(mpx:GFP/mpeg1:mCherry)* at 2dpf were injected in the notochord with indicated amount of LPS or RNA from *E. coli*. The low dose infections of *E. coli-DsRed* were performed with live bacteria or dead bacteria killed by heating or fixing with PFA 4%, PBS injection was used as control. White arrowheads show recruitment of neutrophils and macrophages, pink arrowheads indicate the presence of *E. coli-DsRed*.

(B) Quantification of recruited neutrophils along the notochord upon different types of injections mentioned in (A). Error bars are means of neutrophils \pm SEM.

Very quickly following the LPS injection neutrophils and macrophages are recruited around the notochord and mount the inflammation in a dose dependent manner. However, even at a very high quantity (200ng/larva) LPS could not maintain the inflammation for more than two days. The low concentration LPS is supposed to diffuse easily across the collagen sheath of the notochord and is sensed quickly by phagocytes. At high concentration LPS molecules tend to aggregate in clusters which need some time to disaggregate before diffusing out of the notochord. This may explain the delay in triggering phagocyte recruitments when injected with 200ng of LPS.

Injections of RNA derived from *E. coli* or heat-killed-, or PFA-fixed *E. coli* did not induce strong and prolonged inflammation as seen in the injection with live bacteria. Interestingly, after fixing with PFA the bacterial cells and the DsRed fluorescent protein become stable. After being injected in the notochord the fixed bacteria were found localized constantly in between the notochordal cell and the collagen sheath without decaying or triggering immune response. These bacteria remain in the notochord for up to more than 2 weeks.

We conclude here that only live *E. coli*, when injected in the notochord, trigger an episode of prolonged inflammation. The debris from dead bacteria could not maintain the inflammation suggesting that before being killed by neutrophils, the live bacteria release certain factor which activates the chronic program of the inflammation.

2. Chronic inflammation affects vertebral column ossification

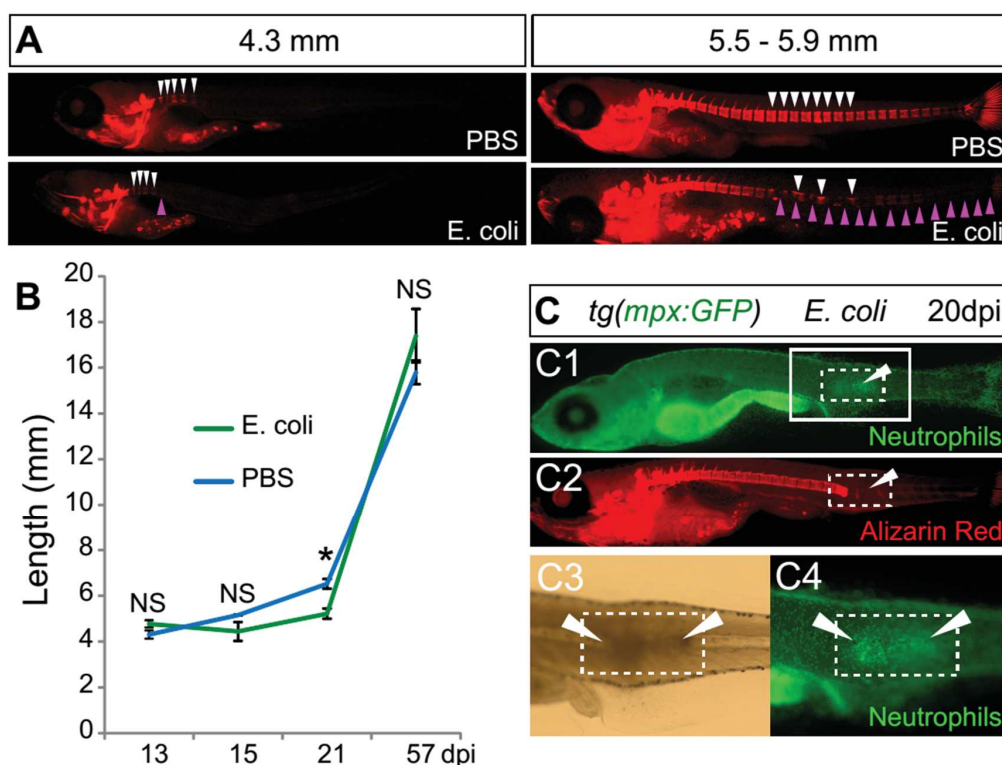


Figure 19: Chronic inflammation affects vertebral column ossification

Tg(mpx:GFP) embryos were injected with *E. coli* or PBS in the notochord at 2dpf. At 13-, 15-, 20-, 21-, 57 dpi fishes were anesthetized with overdose of tricaine and fixed in PFA 4% for 1 day. These fishes were then washed with PBS and later stained with 0.001% Alizarin Red in 0.5% KOH for 24 hours. Images in (A) and (C) were taken using red channel of fluorescent microscope MVX10 Olympus. (A) Inflammation delays vertebral column calcification. Due to the developmental variation larvae were categorized according their lengths. White arrowheads in (A) indicate normal ossification of the vertebrae, pink arrowheads show loss of bone ossification. (B) *E. coli* infected larvae experience slower development and have shorter bodies than that of the control larvae at 21dpi. Error bars show means \pm SEM, $P < 0.05$, $n > 20$. (C) Transient infection induced chronic inflammation which subsequently led to malformation of the bone. While infection is cleared 1 day after infection, the inflammation is prolonged until juvenile stage. Dashed boxes and arrowheads show the sites of inflammation. C2, severe bone loss at the inflammation site; C3 and C4, region in box in C1.

In zebrafish the calcification of vertebral column occurs on the anterior-posterior direction with contribution of intact notochordal cells (Bensimon-Brito et al., 2012). Infection of *E. coli* in the notochord results in chronic inflammation along the notochord, which in turn causes severe damages and abnormal appearance of cells in the notochord. To understand whether defect of the notochord affects vertebrate ossification we infected the notochord with *E. coli* and follow the infected fishes up to their juvenile stages. We observed that fishes with notochord defects experienced delay in their vertebrate calcification. Surprisingly, in some fishes the inflammations were not resolved for very long duration. These chronic inflammations devastatingly prevent the correct formation of the vertebral columns.

LIST OF TABLES

Table 1: Receptors involved in the phagocytosis.....	21
Table 2: NOX enzymes expression in different tissues	25
Table 3: Cytokines production and function	29
Table 4: Active cytokines of the immune responses.....	39

ABBREVIATIONS

RAC: Ras-related C3 botulinum toxin substrate

RAS: Rat sarcoma

NETs: Neutrophil Extracellular Traps

NOX: nicotinamide adenine dinucleotide phosphate-oxidase

DOUX: Dual Oxidase

MPX: Myeloperoxidase

MPEG1: Macrophage expressed gene 1

GCSF: Granulocyte colony stimulating factor

GCSFR: Granulocyte colony stimulating factor receptor

LISTS OF FIGURES

Figure 1: Neutrophils deliver multiple anti-microbial molecules.....	9
Figure 2: Killing mechanisms of neutrophil.....	12
Figure 3: Killing of bacteria in neutrophil phagosome.....	14
Figure 4: Embryonic macrophage development.....	16
Figure 5: Monocyte-derived macrophage development.....	17
Figure 6: Phagocytic function of macrophages.....	19
Figure 7: Process of the phagocytosis.....	22
Figure 8: NADPH oxidase and DUOX isoforms.....	24
Figure 9: Distribution of ROS and their interactions with NETs formation.....	27
Figure 10: Some cytokines and their receptors.....	30
Figure 11: Causes, physiopathology and outcomes of inflammation.....	35
Figure 12: Zebrafish. Most organs are functionally formed at larval stage.....	37
Figure 13: Scheme of primitive and definitive hematopoiesis during zebrafish embryogenesis	38
Figure 14: Zebrafish notochord	39
Figure 15: Structural aspects of the notochord.....	41
Figure 16: Modulations of IL1b and TNFa during chronic inflammation.....	102
Figure 17: Embryo needs proper neutrophil density to fight different severity of infections.....	106
Figure 18: Only live <i>E. coli</i> bacteria induce chronic inflammation.....	107
Figure 19: Chronic inflammation affects vertebrate column ossification.....	109

REFERENCES

- Abdel-Latif, D., Steward, M. and Lacy, P.** (2005). Neutrophil primary granule release and maximal superoxide generation depend on Rac2 in a common signalling pathway. *Can. J. Physiol. Pharmacol.* **83**, 69–75.
- Ablain, J. and Zon, L. I.** (2013). Of fish and men: using zebrafish to fight human diseases. *Trends Cell Biol.* **23**, 584–6.
- Aggarwal, N. R., King, L. S. and D'Alessio, F. R.** (2014). Diverse macrophage populations mediate acute lung inflammation and resolution. *Am. J. Physiol. Lung Cell. Mol. Physiol.* **306**, L709–25.
- Albiger, B., Dahlberg, S., Henriques-Normark, B. and Normark, S.** (2007). Role of the innate immune system in host defence against bacterial infections: focus on the Toll-like receptors. *J. Intern. Med.* **261**, 511–28.
- Alibaud, L., Rombouts, Y., Trivelli, X., Burguière, A., Cirillo, S. L. G., Cirillo, J. D., Dubremetz, J.-F., Guérardel, Y., Lutfalla, G. and Kremer, L.** (2011). A *Mycobacterium marinum* TesA mutant defective for major cell wall-associated lipids is highly attenuated in *Dictyostelium discoideum* and zebrafish embryos. *Mol. Microbiol.* **80**, 919–34.
- Allen, J. P. and Neely, M. N.** (2010). Trolling for the ideal model host: zebrafish take the bait. *Future Microbiol.* **5**, 563–9.
- Amatruda, J. F. and Zon, L. I.** (1999). Dissecting hematopoiesis and disease using the zebrafish. *Dev. Biol.* **216**, 1–15.
- Arango Duque, G. and Descoteaux, A.** (2014). Macrophage cytokines: involvement in immunity and infectious diseases. *Front. Immunol.* **5**, 491.
- ATHENS, J. W., HAAB, O. P., RAAB, S. O., MAUER, A. M., ASHENBRUCKER, H., CARTWRIGHT, G. E. and WINTROBE, M. M.** (1961). Leukokinetic studies. IV. The total blood, circulating and marginal granulocyte pools and the granulocyte turnover rate in normal subjects. *J. Clin. Invest.* **40**, 989–95.
- Balla, K. M., Lugo-Villarino, G., Spitsbergen, J. M., Stachura, D. L., Hu, Y., Bañuelos, K., Romo-Fewell, O., Aroian, R. V and Traver, D.** (2010). Eosinophils in the zebrafish: prospective isolation, characterization, and eosinophilia induction by helminth determinants. *Blood* **116**, 3944–54.
- Barnes, P. J.** (2008). The cytokine network in asthma and chronic obstructive pulmonary disease. *J. Clin. Invest.* **118**, 3546–56.
- Barton, G. M.** (2008). A calculated response: control of inflammation by the innate immune system. *J. Clin. Invest.* **118**, 413–20.
- Baum, R. and Gravalles, E. M.** (2014). Impact of inflammation on the osteoblast in rheumatic diseases. *Curr. Osteoporos. Rep.* **12**, 9–16.
- Becken, U., Jeschke, A., Veltman, K. and Haas, A.** (2010). Cell-free fusion of bacteria-containing phagosomes with endocytic compartments. *Proc. Natl. Acad. Sci.* **107**, 20726–20731.
- Bedard, K. and Krause, K.-H.** (2007). The NOX family of ROS-generating NADPH oxidases: physiology and pathophysiology. *Physiol. Rev.* **87**, 245–313.

- Belon, C., Soscia, C., Bernut, A., Laubier, A., Bleves, S. and Blanc-Potard, A.-B.** (2015). A Macrophage Subversion Factor Is Shared by Intracellular and Extracellular Pathogens. *PLoS Pathog.* **11**, e1004969.
- Benoit, M., Desnues, B. and Mege, J.-L.** (2008). Macrophage Polarization in Bacterial Infections. *J. Immunol.* **181**, 3733–3739.
- Bensimon-Brito, A., Cardeira, J., Cancela, M., Huysseune, A. and Witten, P.** (2012). Distinct patterns of notochord mineralization in zebrafish coincide with the localization of Osteocalcin isoform 1 during early vertebral centra formation. *BMC Dev. Biol.* **12**, 28.
- Bernut, A., Herrmann, J.-L., Kissa, K., Dubremetz, J.-F., Gaillard, J.-L., Lutfalla, G. and Kremer, L.** (2014). Mycobacterium abscessus cording prevents phagocytosis and promotes abscess formation. *Proc. Natl. Acad. Sci. U. S. A.* **111**, E943–52.
- Bird, S. and Tafalla, C.** (2015). Teleost Chemokines and Their Receptors. *Biology (Basel)*. **4**, 756–84.
- Björnsdóttir, H., Welin, A., Michaëlsson, E., Osla, V., Berg, S., Christenson, K., Sundqvist, M., Dahlgren, C., Karlsson, A. and Bylund, J.** (2015). Neutrophil NET formation is regulated from the inside by myeloperoxidase-processed reactive oxygen species. *Free Radic. Biol. Med.* **89**, 1024–1035.
- Bordon, J., Aliberti, S., Fernandez-Botran, R., Uriarte, S. M., Rane, M. J., Duvvuri, P., Peyrani, P., Morlacchi, L. C., Blasi, F. and Ramirez, J. A.** (2013). Understanding the roles of cytokines and neutrophil activity and neutrophil apoptosis in the protective versus deleterious inflammatory response in pneumonia. *Int. J. Infect. Dis.* **17**, e76–83.
- Bozza, F. a, Salluh, J. I., Japiassu, A. M., Soares, M., Assis, E. F., Gomes, R. N., Bozza, M. T., Castro-Faria-Neto, H. C. and Bozza, P. T.** (2007). Cytokine profiles as markers of disease severity in sepsis: a multiplex analysis. *Crit. Care* **11**, R49.
- Brandt, D. T., Marion, S., Griffiths, G., Watanabe, T., Kaibuchi, K. and Grosse, R.** (2007). Dia1 and IQGAP1 interact in cell migration and phagocytic cup formation. *J. Cell Biol.* **178**, 193–200.
- Branzk, N., Lubojemska, A., Hardison, S. E., Wang, Q., Gutierrez, M. G., Brown, G. D. and Papayannopoulos, V.** (2014). Neutrophils sense microbe size and selectively release neutrophil extracellular traps in response to large pathogens. *Nat. Immunol.* **15**, 1017–1025.
- Brinkmann, V., Reichard, U., Goosmann, C., Fauler, B., Uhlemann, Y., Weiss, D. S., Weinrauch, Y. and Zychlinsky, A.** (2004). Neutrophil extracellular traps kill bacteria. *Science* **303**, 1532–5.
- Candel, S., de Oliveira, S., López-Muñoz, A., García-Moreno, D., Espín-Palazón, R., Tyrkalska, S. D., Cayuela, M. L., Renshaw, S. A., Corbalán-Vélez, R., Vidal-Abarca, I., et al.** (2014). Tnfa signaling through tnfr2 protects skin against oxidative stress-induced inflammation. *PLoS Biol.* **12**, e1001855.
- Caron, E. and Hall, A.** (1998). Identification of two distinct mechanisms of phagocytosis controlled by different Rho GTPases. *Science* **282**, 1717–21.
- Charles A Janeway, J., Travers, P., Walport, M. and Shlomchik, M. J.** (2001). The front line of host defense.

- Chatani, M., Takano, Y. and Kudo, A.** (2011). Osteoclasts in bone modeling, as revealed by in vivo imaging, are essential for organogenesis in fish. *Dev. Biol.* **360**, 96–109.
- Chimen, M., McGettrick, H. M., Apta, B., Kuravi, S. J., Yates, C. M., Kennedy, A., Odedra, A., Alassiri, M., Harrison, M., Martin, A., et al.** (2015). Homeostatic regulation of T cell trafficking by a B cell-derived peptide is impaired in autoimmune and chronic inflammatory disease. *Nat. Med.* **21**, 467–75.
- Clemens, D. L., Lee, B.-Y. and Horwitz, M. A.** (2004). Virulent and avirulent strains of *Francisella tularensis* prevent acidification and maturation of their phagosomes and escape into the cytoplasm in human macrophages. *Infect. Immun.* **72**, 3204–17.
- Colucci-Guyon, E., Tinevez, J.-Y., Renshaw, S. A. and Herbomel, P.** (2011). Strategies of professional phagocytes in vivo: unlike macrophages, neutrophils engulf only surface-associated microbes. *J. Cell Sci.* **124**, 3053–9.
- Corleis, B., Korb, D., Wilson, R., Bylund, J., Chee, R. and Schaible, U. E.** (2012). Escape of *Mycobacterium tuberculosis* from oxidative killing by neutrophils. *Cell. Microbiol.* **14**, 1109–1121.
- Courtney, D. M., Aldeen, A. Z., Gorman, S. M., Handler, J. A., Trifilio, S. M., Parada, J. P., Yarnold, P. R. and Bennett, C. L.** (2007). Cancer-associated neutropenic fever: clinical outcome and economic costs of emergency department care. *Oncologist* **12**, 1019–26.
- Covarrubias, L., Hernández-García, D., Schnabel, D., Salas-Vidal, E. and Castro-Obregón, S.** (2008). Function of reactive oxygen species during animal development: Passive or active? *Dev. Biol.* **320**, 1–11.
- Dancey, J. T., Deubelbeiss, K. A., Harker, L. A. and Finch, C. A.** (1976). Neutrophil kinetics in man. *J. Clin. Invest.* **58**, 705–15.
- Davidson, A. J. and Zon, L. I.** (2004). The “definitive” (and “primitive”) guide to zebrafish hematopoiesis. *Oncogene* **23**, 7233–46.
- Davis, C. P.** (1996). Normal Flora.
- De Deken, X., Wang, D., Many, M.-C., Costagliola, S., Libert, F., Vassart, G., Dumont, J. E. and Miot, F.** (2000). Cloning of Two Human Thyroid cDNAs Encoding New Members of the NADPH Oxidase Family. *J. Biol. Chem.* **275**, 23227–23233.
- de Haas, C. J. C., Veldkamp, K. E., Peschel, A., Weerkamp, F., Van Wamel, W. J. B., Heezius, E. C. J. M., Poppelier, M. J. J. G., Van Kessel, K. P. M. and van Strijp, J. A. G.** (2004). Chemotaxis inhibitory protein of *Staphylococcus aureus*, a bacterial antiinflammatory agent. *J. Exp. Med.* **199**, 687–95.
- DeVries, M. E., Kelvin, A. A., Xu, L., Ran, L., Robinson, J. and Kelvin, D. J.** (2005). Defining the Origins and Evolution of the Chemokine/Chemokine Receptor System. *J. Immunol.* **176**, 401–415.
- Dinarello, C. A.** (2009). Immunological and inflammatory functions of the interleukin-1 family. *Annu. Rev. Immunol.* **27**, 519–50.
- Dinarello, C. A., Simon, A. and van der Meer, J. W. M.** (2012). Treating inflammation by blocking interleukin-1 in a broad spectrum of diseases. *Nat. Rev. Drug Discov.* **11**, 633–52.

- Dinh, Q. N., Drummond, G. R., Sobey, C. G. and Chrissobolis, S.** (2014). Roles of inflammation, oxidative stress, and vascular dysfunction in hypertension. *Biomed Res. Int.* **2014**, 406960.
- Donadieu, J., Beaupain, B., Rety-Jacob, F. and Nove-Josserand, R.** (2009). Respiratory distress and sudden death of a patient with GSD1b chronic neutropenia: possible role of pegfilgrastim. *Haematologica* **94**, 1175–7.
- Dooley, K.** (2000). Zebrafish: a model system for the study of human disease. *Curr. Opin. Genet. Dev.* **10**, 252–256.
- Dupré-Crochet, S., Erard, M. and Nüße, O.** (2013). ROS production in phagocytes: why, when, and where? *J. Leukoc. Biol.* **94**, 657–70.
- Dupuy, C., Ohayon, R., Valent, A., Noël-Hudson, M. S., Dème, D. and Virion, A.** (1999). Purification of a novel flavoprotein involved in the thyroid NADPH oxidase. Cloning of the porcine and human cdnas. *J. Biol. Chem.* **274**, 37265–9.
- Elenkov, I. J., Iezzoni, D. G., Daly, A., Harris, A. G. and Chrousos, G. P.** (2005). Cytokine dysregulation, inflammation and well-being. *Neuroimmunomodulation* **12**, 255–69.
- Elks, P. M., van der Vaart, M., van Hensbergen, V., Schutz, E., Redd, M. J., Murayama, E., Spaink, H. P. and Meijer, A. H.** (2014). Mycobacteria counteract a TLR-mediated nitrosative defense mechanism in a zebrafish infection model. *PLoS One* **9**, e100928.
- Ellett, F., Pase, L., Hayman, J. W., Andrianopoulos, A. and Lieschke, G. J.** (2011). mpeg1 promoter transgenes direct macrophage-lineage expression in zebrafish. *Blood* **117**, e49–56.
- Ellett, F., Elks, P. M., Robertson, A. L., Ogryzko, N. V and Renshaw, S. A.** (2015). Defining the phenotype of neutrophils following reverse migration in zebrafish. *J. Leukoc. Biol.* **98**, 975–81.
- Ellis, K., Bagwell, J. and Bagnat, M.** (2013). Notochord vacuoles are lysosome-related organelles that function in axis and spine morphogenesis. *J. Cell Biol.* **200**, 667–79.
- Emery, P.** (2012). Optimizing outcomes in patients with rheumatoid arthritis and an inadequate response to anti-TNF treatment. *Rheumatology (Oxford)*. **51 Suppl 5**, v22–30.
- Ernst, R. K., Guina, T. and Miller, S. I.** Salmonella typhimurium outer membrane remodeling: role in resistance to host innate immunity. *Microbes Infect.* **3**, 1327–34.
- Fang, F. C.** (2011). Antimicrobial actions of reactive oxygen species. *MBio* **2**, e00141–11–.
- Feng, Y., Santoriello, C., Mione, M., Hurlstone, A. and Martin, P.** (2010). Live imaging of innate immune cell sensing of transformed cells in zebrafish larvae: parallels between tumor initiation and wound inflammation. *PLoS Biol.* **8**, e1000562.
- Fleming, A., Jankowski, J. and Goldsmith, P.** (2010). In vivo analysis of gut function and disease changes in a zebrafish larvae model of inflammatory bowel disease: a feasibility study. *Inflamm. Bowel Dis.* **16**, 1162–72.
- Forteza, R., Salathe, M., Miot, F., Forteza, R. and Conner, G. E.** (2005). Regulated hydrogen peroxide production by Duox in human airway epithelial cells. *Am. J.*

Respir. Cell Mol. Biol. **32**, 462–9.

- Foster, J. R.** (2001). The functions of cytokines and their uses in toxicology. *Int. J. Exp. Pathol.* **82**, 171–92.
- Fradin, C., De Groot, P., MacCallum, D., Schaller, M., Klis, F., Odds, F. C. and Hube, B.** (2005). Granulocytes govern the transcriptional response, morphology and proliferation of *Candida albicans* in human blood. *Mol. Microbiol.* **56**, 397–415.
- Fridovich, I.** (1997). Superoxide anion radical (O₂⁻), superoxide dismutases, and related matters. *J. Biol. Chem.* **272**, 18515–7.
- Fuchs, T. A., Abed, U., Goosmann, C., Hurwitz, R., Schulze, I., Wahn, V., Weinrauch, Y., Brinkmann, V. and Zychlinsky, A.** (2007). Novel cell death program leads to neutrophil extracellular traps. *J. Cell Biol.* **176**, 231–41.
- Garcia-Carbonero, R., Mayordomo, J. I., Tornamira, M. V., Lopez-Brea, M., Rueda, A., Guillem, V., Arcediano, A., Yubero, A., Ribera, F., Gomez, C., et al.** (2001). Granulocyte Colony-Stimulating Factor in the Treatment of High-Risk Febrile Neutropenia: a Multicenter Randomized Trial. *JNCI J. Natl. Cancer Inst.* **93**, 31–38.
- Gauron, C., Rampon, C., Bouzaffour, M., Ipendey, E., Teillon, J., Volovitch, M. and Vrız, S.** (2013). Sustained production of ROS triggers compensatory proliferation and is required for regeneration to proceed. *Sci. Rep.* **3**, 2084.
- Gautier, E. L., Shay, T., Miller, J., Greter, M., Jakubzick, C., Ivanov, S., Helft, J., Chow, A., Elpek, K. G., Gordonov, S., et al.** (2012). Gene-expression profiles and transcriptional regulatory pathways that underlie the identity and diversity of mouse tissue macrophages. *Nat. Immunol.* **13**, 1118–28.
- Geiler, J., Buch, M. and McDermott, M. F.** (2011). Anti-TNF treatment in rheumatoid arthritis. *Curr. Pharm. Des.* **17**, 3141–54.
- Geiszt, M., Kapus, A. and Ligeti, E.** (2001). Chronic granulomatous disease: more than the lack of superoxide? *J. Leukoc. Biol.* **69**, 191–196.
- Geiszt, M., Witta, J., Baffi, J., Lekstrom, K. and Leto, T. L.** (2003). Dual oxidases represent novel hydrogen peroxide sources supporting mucosal surface host defense. *FASEB J.* **17**, 1502–4.
- Georgopoulos, K., Winandy, S. and Avitahl, N.** (1997). The role of the Ikaros gene in lymphocyte development and homeostasis. *Annu. Rev. Immunol.* **15**, 155–76.
- Ghysen, A. and Dambly-Chaudière, C.** (2007). The lateral line microcosmos. *Genes Dev.* **21**, 2118–30.
- Ginhoux, F. and Jung, S.** (2014). Monocytes and macrophages: developmental pathways and tissue homeostasis. *Nat. Rev. Immunol.* **14**, 392–404.
- Glickman, N. S.** (2003). Shaping the zebrafish notochord. *Development* **130**, 873–887.
- Goodman, R. B., Pugin, J., Lee, J. S. and Matthay, M. A.** (2003). Cytokine-mediated inflammation in acute lung injury. *Cytokine Growth Factor Rev.* **14**, 523–35.
- Gresser, I., Bourali, C., Levy, J. P., Fontaine-Brouty-Boye, D. and Thomas, M. T.** (1969). INCREASED SURVIVAL IN MICE INOCULATED WITH TUMOR CELLS AND TREATED WITH INTERFERON PREPARATIONS. *Proc. Natl. Acad. Sci.* **63**, 51–57.

- Guimarães-Costa, A. B., Nascimento, M. T. C., Froment, G. S., Soares, R. P. P., Morgado, F. N., Conceição-Silva, F. and Saraiva, E. M.** (2009). Leishmania amazonensis promastigotes induce and are killed by neutrophil extracellular traps. *Proc. Natl. Acad. Sci. U. S. A.* **106**, 6748–53.
- H. Meijer, A. and P. Spaik, H.** (2011). Host-Pathogen Interactions Made Transparent with the Zebrafish Model. *Curr. Drug Targets* **12**, 1000–1017.
- Hagedorn, M., McCarthy, M., Carter, V. L. and Meyers, S. A.** (2012). Oxidative stress in zebrafish (*Danio rerio*) sperm. *PLoS One* **7**, e39397.
- Hall, C., Flores, M. V., Storm, T., Crosier, K. and Crosier, P.** (2007). The zebrafish lysozyme C promoter drives myeloid-specific expression in transgenic fish. *BMC Dev. Biol.* **7**, 42.
- Halverson, T. W. R., Wilton, M., Poon, K. K. H., Petri, B. and Lewenza, S.** (2015). DNA is an antimicrobial component of neutrophil extracellular traps. *PLoS Pathog.* **11**, e1004593.
- Hamann, A.** (2000). T-cell trafficking into sites of inflammation. *Rheumatology* **39**, 696–699.
- Hanada, T. and Yoshimura, A.** Regulation of cytokine signaling and inflammation. *Cytokine Growth Factor Rev.* **13**, 413–21.
- Harrison, M. R. M., Bussmann, J., Huang, Y., Zhao, L., Osorio, A., Burns, C. G., Burns, C. E., Sucov, H. M., Siekmann, A. F. and Lien, C.-L.** (2015a). Chemokine-guided angiogenesis directs coronary vasculature formation in zebrafish. *Dev. Cell* **33**, 442–54.
- Harrison, M. R. M., Bussmann, J., Huang, Y., Zhao, L., Osorio, A., Burns, C. G., Burns, C. E., Sucov, H. M., Siekmann, A. F. and Lien, C.-L.** (2015b). Chemokine-guided angiogenesis directs coronary vasculature formation in zebrafish. *Dev. Cell* **33**, 442–54.
- Harvie, E. A. and Huttenlocher, A.** (2015). Neutrophils in host defense: new insights from zebrafish. *J. Leukoc. Biol.* **98**, 523–37.
- Harvie, E. A., Green, J. M., Neely, M. N. and Huttenlocher, A.** (2013). Innate immune response to *Streptococcus iniae* infection in zebrafish larvae. *Infect. Immun.* **81**, 110–21.
- Hennigan, S. and Kavanaugh, A.** (2008). Interleukin-6 inhibitors in the treatment of rheumatoid arthritis. *Ther. Clin. Risk Manag.* **4**, 767–75.
- Henrotin, Y., Bruckner, P. and Pujol, J.-P.** (2003). The role of reactive oxygen species in homeostasis and degradation of cartilage. *Osteoarthr. Cartil.* **11**, 747–755.
- Henry, K. M., Loynes, C. A., Whyte, M. K. B. and Renshaw, S. A.** (2013). Zebrafish as a model for the study of neutrophil biology. *J. Leukoc. Biol.* **94**, 633–42.
- Herbomel, P., Thisse, B. and Thisse, C.** (1999). Ontogeny and behaviour of early macrophages in the zebrafish embryo. *Development* **126**, 3735–45.
- Hu, Y.-L., Pan, X.-M., Xiang, L.-X. and Shao, J.-Z.** (2010). Characterization of C1q in teleosts: insight into the molecular and functional evolution of C1q family and classical pathway. *J. Biol. Chem.* **285**, 28777–86.

- Hume, D. a** (2008). Macrophages as APC and the dendritic cell myth. *J. Immunol.* **181**, 5829–5835.
- Italiani, P. and Boraschi, D.** (2014). From Monocytes to M1/M2 Macrophages: Phenotypical vs. Functional Differentiation. *Front. Immunol.* **5**,.
- Jault, C., Pichon, L. and Chluba, J.** (2004). Toll-like receptor gene family and TIR-domain adapters in *Danio rerio*. *Mol. Immunol.* **40**, 759–71.
- Jones, R. E. and Moreland, L. W.** (1999). Tumor necrosis factor inhibitors for rheumatoid arthritis. *Bull. Rheum. Dis.* **48**, 1–4.
- Kapetanovic, R., Nahori, M.-A., Balloy, V., Fitting, C., Philpott, D. J., Cavillon, J.-M. and Adib-Conquy, M.** (2007). Contribution of phagocytosis and intracellular sensing for cytokine production by *Staphylococcus aureus*-activated macrophages. *Infect. Immun.* **75**, 830–7.
- Kar, B.** (2013). Zebrafish: An in Vivo Model for the Study of Human Diseases. *Int. J. Genet. Genomics* **1**, 6.
- Karin, M., Lawrence, T. and Nizet, V.** (2006). Innate immunity gone awry: linking microbial infections to chronic inflammation and cancer. *Cell* **124**, 823–35.
- Karmakar, S., Kay, J. and Gravallesse, E. M.** (2010). Bone damage in rheumatoid arthritis: mechanistic insights and approaches to prevention. *Rheum. Dis. Clin. North Am.* **36**, 385–404.
- Karmakar, M., Sun, Y., Hise, A. G., Rietsch, A. and Pearlman, E.** (2012). Cutting edge: IL-1 β processing during *Pseudomonas aeruginosa* infection is mediated by neutrophil serine proteases and is independent of NLRC4 and caspase-1. *J. Immunol.* **189**, 4231–5.
- Kawahara, T., Quinn, M. T. and Lambeth, J. D.** (2007). Molecular evolution of the reactive oxygen-generating NADPH oxidase (Nox/Duox) family of enzymes. *BMC Evol. Biol.* **7**, 109.
- Kissa, K., Murayama, E., Zapata, A., Cortés, A., Perret, E., Machu, C. and Herbomel, P.** (2008). Live imaging of emerging hematopoietic stem cells and early thymus colonization. *Blood* **111**, 1147–56.
- Klebanoff, S. J.** (2005). Myeloperoxidase: friend and foe. *J. Leukoc. Biol.* **77**, 598–625.
- Klebanoff, S. J., Kettle, A. J., Rosen, H., Winterbourn, C. C. and Nauseef, W. M.** (2013). Myeloperoxidase: a front-line defender against phagocytosed microorganisms. *J. Leukoc. Biol.* **93**, 185–98.
- Kobayashi, S. D. and DeLeo, F. R.** Role of neutrophils in innate immunity: a systems biology-level approach. *Wiley Interdiscip. Rev. Syst. Biol. Med.* **1**, 309–33.
- Kolaczowska, E. and Kubes, P.** (2013a). Neutrophil recruitment and function in health and inflammation. *Nat. Rev. Immunol.* **13**, 159–75.
- Kolaczowska, E. and Kubes, P.** (2013b). Neutrophil recruitment and function in health and inflammation. *Nat. Rev. Immunol.* **13**, 159–75.
- Koppensteiner, H., Brack-Werner, R. and Schindler, M.** (2012). Macrophages and their relevance in Human Immunodeficiency Virus Type I infection. *Retrovirology* **9**, 82.

- Krishnan, B. R.** (1999). Interleukin-1 receptor antagonist gene therapy for arthritis. *Curr. Opin. Mol. Ther.* **1**, 454–7.
- Kulkeaw, K. and Sugiyama, D.** (2012). Zebrafish erythropoiesis and the utility of fish as models of anemia. *Stem Cell Res. Ther.* **3**, 55.
- Lalor, P. F., Shields, P., Grant, A. and Adams, D. H.** (2002). Recruitment of lymphocytes to the human liver. *Immunol. Cell Biol.* **80**, 52–64.
- Lamason, R. L., Mohideen, M.-A. P. K., Mest, J. R., Wong, A. C., Norton, H. L., Aros, M. C., Jurynech, M. J., Mao, X., Humphreville, V. R., Humbert, J. E., et al.** (2005). SLC24A5, a putative cation exchanger, affects pigmentation in zebrafish and humans. *Science* **310**, 1782–6.
- Langenau, D. M., Ferrando, A. A., Traver, D., Kutok, J. L., Hezel, J.-P. D., Kanki, J. P., Zon, L. I., Look, A. T. and Trede, N. S.** (2004). In vivo tracking of T cell development, ablation, and engraftment in transgenic zebrafish. *Proc. Natl. Acad. Sci. U. S. A.* **101**, 7369–74.
- Laplace-Builhe, B., Nguyen-Chi, M., Travnickova, J., Luz-Crawford, P., Tejedor, G., Kissa, K., Lutfalla, G., Jorgensen, C. and Djouad, F.** (2015). A2.2 Pro-inflammatory macrophages mediated TNF-alpha signalling is required for caudal fin regeneration in zebrafish larvae. *Ann. Rheum. Dis.* **74**, A16–A16.
- Lawrence, T., Willoughby, D. A. and Gilroy, D. W.** (2002). Anti-inflammatory lipid mediators and insights into the resolution of inflammation. *Nat. Rev. Immunol.* **2**, 787–95.
- Lawrence, C., Sanders, E. and Henry, E.** (2012). Methods for culturing saltwater rotifers (*Brachionus plicatilis*) for rearing larval zebrafish. *Zebrafish* **9**, 140–6.
- Le Guyader, D., Redd, M. J., Colucci-Guyon, E., Murayama, E., Kissa, K., Briolat, V., Mordelet, E., Zapata, A., Shinomiya, H. and Herbomel, P.** (2008). Origins and unconventional behavior of neutrophils in developing zebrafish. *Blood* **111**, 132–41.
- Lee, N. K., Choi, Y. G., Baik, J. Y., Han, S. Y., Jeong, D.-W., Bae, Y. S., Kim, N. and Lee, S. Y.** (2005). A crucial role for reactive oxygen species in RANKL-induced osteoclast differentiation. *Blood* **106**, 852–9.
- Levrard, J.-P., Boudinot, P., Colin, I., Benmansour, A., Peyrieras, N., Herbomel, P. and Lutfalla, G.** (2007). Identification of the Zebrafish IFN Receptor: Implications for the Origin of the Vertebrate IFN System. *J. Immunol.* **178**, 4385–4394.
- Li, K., Sacks, S. H. and Zhou, W.** (2007). The relative importance of local and systemic complement production in ischaemia, transplantation and other pathologies. *Mol. Immunol.* **44**, 3866–3874.
- Li, L., Yan, B., Shi, Y.-Q., Zhang, W.-Q. and Wen, Z.-L.** (2012). Live imaging reveals differing roles of macrophages and neutrophils during zebrafish tail fin regeneration. *J. Biol. Chem.* **287**, 25353–60.
- Lieschke, G. J.** (2001). Morphologic and functional characterization of granulocytes and macrophages in embryonic and adult zebrafish. *Blood* **98**, 3087–3096.
- Lieschke, G. J. and Currie, P. D.** (2007). Animal models of human disease: zebrafish swim into view. *Nat. Rev. Genet.* **8**, 353–67.
- Lieschke, G. J., Oates, A. C., Crowhurst, M. O., Ward, A. C. and Layton, J. E.** (2001).

Morphologic and functional characterization of granulocytes and macrophages in embryonic and adult zebrafish. *Blood* **98**, 3087–96.

- Litvack, M. L. and Palaniyar, N.** (2010). Review: Soluble innate immune pattern-recognition proteins for clearing dying cells and cellular components: implications on exacerbating or resolving inflammation. *Innate Immun.* **16**, 191–200.
- Lucey, D. R., Clerici, M. and Shearer, G. M.** (1996). Type 1 and type 2 cytokine dysregulation in human infectious, neoplastic, and inflammatory diseases. *Clin. Microbiol. Rev.* **9**, 532–62.
- Lugo-Villarino, G., Balla, K. M., Stachura, D. L., Bañuelos, K., Werneck, M. B. F. and Traver, D.** (2010). Identification of dendritic antigen-presenting cells in the zebrafish. *Proc. Natl. Acad. Sci. U. S. A.* **107**, 15850–5.
- Lushchak, V. I.** (2014). Free radicals, reactive oxygen species, oxidative stress and its classification. *Chem. Biol. Interact.* **224**, 164–175.
- Ma, D., Zhang, J., Lin, H., Italiano, J. and Handin, R. I.** (2011). The identification and characterization of zebrafish hematopoietic stem cells. *Blood* **118**, 289–97.
- Manz, M. G. and Boettcher, S.** (2014). Emergency granulopoiesis. *Nat. Rev. Immunol.* **14**, 302–14.
- Martins, A., Han, J. and Kim, S. O.** (2010). The multifaceted effects of granulocyte colony-stimulating factor in immunomodulation and potential roles in intestinal immune homeostasis. *IUBMB Life* **62**, 611–7.
- Maskrey, B. H., Megson, I. L., Whitfield, P. D. and Rossi, A. G.** (2011). Mechanisms of resolution of inflammation: a focus on cardiovascular disease. *Arterioscler. Thromb. Vasc. Biol.* **31**, 1001–6.
- Mastroeni, P., Grant, A., Restif, O. and Maskell, D.** (2009). A dynamic view of the spread and intracellular distribution of *Salmonella enterica*. *Nat. Rev. Microbiol.* **7**, 73–80.
- Matsumoto, K. and Kanmatsuse, K.** (2000). Interleukin-18 and interleukin-12 synergize to stimulate the production of vascular permeability factor by T lymphocytes in normal subjects and in patients with minimal-change nephrotic syndrome. *Nephron* **85**, 127–33.
- McInnes, I. B. and Schett, G.** (2007). Cytokines in the pathogenesis of rheumatoid arthritis. *Nat. Rev. Immunol.* **7**, 429–442.
- Medzhitov, R.** (2008). Origin and physiological roles of inflammation. *Nature* **454**, 428–35.
- Metzler, K. D., Fuchs, T. A., Nauseef, W. M., Reumaux, D., Roesler, J., Schulze, I., Wahn, V., Papayannopoulos, V. and Zychlinsky, A.** (2011). Myeloperoxidase is required for neutrophil extracellular trap formation: implications for innate immunity. *Blood* **117**, 953–9.
- Mikkelsen, R. B. and Wardman, P.** (2003). Biological chemistry of reactive oxygen and nitrogen and radiation-induced signal transduction mechanisms. *Oncogene* **22**, 5734–54.
- Mills, C. D. and Ley, K.** (2014). M1 and M2 macrophages: the chicken and the egg of immunity. *J. Innate Immun.* **6**, 716–26.

- Morsch, M., Radford, R., Lee, A., Don, E. K., Badrock, A. P., Hall, T. E., Cole, N. J. and Chung, R.** (2015). In vivo characterization of microglial engulfment of dying neurons in the zebrafish spinal cord. *Front. Cell. Neurosci.* **9**, 321.
- Mostowy, S. and Shenoy, A. R.** (2015). The cytoskeleton in cell-autonomous immunity: structural determinants of host defence. *Nat. Rev. Immunol.* **15**, 559–73.
- Müller-Redetzky, H., Lienau, J., Suttorp, N. and Witzenth, M.** (2015). Therapeutic strategies in pneumonia: going beyond antibiotics. *Eur. Respir. Rev.* **24**, 516–24.
- Murayama, E., Kissa, K., Zapata, A., Mordelet, E., Briolat, V., Lin, H.-F., Handin, R. I. and Herbomel, P.** (2006). Tracing hematopoietic precursor migration to successive hematopoietic organs during zebrafish development. *Immunity* **25**, 963–75.
- Nathan, C.** (2006). Neutrophils and immunity: challenges and opportunities. *Nat. Rev. Immunol.* **6**, 173–182.
- Neurath, M. F.** (2014). Cytokines in inflammatory bowel disease. *Nat. Rev. Immunol.* **14**, 329–42.
- Newburger, P. E.** (2006). Disorders of neutrophil number and function. *Hematology Am. Soc. Hematol. Educ. Program* **2006**, 104–10.
- Nguyen-Chi, M., Phan, Q. T., Gonzalez, C., Dubremetz, J.-F., Levraud, J.-P. and Lutfalla, G.** (2014). Transient infection of the zebrafish notochord with *E. coli* induces chronic inflammation. *Dis. Model. Mech.* **7**, 871–82.
- Nguyen-Chi, M., Laplace-Builhe, B., Travnickova, J., Luz-Crawford, P., Tejedor, G., Richard, I., Kissa, K., Lutfalla, G., Jorgensen, C. and Djouad, F.** (2015). A1.19 Identification of macrophage subsets in zebrafish larvae. *Ann. Rheum. Dis.* **74**, A8–A8.
- Niethammer, P., Grabher, C., Look, A. T. and Mitchison, T. J.** (2009a). A tissue-scale gradient of hydrogen peroxide mediates rapid wound detection in zebrafish. *Nature* **459**, 996–9.
- Niethammer, P., Grabher, C., Look, A. T. and Mitchison, T. J.** (2009b). A tissue-scale gradient of hydrogen peroxide mediates rapid wound detection in zebrafish. *Nature* **459**, 996–9.
- O’Shea, J. J., Ma, A. and Lipsky, P.** (2002). Cytokines and autoimmunity. *Nat. Rev. Immunol.* **2**, 37–45.
- Ogryzko, N. V., Hoggett, E. E., Solaymani-Kohal, S., Tazzyman, S., Chico, T. J. A., Renshaw, S. A. and Wilson, H. L.** (2014). Zebrafish tissue injury causes upregulation of interleukin-1 and caspase-dependent amplification of the inflammatory response. *Dis. Model. Mech.* **7**, 259–64.
- Olavarría, V. H., Sepulcre, M. P., Figueroa, J. E. and Mulero, V.** (2010). Prolactin-induced production of reactive oxygen species and IL-1 β in leukocytes from the bony fish gilthead seabream involves Jak/Stat and NF- κ B signaling pathways. *J. Immunol.* **185**, 3873–83.
- Orman, M. A., Nguyen, T. T., Ierapetritou, M. G., Berthiaume, F. and Androulakis, I. P.** (2011). Comparison of the cytokine and chemokine dynamics of the early inflammatory response in models of burn injury and infection. *Cytokine* **55**, 362–71.
- Paik, E. J. and Zon, L. I.** (2010). Hematopoietic development in the zebrafish. *Int. J. Dev.*

Biol. **54**, 1127–37.

- Paiva, C. N. and Bozza, M. T.** (2014). Are reactive oxygen species always detrimental to pathogens? *Antioxid. Redox Signal.* **20**, 1000–37.
- Palić, D., Andreasen, C. B., Ostojić, J., Tell, R. M. and Roth, J. A.** (2007). Zebrafish (*Danio rerio*) whole kidney assays to measure neutrophil extracellular trap release and degranulation of primary granules. *J. Immunol. Methods* **319**, 87–97.
- Palti, Y.** (2011). Toll-like receptors in bony fish: from genomics to function. *Dev. Comp. Immunol.* **35**, 1263–72.
- Panopoulos, A. D. and Watowich, S. S.** (2008). Granulocyte colony-stimulating factor: Molecular mechanisms of action during steady state and “emergency” hematopoiesis. *Cytokine* **42**, 277–288.
- Papayannopoulos, V. and Zychlinsky, A.** (2009). NETs: a new strategy for using old weapons. *Trends Immunol.* **30**, 513–21.
- Papayannopoulos, V., Metzler, K. D., Hakkim, A. and Zychlinsky, A.** (2010). Neutrophil elastase and myeloperoxidase regulate the formation of neutrophil extracellular traps. *J. Cell Biol.* **191**, 677–91.
- Parichy, D. M., Elizondo, M. R., Mills, M. G., Gordon, T. N. and Engeszer, R. E.** (2009). Normal table of postembryonic zebrafish development: staging by externally visible anatomy of the living fish. *Dev. Dyn.* **238**, 2975–3015.
- Pase, L., Layton, J. E., Wittmann, C., Ellett, F., Nowell, C. J., Reyes-Aldasoro, C. C., Varma, S., Rogers, K. L., Hall, C. J., Keightley, M. C., et al.** (2012). Neutrophil-delivered myeloperoxidase dampens the hydrogen peroxide burst after tissue wounding in zebrafish. *Curr. Biol.* **22**, 1818–24.
- Patton, E. E., Dhillon, P., Amatruda, J. F. and Ramakrishnan, L.** (2014). Spotlight on zebrafish: translational impact. *Dis. Model. Mech.* **7**, 731–3.
- Pène, J., Chevalier, S., Preisser, L., Vénéreau, E., Guilleux, M.-H., Ghannam, S., Molès, J.-P., Danger, Y., Ravon, E., Lesaux, S., et al.** (2008). Chronically inflamed human tissues are infiltrated by highly differentiated Th17 lymphocytes. *J. Immunol.* **180**, 7423–30.
- Petrie, T. A., Strand, N. S., Yang, C.-T., Tsung-Yang, C., Rabinowitz, J. S. and Moon, R. T.** (2014). Macrophages modulate adult zebrafish tail fin regeneration. *Development* **141**, 2581–91.
- Pfeffer, K., Matsuyama, T., Kündig, T. M., Wakeham, a, Kishihara, K., Shahinian, a, Wiegmann, K., Ohashi, P. S., Krönke, M. and Mak, T. W.** (1993). Mice deficient for the 55 kd tumor necrosis factor receptor are resistant to endotoxic shock, yet succumb to *L. monocytogenes* infection. *Cell* **73**, 457–467.
- Pozzoli, O., Vella, P., Iaffaldano, G., Parente, V., Devanna, P., Lacovich, M., Lamia, C. L., Fascio, U., Longoni, D., Cotelli, F., et al.** (2011). Endothelial fate and angiogenic properties of human CD34+ progenitor cells in zebrafish. *Arterioscler. Thromb. Vasc. Biol.* **31**, 1589–97.
- Pressley, M. E., Phelan, P. E., Witten, P. E., Mellon, M. T. and Kim, C. H.** (2005). Pathogenesis and inflammatory response to *Edwardsiella tarda* infection in the zebrafish. *Dev. Comp. Immunol.* **29**, 501–13.

- Quiniou, S. M. A., Boudinot, P. and Bengtén, E.** (2013). Comprehensive survey and genomic characterization of Toll-like receptors (TLRs) in channel catfish, *Ictalurus punctatus*: identification of novel fish TLRs. *Immunogenetics* **65**, 511–30.
- Rada, B. and Leto, T. L.** (2008). Oxidative innate immune defenses by Nox/Duox family NADPH oxidases. *Contrib. Microbiol.* **15**, 164–87.
- Reeves, E. P., Lu, H., Jacobs, H. L., Messina, C. G. M., Bolsover, S., Gabella, G., Potma, E. O., Warley, A., Roes, J. and Segal, A. W.** (2002). Killing activity of neutrophils is mediated through activation of proteases by K⁺ flux. *Nature* **416**, 291–7.
- Remijsen, Q., Vanden Berghe, T., Wirawan, E., Asselbergh, B., Parthoens, E., De Rycke, R., Noppen, S., Delforge, M., Willems, J. and Vandenabeele, P.** (2011a). Neutrophil extracellular trap cell death requires both autophagy and superoxide generation. *Cell Res.* **21**, 290–304.
- Remijsen, Q., Vanden Berghe, T., Wirawan, E., Asselbergh, B., Parthoens, E., De Rycke, R., Noppen, S., Delforge, M., Willems, J. and Vandenabeele, P.** (2011b). Neutrophil extracellular trap cell death requires both autophagy and superoxide generation. *Cell Res.* **21**, 290–304.
- Remijsen, Q., Kuijpers, T. W., Wirawan, E., Lippens, S., Vandenabeele, P. and Vanden Berghe, T.** (2011c). Dying for a cause: NETosis, mechanisms behind an antimicrobial cell death modality. *Cell Death Differ.* **18**, 581–8.
- Rendueles, O., Ferrières, L., Frétaud, M., Bégaud, E., Herbomel, P., Levraud, J.-P. and Ghigo, J.-M.** (2012). A new zebrafish model of oro-intestinal pathogen colonization reveals a key role for adhesion in protection by probiotic bacteria. *PLoS Pathog.* **8**, e1002815.
- Renshaw, S. A., Loynes, C. A., Trushell, D. M. I., Elworthy, S., Ingham, P. W. and Whyte, M. K. B.** (2006). A transgenic zebrafish model of neutrophilic inflammation. *Blood* **108**, 3976–8.
- Robertson, A. L., Holmes, G. R., Bojarczuk, A. N., Burgon, J., Loynes, C. A., Chimen, M., Sawtell, A. K., Hamza, B., Willson, J., Walmsley, S. R., et al.** (2014). A zebrafish compound screen reveals modulation of neutrophil reverse migration as an anti-inflammatory mechanism. *Sci. Transl. Med.* **6**, 225ra29.
- Robinson, J. M.** (2008). Reactive oxygen species in phagocytic leukocytes. *Histochem. Cell Biol.* **130**, 281–97.
- Rock, K. L. and Kono, H.** (2008). The inflammatory response to cell death. *Annu. Rev. Pathol.* **3**, 99–126.
- Rodrigues Viana, C. T., Castro, P. R., Marques, S. M., Paz Lopes, M. T., Gonçalves, R., Campos, P. P. and Andrade, S. P.** (2015). Differential Contribution of Acute and Chronic Inflammation to the Development of Murine Mammary 4T1 Tumors. *PLoS One* **10**, e0130809.
- Rosenbauer, F. and Tenen, D. G.** (2007). Transcription factors in myeloid development: balancing differentiation with transformation. *Nat. Rev. Immunol.* **7**, 105–17.
- Rubbert-Roth, A. and Finckh, A.** (2009). Treatment options in patients with rheumatoid arthritis failing initial TNF inhibitor therapy: a critical review. *Arthritis Res. Ther.* **11** Suppl 1, S1.

- Rubin-Bejerano, I., Fraser, I., Grisafi, P. and Fink, G. R.** (2003). Phagocytosis by neutrophils induces an amino acid deprivation response in *Saccharomyces cerevisiae* and *Candida albicans*. *Proc. Natl. Acad. Sci. U. S. A.* **100**, 11007–12.
- Russell, D. G., Vandervan, B. C., Glennie, S., Mwandumba, H. and Heyderman, R. S.** (2009). The macrophage marches on its phagosome: dynamic assays of phagosome function. *Nat. Rev. Immunol.* **9**, 594–600.
- Santoriello, C. and Zon, L. I.** (2012). Hooked! Modeling human disease in zebrafish. *J. Clin. Invest.* **122**, 2337–43.
- Scheller, J., Chalaris, A., Schmidt-Arras, D. and Rose-John, S.** (2011). The pro- and anti-inflammatory properties of the cytokine interleukin-6. *Biochim. Biophys. Acta* **1813**, 878–88.
- Schett, G.** (2011). Effects of inflammatory and anti-inflammatory cytokines on the bone. *Eur. J. Clin. Invest.* **41**, 1361–6.
- Schorpp, M., Bialecki, M., Diekhoff, D., Walderich, B., Odenthal, J., Maischein, H.-M., Zapata, A. G. and Boehm, T.** (2006). Conserved Functions of Ikaros in Vertebrate Lymphocyte Development: Genetic Evidence for Distinct Larval and Adult Phases of T Cell Development and Two Lineages of B Cells in Zebrafish. *J. Immunol.* **177**, 2463–2476.
- Schuerwegh, A. J., Dombrecht, E. J., Stevens, W. J., Van Offel, J. F., Bridts, C. H. and De Clerck, L. S.** (2003). Influence of pro-inflammatory (IL-1 alpha, IL-6, TNF-alpha, IFN-gamma) and anti-inflammatory (IL-4) cytokines on chondrocyte function. *Osteoarthritis Cartilage* **11**, 681–7.
- Schwarzer, C., Machen, T. E., Illek, B. and Fischer, H.** (2004). NADPH oxidase-dependent acid production in airway epithelial cells. *J. Biol. Chem.* **279**, 36454–61.
- Segal, A. W.** (2006). How superoxide production by neutrophil leukocytes kills microbes. *Novartis Found. Symp.* **279**, 92–8; discussion 98–100, 216–9.
- Serhan, C. N., Brain, S. D., Buckley, C. D., Gilroy, D. W., Haslett, C., O'Neill, L. A. J., Perretti, M., Rossi, A. G. and Wallace, J. L.** (2007). Resolution of inflammation: state of the art, definitions and terms. *FASEB J.* **21**, 325–32.
- Seruga, B., Zhang, H., Bernstein, L. J. and Tannock, I. F.** (2008). Cytokines and their relationship to the symptoms and outcome of cancer. *Nat. Rev. Cancer* **8**, 887–99.
- Sharif, F., de Bakker, M. A. G. and Richardson, M. K.** (2014). Osteoclast-like Cells in Early Zebrafish Embryos. *Cell J.* **16**, 211–24.
- Shenoy, G. N., Chatterjee, P., Kaw, S., Mukherjee, S., Rathore, D. K., Bal, V., Rath, S. and George, A.** (2012). Recruitment of memory B cells to lymph nodes remote from the site of immunization requires an inflammatory stimulus. *J. Immunol.* **189**, 521–8.
- Slauch, J. M.** (2011). How does the oxidative burst of macrophages kill bacteria? Still an open question. *Mol. Microbiol.* **80**, 580–3.
- Smith, M. W., Schmidt, J. E., Rehg, J. E., Orihuela, C. J. and McCullers, J. A.** (2007). Induction of pro- and anti-inflammatory molecules in a mouse model of pneumococcal pneumonia after influenza. *Comp. Med.* **57**, 82–9.
- Solau-Gervais, E., Laxenaire, N., Cortet, B., Dubucquoi, S., Duquesnoy, B. and Flipo, R.-M.** (2006). Lack of efficacy of a third tumour necrosis factor alpha

- antagonist after failure of a soluble receptor and a monoclonal antibody. *Rheumatology (Oxford)*. **45**, 1121–4.
- Song, H.-D., Sun, X.-J., Deng, M., Zhang, G.-W., Zhou, Y., Wu, X.-Y., Sheng, Y., Chen, Y., Ruan, Z., Jiang, C.-L., et al.** (2004). Hematopoietic gene expression profile in zebrafish kidney marrow. *Proc. Natl. Acad. Sci. U. S. A.* **101**, 16240–5.
- Stasia, M. J. and Li, X. J.** (2008). Genetics and immunopathology of chronic granulomatous disease. *Semin. Immunopathol.* **30**, 209–35.
- Stemple, D. L.** (2005). Structure and function of the notochord: an essential organ for chordate development. *Development* **132**, 2503–12.
- Stöger, J. L., Gijbels, M. J. J., van der Velden, S., Manca, M., van der Loos, C. M., Biessen, E. A. L., Daemen, M. J. A. P., Lutgens, E. and de Winther, M. P. J.** (2012). Distribution of macrophage polarization markers in human atherosclerosis. *Atherosclerosis* **225**, 461–8.
- Stoiber, W., Obermayer, A., Steinbacher, P. and Krautgartner, W.-D.** (2015). The Role of Reactive Oxygen Species (ROS) in the Formation of Extracellular Traps (ETs) in Humans. *Biomolecules* **5**, 702–23.
- Sumimoto, H.** (2008). Structure, regulation and evolution of Nox-family NADPH oxidases that produce reactive oxygen species. *FEBS J.* **275**, 3249–77.
- Suzuki, T. and Sasakawa, C.** (2001). Molecular basis of the intracellular spreading of Shigella. *Infect. Immun.* **69**, 5959–66.
- Svahn, A. J., Graeber, M. B., Ellett, F., Lieschke, G. J., Rinkwitz, S., Bennett, M. R. and Becker, T. S.** (2013). Development of ramified microglia from early macrophages in the zebrafish optic tectum. *Dev. Neurobiol.* **73**, 60–71.
- Tanaka, T. and Kishimoto, T.** (2012). Targeting interleukin-6: All the way to treat autoimmune and inflammatory diseases. *Int. J. Biol. Sci.* **8**, 1227–1236.
- Torraca, V., Masud, S., Spaink, H. P. and Meijer, A. H.** (2014). Macrophage-pathogen interactions in infectious diseases: new therapeutic insights from the zebrafish host model. *Dis. Model. Mech.* **7**, 785–97.
- Trede, N. S., Langenau, D. M., Traver, D., Look, A. T. and Zon, L. I.** (2004). The Use of Zebrafish to Understand Immunity. *Immunity* **20**, 367–379.
- Turner, M. D., Nedjai, B., Hurst, T. and Pennington, D. J.** (2014). Cytokines and chemokines: At the crossroads of cell signalling and inflammatory disease. *Biochim. Biophys. Acta* **1843**, 2563–2582.
- Underhill, D. M. and Goodridge, H. S.** (2012). Information processing during phagocytosis. *Nat. Rev. Immunol.* **12**, 492–502.
- Urban, C. F., Lourido, S. and Zychlinsky, A.** (2006). How do microbes evade neutrophil killing? *Cell. Microbiol.* **8**, 1687–96.
- van der Vaart, M., Spaink, H. P. and Meijer, A. H.** (2012). Pathogen recognition and activation of the innate immune response in zebrafish. *Adv. Hematol.* **2012**, 159807.
- van Ham, T. J., Kokel, D. and Peterson, R. T.** (2012). Apoptotic cells are cleared by directional migration and elmo1- dependent macrophage engulfment. *Curr. Biol.* **22**, 830–6.

- Van Kampen, C., Gauldie, J. and Collins, S. M.** (2005). Proinflammatory properties of IL-4 in the intestinal microenvironment. *Am. J. Physiol. Gastrointest. Liver Physiol.* **288**, G111–7.
- Varela, M., Dios, S., Novoa, B. and Figueras, A.** (2012). Characterisation, expression and ontogeny of interleukin-6 and its receptors in zebrafish (*Danio rerio*). *Dev. Comp. Immunol.* **37**, 97–106.
- Vergunst, A. C., Meijer, A. H., Renshaw, S. A. and O’Callaghan, D.** (2010). *Burkholderia cenocepacia* creates an intramacrophage replication niche in zebrafish embryos, followed by bacterial dissemination and establishment of systemic infection. *Infect. Immun.* **78**, 1495–508.
- Vilcek, J. and Feldmann, M.** (2004). Historical review: Cytokines as therapeutics and targets of therapeutics. *Trends Pharmacol. Sci.* **25**, 201–9.
- Warga, R. M., Kane, D. A. and Ho, R. K.** (2009). Fate mapping embryonic blood in zebrafish: multi- and unipotential lineages are segregated at gastrulation. *Dev. Cell* **16**, 744–55.
- Weiss, G. and Schaible, U. E.** (2015). Macrophage defense mechanisms against intracellular bacteria. *Immunol. Rev.* **264**, 182–203.
- Winkelstein, J. A., Marino, M. C., Johnston, R. B., Boyle, J., Curnutte, J., Gallin, J. I., Malech, H. L., Holland, S. M., Ochs, H., Quie, P., et al.** (2000). Chronic granulomatous disease. Report on a national registry of 368 patients. *Medicine (Baltimore)*. **79**, 155–69.
- Wright, T. W., Notter, R. H., Wang, Z., Harmsen, A. G. and Gigliotti, F.** (2001). Pulmonary inflammation disrupts surfactant function during *Pneumocystis carinii* pneumonia. *Infect. Immun.* **69**, 758–64.
- Wynn, T. A., Chawla, A. and Pollard, J. W.** (2013). Macrophage biology in development, homeostasis and disease. *Nature* **496**, 445–55.
- Yang, S., Madyastha, P., Bingel, S., Ries, W. and Key, L.** (2001). A new superoxide-generating oxidase in murine osteoclasts. *J. Biol. Chem.* **276**, 5452–8.
- Yeh, D.-W., Liu, Y.-L., Lo, Y.-C., Yuh, C.-H., Yu, G.-Y., Lo, J.-F., Luo, Y., Xiang, R. and Chuang, T.-H.** (2013). Toll-like receptor 9 and 21 have different ligand recognition profiles and cooperatively mediate activity of CpG-oligodeoxynucleotides in zebrafish. *Proc. Natl. Acad. Sci. U. S. A.* **110**, 20711–6.
- Zimmerli, S., Majeed, M., Gustavsson, M., Stendahl, O., Sanan, D. A. and Ernst, J. D.** (1996). Phagosome-lysosome fusion is a calcium-independent event in macrophages. *J. Cell Biol.* **132**, 49–61.
- Zwerina, J., Hayer, S., Tohidast-Akrad, M., Bergmeister, H., Redlich, K., Feige, U., Dunstan, C., Kollias, G., Steiner, G., Smolen, J., et al.** (2004). Single and combined inhibition of tumor necrosis factor, interleukin-1, and RANKL pathways in tumor necrosis factor-induced arthritis: effects on synovial inflammation, bone erosion, and cartilage destruction. *Arthritis Rheum.* **50**, 277–90.

SUMMARY

In bacterial infections, according to the infected tissue and the nature of pathogens, the body responds by mobilizing various actors. I decided to use zebrafish or *Danio rerio* model to study the innate immune response to bacterial infection in the situations that professional phagocytes cannot come in direct contact with the bacteria. For this, I developed a model of infection in the notochord of zebrafish embryo. Upon injection of bacteria in this compartment, the microbes find themselves protected by the thick collagen sheath where the phagocytes cannot penetrate. While mycobacteria are not detected by phagocytes; *E. coli* bacteria are sensed and a significant local inflammation around the notochord is mounted. The *E. coli*, although inaccessible to phagocytosis are eliminated within the first 24 hours after injection, the inflammation lasts several days.

I studied the mechanisms that lead to this persistent inflammation and its long term consequences on the development of the fish. I showed the central role of the cytokine IL1B in this process, and I developed a transgenic line that allows studying *in vivo* the induction of this cytokine in fish.

I then studied the roles of the two main populations of phagocytes in the elimination of *E. coli*. I revealed that macrophages are not involved in the removal of bacteria but neutrophils, although unable to penetrate inside the collagen casing, are necessary for the bacterial elimination.

I also confirmed that myeloperoxidase and nitrogen monoxide are not involved in the removal of bacteria, rather the reactive oxygen species produced by neutrophils are needed to eradicate the infection.